

WestminsterResearch

<http://www.westminster.ac.uk/westminsterresearch>

**The effect of single nucleotide polymorphisms and mutations on
congenital thrombotic thrombocytopenic purpura phenotype**

Tate, H.

This is an electronic version of a PhD thesis awarded by the University of Westminster.
© Ms Helena Tate, 2017.

The WestminsterResearch online digital archive at the University of Westminster aims to make the research output of the University available to a wider audience. Copyright and Moral Rights remain with the authors and/or copyright owners.

Whilst further distribution of specific materials from within this archive is forbidden, you may freely distribute the URL of WestminsterResearch: (<http://westminsterresearch.wmin.ac.uk/>).

In case of abuse or copyright appearing without permission e-mail repository@westminster.ac.uk

**The effect of single nucleotide polymorphisms and mutations
on congenital thrombotic thrombocytopenic purpura
phenotype**

Helena Tate

**A thesis submitted in partial fulfilment of the
requirements of the University of Westminster for the
degree of Doctor of Philosophy**

November 2017

Abstract

Thrombotic thrombocytopenic purpura (TTP) is a rare, life-threatening disease with a reported incidence of 6 cases per million per year in the UK. It is characterised by episodes of microangiopathic haemolytic anaemia and thrombocytopenia, with the widespread presence of platelet-rich thrombi in the microcirculation, leading to end-organ damage. TTP is a clinically heterogeneous disorder caused by autoantibody inhibition or clearance or by a deficiency in activity or secretion of the von Willebrand factor cleaving protease (ADAMTS13). Over 100 mutations have been identified in ADAMTS13 yet, in some cases, these mutations in congenital TTP alone do not explain the disease phenotype, particularly in late-onset congenital TTP. One aim of this study was to analyse the effect of single nucleotide polymorphisms (SNPs), in conjunction with ADAMTS13 mutations, which have been identified in a cohort of TTP patients with varied clinical phenotype. Twenty mutant expression plasmids containing an ADAMTS13 mutation and/or SNP have been constructed by site-directed mutagenesis (SDM). Fourteen plasmids contained a new non-synonymous mutation (C3484T) which has been rectified by further SDM. After full sequencing of the plasmid ADAMTS13 insert, 24 clones were identified as viable and the resultant protein was expressed in HEK293T cells and analysed by Western blot and ADAMTS13 antigen ELISA. Blots were scanned by densitometry and the intensity of the protein species corresponding to ADAMTS13 determined using ImageJ. The predicted effects of mutations and/or SNPs were annotated by the *in silico* computational tools SIFT, PolyPhen2, I-Mutant 2.0 and SNPEffect 4.0. Results from this genotype study were compared to clinical phenotype by correlating data held within the TTP Registry at University College London. The resultant analysis showed the mutations located in the N-terminal end of ADAMTS13 protein induced more secretory defects and SNPs had less of an effect on phenotype. The p.R7W and p.A1033T SNPs showed more of an effect on secretion of ADAMTS13 when the mutation was located in the C-terminal end (p.R1060W) which is associated with late-onset phenotype. However, other environmental factors such as changes in the ADAMTS13-

VWF axis during pregnancy and infection make a correlation between genotype and phenotype in TTP more challenging.

Table of Contents

Abstract.....	ii
Table of Contents.....	iv
Table of Figures.....	ix
Table of Tables.....	xiii
Declaration.....	xvi
Abbreviations.....	xvii
Acknowledgements.....	xix
Chapter 1 Introduction.....	1
1.0 Historical context.....	1
1.1 von Willebrand factor.....	5
1.1.1 VWF synthesis.....	6
1.1.2 Platelet binding to VWF.....	7
1.1.3 von Willebrand's disease (VWD).....	8
1.2 ADAMTS13.....	9
1.2.1 Overview of ADAMTS proteases.....	9
1.2.3 Post-translational modifications.....	15
1.2.4 ADAMTS13 biosynthesis and secretion.....	16
1.3 ADAMTS13 – VWF interactions.....	16
1.3.1 Sites of VWF proteolysis by ADAMTS13.....	19
1.4 Pathologies of the ADAMTS13-VWF axis.....	21
1.4.1 Thrombotic thrombocytopenic purpura (TTP).....	21
1.5 Single nucleotide polymorphisms.....	25
1.6 TTP Animal models.....	27
1.6.1 Murine models.....	27
1.6.2 Baboon model.....	28
1.7 Additional factors and triggers of TTP.....	28
1.7.1 Inhibition.....	28
1.7.2 Pregnancy.....	29
1.7.3 Infection.....	29
1.7.4 The role of complement in endothelial activation.....	29
1.8 The role of ADAMTS13 in stroke and myocardial infarction.....	31
Aims.....	32

Objectives	32
Chapter 2 Materials and methods	33
2.1 Construction of <i>ADAMTS13</i> single nucleotide polymorphisms (SNPs), missense and deletion mutations.....	33
2.1.1 The pcDNA3.1(+) vector	37
2.2 Single-site directed mutagenesis (SDM)	37
2.2.1 Mutant strand synthesis reaction (polymerase chain reaction).....	37
2.2.2. Digestion of amplification products and transformation	38
2.3 Multi-site directed mutagenesis (multi-SDM)	39
2.3.1 Control reaction for multi-SDM	40
2.3.2 Mutant strand PCR for multi-SDM	41
2.4 Mini preparation of colonies.....	42
2.5 Sanger sequencing to verify successful nucleotide change	43
2.6 Plasmid copy amplification	44
2.6.1 QIAGEN HiSpeed® Plasmid Maxi preparation.....	44
2.6.2 Invitrogen PureLink® HiPure Plasmid DNA purification Midi preparation	45
2.6 Preparation of HEK293T cells.....	46
2.7 Transfection of HEK293T cells.....	46
2.7.1 Transfection agent	46
2.7.2 Transfection	47
2.8 Measure of transfection efficiency	47
2.9 Cell lysate preparation	48
2.10 Concentration of conditioned media.....	49
2.11 Protein quantification	49
2.11.1 Analysis of protein quantification results	50
2.12 Western blot	50
2.12.1 Sodium dodecyl sulphate polyacrylamide gel electrophoresis (SDS PAGE)	50
2.12.2 Running SDS PAGE	51
2.12.3 Transfer and western blot.....	51
2.12.4 Visualisation using enhanced chemiluminescence (ECL) reagent	52
2.12.5 Determination of the appropriate sample load for Western blot	52
2.12.6 Densitometry analysis.....	53
2.13 Commercial <i>ADAMTS13</i> antigen quantification: IMUBIND® <i>ADAMTS13</i> ELISA	53
2.13.1 Preparation of <i>ADAMTS13</i> standards	53

2.13.2 ADAMTS13 assay.....	53
2.14.3 Analysis of results	54
Chapter 3 In silico analysis of mutations and single nucleotide polymorphisms	55
3.1 Introduction	55
3.2 Methods.....	56
3.2.1 MUSCLE alignment.....	57
3.2.2 FOLD X.....	57
3.2.3 I-Mutant2.0.....	58
3.2.4 Sorting intolerant from tolerant (SIFT)	58
3.2.5 PolyPhen2.0	58
3.3 Results.....	59
3.3.1 MUSCLE alignments	59
3.3.2 FOLD X.....	62
3.3.3 I-Mutant2.0	64
3.3.4 Sorting intolerant from tolerant (SIFT) analysis.....	64
3.3.5 PolyPhen2.0	65
3.3.6 Frequency of SNPs in the population.....	66
3.3.7 Predict SNP.....	67
3.4 Discussion.....	68
3.4.1 Analyses of polymorphisms	69
3.4.2 Analyses of mutations.....	72
3.5 Concluding remarks	75
Chapter 4 Pregnancy-associated congenital TTP (Upshaw-Schulman syndrome)	76
4.1 Introduction	76
4.1.1 Thrombotic microangiopathies.....	76
4.2 Pathophysiology of pregnancy-associated TTP.....	78
4.2.1 Genotype of pregnancy-associated TTP	78
4.2.2 Location of p.R1060W and SNPs in ADAMTS13.....	79
4.3 Previous expression studies of mutation p.R1060W and SNPs	80
4.3.1 Expression studies of p.R1060W mutation.....	80
4.3.2 Expression studies of p.R7W and p.A1033T SNPs with mutation p.R1060W	81
4.4 Aims of this study.....	82
4.5 Methods.....	82
4.5.1 In silico modelling of mutation p.R1060W and SNPs R7W and A1033T.....	82

4.5.2 In vitro expression studies of mutation p.R1060W and SNPs p.R7W and p.A1033T	83
4.6 Results of transient expression studies of mutation p.R1060W mutation and SNPs..	85
4.6.1 Sanger sequencing of WT ADAMTS13 cDNA insert	85
4.6.2 Transfection efficiencies	89
4.6.3 Western blot analysis of cell lysates	92
4.6.4 Western blot analysis of conditioned media	94
4.6.5 Western blot analysis of cell lysates, repeat transient transfections	95
4.6.6 Western blot analyses of conditioned media, repeat transient transfections	95
4.6.7 ImageJ analysis of western blots: cell lysates	96
4.6.8 ImageJ analysis of western blots: conditioned media	98
4.6.9 ImageJ analysis of cell lysates, repeat transient transfections	99
4.6.10 ImageJ analysis of concentrated conditioned media, repeat transient transfections	100
4.6.11 ADAMTS13 ELISA analysis of concentrated conditioned media samples.....	101
4.7 Statistical analysis	103
4.8 Discussion.....	103
4.9 Concluding remarks	108
Chapter 5 The effect of SNPs and mutations on congenital TTP phenotype	111
5.1 ADAMTS13 polymorphisms	111
5.2 Methods.....	117
5.2.1 In silico analysis.....	117
5.2.2 In vitro expression studies	117
5.3 Results.....	119
5.3.1 Sequencing data of expression vectors	119
5.3.2 Transfection efficiencies of expression vectors	125
5.3.3 Western blot analyses.....	125
5.4 Discussion.....	153
5.4.1 Challenges in the methodology	153
5.4.2 Mutation p.R102H series	154
5.4.3 Mutation p.D217H series	155
5.4.4 Mutation p.T196I series	156
5.4.5 Mutation p.R409W.....	157
5.4.6 Mutation p.R398H.....	157

5.4.7 Mutation p.Q436H	158
5.4.8 Mutation p.A596V	158
5.4.9 Mutation p.A690T	159
5.4.10 Mutation p.C977F	159
5.4.11 Single nucleotide polymorphisms	159
5.5 Concluding remarks	160
Chapter 6 Discussion and conclusions	161
6.1 Aim of this study	161
6.2 Discussion of methods used	162
6.3 The relationship between patient genotype and clinical phenotype	166
6.4 The effect of mRNA processing on ADAMTS13 expression	167
6.5 Improvement of the method of protein detection.....	168
6.6 Synonymous SNPs.....	169
6.7 Concluding remarks	169
References.....	170
Appendices	183

Table of Figures

Figure 1.1 Regulation of ULWF in the A2 domain by ADAMTS13	6
Figure 1.2 Crystal structure of ADAMTS13	12
Figure 1.3 PDB crystal structure of the exosite structure of ADAMTS13	13
Figure 1.4 Secondary structures of ADAMTS13 domains mapped to the amino acid sequence	16
Figure 1.5 ADAMTS13-VWF interactions	18
Figure 1.6 Seven-step model of ADAMTS13-VWF exosite binding.....	19
Figure 3.1 Mutation p.R409W from FOLD X analysis.....	62
Figure 3.2 Mutation p.A596V from FOLD X analysis.....	63
Figure 3.3 SNP p.P475S from FOLD X analysis	63
Figure 3.4 SNP p.P618A from FOLD X analysis.....	63
Figure 4.1: Position of mutation p.R1060W and SNPs p.R7W and p.A1033T in ADAMTS13	78
Figure 4.2 Wild type full sequencing <i>ADAMTS13</i> cDNA.....	85
Figure 4.3 Non-synonymous mutation primer design C3484T	86
Figure 4.4 Sequencing results of expression vector p.A1033T SNP.....	87
Figure 4.5 Sequencing results of expression vector p.R1060W mutation.....	87
Figure 4.6 Sequencing results expression vector p.R7W SNP.....	88
Figure 4.7 Sequencing results expression vector p.R7W + p.R1060W	88
Figure 4.8 Sequencing results expression vector p.R1060W + p.A1033T.....	89
Figure 4.9 Sequencing results expression vector p.R1060W + p.R7W + p.A1033T	89
Figure 4.10: Co-transfection negative control	90
Figure 4.11 Co-transfection positive control	90
Figure 4.12 Co-transfection p.R1060W.....	90
Figure 4.13 Co-transfection p.R7W.....	90
Figure 4.14 Co-transfection p.A1033T	90
Figure 4.15 Co-transfection p.R1060W + p.R7W	90
Figure 4.16 Co-transfection p.R1060W + p.A1033T	91
Figure 4.17 Co-transfection p.R1060W + p.R7W + p.A1033T.....	91
Figure 4.18 Western blot analysis cell lysates (untreated).....	92
Figure 4.19 Western blot analysis cell lysates p.A1033T, p.A1033T + p.R1060W	93
Figure 4.20 Western blot analysis cell lysate p.R1060W, p.R1060W + p.R7W, p.R1060W + p.R7W + p.A1033T	93

Figure 4.21 Western blot analysis p.R7W	93
Figure 4.22 Western blot analysis conditioned media (CM) p.R1060W + p.R7W + p.A1033T	94
Figure 4.23 Western blot analysis CM p.R1060W, p.R1060W + p.A1033T, p.A1033T	94
Figure 4.24 Western blot analysis CM p.R1060W + p.R7W + p.A1033T, p.R1060W + p.R7W, p.R7W.....	94
Figure 4.25 Western blot analysis CM p.A1033T, p.R1060W + p.A1033T + p.R7W, R1060W + p.R7W.....	95
Figure 4.26 Western blot analysis cell lysate (rpt) p.R1060W, p.R1060W + p.A1033T	95
Figure 4.27 Western blot analysis CM (rpt) p.R1060W, p.A1033T, p.R1060W + p.A1033T ..	96
Figure 4.28 Western blot analysis CM (rpt) p.R1060W + p.R7W, p.R1060W + p.R7W + p.A1033T, p.R7W	96
Figure 4.29 Comparison of ADAMTS13 expression cell lysates p.R1060W series	97
Figure 4.30 Comparison of ADAMTS13 expression conditioned media, p.R1060W series ...	98
Figure 4.31 Comparison of ADAMTS13 expression cell lysates (rpt), p.A1033T, p.R1060W, p.R1060W + p.R7W, p.R1060W + p.A1033T, p.R1060W multi	100
Figure 4.32 Comparison ADAMTS13 expression CM (rpt) p.R1060W, p.A1033T, p.R1060W + p.A1033T, p.R1060W + p.R7W, p.R1060W multi	101
Figure 4.33 Comparison of ADAMTS13 antigen concentration p.R1060W + SNPs, CM	102
Figure 5.1 Position of mutations within the ADAMTS13 protein	115
Figure 5.2 Position of SNPs within the ADAMTS13 protein	115
Figure 5.3 Sequencing results of expression vector G305A and SNPs.....	120
Figure 5.4 Sequencing results of expression vector C587T + C1342G	120
Figure 5.5 Sequencing results of expression vector G649C + SNPs	120
Figure 5.6 Sequencing results of expression vector C1192T + C1342G	121
Figure 5.7 Sequencing results of expression vector C1225T	121
Figure 5.8 Sequencing results of expression vector G1308C.....	121
Figure 5.9 Sequencing results of expression vector C1787T + C1423T	121
Figure 5.10 Sequencing results of expression vector G2068A.....	121
Figure 5.11 Sequencing results of expression vector G2930T	122
Figure 5.12 Sequencing results of expression vector C1423T	122
Figure 5.13 Sequencing results of expression vector C1852G.....	122
Figure 5.14 Sequencing results of expression vector C2195T	122
Figure 5.15 Sequencing results of expression vector C2699T	122

Figure 5.16 Western blot analysis cell lysate p.A900V, p.R102H.....	126
Figure 5.17 Western blot analyses cell lysates p.R102H + SNPs.....	126
Figure 5.18 Western blot analyses conditioned media p.R102H + SNPs.....	127
Figure 5.19 Comparison of ADAMTS13 expression p.R102H + SNPs cell lysates	128
Figure 5.20 Comparison of ADAMTS13 expression p.R120H + SNPs conditioned media....	129
Figure 5.21 Comparison of ADAMTS13 antigen concentration, p.R102H + SNPs	130
Figure 5.22 Western blot analyses p.D217H + SNPs, cell lysate	131
Figure 5.23 Western blot analyses p.D217H + multiple SNPs, cell lysates	131
Figure 5.24 Western blot analyses p.D217H + SNPs, conditioned media.....	132
Figure 5.25 Comparison of ADAMTS13 expression p.D217H, cell lysates	133
Figure 5.26 Comparison of ADAMTS13 expression p.D217H, conditioned media	134
Figure 5.27 Comparison of ADAMTS13 antigen concentration p.D217H + SNPs	135
Figure 5.28 Western blot analyses SNPs, cell lysates	136
Figure 5.29 Western blot analyses SNPs cell lysates	136
Figure 5.30 Western blot analyses SNPs, conditioned media	137
Figure 5.31 Comparison of ADAMTS13 expression cell lysates, SNP series	138
Figure 5.32 Comparison of ADAMTS13 expression, conditioned media, SNP series	139
Figure 5.33 Comparison of ADAMTS13 antigen concentration, SNP series	140
Figure 5.34 Western blot analyses cell lysates p.398C, p.398C + p.Q448E, p.409W,.....	141
Figure 5.35 Western blot analyses conditioned media p.398C, p.398C + p.Q448E, p.409W	141
Figure 5.36 Comparison ADAMTS13 expression p.R409W, p.R398C series cell lysates.....	142
Figure 5.37 Comparison ADAMTS13 expression p.R409W, p.R398C series, conditioned media	143
Figure 5.38 Comparison of ADAMTS13 antigen concentration p.R409W, p.R398C series .	144
Figure 5.39 Western blot analyses cell lysates p.A596V, p. A596V + p.P475S, p.A690T	145
Figure 5.40 Western blot analyses conditioned media p.A596V, p.A596V + p.P475S, p.A690T	145
Figure 5.41 Western blot analyses cell lysates p.T196I, p.T196I + p.Q448E.....	147
Figure 5.42 Western blot analyses conditioned media p.T196I, p.T196I + p.Q448E.....	147
Figure 5.43 Comparison ADAMTS13 expression cell lysates p.A596V series, p.A690T, p.T196I series	148
Figure 5.44 Comparison ADAMTS13 expression, conditioned media p.A596V series, p.A690T, T196I series.....	149

Figure 5.45 Western blot analyses cell lysates and conditioned media p.Q436H.....	150
Figure 5.46 Comparison of ADAMTS13 expression cell lysates and conditioned media p.Q436H	151
Figure 5.47 Western blot analyses cell lysates p.C977F	152
Figure 5.48 Western blot analyses conditioned media p.C977F	152
Figure 5.49 Comparison of ADAMTS13 expression cell lysates and conditioned media p.C977F.....	153

Table of Tables

Table 1.1 Amino acid positions of cations binding in functional domains	10
Table 1.2 Summary of exosite properties.....	15
Table 1.3 SNP reference numbers	26
Table 2.1 Mutations and SNP inserted into ADAMTS13 cDNA vector.....	33
Table 2.2 Parameters used to calculate T_m oligonucleotide primers	34
Table 2.3 Mutagenic oligonucleotide primers	36
Table 2.4 Preparation of sample reaction, single-site SDM.....	38
Table 2.5 SDM primer length used in multi-site SDM.....	40
Table 2.6 Preparation of sample reaction multi-site SDM.....	40
Table 2.7 Cycling parameters for multi-site SDM	41
Table 2.8 PCR components for multi-site SDM.....	42
Table 2.9 Oligonucleotide primers used to sequence <i>ADAMTS13</i> cDNA	44
Table 2.10 The concentration of conditioned media.....	49
Table 2.11 BCA protein standard concentrations.....	49
Table 3.1 Conservation of amino acid residues among orthologs: SNPs and mutations	59
Table 3.2 FOLD X scores for mutations and SNPs	62
Table 3.3 Summary of SNP Effect 4.0: FOLD X findings	63
Table 3.4 Results from I-Mutant algorithm for mutations and SNPs	64
Table 3.5 SIFT scores for mutations and SNPs	64
Table 3.6 Results of PolyPhen2.0 analysis for mutations and SNPs	65
Table 3.7 Frequencies of SNPs in the European population.....	66
Table 3.8 Frequencies of SNPs in the global population	66
Table 3.9 Summary of prediction and expected accuracy of prediction for each analytical tool	67
Table 4.1 Summary of <i>in silico</i> analysis.....	83
Table 4.2 Expression vectors created by SDM	83
Table 4.3 Nucleotide substitutions for SDM primers.....	83
Table 4.4 Synonymous changes in WT <i>ADAMTS13</i> cDNA insert	86
Table 4.5 DNA concentration of expression vectors.....	86
Table 4.6 Estimated transfection efficiencies of expression vectors.....	91
Table 4.7 Normalized protein ratio of expressed ADAMTS13 in cell lysates.....	97
Table 4.8 Normalized protein ratio of expressed ADAMTS13 in CM.....	98

Table 4.9 Normalized protein ratio of expressed ADAMTS13 in cell lysates, repeat transfection.....	99
Table 4.10 Normalized protein ratio of expressed ADAMTS13 in CM, repeat transfection	100
Table 4.11 Normalized ADAMTS13 antigen ratio of expressed ADAMTS in CM	102
Table 4.12 Results of one way ANOVA analysis.....	103
Table 4.13 Summary of ADAMTS13 expression in cell lysates, first transfection	105
Table 4.14 Summary of ADAMTS13 expression in CM, first transfection	106
Table 4.15 Summary of ADAMTS13 antigen concentration in CM, first transfection	107
Table 4.16 Summary of ADAMTS13 expression in cell lysates, second transfection	107
Table 4.17 Summary of ADAMTS13 expression in CM, second transfection	108
Table 5.1 Missense non-synonymous SNPs identified in the <i>ADAMTS13</i> cDNA	112
Table 5.2 Genotype of patients diagnosed with pregnancy-associated TTP	113
Table 5.3 Genotype of patients diagnosed with neonatal TTP	113
Table 5.4 Genotype of patients diagnosed with childhood TTP	113
Table 5.5 Clinical details and genotype of TTP patients	114
Table 5.6 Previous expression studies of the effect of mutations and SNPs on the secretion and activity of ADAMTS13	115
Table 5.7 Expected effect of SNPs on secretion of ADAMTS13.....	116
Table 5.8 Expected effect of mutations on secretion of ADAMTS13.....	117
Table 5.9 Expression vectors constructed by SDM.....	118
Table 5.10 Expression vectors not created	118
Table 5.11 Expression vectors carrying C3484T non-synonymous mutation	123
Table 5.12 DNA concentrations of expression vectors	124
Table 5.13 Transfection efficiencies of expression vectors	125
Table 5.14 ImageJ analysis of p.R102H series, cell lysates	127
Table 5.15 ImageJ analysis of p.R102H series, CM	128
Table 5.16 ELISA ADAMTS13 antigen concentration p.R102H series	129
Table 5.17 One way ANOVA analysis of p.R102H + SNPs	130
Table 5.18 ImageJ analysis of p.D217H series, cell lysates	132
Table 5.19 ImageJ analysis of p.D217H series, CM	133
Table 5.20 ELISA ADAMTS13 antigen concentration, p.D217H	134
Table 5.21 One way ANOVA results, p.D217H + SNPs	135
Table 5.22 ImageJ analysis of SNP series, cell lysates.....	137
Table 5.23 ImageJ analysis SNP series, CM	138

Table 5.24 ELISA ADAMTS13 antigen concentration SNP series	139
Table 5.25 One way ANOVA results, SNP series	140
Table 5.26 ImageJ analysis of p.R409W and p.R398C series, cell lysates	142
Table 5.27 ImageJ analysis p.R409W and p.R398C series, CM	142
Table 5.28 ELISA ADAMTS13 antigen concentration p.R409W and p.R398C series.....	143
Table 5.29 ImageJ analysis of cell lysates p.A596V series and p.A690T	145
Table 5.30 ImageJ analysis of p.596V series and p.A690T, CM	146
Table 5.31 ImageJ analysis of p.T196I series, cell lysates	147
Table 5.32 ImageJ analysis of p.T196I series, CM	148
Table 5.33 ImageJ analysis of p.Q436H, cell lysates	150
Table 5.34 ImageJ analysis of p.Q436H, CM	150
Table 5.35 ADAMTS13 antigen concentration p.Q436H	151
Table 5.36 ImageJ analysis of p.C977F cell lysate	152
Table 5.37 ImageJ analysis of p.C977F CM	153
Table 6.1 Summary of predicted effect of SNPs and mutations on ADAMTS13 expression	161
Table 6.2 Restriction enzymes not targetting <i>ADAMTS13</i> cDNA.....	164

Declaration

I declare that the present work was carried out in accordance with the Guidelines and Regulations of the University of Westminster. The work is original except where indicated by special reference in the text.

The submission as a whole or part is not substantially the same as any that I previously or am currently making, whether in published or unpublished form, for a degree, diploma or similar qualification at any university or similar institution.

Until the outcome of the current application to the University of Westminster is known, the work will not be submitted for any such qualification at another university or similar institution.

Any views expressed in this work are those of the author and in no way represent those of the University of Westminster.

Signed: *Helena Tate*

Date: 29 November 2016

Abbreviations

ADAMTS13	A disintegrin-like and metalloprotease with thrombospondin-type type 13 motifs
APS	Ammonium persulphate
BCA	Bicinchoninic
BSA	Bovine serum albumin
CAT	Chloramphenicol acetyl transferase
CM	Conditioned media
CMV	Cytomegalovirus
CUB	Complement C1r/C1s, UEGF, bone morphogenic protein
CWR core	Cysteine-tryptophan-arginine core
DCTS	Disintegrin-cystiene-rich-thrombospondin-spacer domains
DMEM	Dulbecco's modified Eagle's medium
DMSO	Dimethyl sufoxide
DNA	Deoxyribonucleic acid
dNTP	Dinucleotide triphosphate
EDTA	Ethylenediaminetetracetic acid
ER	Endoplasmic reticulum
FASTA	Fast all (program)
FFP	Fresh frozen plasma
FRETs	Fluorescence resonance energy transfer assay
GFP	Green fluorescent protein
GWA	Genome-wide association study
HCl	Hydrochloric acid
HEK	Human embryonic kidney
HELLP	Haemolysis elevated liver enzymes low platelet count
HPLC	High performance liquid chromatography
HRP	Horseradish peroxidase
HUS	Haemolytic uraemia syndrome
HUVEC	Human umbilical vein endothelial cells
IPTG	Isopropyl-1-thio- β -D-galactopyranoside
ISTH-SCC	International Society of Thrombosis and Haemostasis Scientific Standardization Committee
MAF	Minor allele frequency
MAHA	Microangiopathic haemolytic anaemia
MEM	Minimum essential medium
MP	Metalloprotease
MUSCLE	Multiple sequence comparison by log expectation
NSM	Non-synonymous mutation
NZY	NZ amine broth
PBS	Phosphate buffered saline
PCR	Polymerase chain reaction
PDB	Protein Data Bank
PEI	Polyethylenimine
PSI-BLAST	Position-specific basic local alignment search tool
PT	Plasma therapy
Rpm	Revolutions per minute
RNA	Ribonucleic acid

rADAMTS13	Recombinant ADAMTS13
RT	Room temperature
SDM	Site directed mutagenesis
SDS	Sodium dodecyl sulfate
SELDITOF	Surface-enhanced laser desorption ionization time-of-flight
SEM	Standard error of the mean
SIFT	Sorting intolerant from tolerant
SNP	Single nucleotide polymorphism
TBS	Tris buffered saline
TBST	Tris buffered saline with Tween® 20
TEMED	N,N,N,N tetramethylethylenediamine
TK	Tyrosine kinase
TMB	5-5'-tetramethylbenzidine
TMA	Thrombotic microangiopathies
TSP	Thrombospondin-type 1
TTP	Thrombotic thrombocytopenic purpura
UCLH	University College London Hospital
ULVWF	Ultra large von Willebrand factor
USS	Upshaw-Schulman syndrome
VWD	Von Willebrand's disease
VWF	Von Willebrand factor
WT	Wild type

Amino acid code	Amino acid
A	Alanine
C	Cysteine
D	Aspartic acid
E	Glutamic acid
F	Phenylalanine
G	Glycine
H	Histidine
I	Isoleucine
K	Lysine
L	Leucine
M	Methionine
N	Asparagine
P	Proline
Q	Glutamine
R	Arginine
S	Serine
T	Threonine
V	Valine
W	Tryptophan
Y	Tyrosine

Acknowledgements

I would like to thank my Director of Studies, Dr Raymond Camilleri, for his help, guidance, support and cups of tea throughout this PhD. I would also like to thank my supervisors Dr Michael Godge, Dr Marie Scully and Dr John Murphy for their insightful comments and clarity of thought.

Thank you also to Dr Pamela Greenwell for allowing me to use bench space in her laboratory, to Dr Edward Wright for the donation of the reporter plasmid and to all the technical staff at the University of Westminster. Their help in the laboratory has been indispensable. Thank you also to the undergraduate and postgraduate students that have worked in the research laboratory and helped me with the SDM cloning work.

Thank you to the University of Westminster for granting me a scholarship, without which this PhD would not have been possible. Thank you to all my friends and fellow PhD students who have brightened my day and made some very useful suggestions.

Lastly thank you to Michael, James and Henry without whose support I would have floundered.

Chapter 1

Introduction

Thrombotic thrombocytopenic purpura (TTP) is a rare, life-threatening haematological disease with a reported incidence of six cases per million per year in the UK (Scully *et al.*, 2008). The disorder is characterised by episodes of microangiopathic haemolytic anaemia (MAHA), thrombocytopenia and the widespread presence of platelet-rich thrombi in the microcirculation. This leads to end-organ ischaemic damage, primarily affecting the heart, kidneys and nervous system. The diagnosis of TTP has traditionally been based on clinical history, examination and routine blood parameters. If left untreated, the disease carries a mortality rate of 90% (Scully *et al.*, 2012). Current first-line treatment is plasma exchange with fresh frozen plasma (FFP), often in conjunction with the anti-CD20 monoclonal antibody rituximab.

1.0 Historical context

TTP was first documented in the literature by the physician Dr Eli Moschcowitz in the USA (Moschcowitz, 1924). A 16-year-old female student had been admitted to the Beth Israel Hospital in New York with a recent history of upper extremity weakness and fever, which progressed over four days after hospital admission. She lapsed into a coma and subsequently died and the histological evidence on post-mortem showed that 'Death...resulted from some powerful poison which had both agglutinative and haemolytic properties'. Baehr *et al.* in 1936 added to this report that hyaline microthrombi observed on post mortem were rich in platelets (Baehr *et al.*, 1936).

Following this, there were few sporadic documented cases until Singer *et al.* reviewed the 11 documented cases to date and were the first to use the term TTP in 1947. Thrombocytopenic purpura was a relatively common occurrence but, in combination with multiple platelet thrombi, the disorder was rare. The patient identified by Singer in 1947 was an 11-year-old girl who presented with ecchymosis and petechiae, together with neurological symptoms including

headache, paraesthesia and confusion. On the sixth day after admission she died and post-mortem histological analysis showed identical features with the previous 11 cases in the literature. All cases reported the presence of many platelet-rich microthrombi in capillaries, arterioles and the smaller arteries of almost all organs. Singer concluded that the disease should be recognised ante-mortem, rather than on post-mortem histological evidence, and suggested thrombotic should be added to the term thrombocytopenic purpura. The disease TTP was thus recognised (Singer *et al.*, 1947).

Schulman in 1960 reported that an eight-year-old patient, who had a history of severe epistaxis and petechiae from birth and no family history of similar problems, also suffered haemolytic anaemia and thrombocytopenia. The epistaxis cleared after treatment with whole blood and the patient underwent a splenectomy. Following this, the patient was transfused several times and the platelet count recovered for eight days whereupon the count fell to pre-transfusion levels. Schulman concluded that the thrombocytopenia was due to '...a deficiency of a factor, present in normal plasma, which is required for megakaryocyte maturation which is neutralised by a factor in normal plasma' (Schulman *et al.*, 1960). The pathophysiology of the disease still proved elusive.

Amorosi and Ultmann in 1966 furthered research in the field by reporting 16 cases and reviewing the literature to date (Amorosi & Ultmann, 1966). By this time, there were a total of 271 cases of reported TTP. Previously, TTP was considered clinically to be a triad of signs and symptoms, namely bleeding or purpura, haemolytic anaemia and neurologic presentations. As fever was observed to be almost always present, as well as renal disease, the authors argued that TTP should be considered to be a pentad of signs and symptoms. The cases they described and reviewed were between the ages of 10-39 years, with more females than males. There was also a greater incidence of pregnancy in the case histories, which the authors argued could be by chance, or there may be an aetiological relationship. With respect to the mechanism of the disease, the authors suggested allergy, or possibly a toxin capable of causing haemolysis and platelet agglutination. It was also suggested that the cause could be auto-immune but it was observed that transfusion of plasma

from a patient with TTP to a healthy volunteer caused no untoward effects (which would possibly not pass ethics today). The authors concluded that TTP is a very variable disease, both in clinical presentation and in outcome, with 72% of patients dying within 90 days. Hereinafter, they recommended the disorder should be considered to be a pentad of signs and symptoms to aid clinical diagnosis.

TTP research continued apace and in 1996, Furlan *et al.* identified unusually large forms of von Willebrand factor (VWF) in patients with TTP. These large multimers disappeared after treatment with fresh frozen plasma. The authors drew the conclusion that '...a proteolytic enzyme is responsible for VWF degradation in normal plasma not yet identified'. It was known that plasmin cleaves several bonds in VWF, leaving a high molecular weight core which retained 70% of its platelet-binding ability. The authors purified the 'factor' which degraded VWF and identified that the 'proteolytic enzyme' cleaved VWF at the Tyr1605-Met1606 bond and that there was a consistent proportion of VWF fragments produced with molecular weights of 189, 176 and 140kDa. They concluded that this VWF cleaving protease was not a serine protease, cathepsin, matrix metalloprotease nor a calpain but the true nature of the VWF-cleaving enzyme had yet to be elucidated (Furlan *et al.*, 1996).

Tsai *et al.* in 1996 concurrently worked on the identification of this VWF-cleaving protease. They performed some elegant experiments placing VWF under shear stress, concluding that VWF in its native form existed as an enclosed structure that was relatively resistant to cleavage by the novel metalloprotease. However, when VWF was placed in conditions of shear stress as found in smaller arteries, arterioles and capillaries in the circulation, this enclosed structure unfurled and the active site was exposed to the protease. They identified that this process required calcium ions and that the unfurled multimeric structure of VWF facilitated the greatest platelet binding. They concluded that, after entering the circulation, proteolysis may only occur when VWF is exposed to shear stress. At this point, it was concluded that TTP induces an excessive release of ultra-large von Willebrand factor (ULVWF) and/or induces increased or impaired degradation of these multimers (Tsai, 1996).

Further work by Furlan *et al.* in 1997 analysed patient pedigree data in four families of patients with chronic relapsing TTP and concluded that TTP was caused by a deficiency of the protease and that this was inherited in an autosomal recessive pattern (Furlan *et al.*, 1997). In 1998 this group analysed samples from 53 patients diagnosed with TTP or haemolytic uremic syndrome (HUS) which is a microvascular disorder with signs and symptoms very similar to TTP. In this cohort, 13 patients had been diagnosed with HUS, 24 with non-familial TTP and 16 with familial TTP. They developed and utilised a WVF-cleaving protease assay and looked for the presence of an inhibitor by measuring protease activity in samples from healthy patients after incubation with patient samples. From this, they recommended that these tests be implemented to aid differential diagnosis and to guide treatment of TTP with differing aetiology. They argued that patients with familial forms may relapse and those with the presence of an inhibitor may require greater volumes of FFP (Furlan *et al.*, 1998).

The identification and classification of the VWF-cleaving protease was finally elucidated in 2001 by two separate groups. Fujikawa purified the protease from commercial factor VIII/VWF and the N-terminal sequence was identified and compared to the human genome sequence published in the same year by the International Human Genome Consortium (Fujikawa, 2001). At the same time, Levy *et al.* studied the molecular pathogenesis of TTP using a genetic approach. They studied four pedigrees of patients with familial TTP. The level of the VWF-cleaving protease in plasma was 2-7% of normal in affected individuals. On analysing the levels of protease in the parents of affected individuals, it was found they corresponded to those consistent with a heterozygous carrier status. It was concluded that the plasma level of the protease could be used as a phenotypic trait for linkage analysis in order to map the locus of the protease. Through techniques such as cDNA cloning, polymerase chain reaction (PCR) with reverse transcription, rapid amplification of cDNA ends and genomic sequence analysis, the full length of the protease cDNA and genomic structure was deduced. The protease was identified as being the thirteenth member of the ADAMTS family (a disintegrin and metalloproteinase with thrombospondin type 1 repeats).

The ADAMTS13 gene was discovered to be located on chromosome 9q34, spanned 29 exons and encoded a protein of 1,427 amino acids. The gene was found to be highly conserved when compared to the mouse genome sequence. On analysis by northern blot, it was found ADAMTS13 was almost exclusively produced in the liver. Levy *et al.* also identified 12 mutations and a total of 25 single nucleotide polymorphisms (SNPs), seven of which resulted in non-synonymous changes which altered the amino acid sequence in the protein (Levy *et al.*, 2001).

Since the identification and classification of ADAMTS13 in 2001, the direct link between ADAMTS13 deficiency and TTP pathogenesis has been firmly established and a significant body of research has been produced in this field (Sadler, 2017). The development of diagnostic assays has also greatly contributed to the advancement of knowledge, in addition to aiding patient diagnosis of TTP.

1.1 von Willebrand factor

The hallmarks of TTP are caused by platelet-rich microthrombi consisting of multimeric ULVWF. VWF is a large, multi-domain, heterogeneous glycoprotein which plays a vital role in primary haemostasis. It consists of 2,050 amino acids in its monomeric form. The gene for VWF is located at the tip of the short arm of chromosome 12 (Ginsburg *et al.*, 1985), is ~178kb in length and contains 52 exons (Mancuso *et al.*, 1989). The messenger RNA encodes a precursor of 2,813 amino acids in length and consists of a signal peptide (22 amino acids), a propeptide (741 amino acids) and the mature peptide subunit (2,050 amino acids); (Sadler, 1998).

VWF is classified as an acute phase protein and is produced constitutively in endothelial cells (Wagner *et al.*, 1982) and megakaryocytes (Nachman *et al.*, 1977) and is secreted into the plasma, where it exists in a globular form. The primary functions of VWF are threefold: to bind to sub-endothelial collagen which has been exposed to vessel injury; to bind to receptor glycoprotein Ib (GPIb) complex on the surface of non-activated platelets and to bind to the

receptor GPIIb/IIIa complex on the surface of activated platelets. A further function of VWF is to bind to factor VIII to protect it from proteolytic cleavage (Weiss *et al.*, 1977).

1.1.1 VWF synthesis

VWF is synthesized in the endoplasmic reticulum (ER) of endothelial cells as monomers consisting of unprocessed precursors termed pre-pro-VWF monomers (Wagner *et al.*, 1982). These monomers are linked via C-terminal disulphide bonds to form dimers (pro-VWF molecules). Further post-translational modification occurs in the Golgi apparatus and the resultant glycosylation leads to the presence of the ABO (H) group antigens (Matsui *et al.*, 1992). As a consequence, populations with blood group O result in lower mean levels of VWF in the plasma (Gill *et al.*, 1987). Further processing facilitates multimerization through N-terminal glycosylation, resulting in the formation of multimers varying in size. The larger size multimers, termed ultra-large VWF (ULVWF) are more functionally active due to increased numbers of platelet-binding receptors. The enzyme ADAMTS13 regulates the size of these multimeric units through cleavage of the VWF A2 domain (see Figure 1.1).

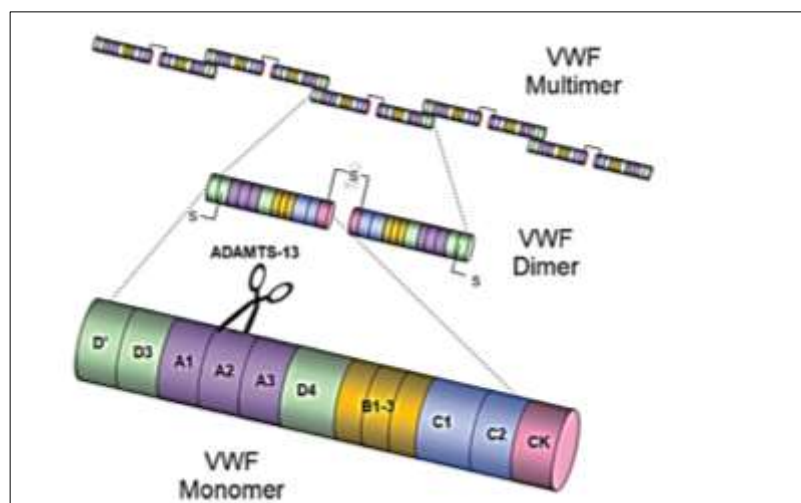


Figure 1.1 Regulation of ULWF in the A2 domain by ADAMTS13 (from Chapman *et al.*, 2012). Reproduced with permission © Georg Thieme Verlag AG.

The enzyme furin processes pro-VWF into the mature VWF multimers by cleavage of the pro-polypeptide von Willebrand propeptide (VW pp) from the

pro-VWF dimers. VWFpp chaperones VWF into storage granules (Weibel-Palade bodies in endothelial cells and α -granules in platelets) ready for release into the plasma (Wagner *et al.*, 1982). Each monomer is ~250 kDa in size but through multimerization is stored as ULVWF; (Sadler, 2002). VWF can exist in the plasma as a series of oligomers whose subunits range from 2-40 to 100-200 multimers or more, with a molecular weight exceeding 20,000 kDa (Sadler, 1998; Zhou 2011). These high molecular-weight multimers (ULVWF) bind platelets and collagen more efficiently and are vital for platelet aggregation at the site of tissue injury (Arya *et al.*, 2002).

Platelets do not release VWF until activated whereas endothelial cells release VWF constitutively, particularly in response to exercise and adrenergic stimulation (Giblin *et al.*, 2008). Once released from the Weibel-Palade bodies into the plasma, VWF exists in a globular form with the collagen-binding A3 domain exposed to enable surveillance of the vasculature and to enable it to bind when the sub-endothelial matrix is exposed at sites of vessel damage. However, the GPIb α binding site in the A1 domain is partly concealed, ensuring no unwanted platelet binding occurs. The ADAMTS13 binding and cleavage sites (the A2 domain) are also buried, ensuring no unwanted proteolysis of VWF (Zhang *et al.*, 2009).

1.1.2 Platelet binding to VWF

With vessel injury, the resultant disruption of the vessel wall exposes the pro-coagulant sub-endothelium. In intermediate- to high-shear conditions in arteries, arterioles, capillaries and in stenosed vessels, platelet adherence to the exposed collagen is indirect, via the interaction between the A1 domain of VWF (Fujimura *et al.*, 1986) and the platelet GPIb-IX-V complex. In this way, VWF acts as a bridge between the platelet surface and exposed collagen. In non-activated platelets this interaction occurs with low affinity, or not at all, as the GPIb-IX-V complex is masked and is therefore haemostatically inactive. If VWF is immobilized by binding to collagen-rich matrices via the A3 domain that have been exposed through damage, the VWF multimers unravel under the forces of shear stress on the tethered molecule by the flowing blood

(Siedlecki *et al.*, 1996). This leads to exposure of the high-affinity platelet-binding complex and the subsequent capture of platelets that are circulating at the periphery of the vessel. The exposure of the linear array of VWF A1 domains facilitates binding to multiple GP1b α receptors on the platelet surface (Sadler, 1998). Once tethered, platelets roll over the exposed VWF receptor complexes in the direction of blood flow and the process of platelet tethering is initiated. As this interaction is unstable due to a fast dissociation rate, further platelet-collagen interactions leading to platelet activation occur. The larger ULVWF are more haemostatically competent, due not only to the large numbers of collagen and platelet-binding sites, but also because they unravel more readily under rheological shear (Zhang *et al.*, 2009). Under normal conditions the VWF polymers, when stretched, can reach up to a length of 100 μ m and represent a dimer containing 5,100 amino acids and this is needed to stop bleeding (Schneider *et al.*, 2007).

The control of multimer length through proteolytic cleavage by ADAMTS13 is a delicate balance between reducing their size to ensure they remain sufficiently functional to stop bleeding and ensuring adequate cleavage to avoid unwanted thromboses.

1.1.3 von Willebrand's disease (VWD)

von Willebrand's disease is an autosomal bleeding disorder of variable clinical severity resulting from a variety of subtypes of VWF deficiency and is the most common inherited haemostatic disorder in the UK. This disorder has led to much analysis of the VWF gene (VWF gene reference sequence ID:7450). Mutations and polymorphisms within VWF have been studied widely and are compiled and maintained for the International Society of Thrombosis and Haemostasis at the University of Sheffield (ISTH-SSC VWF online database). Specific mutations within VWF are known to affect exosite binding of ADAMTS13 (de Groot *et al.*, 2009; Pos *et al.*, 2010) and ADAMTS13 activity (de Groot *et al.*, 2010). In patients with severe VWD, Factor VIII levels have also been found to be less than 10% of normal controls (Sadler, 1998).

1.2 ADAMTS13

1.2.1 Overview of ADAMTS proteases

ADAMTS13 belongs to the ADAMTS family of multi-domain extracellular proteases which all contain a reprotolysin-like metalloprotease. There are 19 members of this family and they can be sub-grouped on the basis of their known substrates such as the proteoglycans, the procollagen N-peptidases, the cartilage oligomeric matrix proteins and the VWF-cleaving protease ADAMTS13 (Kelwick *et al.*, 2015). Generally they are considered to be remodelling enzymes of the extracellular matrix and as a family, they have important roles in connective tissue organization, coagulation, inflammation, angiogenesis and cell migration (Apte, 2004; Porter, 2005). The proteases are highly conserved structures containing the metalloprotease catalytic domain, a carboxy-terminal ancillary domain and at least one thrombospondin type 1 repeat.

1.2.2 ADAMTS13 structure

ADAMTS13 is a ~180 kDa metalloprotease consisting of 1,427 amino acids. The protease contains a signal peptide, a propeptide, a metalloprotease domain, a disintegrin-like domain, a thrombospondin type 1 motif (TSP-1), a cysteine-rich domain, a spacer domain, seven TSP-1 repeats and 2 complement C1r/C1s, sea urchin epidermal growth factor and bone morphogenetic protein 1 (CUB) domains (Zheng *et al.*, 2001); see Figure 1.2. The ADAMTS13 gene is located on chromosome 9q34, and is approximately 45kb in humans. The gene consists of 24 exons (Levy *et al.*, 2001).

1.2.2.1 The propeptide domain

The ADAMTS13 propeptide is short and poorly conserved compared to those of other proteases in the ADAM or ADAMTS family and is not required for its secretion or activation. This region in other ADAMTS proteases functions as a molecular chaperone to direct protein folding, or the domain provides enzymatic latency and is cleaved during biosynthesis. This role is not apparent in ADAMTS13 (Majerus *et al.*, 2003). The signal and propeptide domains encompass amino acid residues 1→79.

1.2.2.2 The metalloprotease domain

The metalloprotease domain contains the active site and encompasses amino acid residues 79→286. Several metal ions bind in this site and these interactions are considered functionally necessary (see Table 1.1). The active site of all the reprotolysin or adamlysin family of metalloproteases contain three histidine residues that co-ordinate the essential Zn^{2+} in the sequence HEXXHXXGXXHD. Three Ca^{2+} binding sites have also been postulated (see Table 1.1). The first is between amino acid residues Glu83, Asp173, Cys281 and Asp284, which is in common with other metalloproteases. The second binding site is projected to be between residues Glu164, Asp166 and Asn162, Asp165 and Asp 168. This appears to be a low-affinity Ca^{2+} binding site and is functionally not important: mutational studies to assess the low affinity site have found that the apparent dissociation constant ($K_{D\ app}$) between the mutants and wild type is similar (51 μ M, 65 μ M and 70 μ M respectively); (Gardner *et al.*, 2014). The third site is between the residues Asp187, Glu212 and Asp182 or Glu184. Through mutational analyses, any alterations in these residues dramatically alter function therefore this latter site is postulated to be a high-affinity Ca^{2+} binding site (Gardner *et al.*, 2014) and aids in the conformation of the active site cleft.

Table 1.1 Amino acid positions of cations binding in functional domains

Description	Amino acid position	Cation
Metal binding	Glu 83	Calcium
Metal binding	Asp 173	Calcium
Metal binding	Asp 182	Calcium; high affinity
Metal binding	Glu 184	Calcium; high affinity
Metal binding	Asp 187	Calcium; high affinity
Metal binding	Glu 212	Calcium; high affinity
Metal binding	His 224	Zinc; catalytic
Active site	Glu 225	
Metal binding	His 228	Zinc; catalytic
Metal binding	His 234	Zinc; catalytic
Metal binding	Cys 281	Calcium
Metal binding	Asp 284	Calcium

There are also other points of recognition found to be important for the interaction of VWF and ADAMTS13. These are residues Leu198, Leu232 and Leu274 that collectively interact with Leu1603 in VWF (Xiang *et al.*, 2011).

Experimental evidence has shown that the metalloprotease domain alone has little or no proteolytic activity towards VWF. However, as more domains are sequentially added, the activity towards its substrate increases, indicating that exosite interactions govern enzymatic activity and substrate specificity, as is seen in other clotting factors (Gao *et al.*, 2008; Soejima *et al.*, 2010; X. Zheng *et al.*, 2003). Other researchers have found that the metalloprotease and the disintegrin-like domain are an inseparable functional unit (Ai *et al.*, 2005; de Groot *et al.*, 2009; Gao *et al.*, 2008); and that the dependence on calcium for proteolytic activity is mediated by the high affinity site (Anderson *et al.*, 2006; Gardner *et al.*, 2014).

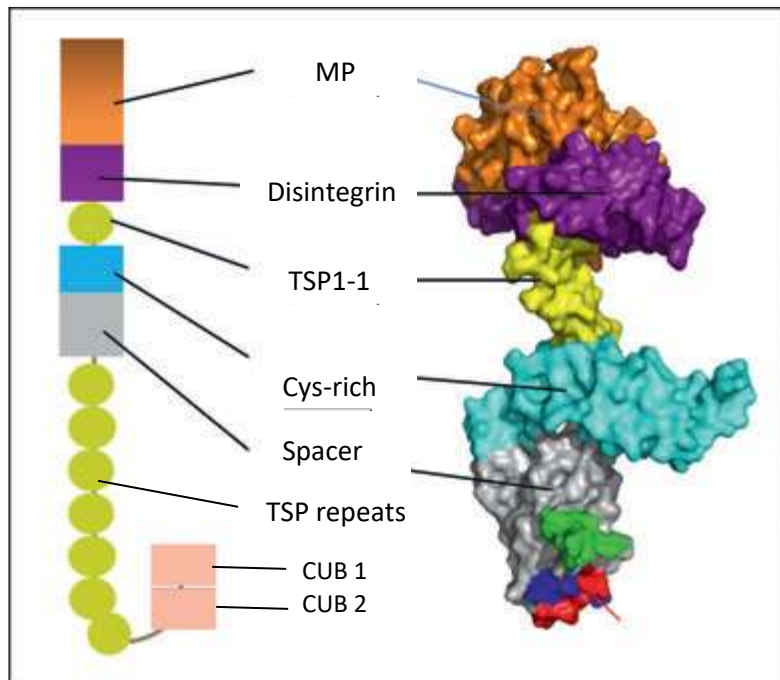
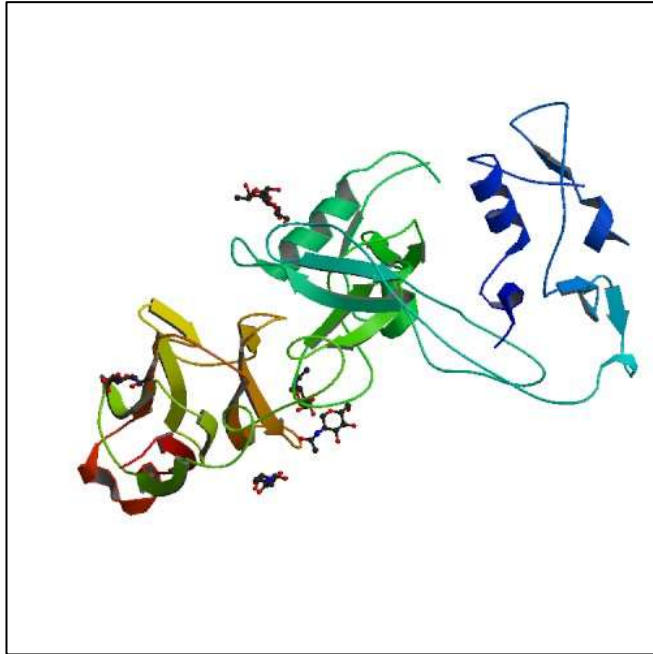


Figure 1.2 Crystal structure of ADAMTS13 (right) with corresponding domains (modified from Zheng *et al.*, 2013); PDB 3GHM. MP: metalloprotease, TSP1-1: thrombospondin type 1, Cys-rich: cysteine-rich domain. The TSP repeats and CUB domains are not within the crystal structure.

1.2.2.3 The disintegrin domain

Mutational studies have shown that the disintegrin domain is important in substrate recognition and assists in positioning the Tyr1605-Met1606 bond of VWF into the active-site cleft (Xiang *et al.*, 2011). This domain harbours an exosite involving residues Arg349 and Leu350 that interact with residue Asp1614 in the VWF A2 domain. Akiyama *et al.* determined two crystal structures of the DCTS (disintegrin, cysteine-rich, TSP1-1 and spacer)

domains and revealed folding similarities between the disintegrin-like domain and the N-terminal portion of the cysteine-rich domain (termed the C_A domain); see Figure 1.3; (Akiyama *et al.*, 2009a). The C_A domain has been found to have multiple interaction sites with the spacer domain.







Legend	
	Spacer domain, amino acids 556-680
	Cysteine-rich domain, amino acids 440-531
	Thrombospondin type 1 domain, amino acids 384-439
	Disintegrin domain, amino acids 306-383

Figure 1.3 Protein data bank crystal structure of the exosite-containing fragment of human ADAMTS13 (form 2) showing the spacer, the cysteine rich, thrombospondin type 1 and disintegrin domains; amino acid residues 286→680. Image from PDB 3GHN. (Akiyama *et al.*, 2009a).

1.2.2.4 The thrombospondin (TSP1-1) domain

The TSP1-1 domain (amino acids 384→439) contains six cysteine amino acid residues and has a stiff, rod-like structure containing stacked layers of tryptophan, arginine and hydrophobic residues which contribute to its rigidity (termed the CWR layered core); (Akiyama *et al.*, 2009a). The role of this domain is to position the VWF binding exosites with the other ADAMTS domains.

1.2.2.5 The cysteine-rich domain

The cysteine-rich domain (amino acid residues 439→555) contains 10 conserved cysteine residues and has a similar tertiary structure to the disintegrin-like domain, despite only sharing 17% homology in their amino acid sequence. The C-terminal is highly conserved in amino acid sequence with other members of the ADAMTS family which highlights its functional importance. It has been found that the exosites DCTS (disintegrin, cysteine-rich, TSP1-and spacer domain) are critical for the interaction between ADAMTS13 and the VWF A2 domain for the proteolysis of VWF and for substrate specificity (De Maeyer *et al.*, 2010; Gao *et al.*, 2008; de Groot *et al.*, 2015). The presence of a VWF-binding exosite (exosite 2) consisting of residues His476, Ser477, Gln478, Arg448, Phe494 and Met496 has been postulated to exist (Akiyama *et al.*, 2009a). ADAMTS13 variants that lack the cysteine-rich and/or spacer domains lack activity to the peptidyl substrate or cell-bound UL-VWF. If each of these non-catalytic domains is added to the metalloprotease domain, the cleavage of VWF substrate increases in a stepwise fashion. However, if the TSP1 2-8 and CUB domains are added, there is no increase in proteolytic activity. These domains collectively are thought to ensure that the scissile bond is brought into position over the active centre of the metalloprotease domain (Xiang *et al.*, 2011).

1.2.2.6 The spacer domain

The spacer domain comprises amino acid residues 555→680 of the mature protein. This domain contains a globular functional unit with a 10-stranded β -sandwich fold (Akiyama *et al.*, 2009a); see Figure 1.2. Several exosites in the spacer domain have been found to be highly conserved among other species, which indicate they may have an important functional or structural role. One of these areas, exosite 3, which is lacking in a murine model, may be important in proteolytic cleavage as the mouse model shows dramatically reduced antithrombotic activity (Xiao *et al.*, 2011). Deletion of certain residues within exosite 3 leads to the reduced cleavage of VWF substrate. The amino acid residues Arg659, Arg660 and Tyr661 and Tyr665 have been shown to be critical for cleavage and are responsible for much of the tight binding between ADAMTS13 and unravelled VWF (Jin *et al.*, 2012; Pos *et al.*, 2010).

A summary of the properties of ADAMTS13 exosite domains can be seen in Table 1.2

1.2.2.7 The thrombospondin (TSP1) repeats

The TSP1 repeats (2-8) after the spacer domain are variable in number and are not well conserved amongst ADAMTS proteases but this domain participates in substrate recognition and cell surface binding in all ADAMTS proteases to some degree. In ADAMTS13, the TSP1 repeats 2-8 (amino acid residues 685→1131) bind VWF through the D4 domain (see Figure 1.5) and all repeats contain the sequence WXXW, which is often modified by the attachment of an α -mannosyl group (Hofsteenge *et al.*, 2001). Seven of the eight repeats are also modified by the addition of the disaccharide Glc-Fuc-O-Ser/Thr but it is not clear what the role these post-translational modifications have *in vivo* (Hofsteenge *et al.*, 2001).

1.2.2.8 The CUB domains

The CUB domains (amino acid residues 1131→1427) are unique to ADAMTS13 and are not found in other ADAMTS and ADAM proteases (Apte, 2009). Their role is not yet fully understood. Human and murine ADAMTS13 variants which lack the TSP1 5-8 repeats and the CUB domains still cleave cell-bound UL-VWF under flow conditions (De Maeyer *et al.*, 2010; Jin *et al.*, 2009). The C-terminal domains (TSP1 2-8 and CUB domains) appear to be important with respect to binding to globular VWF (Feys *et al.*, 2009; Zanardelli *et al.*, 2009). This is estimated to be approximately 3% of total ADAMTS13 (Feys *et al.*, 2009). The binding of ADAMTS13 to globular VWF through the ADAMTS13 C-terminal domains and the VWF C4-CK domains has led to the discovery that a small proportion of ADAMTS13 circulates in the plasma in combination with VWF. The secondary structures of the ADAMTS13 domains mapped to amino acid sequence can be seen in Figure 1.4.

Table 1.2 Summary of exosite properties

Domain	Amino acid	Role
Disintegrin-like	306-383	Interaction of Arg 349 in ADAMTS13 and Asp1614 in VWF assists in positioning the scissile bond within the active site of ADAMTS13 enabling substrate recognition and proteolysis
Thrombospondin type 1 repeat	384-439	The stiff, rod like structure of this domain contributes to the stability of ADAMTS13 and aids in correct positioning of the scissile bond.
Cysteine rich	440-531	The disulphide bond reducing activity in this domain prevents lateral association and increased platelet adherence of VWF mutimers induced by high fluid stress (Zhou <i>et al.</i> , 2010)
Spacer	556-680	This domain interacts with the C-terminal part of VWF A2 domain which mediates much of the binding affinity between ADAMTS13 and VWF

260	270	280	290	300
SDGAAPRAGL	AWSPCSRRL	LILLSAGRAR	CVWDPPRPQP	GSAGHPPDAQ
310	320	330	340	350
PGLYYSANEQ	CRVAFGPKAV	ACTFAREHLD	MCQALSCHTD	PLDQSSCSRL
360	370	380	390	400
LVPLLDGTEC	GVEKWCSEKGR	CRSLVELTPI	AAVHGRWSSW	GPRSPCSRSC
410	420	430	440	450
GGGVVTRRRQ	CNNPRPAFGG	RACVGADLQA	EMCNTQACEK	TQLEFMSQQC
460	470	480	490	500
ARTDQPLRS	SPGGASFYHW	GAAVPHSQGD	ALCRHMCRAI	GESFIMKRGD
510	520	530	540	550
SFLDGTRCMP	SGPREDGTLS	LCVSGSCRTE	GCDGRMDSQQ	VWDRQCVCQG
560	570	580	590	600
DNSTCSPRKG	SFTAGRAREY	VTFLTVPNL	TSVYIANHRP	LFTHLAVRIG
610	620	630	640	650
GRYVVAGKMS	ISPNTTYPSTL	LEDGRVEYRV	ALTEDRLPRL	EEIRIWGPLQ
660	670	680	690	700
EDADIQVYRR	YGEEYGNLTR	PDITFTYFQF	KPRQAWVWAA	VRGPCSVSCG
710	720	730	740	750
AGLRWVNYSC	LDQARKELVE	TVQCQGSQQP	PAWPEACVLE	PCPPYWAVGD

Figure 1.4 Secondary structures of ADAMTS13 domains mapped to the amino acid sequence domain: amino acids 286→382; TSP1-1 383→439, Cysteine-rich 439→555, spacer 555→680. Key: Helix, β -pleated sheet, turn

1.2.3 Post-translational modifications

Plasma ADAMTS13 is highly glycosylated, with putative N-linked glycosylation and O-fucosylation sites identified. O-fucosylation is thought to mediate the efficient secretion of ADAMTS13 (Ricketts *et al.*, 2007). It occurs on serine or

threonine residues within the consensus sequence C1-X(2)-S/T-C2-G which occurs in the TSP1-1 repeat domains (where C1 and C2 are the first and second cysteine residue of the repeat). ADAMTS13 has seven predicted fucosylation sites; one in each TSP1 domain with the exception of TSP1-4 (Zheng *et al.*, 2001). The N-glycosylation of residues may also facilitate secretion (Akiyama *et al.*, 2009b; Jia *et al.*, 2009; Liu *et al.*, 2005; Zheng *et al.*, 2001). Ten potential N-glycosylation sites have been identified; two in the metalloprotease domain, one in the cysteine-rich, three in the spacer, one in the TSP1-2 and two in the CUB domains (Zheng *et al.*, 2001). Several potential C-mannosylation sites have also been identified (Sorvillo *et al.*, 2014) although the role of this glycosylation has not been elucidated.

1.2.4 ADAMTS13 biosynthesis and secretion

ADAMTS13 is primarily synthesized in the liver and is localized to the hepatic stellate cells (Uemura *et al.*, 2005). The full-length *ADAMTS13* mRNA is approximately 4.3kb (Zheng *et al.*, 2001) and protein expression in rat hepatic stellate cells is up-regulated upon mechanical pressure and inflammatory cytokines such as transforming growth factor β (TGF- β). It has been suggested therefore that ADAMTS13 may have a role in tissue remodelling after injury (Niiya *et al.*, 2006). *ADAMTS13* mRNA and protein have also been detected in vascular endothelial cells *in vitro* and *in vivo* (Shang *et al.*, 2006; Zheng, 2015). The function of ADAMTS13 secreted from endothelial cells is not known but the large surface coverage of endothelium in the body could potentially contribute a substantial quantity of the protease. ADAMTS13 released from endothelial cells could arguably cleave newly formed ULVWF strings on the cell surface.

1.3 ADAMTS13 – VWF interactions

ADAMTS13 regulates VWF proteolysis by the cleavage of a single Tyr-1605-Met-1606 scissile bond within the A2 domain of VWF and hence reduces thrombus formation. As a specific inhibitor of ADAMTS13 has not been identified, this process is in a sense unregulated. However, its activity is largely

controlled by the substrate, i.e. by the conformational change of VWF under shear stress which unveils the scissile bond, multiple platelet binding sites and other specific exosites for binding (Sadler, 1998). When the globular form of VWF unravels it reveals its A1 platelet-binding sites and at the same time the cryptic ADAMTS13 binding sites, allowing cleavage at the scissile bond (Zhang *et al.*, 2009); see Figure 1.5.

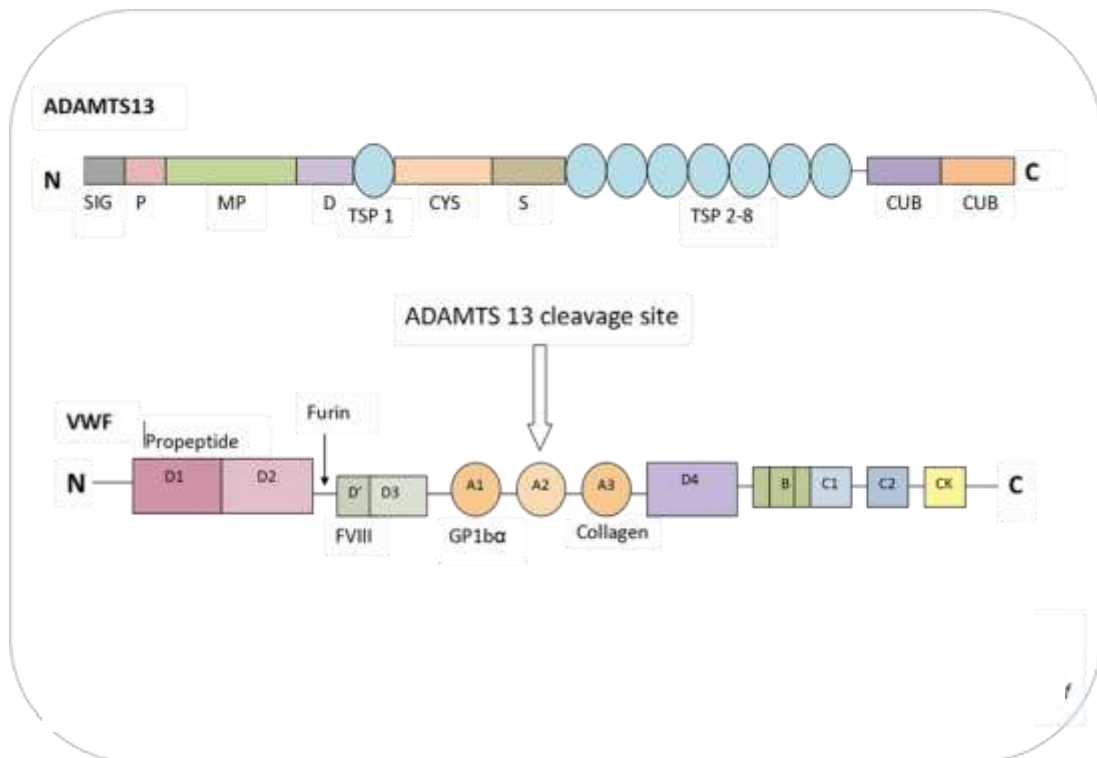


Figure 1.5 ADAMTS13-VWF interactions. ADAMTS13 contains a signal peptide(SIG), a propeptide (P), a metalloprotease domain (MP), a disintegrin-like domain (D), a TSP motif (TSP 1), a cysteine-rich domain (CYS), a spacer domain (S), seven TSP repeats (TSP 2-8) and 2 CUB domains. ADAMTS13 cleaves vWF at a scissile bond in the A2 domain of vWF. The A1 domain binds GP1b α receptors on the platelet surface and the A3 collagen binding site adheres to the subendothelial matrix,

A model of the interactions between VWF and ADAMTS13 has been proposed by Crawley and co-workers (2011) and defines a 7-step process of precise exosite binding between ADAMTS13 and VWF, which can be visualised like a 'molecular zipper'. This allows the accurate delivery of the active site of ADAMTS13 to the scissile bond within the A2 domain of VWF (Crawley *et al.*, 2011); (see Figure 1.6).

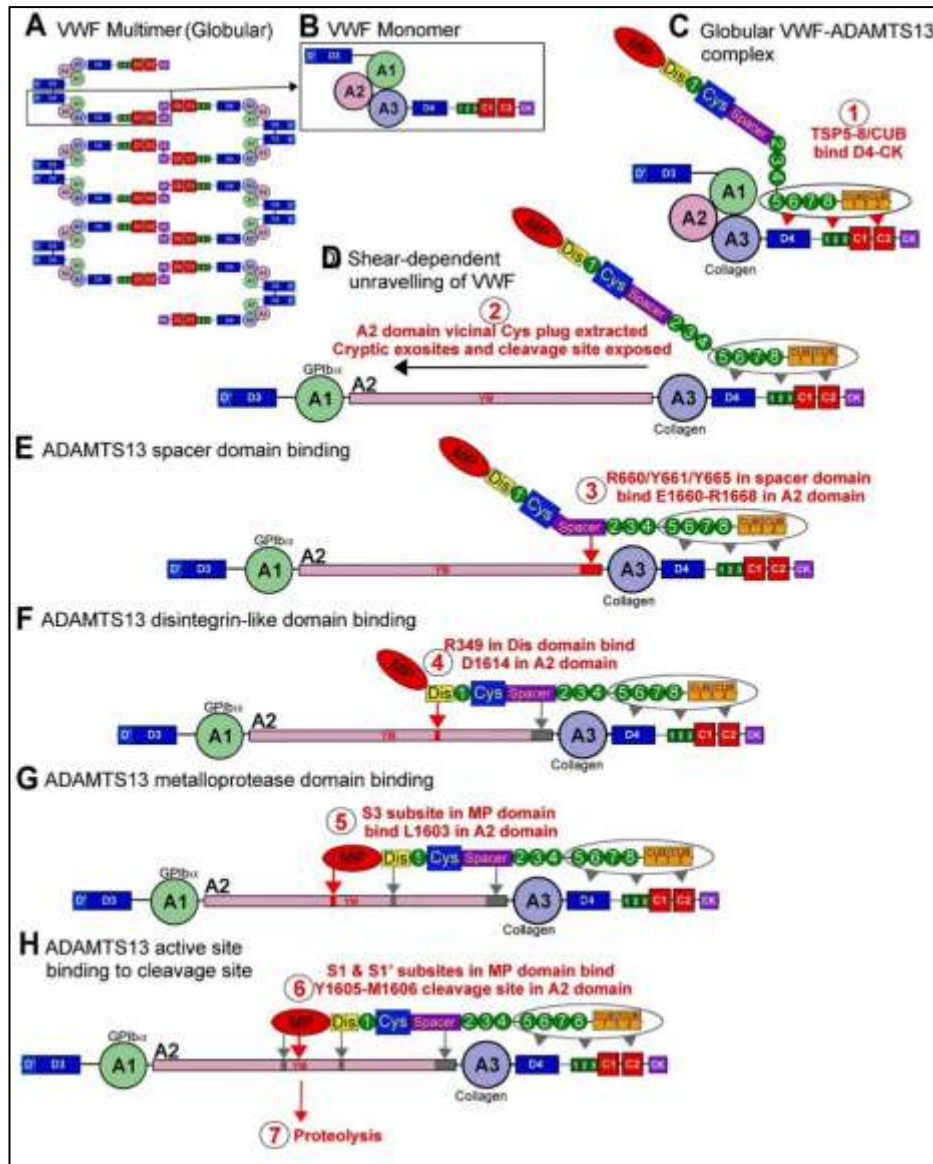


Figure 1.6 Seven-step model of ADAMTS13-VWF exosite binding as proposed by Crawley & Lane (from Crawley *et al.*, 2011) Reproduced with permission © American Society Hematology.)

From Figure 1.6 (A) it can be seen that VWF exists in the circulation in globular form, some of which is reversibly bound to ADAMTS13 through the ADAMTS13 TSP1 5-8 and the VWF D4-CK domains (step 1). On binding to collagen through the A3 domain, VWF unfurls under shear stress in the microvasculature revealing cryptic exosite binding sites and cleavage sites in the VWF A2 domain (step 2). Through the extraction of the vicinal cysteine plug from the hydrophobic core of the VWF A2 domain, the ADAMT13 spacer domain recognises the residues Glu1660-Arg1668 of the A2 VWF domain. Interaction between these sites lead to tight binding (step 3). The interaction

between the ADAMTS13 exosite residues Arg349/Leu350 in the disintegrin-like domain then forms a low-affinity interaction with Asp1614 in VWF (step 4) allowing the essential binding between Leu1603 and the complementary S3 subsite in the ADAMTS13 metalloprotease domain (residues Leu198, Leu232 and Leu 274); (step 5). Collectively, these interactions position the Tyr1605-Met1606 scissile bond over the ADAMTS13 active site (step 6) allowing further interactions between subsites in this area, leading to the proteolysis of VWF (step 7) (Crawley *et al.*, 2011). Cleavage of the scissile bond reduces the affinity between ADAMTS13 and VWF, allowing recycling of ADAMTS13.

1.3.1 Sites of VWF proteolysis by ADAMTS13

It has been suggested that there are three sites where VWF proteolysis occurs: at the site of vessel damage, in free circulation and at the endothelial surface (Crawley & Scully, 2013).

1.3.1.1 Site of vessel damage

At the site of vessel damage the unravelling of VWF not only exposes the platelet-binding sites, which enable it to perform its critical role in primary haemostasis, but also exposes the ADAMTS13 cleavage site, which allows proteolysis. Hence there is a balance between pro- and anti-platelet-binding functions. The binding of platelet GPIIb α to VWF occurs rapidly at a rate that exceeds VWF proteolysis (Kim *et al.*, 2010). At the site of vessel damage, collagen and thrombin are activators of activated platelets that promote more adhesion and aggregation, leading to formation of the haemostatic plug. At this point the platelets become resistant to the consequences of VWF proteolysis but as the plug extends further, exposure to collagen and thrombin is lessened and ADAMTS13 is able to cleave VWF and limit platelet plug formation to the site of vessel damage (Shida *et al.*, 2008).

1.3.1.2 Free circulation

The microvasculature is a high shear environment, as are vessels that are stenosed. Typical shear rates in small arteries are in the range of 1,000s⁻¹ (Schneider *et al.*, 2007). Some ULVWF is released into the circulation but

exists in globular form with platelet-binding sites hidden. In high shear environments these multimers uncoil, which could lead to unwanted platelet binding but unravelling also exposes the ADAMTS13 proteolytic site. Larger VWF multimers are thus processed into sizes that are less susceptible to uncoiling by shear force unless bound to collagen.

1.3.1.3 Endothelial surface

VWF released from the endothelia can be in the hyper-reactive ULVWF form which must be processed. If unprocessed, this could lead to the development of microthrombi. It has been found that the Weibel-Palade bodies containing VWF fuse with the plasma membrane of the endothelial cell to release the multimeric VWF. The VWF unravels as it is released through this aperture in the plasma membrane and is transiently tethered to the endothelial surface. The shear forces in the circulation unravel the VWF and allow it to conform to a string-like conformation, allowing processing of the multimers by ADAMTS13. The multimers that are released then adopt a globular form in the free circulation (Crawley & Scully, 2013). Another level of control exhibited by ADAMTS13 may be due to its apparent localization at the endothelial surface, thereby enabling the cleavage of ULVWF multimers at the site of release from the Weibel-Palade bodies (Vomund & Majerus, 2009). It has been found that there is an increased proteolysis of VWF by endothelial-bound ADAMTS13 compared to ADAMTS13 in solution and the thrombospondin (TSP1) repeats are necessary for this endothelial localization. It has been postulated that the glycoprotein CD36 is responsible for this binding (Davis *et al.*, 2009). Due to this localization, which would more likely occur during an acute phase as VWF is an acute phase protein, the apparent concentration of ADAMTS13 in the circulation would drop. This has been seen clinically (Rossi *et al.*, 2001). Decreased levels of plasma ADAMTS13 have been seen in patients post-surgery, in those with acute inflammatory illnesses and in pregnant patients in the second and third trimesters. Interestingly, in patients with congenital TTP, infusions of fresh frozen plasma are given every 2-3 weeks, allowing prolonged protection from thromboses by the reserve store of endothelial-bound ADAMTS13.

1.4 Pathologies of the ADAMTS13-VWF axis

Several pathologies have been associated with the imbalance of VWF size caused by the dysfunction of ADAMTS13-mediated regulation. The hallmark of Type 2A von Willebrand's disease is the absence of high molecular weight VWF multimers which is brought about by two broad mechanisms. Firstly, mutations in the A2 domain of VWF lead to destabilisation and unfolding of the protein in the circulation, leading to excessive proteolysis by ADAMTS13 (i.e. extracellular processing by ADAMTS13); (see section 1.1.3). This reduces platelet binding and as a result leads to excessive bleeding (Xu & Springer, 2013). The second mechanism is due to intracellular processing of VWF, leading to qualitative abnormalities in VWF.

Reduced levels of ADAMTS13 or reduced function may be due to the presence of autoantibodies to ADAMTS13, leading to unwanted platelet tethering, excessive platelet aggregation and disseminated microvascular VWF with platelet-rich thrombus formation. This results in thrombotic thrombocytopenic purpura.

1.4.1 Thrombotic thrombocytopenic purpura (TTP)

1.4.1.1 Incidence

TTP is rare, with a reported incidence of ~6 cases per million per year (Scully *et al.*, 2008). Two main subgroups of TTP have been identified: acute idiopathic or acquired TTP and congenital TTP (cTTP or Upshaw-Schulman syndrome). The latter occurs more rarely, with approximately 100 patients described worldwide (Scully *et al.*, 2012). TTP may present at any age, from neonate to adult, but the mean age of acute presentation is 20-30 years of age. Approximately 7% present as neonates/in childhood (<18 years old); (Moatti-Cohen *et al.*, 2012). The disease affects more women with a ratio of 1:2 male to female, which also applies to autoimmune disorders in general.

1.4.1.2 Pathophysiology of TTP

As described previously, where control breaks down in ADAMTS13 deficiency, the decreased VWF proteolysis results in platelet-rich thrombus formation,

which breaks off as microthrombi into the microcirculation (Levy *et al.*, 2001). These result in the fragmentation of erythrocytes, leading to microangiopathic haemolytic anaemia (MAHA), and often embolise to distal sites causing end-organ damage. The consumption of platelets also leads to thrombocytopenia. These processes define the characteristics of TTP.

1.4.1.3 Signs and symptoms of TTP

Although TTP was originally defined as a pentad of symptoms, patients do not frequently present with all five. Approximately 65% present with neurological symptoms such as confusion, headache, dysarthria or visual problems and 42% presented with cardiac involvement such as chest pain, heart failure and hypotension (Scully *et al.*, 2008). However, all patients present with thrombocytopenia (platelet count $10-30 \times 10^9/L$);(Scully *et al.*, 2012). This is due to the sequestration of platelets in microvascular thrombi. Low haemoglobin levels (80-100g/L), the presence of schistocytes on blood film and elevated lactate dehydrogenase are evidence of MAHA, which is pathognomonic. A raised reticulocyte count and low haptoglobin levels as a result of MAHA is also seen. The direct Coombs test is negative (Scully *et al.*, 2012).

1.4.1.3 Acquired TTP

Deficiency in idiopathic or acquired TTP is usually due to the presence of autoantibodies (usually IgG and, less frequently, IgA or IgM) directed against ADAMTS13, which reduce its activity/availability (Furlan *et al.*, 1997; Scheiflinger *et al.*, 2003). This is the more common form of TTP, affecting 95% of cases and has not been associated with any particular precipitant (Scully *et al.*, 2008). Several studies have found that the autoantibodies are directed towards epitopes in the cysteine-rich/spacer domains, particularly the residues Pro660, Tyr661 and Tyr665 (Klaus *et al.*, 2004; Pos *et al.*, 2010). These domains are important in mediating tight binding between ADAMTS13 and VWF. Autoantibodies to the C-terminal domain of ADAMTS13 (TSP2-8 and CUB domains) have also been identified but are thought not to have inhibitory effects by comparison (Zheng, 2010). Antibodies may inhibit

ADAMTS13 itself (Peyvandi *et al.*, 2004; Tsai & Lian, 1998) or promote enhanced clearance of the protein (Scheifflinger *et al.*, 2003). Approximately 15% of cases have been associated with certain drugs such as quinine, simvastatin, trimethoprim and PEGylated interferon (Scully *et al.*, 2012). Acquired TTP may also develop secondary to other diseases such as HIV, infection or transplantation.

1.4.1.4 Inherited (congenital) TTP

The main pathophysiological mechanisms of congenital TTP are defects in ADAMTS13 secretion and/or catalytic activity due to one or more mutations in the ADAMTS13 gene. It is inherited as an autosomal recessive disease (Levy *et al.*, 2001) and is also known as Upshaw-Schülman syndrome (USS); (OMIM accession number 274150). Diagnosis of the subtypes is now characterised by ADAMTS13 activity being less than 5% of normal and the presence of autoantibodies and/or inhibitors (Scully *et al.*, 2011).

To date, there have been over 100 mutations reported throughout the *ADAMTS13* gene (Lotta *et al.*, 2010) including missense, insertions, deletions and splice site mutations. Approximately 60% are missense mutations and localize primarily in the 5' half of the gene, towards the N-terminal end of the protein. Variations in ADAMTS13 activity or secretion have been documented and reviewed (Lotta *et al.*, 2010). This diversity goes some way to explaining the clinical variability seen in congenital TTP. Some patients present in the neonatal period; others present in childhood or as adults whereas others may present only after a physiologically challenging event such as pregnancy or sepsis, despite having persistently low levels of ADAMTS13. After diagnosis of TTP some patients require frequent treatment whereas others may require treatment only after an infection (Camilleri *et al.*, 2012; Donadelli *et al.*, 2006). The clinical severity of disease episodes is also variable, with some patients presenting with asymptomatic thrombocytopenia and anaemia, through to multi-organ failure. Adult-onset disease may prove fatal or patients may develop a relapsing disease (Tao *et al.*, 2006, Palla *et al.*, 2009).

A recent study has linked the genotype to the amount of residual ADAMTS13 activity and the clinical features of the disease, but individual exceptions have been found with relatively high residual activity having early disease episodes or frequent recurrences (Lotta *et al.*, 2012). Most patients with TTP are compound heterozygotes although homozygotes have been reported, particularly in consanguineous families (Palla *et al.*, 2009). Usually, to cause severe ADAMTS13 deficiency (<5% activity) both alleles must be affected. Heterozygous carriers of an *ADAMTS13* mutation are usually asymptomatic and free of TTP-like symptoms. The majority of mutations that have been analysed cause a severe deficiency due to aberrant folding of the protease, leading to intracellular retention. However, less severe phenotypes have also been associated with only one heterozygous mutation (Camilleri *et al.*, 2008; Donadelli *et al.*, 2006) which could be explained by the presence of a combination of single nucleotide polymorphisms (SNPs) contributing to the phenotype (Camilleri *et al.*, 2012; Lotta *et al.*, 2010; Plaimauer *et al.*, 2006). SNPs may be defined and differentiated from mutations by being genetic variants with an allele frequency of greater than 1% in the population and are present in the germline (Tseng & Kimchi-Safarty, 2011). These SNPs, in the presence or absence of mutations, could contribute to gain-of-function or loss-of-function phenotypes (Camilleri *et al.*, 2012; Plaimauer *et al.*, 2006).

1.4.1.5 Treatment of TTP

TTP is an acute, life-threatening illness that requires prompt and effective treatment. The standard treatment is daily plasma exchange therapy which has led to a reduction in mortality from ~ 90% to between 10 and 20% (Scully *et al.*, 2008). This removes circulating anti-ADAMTS13 antibodies in the acquired form of TTP and replaces ADAMTS13 in the inherited form. The number of exchanges required is patient-specific but is generally more frequent in antibody-mediated TTP due to the continual synthesis of auto-antibodies. Treatment is continued until two days after normalization of platelet count. As low levels of ADAMTS13 are needed to normalize ULVWF size in the plasma, treatment for the inherited form is typically every 3-4 weeks (Scully *et al.*, 2008).

1.5 Single nucleotide polymorphisms

Variation in the human genome can be brought about by single nucleotide polymorphisms and copy number variation. SNPs are associated with obvious phenotype variations such as blood group and eye colour and with less obvious factors such as responses to drugs and susceptibility to disease. With the full sequencing and mapping of the human genome, linking the effects of these SNPs to functional outcomes has become a major focus in structural bioinformatics.

There are an estimated 150,482,730 common non synonymous SNPs in the human population (NCBI dbSNP Human Build 146), with each person expected to be heterozygous for 24,000-40,000 of these variants (Ng & Henikoff, 2006). SNPs in the human population are observed less frequently than expected from the overall mutation rate. It could be argued that this is evidence that they are under selection pressures. If a random mutation occurs in a coding region it should lead to an amino acid change approximately 2/3 of the time (in consideration of the degeneracy of the genetic code) but non synonymous SNPs lead to only half of the observed coding SNPs in the human genome. Also, non-conservative amino acid substitutions (i.e. substitution of amino acid with one of different physio-chemical properties) occur at approximately half the rate of conservative amino acid substitutions (one of similar properties), indicating they are under selection pressures. Non-synonymous SNPs therefore may play a role in human health by altering protein expression and function (Ng & Henikoff, 2006). Thirty five non-synonymous SNPs have been identified in the coding region of the ADAMTS13 gene (from SNPedia<<http://www.snpedia.com/index.php/ADAMTS13>> [accessed 13/9/2017]); (see Table 1.3).

Table 1.3 SNP reference numbers (from SNPedia)

	dbSNP reference
1	rs786205078
2	rs786205077
3	rs739469
4	rs4962153
5	rs41314453
6	rs387906346
7	rs387906345
8	rs387906344
9	rs387906343
10	rs387906342
11	rs387906341
12	rs36222275
13	rs3118667
14	rs28647808
15	rs281875305
16	rs2301612
17	rs2285489
18	rs148312697
19	rs142572218
20	rs121908478
21	rs121908477
22	rs121908476
23	rs121908475
24	rs121908474
25	rs121908473
26	rs121908472
27	rs121908471
28	rs121908470
29	rs121908469
30	rs121908468
31	rs121908467
32	rs121908467
33	rs11575933
34	rs1060499780
35	rs105720680

The effect of SNPs has been further analysed (Kokame *et al.*, 2002). Two Japanese families with USS (with neonatal onset and frequent relapse) were analysed and the resultant mutations/SNPs expressed *in vitro* using HeLa cells. The mutations R268P (G803C), Q449stop, C508Y and the SNP P475S were expressed and it was found the two former mutations caused non-secretion whereas the other mutation and SNP showed normal secretion but minimal activity. On analysing the ADAMTS13 gene of 304 normal, healthy

controls, approximately 10% carried the p.P475S SNP. Activity in the control group showed wide variation, with ranges between 60-150% that of pooled normal plasma. It was postulated that the mutation leading to decreased secretion would affect protein folding or stability. Other synonymous changes were found whereupon the same amino acid would be found in the protein, which were T420C, C546T, G1716A, C2280T and C4421A. These synonymous changes would not alter amino acid sequence but could possibly affect expression level through gene transcription or RNA processing (Edwards *et al.*, 2012).

1.6 TTP Animal models

1.6.1 Murine models

The use of animal models has been used to further understand the pathophysiology of congenital TTP. Two groups have generated *Adamts13*-knockout mice. Motto *et al.* disrupted the *ADAMTS13* gene by replacing exons 1-6. This resulted in a complete loss of activity but none of the *Adamts13*-/- knockout mice showed evidence of TTP such as thrombocytopenia, schistocytosis or evidence of VWF-rich thrombi (Motto *et al.*, 2005). Banno *et al.* also created *ADAMTS13*-deficient mice by eliminating exons 3-6 in the *ADAMTS13* gene (Banno *et al.*, 2006). There were no differences between the knockout mice and *Adamts13*+/+ in response; both strains produced viable offspring exhibiting normal development and survival. Motto *et al.* then backcrossed this pedigree with *Adamts13*-/- mice. This resulted in *ADAMTS13*-deficient mice that exhibited lower average platelet counts and decreased survival rates and showed a clear thrombotic phenotype such as increased longevity of VWF strings and an increase in VWF-mediated platelet-endothelial interactions. These mice also exhibited a proinflammatory state (as observed by increased leukocyte rolling and adhesion in stimulated venules and enhanced extravasation of neutrophils). This suggests *ADAMTS13* has antithrombotic and anti-inflammatory effects.

Considering that lack of *ADAMTS13* does not induce TTP in knockout mice, it has been suggested that a second hit is necessary. Two 'second hits' have

been shown to successfully induce TTP-like symptoms in murine models. The first is a shiga toxin (this is mainly produced by *Shigella dysenteriae* and certain strains of *Escherichia coli*). It has been shown that the pentameric B subunits of the shiga toxin are sufficient to induce UL-VWF secretion from endothelial cells via the GbIII receptor present in lipid rafts. The administration of shiga toxin in *Adamts13*^{-/-} mice gave rise to symptoms closely resembling human TTP. CASA/Rk mice (deficient in both VWF and ADAMTS13) were not susceptible to shiga toxin. There was no correlation found between elevated VWF plasma levels and mortality or thrombocytopenia. Other genetic and/or environmental factors may be involved which determine the response of these mice to shiga toxin, protecting them from the more severe phenotype.

1.6.2 Baboon model

Feys *et al.* used the baboon (*Papio ursinus*) to model congenital TTP. A series of monoclonal antibodies (mAb) was generated and one was identified *in vitro* which fully inhibited human ADAMTS13. This inhibitory mAb was administered to healthy baboons and it was found that the activity of ADAMTS13 fell below the detectable limit of <5%. This effect was not observed in knockout mice. The inhibition of ADAMTS13 immediately provoked TTP symptoms in all test animals resulting in severe thrombocytopenia and haemolytic anaemia, reflecting early-stage TTP. It was observed that endothelial activation with concomitant VWF release were major contributions to TTP. However, early-stage symptoms only were observed, suggesting an additional trigger would be necessary to provoke the end-stage symptoms seen in humans (Feys *et al.*, 2010).

1.7 Additional factors and triggers of TTP

1.7.1 Inhibition

ADAMTS13 has been found to be susceptible to proteolytic degradation by plasmin and thrombin (Crawley *et al.*, 2005). It is also susceptible to inhibition by free haemoglobin (Klaus *et al.*, 2004) and interleukin-6 (Bernardo *et al.*, 2004). These other factors may contribute to the TTP phenotype.

1.7.2 Pregnancy

Pregnancy has been found to be a trigger for congenital TTP and has been reported to represent 5-10% of all adult TTP cases (George *et al.*, 2008; Moatti-Cohen *et al.*, 2012; Scully *et al.*, 2008). This is discussed further in Chapter 4.

1.7.3 Infection

Acute infection has been associated with a TTP trigger in patients with low residual ADAMTS activity due to the presence of autoantibodies. In a French cohort of patients, 41% of acute episodes of TTP were associated with infection, particularly in patients with polymorphisms in the toll-like receptor 9 (TLR 9), which may be associated with acquired TTP (Morgand *et al.*, 2014). It has been suggested that infectious diseases may trigger episodes of TTP through the release of polymorphonuclear components such as circulating DNA and histone fragments (Fuchs *et al.*, 2013). This may also explain the development of TTP in mice after endothelial activation with shiga toxin (Motto *et al.*, 2005).

1.7.4 The role of complement in endothelial activation

There may also be a significant role of complement, which is part of the innate immune response, in the development of microvascular thromboses seen in TTP. In a recent review it was argued that complement activation is a common effector leading to endothelial injury and microvascular thrombosis in TTP, atypical HUS (aHUS) and Stx-producing *Escherichia coli*- associated HUS (Noris *et al.*, 2012). In a recent study (Ruiz-Torres, 2005), two out of four patients with congenital TTP showed lower serum levels of C3 in the acute phase of the disease compared with healthy controls, indicating complement consumption.

Noris *et al.* researched a case series whereby 15 patients with familial microangiopathy were assessed for serum levels of C3. It was found that 11 patients had reduced levels, irrespective of a diagnosis of TTP or HUS, indicating C3 consumption through the activation of complement (Noris *et al.*, 1999). In a separate *ex vivo* study, sera from patients with acute TTP induced

more C3 and C5b-9 deposits on microvascular endothelial cells compared with sera from healthy controls. There was no observed difference in C4 deposits, indicating that the alternative pathway was activated. Pre-incubation with sera from patients with TTP showed upregulation of the expression of P selectin on human microvascular cells, resulting in a prothrombotic effect.

In another study by Ruiz-Torres *et al.* it was found that sera from patients with TTP also had a marked effect on neutrophils by increasing the oxidative burst and degranulation, increasing the cytotoxic effects towards endothelial cells. Furthermore, the effects of TTP sera on the endothelium and neutrophils were abrogated by a blockade in complement. The researchers concluded there is a role of complement in microvascular thrombosis of TTP. (Ruiz-Torres *et al.*, 2005).

Further research groups have measured complement activation in 13 patients with acute acquired TTP (Reti *et al.*, 2012). It was found that levels of C3a and C5b-9 correlated with disease activity and these markers decreased with plasma exchange and normalised in remission. A decrease in complement C3 levels indicative of consumption was seen in 15% of patients. There was no significant difference in the classical or lectin pathway activation markers, further indicating activation of the alternative pathway (Reti *et al.*, 2012). Endothelial deposition of C3d, C4d and C5b-9 has also been observed on skin biopsy in a patient with severe acquired TTP, indicating complement activation (Tsai *et al.*, 2013).

With respect to the mechanism of complement activation in TTP, Polley *et al.* have postulated that endothelial damage and platelet thrombi initiate the coagulation and fibrinolytic pathways which may amplify complement activation through the direct cleavage of C3 and C5 by thrombin or other activated proteases (Polley & Nachman, 1978). Interestingly, it has been documented that a patient with acquired TTP did not respond to the usual established treatment but did respond to the anti-C5 humanized monoclonal antibody eculizumab which is further evidence of complement activity in TTP (Tsai *et al.*, 2013).

1.8 The role of ADAMTS13 in stroke and myocardial infarction

An association between low ADAMTS13 plasma levels and the risk of myocardial infarction (MI) has been found (Crawley *et al.*, 2008). Low levels of ADAMTS13 have also been observed in severe sepsis, disseminated intravascular coagulation (DIC) and complicated malarial infection (Schwameis *et al.*, 2015). De Vries *et al.* recently carried out a large population-based cohort study (the Rotterdam Study) which looked at the contribution of genetic variation to ADAMTS13 with a hypothesis-free genome wide association study (GWA); (De Vries *et al.*, 2015). This study was undertaken to investigate the association between ADAMTS13 levels and MI. ADAMTS13 activity was measured in more than 6,000 individuals and SNPs for common and rare genetic variants genotyped. After analysis, the SNP p.A732V was the strongest determinant of ADAMTS13 activity and was associated with a decrease of more than 20%. An independent association was found with a common variant in the *SUPT3H* gene outside the *ADAMTS13* locus and five other genetic variants including p.R1060W. The gene *SUPT3H* codes for the transcription initiation protein SPT3. The p.R1060W mutation was found with a frequency of 0.06% in this population and was associated with a decrease of 47.6% in plasma activity. The more common insertion mutation 4143insA, found predominantly in north and central Europe, was not found in this population. This may be due to rare genetic variants showing greater geographic clustering than common variants (Miyata, 2015). The allele frequency of the p.R1060W variant was established as 0.06%, indicating a significant number of individuals carry this variant and may have a greater risk for TTP or an increased risk of MI or stroke. This information could aid in the risk profiling of patients (De Vries *et al.*, 2015).

Aims

To analyse the effect of SNPs within the *ADAMTS13* gene, singly and in combination with mutations, on the expression of ADAMTS13 *in vitro* and relate these findings to clinical phenotype

Objectives

The objectives of this study were:

- to create expression vectors containing *ADAMTS13* mutations and/or SNPs that have been found clinically and to express the resultant ADAMTS13 on western blot and semi-quantify the level of ADAMTS13 secretion by densitometry.
- To compare the level of expression of ADAMTS13 *in vitro* with previous published findings and to relate experimental results to clinical phenotype.

Chapter 2

Materials and methods

2.1 Construction of *ADAMTS13* single nucleotide polymorphisms (SNPs), missense and deletion mutations

The sequence for human *ADAMTS13* cDNA was obtained from EMBL-EBI (www.ebi.ac.uk, gene ENSG 00000160323, CCDS 6970.1, accessed 21.11.13). The genotypes of 17 congenital TTP patients referred to the UK TTP Registry at UCL have been previously elucidated (Camilleri *et al.*, 2012). In order to locate mutagenic primer sites, the nucleotide substitutions and one deletion identified in the genotype of patients (see Table 2.1) were mapped onto the *ADAMTS13* cDNA sequence. Some patients carried more than one mutation (see Table 2.1).

Table 2.1 Mutations and single nucleotide polymorphisms inserted into *ADAMTS13* cDNA vector plasmid pcDNA3.1(+) (Invitrogen) with WT *ADAMTS13* cDNA insert (from Camilleri *et al.*, 2012)

Nucleotide change (mutation)	Amino acid change
G305A	R102H
C587T	T196I
C649C	D217H
719_724del	G241_C242del
G794C+A794T	R265S+S266C
G803C	R268P
C1192T	R398C
C1225T	R409W
G1308C	Q436H
G1368T	Q456H
C1787T	A596V
G2068A	A690T
T2260C	C754R
C2728T	R910X
G2930T	C977F
C3178T	R1060W
Nucleotide change (SNP)	Amino acid change
C19T	R7W
C1342G	Q448E
C1423T	P475S
C1852G	P618A
C2195T	A732V

C2699T	A900V
G3097A	A1033T

2.1.1 Mutagenesis primer design

Mutagenic oligonucleotide primers were designed individually according to the desired mutation/SNP. The required nucleotide change(s) were located in the centre of the primer and the number of nucleotides on both sides of the mutation/SNP in both forward and reverse primers was between 10-15 bases. The minimum GC content was 40% and the primers terminated in one or more C or G bases. The following formula was used to calculate the melting temperature (T_m) of the primers for substitution (missense) mutations (see Table 2.2):

$$T_m = 81.5 + 0.41(\%GC) - (675/N) - \% \text{ mismatch}$$

For deletion mutations, the following formula was used to calculate the T_m (see Table 2.2):

$$T_m = 81.5 + 0.41(\%GC) - (675/N)$$

where N = the primer length in bases and values for % GC and % mismatch (between the forward and reverse primers) were whole numbers.

The designed primers were checked and validated against the QuikChange T_m calculator at www.genomics.agilent.com.

Table 2.2 Parameters used to calculate T_m of mutagenic oligonucleotide primers

Mutation	Number of nucleotides	% GC	% mismatch	Calculated T_m	T_m (Agilent)
G305A	33	55	3	80.6	80.4
C587T	24	75	4	80.1	80.0
C649C	27	63	4	76.3	78.6
719_724del	20	95	n/a	81.7	81.7
G794C+A796T	26	85	7	83.3	80.9
G803C	23	74	4	78.5	78.1
C1192T	31	65	3	83.3	78.6
C1225T	31	61	3	81.7	78.8
G1308C	31	58	3	80.5	78.6
G1368T	25	76	4	81.6	80.0
C1787T	31	55	3	79.2	79.0
G2068A	27	74	3	83.8	78.1
T2260C	31	71	3	85.9	78.4

C2728T	25	68	4	78.3	78.4
G2930T	29	59	3	79.2	78.1
C3178T	23	83	4	78.4	81.6
C19T	25	68	4	78.3	78.3
SNP					
C1342G	29	59	3	79.2	78.8
C1423T	30	60	3	80.6	80.3
C1852G	29	62	3	80.6	78.9
C2195T	25	68	4	78.3	78.8
C2699T	25	68	4	78.3	78.3
G3097A	29	62	3	70.6	80.2

Primers were designed between 20 and 33 bases long with a T_m of >77 °C (see Table 2.3). The primers were manufactured and HPLC purified by Eurofins Genomics, Germany. Each primer was diluted as a stock solution with molecular grade water to a concentration of 625 ng/ μ l and stored at -80°C. The final working solution was diluted to 125 ng/ μ l and stored at -20 °C.

Table 2.3 Mutagenic oligonucleotide primers used to generate specific *ADAMTS13* mutations/SNPs

Mutation/SNP	Forward primer 5'-3'	Reverse primer 5'-3'
G305A	CAG GAG GAC ACA GAG CAC TAT GTG CTC ACC AAC	GTT GGT GAG CAC ATA GTG CTC TGT GTC CTC CTG
C587T	GGT GCG GGG CGT CAT CCA GCT GGG	CCC AGC TGG ATG ACG CCC CGC ACC
G649C	GGA CAC TGG CTT CA CCT GGG AGT CAC	GTG ACT CCC AGG TCG AAG CCA GTG TCC
G794C+A796T	TCG CCT GGT CCC CTT CCT GCC GCC GG	CCG GCG GCA GGA GGG GGA CCA GGC GA
G803C	CTG CAG CCG CC GCA GCT GCT GA	TCA GCA GCT GCG GGC GGC TGC AG
C1192T	CGA AGT CCT TGC TCC TGC TCC TGC GGA GGA G	CTC CTC CGC AGG AGC AAG AGC AAG GAC TTC G
C1225T	GTG GTC ACC AGG AGG TGG CAG TGC AAC AAC C	GGT TGT TGC ACT GCC ACC TCC TGG TGA CCA C
G1308C	GAT GTG CAA CAC TCA CGC CTG CGA GAA GAC C	GGT CTT CTC GCA GGC GTG AGT GTT GCA CAT C
G1368T	GAC CGA CGG CCA TCC GCT GCG CTC C	GGA GCG CAG CGG ATG GCC GTC GGT C
C1787T	TCT TCA CAC ACT TGG TGG TGA GGA TCG GAG G	CCT CCG ATC CTC ACC ACC AAG TGT GTG AAG A
G2068A	CTG GGT GTG GGC CAC TGT GCG TGG GCC	GGC CCA CGC ACA GTG GCC CAC ACC CAG
C2195T	AGC AGC CAC CAG TGT GGC CAG AGG C	GCC TCT GGC CAC ACT GGT GGC TGC T
T2260C	GGA GAC TTC GGC CCA CGC AGC GCC TCC TGT G	CAC AGG AGG CGC TGC GTG GGC CGA AGT CTC C
C2728T	CTC CTG CGG GCG TGG TCT GAT GGA G	CTC CAT CAG ACC ACG CCC GCA GGA G
G2930T	GAG GAT CCT GTA TTT TGC CCG GGC CCA TG	CAT GGG CCC GGG CAA AAT ACA GGA TCC TC
C3178T	CGG CGC TGG TGTGGC CCG AGG CC	GGC CTC GGG CCA CAC CAG CGC CG
C3484T	CCC TGG AGT GGT TCC AGG CCC GG	CCG GGC CTG GAA CCA CTC CAG GG
SNP		
C19T	CAG CGT CAC CCC TGG GCA AGA TGC C	GGC ATC TTG CCC AGG GGT GAC GCT G
C1342G	TGG AGT TCA TGT CGG AAC AGT GCG CCA GG	CCT GGC GCA CTG TTC CGA CAT GAA CTC CA
C1423T	CTG GGG TGC TGC TGT ATC ACA CAG CCA AGG	CCT TGG CTG TGT GAT ACA GCA GCA CCC CAG
C1852G	CTA ACA CCA CCT ACG CCT CCC TCC TGG AG	CTC CAG GAG GGA GGC GTA GGT GGT GTT AG
C2195T	AGC AGC CAC CAG TGT GGC CAG AGG C	GCC TCT GGC CAC ACT GGT GGC TGC T
C2699T	TGT GGA CCC CTG TGG CAG GGT CGT G	CAC GAC CCT GCC ACA GGG GTC CAC A
G3097A	GTG GCC TTG GCA CTA CTA GAC GCT CGG TG	CAC CGA GCG TCT AGT AGT GCC AAG GCC AC

Shaded nucleotide denotes substitution

The mutations/SNPs in Table 2.1 were introduced into the ADAMTS13 cDNA insert of the pcDNA3.1(+) vector (Invitrogen), using the QuikChange Lightning Site Directed Mutagenesis kit (Stratagene, Agilent Technologies, UK) according to the manufacturer's instructions.

2.1.2 The pcDNA3.1(+) vector

The pcDNA3.1(+) vector (Invitrogen) containing the 5' sequencing primer T7 and the ampicillin resistance gene was kindly donated by Dr James Crawley at Imperial College, London. A myc tag (comprised of 10 amino acids: N-EQKLISEEDL-C) had previously been ligated into the insert immediately before the stop codon sequence. The size of the plasmid to include the ADAMTS13 cDNA insert was approximately 5,500 base pairs (5458bp) and with ADAMTS13 insert is 9739 bp long. The vector pcDNA 3.0 (Invitrogen) with no insert acted as a negative control in transient transfection studies and was also approximately 5,500 base pairs in size (5,446bp).

2.2 Single-site directed mutagenesis (SDM)

2.2.1 Mutant strand synthesis reaction (polymerase chain reaction)

The size of the plasmid to include the ADAMTS13 cDNA insert was 9739 base pairs. In consideration of this relatively large double stranded (ds) DNA vector, the PCR conditions using the Techne Prime™ thermal cycler were optimised as follows: 1 cycle at 95 °C for 2 min to denature the DNA template initially; 95 °C for 20 s to denature the DNA template product; 60°C for 20 s to anneal the mutagenic primers to the template; and 68 °C for 8 min to extend the primers with *Pfu* DNA polymerase, (18 cycles) and 68 °C for 8 min (1 cycle) as a final extension step. To minimise the number of second site errors, a low concentration of ADAMTS13 DNA template (1 µL of 50 ng/µL solution, giving a final concentration of 1ng/µL) and low number of thermal cycles was used (18 cycles). An excess of oligonucleotide primers was used to increase mutagenesis efficiency (1 µL of 125 ng oligonucleotide primers forward and reverse); see Table 2.4.

Table 2.4 Preparation of sample reaction, single site SDM

PCR reaction component	Volume (μL)
10x reaction buffer	5
50ng dsDNA template	1
125 oligonucleotide primer 1	1
125 oligonucleotide primer 2	1
dNTP mix	1
QuikSolution reagent (Agilent Technologies, UK)	1.5
Molecular grade water	39.5

All other cycling parameters were as per the manufacturer's protocol.

2.2.2. Digestion of amplification products and transformation

The treatment of PCR products with *DpnI* restriction enzyme (Agilent Technologies, UK) to digest the parental methylated and hemi-methylated non-mutated plasmid DNA was optimised to 1 hour at 37 °C. In brief, 2 μL *DpnI* was added and thoroughly mixed with the amplification products and incubated at 37 °C for 1 hour. The digested products were then transformed into XL10-Gold ultracompetent *E.coli* cells for nick repair: 45 μL cells thawed on wet ice were added to a pre-chilled round bottomed polypropylene Falcon[®] BD tube (Fisher Scientific, UK) and 2 μL β -mercaptoethanol was added and swirled to mix. After 2 min incubation on wet ice, 2 μL *Dpn I* treated amplification product was added, gently mixed and further incubated on wet ice for 30 min. Following this step, the Falcon tube was heat pulsed in a water bath for 30 s at 42 °C and further incubated on wet ice for 2 min. A volume of 0.5 ml preheated (42 °C) NZY⁺ broth (see Appendix 1) was added and the tube incubated at 37 °C with shaking at 240 rpm for 1 hour.

The products of the transformation reaction were spread on Luria Bertani (LB) agar plates (see Appendix 1) containing 0.1mg/ml ampicillin at volumes of 50, 100, 150 and 200 μL . The plates were incubated at 37 °C for >16 hours and stored at 4 °C until further analysis. If no or a low number of colonies were found the volume of Quik solution (Agilent Technologies, UK) was increased to 2 μL , and/or 5 μL 5 % DMSO (Applichem, Germany) was added to the PCR mixture and the volume of water adjusted accordingly.

2.3 Multi-site directed mutagenesis (multi-SDM)

To introduce more than one SNP together with a mutation into the dsDNA plasmid, the QuikChange Multi site-directed mutagenesis kit was used (Agilent Technologies, UK). This was performed on mutations G649C and G305A to introduce three SNPs together with the mutation. The dsDNA template already containing the required mutation was used and up to three nucleotide changes, reflecting the patient genotype, were inserted. Initially, thermal cycling was performed to denature the mutant DNA template and the mutagenic primers of the SNPs were annealed to the template, with all primers binding to the same strand. The *PfuTurbo* polymerase then extended the primers, generating dsDNA molecules, with one strand containing multiple mutations together with nicks, which were then sealed by the enzyme blend. The parental blend was then digested with *Dpn I*, as per the single site SDM method described previously. To transform XL10-gold Ultracompetent cells (Agilent Technologies, UK), 45 μ l cells were gently thawed on wet ice and added to a pre-chilled round bottomed polypropylene Falcon[®] BD tube (Fisher Scientific, UK). As per the single SDM reaction, 2 μ l β -mercaptoethanol was added and the mixture swirled every 2 min for a total of 10 mins, after which 1.5 μ l *Dpn I* treated DNA from each mutagenesis reaction product was added to the ultracompetent cells. This was gently mixed and further incubated on wet ice for 30 min. Following this step, the Falcon tube was heat pulsed in a water bath for 30 s at 42 °C and further incubated on wet ice for 2 min. A volume of 0.5 ml preheated (42 °C) NZY⁺ broth (see Appendix 1) was added and the tube incubated at 37 °C with shaking at 240 rpm for 1 hour.

The products of the transformation reaction were spread on Luria Bertani (LB) agar plates (see Appendix 1) containing 0.1mg/ml ampicillin at volumes of 1 μ l, 10 μ l, and 100 μ l. The plates were incubated at 37 °C for >16 hours and stored at 4 °C until further analysis. The mutant, closed circle ssDNA was converted into dsDNA *in vivo*.

The primers used for single site SDM were used as per the multi-site method. In order to add primers in approximately equimolar amounts, the length between primers was established and, as there was less than 20% difference,

no adjustment in volume was made (see Table 2.5). The primers were diluted to a concentration of 100 ng/μl from the working solution of 125 ng/μl.

Table 2.5 SDM primer length used in multi-site SDM

Mutations incorporated within dsDNA template	SNP primer	Primer length (nucleotides)
G305A	C1342G (p.Q448E)	29
	C1852G (p.P618A)	29
	C2699T (p.A900V)	25
G649C	C19T (p.R7W)	25
	G3097T (p.A1033T)	29
	C1342G (p.Q448E)	29

2.3.1 Control reaction for multi-SDM

A control reaction was first performed to test the efficiency of simultaneous SDM at three independent sites. The principle of this control method was based on the production of β-galactosidase, encoded by the *LacZ* gene, resulting in blue colonies on media containing X-gal in the presence of the inducer IPTG (see Appendix 1). The template encoded the first 146 amino acids of β-galactosidase and contained stop codons at three positions in the *LacZ* coding sequence. These modifications prevented the production of β-galactosidase and resulted in the appearance of white colonies on X-gal media. The control primers converted the individual stop codons to wild type in the *LacZ* gene. All three reversion events were required to produce blue β gal⁺ colonies. Each plate was scored for the triple mutant plasmid (blue vs white colonies).

The control reaction was prepared and components added in the order shown in Table 2.6.

Table 2.6 Preparation of sample reaction multi-site SDM

Reaction component	Volume (μl)
10X reaction buffer	2.5
Molecular grade water	18.5
Quik solution	-
dsDNA template (50ng)	1
Mutagenic primers (100 ng per primer)	1
dNTP mix	1
QuikChange Multi enzyme blend	1

The cycling parameters seen in Table 2.7 were used:

Table 2.7 Cycling parameters for multi-site SDM PCR

Stage	Number of cycles	Temperature	Time (min)
1	1	95 °C	1
2	30	95 °C	1
		55 °C	1
		65 °C	17
3	1	65 °C	8

For *Dpn I* digestion of the amplification products, 1 µl restriction enzyme was added, mixed thoroughly and incubated at 37 °C for 1 hour. For the transformation, 45 µl slowly thawed XL10-Gold ultracompetent cells were aliquoted into 14 ml Falcon® round-bottomed polypropylene tubes. β-mercaptoethanol (2 µl) was added, gently mixed and incubated on ice for 10 min, swirling gently every 2 min. *Dpn I* treated DNA (1.5 µl) from the control reaction was then added to the cells, swirled and incubated on wet ice for 30 min. The heat pulse and incubation steps were carried out as per the single site SDM protocol. A volume of 10 µl of the control transformation reaction was plated onto LB-ampicillin agar plates that were prepared with 80 µg/ml X-gal and 20 mM IPTG and incubated at 37 °C overnight (<16h) (see Appendix 1).

It was expected that >50% colonies from the control mutagenesis transformation should appear as blue colonies on X-gal agar plates. The expected number of colonies per plate was between 50 to 800.

2.3.2 Mutant strand PCR for multi-SDM

The parameters for thermal cycling of mutant strand synthesis can be seen in Table 2.7 and the PCR reaction components in Table 2.8.

Table 2.8 PCR components for multi-site (Agilent Technologies, UK)

Reaction component	Volume
10 X reaction buffer	2.5 μ l
Molecular grade water	Final volume 25 μ l
Quik solution	0.5 μ l
dsDNA template (50-100ng)	1 μ l (100 ng)
Mutagenic primers (100 ng per primer)	1 μ l (100 ng for each primer)
dNTP mix	2 μ l
QuikChange Multi enzyme blend	1 μ l

All other parameters were followed as per the Multi site control reaction, with the exception of the plating out volumes on LB agar, which were 1 μ l, 10 μ l and 100 μ l.

2.4 Mini preparation of colonies

Eight colonies were picked from a range of plates and incubated overnight (16 h) in 5 mL LB media containing 0.1 mg/ml ampicillin sodium salt (Calbiochem) to an optical density at 600nm (OD₆₀₀) of 1.2-1.6. A negative control was performed with each run, using 5 ml media with no inoculation. Following incubation, plasmid glycerol stocks were prepared by mixing 810 μ L LB culture with 190 μ L 80 % glycerol (VWR, UK) for storage at -80 °C. Plasmid DNA was extracted from the remaining inoculum using the QIAGEN QIAprep Spin Miniprep kit (QIAGEN, Manchester, UK) according to the manufacturer's protocol. This method utilises the alkaline method of bacterial lysis. In brief, the bacteria were pelleted at 5000 rpm for 5 min and the supernatant discarded. Using 250 μ l Buffer P1 (50mM Tris-HCl, pH 8.0, 10mM EDTA, 100 μ g/ml RNase), the cells were re-suspended and lysed under alkaline conditions using 250 μ l Buffer P2 (200mM NaOH, 1%SDS). This was subsequently neutralised with 250 μ l Buffer N3 (4.2M guanidinium-HCl, 0.9M potassium acetate), adjusting to high salt binding conditions. The genomic DNA and cell debris were pelleted by centrifugation at 13,000 rpm for 10 min and the plasmid DNA in the supernatant adsorbed onto the silica membrane of the QIAprep spin column in high salt buffer. Subsequent washes with 500 μ l Buffer PB (5M guanidinium-HCl, 30% isopropanol) removed endonucleases

and salts were removed with 500 µl Buffer PE (10mM Tris-HCl, pH 7.5, 80% ethanol). Plasmid DNA was eluted with 50 µl Buffer EB (10mM Tris-HCl), ensuring a pH of 7.0-8.5 which allowed storage of the plasmid solution at 4 °C. The DNA concentration of the resultant plasmids was quantified using the Nanodrop 2000 spectrophotometer (Thermo Scientific).

2.5 Sanger sequencing to verify successful nucleotide change

The presence of the expected mutation or SNP and the absence of unwanted non-synonymous mutations (NSM) were verified by Sanger sequencing (GATC Biotech, Germany), which utilised the KB™ Basecaller (Applied Biosystems). Prior to sequencing, plasmid DNA samples were diluted to a concentration of 100 ng/µL. In order to sequence the whole plasmid insert, a total of 6 forward and reverse sequencing primers were designed using Primer 3 software (www.primer3.ut.ee), ensuring an approximate overlap of 200 nucleotides between each amplification product. The T7 promoter site on the pcDNA3.1+ plasmid was utilised for sequence 1. Primers were designed with a T_m between 57 °C and 61 °C and were between 18 and 20 nucleotides in length (see Table 2.9). Chromas Lite (Technylesium Pty Ltd,) software was used to open chromatograms for analysis (<http://www.technylesium.com.au/wp/chromas>). The sequence data was then exported in FASTA format to the multiple sequence alignment tool Clustal Omega (<http://www.ebi.ac.uk/Tools/msa/clustalo/>). Prior to initial SDM cloning, sequencing of the wild type insert was performed to ensure no unwanted nucleotide changes leading to non-synonymous amino acid changes were present in the insert. The alignments were scrutinised for any variation from the wild type cDNA sequence. If variations were present, these were compared to the reference amino acid/codon sequence alignment. The nucleotide sequence was aligned to the amino acid sequence by using the online translate tool ExPASy (expasy.org/translate) to establish whether the resultant codon would generate a non-synonymous or synonymous mutation.

Table 2.9 Oligonucleotide primers used to sequence *ADAMTS13* cDNA

Primer name	Forward primer 5'-3'
New seq 01	CAG CCT GGC CTC TAC TAC AG
Seq 02	CAG CCT GGC CTC TAC TAC AG
Seq 03	GTA CCA CAC AGC CAA GGG
Seq 04	ACC TTC ACC TAC TTC CAG CC
Seq 05	GCA CAT CAG CTG GTG GAG
Seq 06	GAA AGT CAT GTC CCT TGG CC
Seq 07	GAA AGT CAT GTC CCT TGG CC

2.6 Plasmid copy amplification

Prior to transfection, plasmid copy numbers were amplified and purified using maxi and midi prep protocols.

2.6.1 QIAGEN HiSpeed® Plasmid Maxi preparation

The maxi procedure was performed according to the manufacturer's protocol. In brief, a single colony was picked from a freshly streaked plate of WT/ mutant *E.coli* containing WT/mutant *ADAMTS13* cDNA and inoculated into 5ml LB medium containing 0.1 mg/ml ampicillin as a starter culture. This was incubated at 37 °C and shaken at 250 rpm for approximately 8 hours. For each mutation or WT, 250 ml LB medium plus 0.1 mg/ml ampicillin was inoculated with 5ml starter culture and grown to a cell density of approximately $3-4 \times 10^9$ cells per ml (3 g/L biomass) by incubating at 37°C and shaking at 240 rpm for 12-16 hours. Cultures were harvested after 12-16 hours during the transition from logarithmic growth to stationary growth phase.

The cells were then harvested by centrifuging at 5000 rpm at 4 °C for 15 min and the supernatant discarded. The resultant pellet was thoroughly re-suspended in 10ml Buffer P1 and the cells lysed by the addition of 10ml Buffer P2. This solution was neutralised by the addition of pre-chilled Buffer N3. The lysate was then loaded into a previously equilibrated QIAfilter cartridge and incubated at room temperature for 10 min, allowing separation of the genomic DNA, proteins and SDS from the plasmid DNA. The filtrate was then loaded into the HiSpeed tip allowing the filtrate to adsorb onto the resin. The resin was washed with 60 ml Buffer QC and plasmid DNA was eluted with 30 ml Buffer

QF. DNA was eluted with the addition of 10.5ml isopropanol (Fisher Scientific, UK) and incubated for 5 min. The isopropanol mixture was then filtered through the QIA precipitator and the membrane dried. DNA was precipitated with the addition of 1 ml Buffer TE and the resultant plasmid stored at 4°C. The DNA concentration of the resultant plasmids was quantified using the Nanodrop 2000 spectrophotometer (Thermo Scientific, UK).

2.6.2 Invitrogen PureLink® HiPure Plasmid DNA purification Midi preparation
Transformed *E.coli* cells were grown overnight (16 h) in 250ml LB medium with 0.1mg/ml ampicillin until the culture was confirmed to have an absorbance of 1-1.5 at 600 nm, or approximately 1×10^9 cells. The cells were harvested by centrifugation at 5,000 rpm at 4 °C and the supernatant discarded. The cells were then thoroughly re-suspended in Buffer R3 with RNase (20 mg/ml). Lysis buffer (4 ml) which contained 0.2 M NaOH and 1% w/v SDS was added, mixed and incubated at room temperature for 5 min. Precipitation buffer (4 ml) containing 3.1 M potassium acetate at pH 5.5 was added and gently mixed to avoid the shearing of DNA and the solution and precipitate centrifuged at 13,000 rpm for 10 min at room temperature (RT). The supernatant was then loaded onto a previously equilibrated HiPure filter midi column, allowing the clearance of bacterial lysates but binding DNA directly to the anion exchange resin. Wash buffer (10 ml) containing sodium acetate at pH 5.0 and 825 mM NaCl was added to the filter column twice, discarding the flow-through. DNA was eluted from the filter column by adding 5 ml elution buffer containing 100 mM Tris-HCl at pH 8.5 and 1.25 M NaCl. This was followed by a precipitation and wash stage. Isopropanol (3.5 ml, Fisher Scientific) was added to the eluate and mixed well. The eluate and precipitated DNA was then centrifuged at 13,000 rpm at 4 °C for 30 min. The supernatant was discarded, ensuring the pellet was not dislodged. Ethanol (3 ml, 70 %) was then added to the pellet and centrifuged at 13,000 rpm for 5 min at 4°C. The supernatant was removed and the pellet air dried for 10 min. Plasmid DNA was then re-suspended in 200µl TE buffer containing 100 nM Tris-HCl at pH 8.0. The DNA concentration of the resultant plasmid was quantified using the Nanodrop 2000 spectrophotometer (Thermo Scientific) and the solution stored at -20°C.

2.6 Preparation of HEK293T cells

Approximately two weeks' prior to transfection, one aliquot (1 mL) of HEK293T cells stored in 10% DMSO was taken out of nitrogen storage (77 K) and thawed slowly on wet ice. The cells were then added to 10 mL pre-warmed (37 °C) Modified Eagle's Medium (MEM) with Earle's salts and L-glutamine (Invitrogen, UK), containing 10 % fetal bovine serum (Invitrogen) and 10 ml penicillin/streptomycin 10,000U/ml (Biochrom AG, Germany). The cells were centrifuged at 1,000 rpm for 5 min and re-suspended in fresh MEM before being transferred to T75 culture flasks and incubated in a humidified incubator (37 °C, 5% CO₂). The cells were checked for recovery after 24 hours' incubation and subsequently passaged using 5 mL Dulbecco's phosphate buffered saline (D-PBS, Invitrogen, UK) and 1mL 0.05 % Trypsin-EDTA (Invitrogen, UK) at 37 °C when the cells reached 70-80 % confluence. Passaging of these cells continued until transfection.

The number of plated cells was counted using a haemocytometer and these were seeded at a density of 5 x 10⁶ live cells per 10 ml plate/ T75 flask or 8 x 10⁵ per 6 well plate. The use of 0.04 % trypan blue (Sigma Aldrich, UK) in a 50/50 dilution with the re-suspended cells in media allowed the differentiation between live and dead cells and this was reflected in the count.

It was important to ensure that over-passaging did not occur which may incur DNA damage/alteration thus changing the nature of the cells and expression of protein. If at any point 20 passaging events were reached, a new aliquot of cells was taken from nitrogen storage and passaged as described previously.

2.7 Transfection of HEK293T cells

2.7.1 Transfection agent

Branched chain polyethylenimine (PEI) (Invitrogen, UK) was used as a transfection agent. A 10 mM solution was prepared by dissolving 4.5 mg PEI in 10 mL distilled water, adjusted to a pH of 6.6-7.5 with 1M hydrochloric acid and subsequently filtered through a 0.2 µm filter, aliquoted and stored at -20°C. Working stock was stored at 4 °C for a maximum of one month.

2.7.2 Transfection

Ensuring 70-80 % confluence of HEK293T cells, the complete media was changed 1 hour prior to transfection. For transfection studies using 10 cm culture dishes, a total quantity of 33 ug plasmid DNA was added to 625 μ L 150 mM sterile NaCl per culture dish. For 6 well plates, a total quantity of 6.6 μ g plasmid DNA was added to 125 μ L 150 mM sterile NaCl per well. The volume required for this quantity of plasmid DNA was calculated from the results of the Maxiprep and Midiprep Nanodrop measurements. Using the optimum PEI (μ L): DNA (μ g) ratio of 2.25 for one 10 ml culture dish, 75 μ L 10 mM PEI was added to 625 μ L 150 mM DNA (33 μ g plasmid DNA) and incubated at RT for no longer than 20 min. For 6 well plates, 15 μ l 10mM PEI was then added to 125 μ l 150mM NaCl. Cells at 70-80% confluency were rinsed with 10 mL pre-warmed Opti-MEM[®] reduced serum medium with L-Glutamine (Invitrogen, UK) to remove serum contents (2 ml for 6 well plates) and 9 mL Opti-MEM[®] was added (2 mL for 6 well plates). The transfection complex consisting of 700 μ L (10 ml)/ 140 μ L (6 well) PEI mixture was added dropwise to the culture dishes/6 well plates containing the cells and Opti-MEM[®], ensuring the transfection complex was evenly distributed. The cells were incubated at 37 °C in 5 % humidified CO₂ for 2-3 days. The conditioned media was then collected from each culture dish and placed on wet ice, subsequently centrifuged at 3000 rpm at 4 °C for 5 min to pellet any cell debris and the supernatant collected in a clean tube and stored at -80°C before analysis. The adherent HEK293T cells were bathed in 1.5 mL (10ml) / 0.8ml (6 well) D-PBS (without calcium or magnesium) and harvested from the surface of the culture dish/6 well plate using a cell scraper or sterile pipette tip and collected in a 15 mL Falcon[®] tube kept on wet ice. The cells were centrifuged at 3000 rpm at 4 °C before the supernatant was discarded. The pelleted cells were then stored at -80°C prior to analysis.

2.8 Measure of transfection efficiency

To measure the efficiency of transfection, a reporter plasmid containing the *Lac Z* gene (kindly donated by Dr Edward Wright, University of Westminster) was co-transfected with the WT or mutated *ADAMTS13* plasmid. The size of

the reporter vector was 8.9kb in total. This allowed the localization of β -galactosidase activity in fixed cells to be visualized by light microscopy and the percentage transfection efficiency to be calculated. With this protocol it was necessary to make the assumption that the reporter plasmid was transfected at the same rate as the *ADAMTS13* plasmid therefore the quantity of plasmid containing the Lac Z reporter and the plasmid containing the ADAMTS13 insert were transfected in a 1:1 ratio.

For 10 cm culture dishes the media was discarded and 2 ml 0.5% v/v glutaraldehyde solution diluted in PBS (Sigma-Aldrich, UK) was added and incubated at 4 °C for 10 min. This was discarded, 2 ml PBS added and incubated at 4 °C for 5 min. The PBS was discarded and 2 ml X-gal solution (final concentration 1mg/ml) added. This was incubated for 1 hour at 37°C and protected from light. Following incubation, the cells were examined under the microscope. Cells successfully transfected appeared blue. The X-gal and buffer were tipped off and cells washed once in PBS. A total of 5 fields were visualised microscopically (X100) and imaged for cell counts. For 6 well plates, 5 μ l X-gal and 400 μ l buffer and PBS were used.

2.9 Cell lysate preparation

Lysates previously stored at -80°C were gently thawed and re-suspended in 0.1% Triton X cell lysis buffer (2ml for 10cm dishes; 800 μ l for 6 well plates) in 15ml tubes. This solution was kept on wet ice and the cell suspension sonicated using the Bandelin SONOPULS homogeniser probe (MS 72 micro tip; Sigma Aldrich, UK) at 35 % power for 5 x 10 s, with 50 s cooling between each iteration. The protein content of the sonicated suspension was quantified by BCA assay, aliquoted into 1.5 ml Eppendorf tubes and stored at -80 °C prior to analysis

2.10 Concentration of conditioned media

A total volume of 10 ml per plate and 2 ml per well of conditioned media was harvested from 10 cm culture dishes and 6 well plates respectively. The media was concentrated using Macrosep™ and Microsep™ Advance Centrifugal devices (PALL Life Sciences, UK); see Table 2.10.

Table 2.10 The concentration of conditioned media

Culture plate	Device	Centrifugal conditions
10 ml	MWCO 30K Omega, Macrosep™	3,000g, 4°C, 6 min
6 well	MWCO 30K Omega, Microsep™	3,000g, 4°C, 2 min

MWCO =molecular weight cut-off. For maximum retention, a device was selected with a MWCO 3 to 6 times less than the molecular weight of the protein to be retained.

The harvested conditioned media was pipetted into the sample reservoir and the cap replaced to prevent evaporation. The device was centrifuged for the required length of time at 4 °C. It was necessary for the membrane paddle of the device to be oriented with the end pointing towards the centre of the rotor to ensure adequate microfiltration. After centrifugation the concentrated conditioned media was retained in the sample reservoir and transferred to a 1.5 ml Eppendorf tube kept on wet ice. The protein content of the conditioned media was quantified by BCA assay and stored at -80°C prior to analysis.

2.11 Protein quantification

Total protein quantification of the cell lysates and conditioned media was carried out using the Pierce™ BCA Protein Assay kit (Thermo Scientific, UK), based on the biuret method. To produce a standard curve the reference standard (bovine serum albumin (BSA), 2mg/ml) was diluted to the concentrations seen in Table 2.11. The blank used was DMEM media.

Table 2.11 BCA protein standard concentrations

Standard	Concentration (µg/ml)
1	750
2	500
3	250
4	125
5	25
6	0

The protocol was followed according to manufacturer's instructions. In brief, the working reagent (WR) was diluted 50 parts reagent A with 1 part reagent B. A volume of 25 µl of each standard or unknown was pipetted into each microwell, with each test performed in triplicate. Working reagent (200 µl) was added to each well and mixed thoroughly, the plate covered and incubated at 37 °C for 30 min then cooled to RT. The absorbance was read at 562nm using the BMG Labtech SPECTROSTAR Nano® microplate reader.

2.11.1 Analysis of protein quantification results

The mean of three absorbance values of standards and unknowns was determined and the average blank standard replicate value subtracted. A standard curve was plotted of BSA concentration (µg/ml) vs average blank corrected absorbance (562nm) for each standard. The concentrations of unknown samples were interpolated from the standard curve.

2.12 Western blot

2.12.1 Sodium dodecyl sulphate polyacrylamide gel electrophoresis (SDS PAGE)

To prepare conditioned media and cell lysis samples, 150 µl sample was added to 50 µl 4x Laemmli buffer (pH 6.8; see Appendix 1) and boiled at 100 °C for 5 min in a 1.5 ml Eppendorf tube. The samples were cooled and stored at -20 °C. To prepare the resolving and stacking buffers, Tris base was dissolved in 15 ml deionized water and the pH adjusted to pH 8.8 (resolving buffer) and pH 6.8 (stacking buffer) using 1M HCl. The final volume was then adjusted to 20 ml (see Appendix 1). Buffers were stored at 4 °C for up to 1 month. To pour the gels, the Bio-Rad Mini-Protean®Tetra casting plates were securely placed in the casting stands, ensuring a tight seal was formed. The 10% acrylamide resolving gel was made up with the APS and TEMED added last (see Appendix 1). The gel was added to the casting plates ensuring no bubbles formed in the solution. A thin layer of butanol (Fisher Chemical, UK) was laid over the top of the gel surface and allowed to set for 30 mins. Once set, the butanol was removed and washed off with deionized water. The 4%

acrylamide stacking gel was prepared, with APS and TEMED added last (see Appendix 1), and laid on the top surface of the resolving gel, again ensuring no bubbles were introduced. The gel comb was placed in the stacking gel and was allowed to set for 20 mins.

2.12.2 Running SDS PAGE

Ensuring the BioRad Mini-Protean[®] gel tank was assembled correctly, the gel combs were removed and the tank half filled with running buffer. The wells were washed with running buffer before sample loading. Lane 1 was loaded with 3 μ l Precision Plus Protein[™] Dual Colour Standard (Bio-Rad, UK) and subsequent lanes loaded with a positive control (WT), cell lysates or conditioned media. Protein loading volumes were normalised according to concentrations established by the BCA assay. The gels were run for 80 min at a voltage of 110V or until the dye front was within 1 cm of the bottom of the gel.

2.12.3 Transfer and western blot

Fifteen min prior to blotting, the nitrocellulose membrane (Hybond[™]-ECL[™], Amersham Biosciences, UK) was activated in 100% HPLC grade methanol (Fisher Scientific). The gels were removed from the casings and placed in chilled transfer buffer for 5 min. Ensuring the correct orientation of the cassette, a fibre pad was submerged in buffer onto the cassette and filter paper placed over the pad. The gel was then placed on the sandwich and the activated membrane placed on top. A second filter paper and fibre pad completed the sandwich and any trapped air bubbles removed. The cassette was submerged in the transfer buffer. The tank was assembled with a magnetic stirrer and ice block in place and filled with chilled transfer buffer. The blot was run for 2 hours at 100 V on a magnetic plate to allow for adequate heat dissipation. On completion, the blot was disassembled and the membrane orientated protein side up. To assess even protein transfer with 0.1% Ponceau S solution, the membrane was allowed to stand in solution for 1 min. Distilled water (20 ml) was used to rinse the membrane until the molecular weight marker and bands became visible. Once the bands were

checked for even transfer, the membrane was rinsed in TBS until the bands were no longer visible. The membrane was then incubated in 3 % w/v blocking buffer in TBS for 1 hour at RT.

Following blocking, the membrane was washed 3 x 5 min in TBST. Primary anti-myc tag antibody (5 μ l, 1 mg/ml mouse monoclonal IgG₁, clone A46, Merck-Millipore, UK) was added and incubated at RT for 1 hour. The membrane was washed 3 x 5 min with TBST and in the case of cell lysis samples, further incubated with 10ml of 1 μ l/ml primary anti-mouse monoclonal β -actin antibody (clone 8226, Abcam, UK) and incubated at RT for 1 hour. For conditioned media samples and following β -actin antibody incubation for cell lysate samples, the membrane was washed 3 x 5 min with TBST and the secondary HRP antibody added (10 ml 0.2 μ l/ml goat anti-mouse IgG, clone A4416, Sigma-Aldrich, UK) and incubated for 1 hour at RT. The membrane was then washed 6 x 5 min in TBST and stored in TBS at 4 °C until visualised.

2.12.4 Visualisation using enhanced chemiluminescence (ECL) reagent

The ECL working solution was prepared by mixing 500 μ l each of the peroxide solution and luminol/enhancer SuperSignal[®] West Femto Maximum Sensitivity Substrate (Thermo Scientific, UK) per blot. The solution was uniformly pipetted onto the blot and incubated for 5 mins. The working solution was drained and the blot visualised with the UVP BioSpectrum[®]515 Imaging System[™] fitted with camera GDS (12.5-75mm, f1.2, motorized Sigma zoom lens).

2.12.5 Determination of the appropriate sample load for Western blot

Prior to running conditioned media or cell lysate samples, the appropriate sample load was determined. A blot was loaded with 1, 4, 8, 12 and 15 μ g WT ADAMTS13 protein in 2 sets of lanes separated by a known concentration of BSA protein standard to assess protein target load for ADAMTS13 anti-myc tag and the housekeeping protein β actin. After transfer, the membrane was cut before the second protein standard lane, producing 2 blots. The anti-myc primary antibody was applied to one blot and the anti- β actin antibody applied to the other blot. The secondary antibody was then added and after incubation

the 2 blots were visualised using the UVP BioSpectrum[®]515 Imaging System[™] fitted with camera GDS (12.5-75mm, f1.2, motorized Sigma zoom lens). Using ImageJ software the target (anti-myc) and housekeeping protein signal intensity was read. The intensity was then plotted against the protein load and the linear dynamic range was determined. The protein load that gave the quantitative reading in the linear dynamic range was selected.

2.12.6 Densitometry analysis

Images of the developed blots were analysed using ImageJ software (<<http://www.imageJ.net>>).

2.13 Commercial ADAMTS13 antigen quantification: IMUBIND[®] ADAMTS13 ELISA

The assay was performed according to manufacturer's instructions.

2.13.1 Preparation of ADAMTS13 standards

Using the supplied 96 well plate, five standards were prepared by serial dilution using the manufacturer's proprietary ADAMTS13 standard supplied. A volume of 200 µl of prepared standard was added to microwell A1/A2. To each microwell from B1/2 to G1/2, 100 µl assay buffer (IMUBIND[®]) was added and 100 µl of standard serially diluted from microwells A1/2 to F1/2, discarding 100 µl from wells F1/2. Wells G1/2 served as a negative control (blank). The concentration of the standards from A1/2 to G1/2 was: 100, 50, 25, 12.5, 6.25, 3.12 and 0 ng/ml respectively.

2.13.2 ADAMTS13 assay

Each sample was diluted 1:20 with assay buffer. To each ADAMTS13 monoclonal antibody (mAb) coated microwell, 100 µl positive control or sample was added, covered and incubated at 37 °C for 1 hour, allowing any ADAMTS13 present in the sample to bind to the mAb in the microwell. The microwells were then emptied and washed 4 times with wash buffer. 100 µl of the detection antibody (biotinylated rabbit anti-ADAMTS13 polyclonal

antibody) was added to each microwell, binding to any ADAMTS13 captured on the plate, covered and incubated at RT (18-25 °C) for 30 min on an orbital microwell plate shaker (250 rpm). The microwells were then emptied and washed 4 times with wash buffer. The enzyme conjugate (100 µl streptavidin-horseradish peroxidase conjugate (SA-HRP)) was added to each microwell plate and incubated at room temperature (18-25 °C) on a microwell shaker (250 rpm) for 30 min, forming the antibody-enzyme detection complex. The microwells were then emptied and washed 4 times with wash buffer. 100 µl perborate-3, 3'-5,5'-tetramethylbenzidine (TMB substrate) was added immediately to each microwell and incubated for 5 min at room temperature. The reaction of TMB and the HRP turned the substrate a blue colour. The reaction was stopped by adding 50 µl 0.5 M sulphuric acid, ensuring even distribution and effecting a colour change from blue to yellow. The absorbance of each well was read at 450 nm using the BMG Labtech Spectrostar Nano microplate reader.

2.14.3 Analysis of results

A standard curve was plotted of ADAMTS13 concentration vs Absorbance reading at 450 nm and values of concentration for the unknown samples interpolated from the standard curve. The reading from the graph was corrected for the 1 in 20 dilution of the sample.

Chapter 3

***In silico* analysis of mutations and single nucleotide polymorphisms**

3.1 Introduction

In silico analysis has been used to predict the association of ADAMTS13 mutations and clinical phenotype (Edwards *et al.*, 2012; Hing *et al.*, 2013; Lotta *et al.*, 2012). The crystallographic structure of the ADAMTS13 protein has been elucidated and can be viewed in the Protein Data Bank (identification codes 3GHM and 3GHN); (Akiyama *et al.*, 2009a). The exosite domains of the disintegrin, thrombospondin type 1, the cysteine rich and signal domain have been analysed but the catalytic metalloprotease domain has not.

The X-ray crystallographic structure has revealed ADAMTS13 to be a complex structural protein with numerous short-range and long-range covalent and non-covalent interactions which provide stability to the functional protein. These interactions are mainly brought about by hydrophobic, hydrogen and disulfide bonding. In consideration of this, mutations found outside of the catalytic region can have consequences on the stability and functionality of ADAMTS13.

As the clinical phenotype of congenital TTP (cTTP) differs amongst patients, and even among siblings with the same genotype, some studies have used *in silico* tools to look at a larger number of patient genotype data in order to assess the correlation between genotype and phenotype (Hing *et al.*, 2013; Lotta *et al.*, 2010; Moatti-Cohen *et al.*, 2012). Hing *et al.* assessed several parameters including the N/C terminal score (the position of the mutation in relation to the catalytic N-terminus of ADAMTS13); the amino acid evolutionary conservation score; the changes in electrostatic charge of the amino acid substitution and phosphorylation. The relative synonymous codon usage and crystal structure *in silico* modelling was also analysed and carried out. This was performed on data from 144 cTTP patients. They found statistically significant associations between homozygous patients with non-synonymous

missense mutations that were found in highly conserved areas and the requirement of increased TP prophylaxis treatment. Additionally, those mutations found in highly conserved areas showed an earlier age of TTP onset. A statistically significant correlation between rarer codon usage and late-onset disease in patients with homozygous missense mutations was also found. Codon usage has been postulated to alter the translation rate of the protein, thereby causing misfolding of the protein and altering function (Edwards *et al.*, 2012).

Interestingly, many missense mutations involve cysteine which is involved in disulfide bond formation. Previous studies have indicated that disulfide bond formation is an important factor in the correct folding of proteins thus mutations involving the substitution of cysteines could result in the misfolding or proteolysis of the protein, triggering its removal and breakdown (Salamanca *et al.*, 2003). Similarly, arginine is an amino acid that is more easily mutated and serves an integral function in hydrogen bonding, leading to stabilisation of the protein.

There is a limitation to *in silico* tools as they can only be applied to the homozygous genotype. In the study performed by Hing *et al.*, this only represented 38.9% of cTTP patients whereas 61.1% of patients were compound heterozygotes. *In silico* tools are also predictive and rely on the parameters written into the algorithm or, if using a machine learning tool, may reflect the biases of the training set. In consideration of siblings with the same genotype presenting a different phenotype, other genes not yet recognized or epigenetic factors could be other areas to consider.

3.2 Methods

In this study, the following *in silico* tools were applied:

- MUSCLE (multiple sequence comparison by log expectation) alignment (<www.ebi.ac.uk/Tools/msa/muscle/> [Accessed 16/6/16]);
- FOLD X (<<http://www.foldx.embl.de/>> [Accessed 2/7/16]);

- SNP Effect 4.0 (<<http://www.snpeffect.switchlab.org/>>[Accessed 20/7/17]);
- I-Mutant2.0 (<<http://www.folding.biofold.org/i-mutant/i-mutant2.0.html>> [Accessed 15/5/17]);
- SIFT (sorting tolerant from intolerant) (<<http://www.sift.jcvi.org>> [Accessed 23/5/17]),
- PolyPhen2.0 (Polymorphism phenotyping 2) (<<http://www.genetics.bwh.harvard.edu/pph2/>> [Accessed 23/5/17]); and
- Predict SNP (<https://loschmidt.chemi.muni.cz/predictsnp> [Accessed 28/7/17]).

The global prevalence of SNPs investigated in this study has also been elucidated from the dbSNP database (<<http://www.ncbi.nlm.nih.gov/snp>>[Accessed 30/7/17]).

3.2.1 MUSCLE alignment

Conservation of amino acids has been postulated to be the second most predictive factor of the impact of a mutation (Lee *et al.*, 2009). To assess the conservation in regions of TTP mutations and SNPs, alignment of orthologs was performed on the following species: *Mus musculus* (the house mouse), *Rattus norvegicus* (the brown rat), *Papio Anubis* (the olive baboon), *Homo sapiens* (the human), *Gorilla gorilla* (the gorilla), *Pan troglodytes* (the common chimpanzee), *Ovis aries* (the sheep) and *Bos Taurus* (the cow); see Figure 3.1.

3.2.2 FOLD X

The FOLDX algorithm is used to calculate the change in free energy the mutation has on the protein. If the mutation destabilizes the structure, the change in Gibbs free energy ($\Delta\Delta G$) is increased whereas if the mutation stabilizes the structure, $\Delta\Delta G$ is decreased. A homology model is built from PDB 3GHM (Schymkowitz *et al.*, 2005). The FOLD X scores for mutations and SNPs can be seen in Table 3.1.

3.2.3 I-Mutant2.0

The I-Mutant $\Delta\Delta G$ *in silico* tool (Capriotti *et al.*, 2006) can evaluate the stability change on single missense mutations based on the protein structure found in the PDB or on the amino acid sequence of the protein. This algorithm has been found to predict whether the mutation stabilises or destabilises the protein in 80% of cases when the three dimensional structure is known and 76% of cases when only the amino acid sequence is known; see

3.2.4 Sorting intolerant from tolerant (*SIFT*)

Previous published studies have used PolyPhen and SIFT as predictors of phenotype based on genotype (Lotta *et al.*, 2012; Moatti-Cohen *et al.*, 2012). Since its release in 2001, the SIFT algorithm has become one of the standard tools for characterizing missense mutations (Sim *et al.*, 2012). The SIFT prediction is based on the degree of conservation of residues in sequence alignments from closely related sequences which have been collected through PSI-BLAST (Position-specific iterative basic local alignment search tool); (Kumar *et al.*, 2009). To assess the effect of an amino acid residue substitution, the programme uses the premise that important positions in the amino acid sequence have been conserved throughout evolution and substitutions in these conserved areas will have a significant effect on protein function. The programme predicts the effects of all possible substitutions at each amino acid position and predicts if the missense mutation will be damaging or tolerated.

3.2.5 PolyPhen2.0

The PolyPhen2 programme uses physical and comparative evolutionary considerations, and utilises functional annotations of SNPs from the UniProtKB/SwissProt databases, maps coding SNPs to gene transcripts, extracts protein sequence annotation and maps to known 3D structures. The programme then estimates the probability of a missense mutation being damaging, based on a combination of these parameters (Adzhubei *et al.*, 2013). The prediction of benign, possibly damaging or probably damaging is then made. Estimates of false positives (the chance that the mutation is classified as damaging when it is in fact non-damaging) and the true positive

(the chance that the mutation is classified as damaging when it is indeed damaging) is scored.

3.2.6 PredictSNP

The PredictSNP is a meta-analysis tool and consensus classifier combining six best performing prediction methods to provide more accurate and robust alternative to the predictions delivered by individual integrated tools (Bendl *et al.*, 2014). The predictions from the computational tools are supplemented by experimental annotations from two databases Uniprot (Q76LX8) and PMD A010243.

3.3 Results

3.3.1 MUSCLE alignments

The results of the alignments can be seen in Table 3.1. The amino acid position of the SNP mutation or is shaded.

Table 3.1 Conservation of amino acid residues among orthologs: SNPs and mutations

Key:

* (asterisk): positions having single, fully conserved residues

: (colon): conservation between groups of strongly similar properties

. (period): conservation between groups of weakly similar properties

- (dash): no corresponding amino acid at this position

<i>Mus musculus</i>	MSQLCLWLTTCQP-CYAVSVRGILTGAIFILGCWGLSDFQKSILQDLEPKDVSSYFGHHA
<i>Rattus norvegicus</i>	MSQLCLWLTTCQP-FLAASIRGILTGAIFILGCWGLSDFQKSFLQDLEPKDLSSFSRHTA
<i>Papio anubis</i>	MHQRHPRARCPS----LCVAGILACG-FLLGCWGPSHFQQSFLQALEPQAVSSYLS-SGA
<i>Homo sapiens</i>	MHQRHPRARCPS----LCVAGILACG-FLLGCWGPSHFQQSCLQALEPQAVSSYLS-PGA
<i>Gorilla gorilla</i>	MHQRHPRARCPS----LCVAGFLACG-FLLGCWGPSHFQQSCLQALEPQAVSSYLS-PGA
<i>Pan troglodytes</i>	MHQRHPRARCPS----LCVAGILACG-FLLGCWGPSHFQQSCLQALEPQAVSSYLS-PGA
<i>Ovis aries</i>	---MIAGSMAPS-TLGRCMQGTLSALFLLSCWALPDRQQFLQALEPGDVTSYFG-PDA
<i>Bos taurus</i>	ESRVSLLGFISPCVTTGRX--GTLTSALFLLSCWALPDRQQFLQVLEPADVTSYFG-PDA
	. * : . * : * . * : . * * * * : : * : . *
SNP p.R7W	
<i>Mus musculus</i>	CVGEDLQAKMCNT-QACEKTQLEFMSQQCAQTDQRPLQLSQGTA-SFYHWDAAVQYSQGD
<i>Rattus norvegicus</i>	CVGEDLQAKMCNT-QACEKTQLEFMSQQCAQTDHRPLQLSQGSA-SFYHWDAAVQYSQGD
<i>Papio anubis</i>	CVGADLQAEMCNTQQACEKTQLEFMSQQCARTDGGQLHSSPGGA-SFYHWGAAVPHSQGD
<i>Homo sapiens</i>	CVGADLQAEMCNT-QACEKTQLEFMSQQCARTDGGQLRSPGGA-SFYHWGAAVPHSQGD
<i>Gorilla gorilla</i>	CVGADLQAEMCNT-QACEKTQLEFMSQQCARTDGGQLRSPGGA-SFYHWGAAVPHSQGD
<i>Pan troglodytes</i>	CVGADLQAEMCNT-QACEKTQLEFMSQQCARTDGGQLRSPGGA-SFYHWGAAVPHSQGD
<i>Ovis aries</i>	CVGSDLQAEMCNT-QACETTQLEFMSQQCAQTDGEPHLHSPGGSTSFYRWGTATLLSPGN
<i>Bos taurus</i>	CVGSDLQAEMCNT-QACEKTQLEFMSQQCAQTDSEPLRLSPGGSTAFYRWGTAEQYSEGN
	*** ***:*** ***:*****:*** ** * . * : :*.*.:* * * :
SNP p.Q448E	
<i>Mus musculus</i>	CVGEDLQAKMCNT-QACEKTQLEFMSEQCAQTDQRPLQLSQGTA-SFYHWDAAVQYSQGD
<i>Rattus norvegicus</i>	CVGEDLQAKMCNT-QACEKTQLEFMSEQCAQTDHRPLQLSQGSA-SFYHWDAAVQYSQGD
<i>Papio anubis</i>	CVGADLQAEMCNTQACEKTQLEFMSEQCARTDGGQLHSSPGGA-SFYHWGAAVPHSQGD
<i>Homo sapiens</i>	CVGADLQAEMCNT-QACEKTQLEFMSQQCARTDGGQLRSPGGA-SFYHWGAAVPHSQGD
<i>Gorilla gorilla</i>	CVGADLQAEMCNT-QACEKTQLEFMSEQCARTDGGQLRSPGGA-SFYHWGAAVPHSQGD
<i>Pan troglodytes</i>	CVGADLQAEMCNT-QACEKTQLEFMSEQCARTDGGQLRSPGGA-SFYHWGAAVPHSQGD
<i>Ovis aries</i>	CVGSDLQAEMCNT-QACETTQLEFMSEQCAQTDGEPHLHSPGGSTSFYRWGTATLLSPGN
<i>Bos taurus</i>	CVGSDLQAEMCNT-QACEKTQLEFMSEQCAQTDSEPLRLSPGGSTAFYRWGTAEQYSEGN
	*** ***:*** ***:*****:*** ** * . * : :*.*.:* * * :
SNP p.P475S	

```

Mus musculus      -----GEMPEPDSL-----YLATDFLVFEMPPPLTPGAWWEKPNSPDPLRAATLTAKLIP
Rattus norvegicus -----GEMTEDPS-----LHLHVLVVFEMPSLWWE-PNSPDLMRAATLTPKLIP
Papio anubis      GRYVVAGKTSISSNTTYPSSLEEDGRVEYRVALTEDRLPRLEEIRIWGFLQEDA-----E
Homo sapiens      GRYVVAGKMSISPNTTYPSSLEEDGRVEYRVALTEDRLPRLEEIRIWGFLQEDA-----D
Gorilla gorilla   GRYVVAGKMSISPNTTYPSSLEEDGRVEYRVALTEDRLPRLEEIRIWGFLQEDA-----D
Pan troglodytes   GRYVVAGKMSISPNTTYPSSLEEDGRVEYRVALTEDRLPHLEEIRIWGFLQEDA-----D
Ovis aries        THAAAGGLGSHSEPTGAPGVL---RAAQRESPAEGPGASREGALQLRPRRQA-----R
Bos taurus        GRYVVAGNGSASATSYPSLEEDNRVEYRVTLSEDRLPRREIRIRGPTRDDM-----E

```

SNPp.P618A

```

Mus musculus      QDKWVKNAQCQGSQPFAWQEPVCSAPCSPYVWAGDFSPCSVSCGGGLRERSLRCVETQD
Rattus norvegicus QNKWVRNAQCQGSQPFAWQEPVCSAPCPHWVADDFGPCSVCSCGGGLRERSLRCVEAHN
Papio anubis      RKELVETARQCQGSQPFAWPEACVLEPCPPYVAVGDFGPCSVCSCGGGLRERPVRCVEAQQ
Homo sapiens      RKELVETVQCQGSQPFAWPEACVLEPCPPYVAVGDFGPCSASCSCGGGLRERPVRCVEAQQ
Gorilla gorilla   RKELVETVQCQGSQPFAWPEACVLEPCPPYVAVGDFGPCSASCSCGGGLRERPVRCVEAQQ
Pan troglodytes   RKELVETVQCQGSQPFAWPEACVLEPCPPYVAVGDFGPCSASCSCGGGLRERPVHCVEAQQ
Ovis aries        RSEWVEAAGCAGSRPEAWSGACTLEPCPPQ-----
Bos taurus        RSEWVEAAHCAGSQPPVWSETCTPGPCPPHWEAGDFGPCSASCSCGGGLREREREVRCVEARG

```

SNP p.A732V

```

Mus musculus      GAQAEHVWTPVGLCSISCGRGLKELYFLCSDSVLKMPVQEEELCGLASKPPSRWEVCRAR
Rattus norvegicus SSQAEHVWTPVGLCSISCGRGLKELYFLCSDSVLKMPVQEEELCGLASKPPSRWEVCRAR
Papio anubis      GAQAAHVWTPVAGPCSVSCGRGLMELRFLCSDSALRVVQEEELCGLASKPGSRWEVCQAV
Homo sapiens      GAQAAHVWTPVAGSCSVSCGRGLMELRFLCSDSALRVVQEEELCGLASKPGSRREVQCQAV
Gorilla gorilla   GAQAAHVWTPVAGSCSVSCGRGLMELRFLCSDSALRVVQEEELCGLASKPGSRQEVQCQAV
Pan troglodytes   GAQAAHMWTPVAGSCSVSCGRGLMELRFLCSDSALRVVQEEELCGLASKPGSRREVQCQAV
Ovis aries        EALAKHVWTPVAGPCSVSCGQGLAELHFVCMDFALRTPVREELCDLASKPGSRREACQAA
Bos taurus        EALAAHVWTPVAGPCSVSCGQGLVELRFVCMDFALRTPVREELCDLASKPGSRREACQAA

```

SNP A900V

```

Mus musculus      PEPCPAR-----
Rattus norvegicus PEPCPAR-----
Papio anubis      LEPCPPRWKVTSLGPCSASCGLGTARRSVACVQLDQGDVEVDEAACAALVRPQASVPCL
Homo sapiens      LEPCPPRWKVMVSLGPCSASCGLGTARRSVACVQLDQGDVEVDEAACAALVRPEASVPCL
Gorilla gorilla   LEPCPPRWKVMVSLGPCSASCGLGTARRSVACVQLDQGDVEVDEAACAALVRPQASVPCL
Pan troglodytes   LEPCPPRWKVMVSLGPCSASCGLGTARRSVACVQLDQGDVEVDEAACAALVRPQASVPCL
Ovis aries        PGPCPPRWKVTSLGPCSASCGLGTARRSVACVRLDRGQDTRVRAACAGLVRPQASIPCI
Bos taurus        LEPCPARWKVTSLGPCSASCGLGTARRSLACVRLDHGQDTEVDGACAGLVQPQASIPCI

```

SNP p.A1033T

```

Mus musculus      LEDILHLELLVAVGPDVSRHQEDTEYVLTNLNIGSELLRNPSLGVQFQVHLVKLITLS
Rattus norvegicus SEDILHLELLVAVGPDVYQAHQEDTEYVLTNLNIGSELLRNPSLGAQLQVHLVKLIILS
Papio anubis      VSHHLHLELLVAVGPDVFQAHQEDTEYVLTNLNIGAE LLRDP SLGAQFRVHLVKMVIIT
Homo sapiens      AGGILHLELLVAVGPDVFQAHQEDTEYVLTNLNIGAE LLRDP SLGAQFRVHLVKMVIIT
Gorilla gorilla   AGGILHLELLVAVGPDVFQAHQEDTEYVLTNLNIGAE LLRDP SLGAQFRVHLVKMVIIT
Pan troglodytes   AGGILHLELLVAVGPDVFQAHQEDTEYVLTNLNIGAE LLRDP SLGAQFRVHLVKMVIIT
Ovis aries        TGHILHLELLVAVGPDVQRTHGEETEYVLTNLNMGSELLRDP SLGAQFRVHLVKMVIIT
Bos taurus        AGHVHLHLELLVAVGPDVHRTHGEETEYVLTNLNMGSELLRDP SLGAQFRVHLVKMVIIT

```

Mutation p.R102H

```

Mus musculus      TQLGGACSLWSCLITEDTGF DLGVTIAHEIGH-----SFGLDHD-GAPGSGSTCKASGH
Rattus norvegicus TQGGGACSPWSCLITEDTGF DLGVTIAHEIGH-----SFGLDHD-GAPGSGSTCEARGH
Papio anubis      TQLGGACSPWWSCLITEDTGF DLGVTIAHEIGH-----SFGLDHD-GAPGSG--CGPSGH
Homo sapiens      TQLGGACSPWWSCLITEDTGF DLGVTIAHEIGH-----SFGLDHD-GAPGSG--CGPSGH
Gorilla gorilla   TQLGGACSPWWSCLITEDTGF DLGVTIAHEIGH-----SFGLDHD-GAPGSG--CGPSGH
Pan troglodytes   TQLGGACSPWWSCLITEDTGF DLGVTIAHEIGH-----SFGLDHD-GAPGSG--CGPSGH
Ovis aries        TQLGGACSSWSCLITEDTGF DLGVTIAHEIGHRTVTRSLGLHGVLGAPQPPPSVLSGE
Bos taurus        TQLGGACSSWSCLITEDTGF DLGVTIAHEIGH-----SFGLDHD-GVPGSG--CGPSGH

```

Mutation p.T196I

```

Mus musculus      TQLGGACSLWSCLITEDTGF DLGVTIAHEIGH-----SFGLDHD-GAPGSGSTCKASGH
Rattus norvegicus TQGGGACSPWSCLITEDTGF DLGVTIAHEIGH-----SFGLDHD-GAPGSGSTCEARGH
Papio anubis      TQLGGACSPWWSCLITEDTGF DLGVTIAHEIGH-----SFGLDHD-GAPGSG--CGPSGH
Homo sapiens      TQLGGACSPWWSCLITEDTGF DLGVTIAHEIGH-----SFGLDHD-GAPGSG--CGPSGH
Gorilla gorilla   TQLGGACSPWWSCLITEDTGF DLGVTIAHEIGH-----SFGLDHD-GAPGSG--CGPSGH
Pan troglodytes   TQLGGACSPWWSCLITEDTGF DLGVTIAHEIGH-----SFGLDHD-GAPGSG--CGPSGH
Ovis aries        TQLGGACSSWSCLITEDTGF DLGVTIAHEIGHRTVTRSLGLHGVLGAPQPPPSVLSGE
Bos taurus        TQLGGACSSWSCLITEDTGF DLGVTIAHEIGH-----SFGLDHD-GVPGSG--CGPSGH

```

Mutation p.D217H

<i>Mus musculus</i>	K-WCSKARCRSLAELAPVAAVHGHWSWGPHSPCSRSCGGGVITRRRCWNNPRPAFGGRA
<i>Rattus norvegicus</i>	K-WCSKARCRSLAELAPVAAVHGHWSWGPHSPCSRSCGGGVITRRRCWNNPRPAFGGRA
<i>Papio anubis</i>	K-WCSKGRCSRSLVELTPIAAVHGHWSWSWSPQSPCSRSCGGGVITRRRCQNNPRPAFGGRA
<i>Homo sapiens</i>	K-WCSKGRCSRSLVELTPIAAVHGRWSSWGPRSPCSRSCGGGVITRRRCQNNPRPAFGGRA
<i>Gorilla gorilla</i>	K-WCSKGRCSRSLVELTPIAAVHGRWSSWGPHSPCSRSCGGGVITRRRCQNNPRPAFGGRA
<i>Pan troglodytes</i>	K-WCSKGRCSRSLVELTPIAAVHGRWSSWGPRSPCSRSCGGGVITRRRCQNNPRPAFGGRA
<i>Ovis aries</i>	KDACSRRARCGGLRTGVWVG--GCLWVWVWALGGGGVGGGGVITRRRCNDNPRPAFGGRA
<i>Bos taurus</i>	K-WCSKGRCSRSLAELAPVGVVHGHWSWGWPSPCSRSCGGGVITRRRCNNPRPAFGGRT

Mutation p.R409W

<i>Mus musculus</i>	K-WCSKARCRSLAELAPVAAVHGHWSWGPHSPCSRSCGGGVITRRRCWNNPRPAFGGRA
<i>Rattus norvegicus</i>	K-WCSKARCRSLAELAPVAAVHGHWSWGPHSPCSRSCGGGVITRRRCWNNPRPAFGGRA
<i>Papio anubis</i>	K-WCSKGRCSRSLVELTPIAAVHGHWSWSWSPQSPCSRSCGGGVITRRRCQNNPRPAFGGRA
<i>Homo sapiens</i>	K-WCSKGRCSRSLVELTPIAAVHGRWSSWGPRSPCSRSCGGGVITRRRCQNNPRPAFGGRA
<i>Gorilla gorilla</i>	K-WCSKGRCSRSLVELTPIAAVHGRWSSWGPHSPCSRSCGGGVITRRRCQNNPRPAFGGRA
<i>Pan troglodytes</i>	K-WCSKGRCSRSLVELTPIAAVHGRWSSWGPRSPCSRSCGGGVITRRRCQNNPRPAFGGRA
<i>Ovis aries</i>	KDACSRRARCGGLRTGVWVG--GCLWVWVWALGGGGVGGGGVITRRRCNDNPRPAFGGRA
<i>Bos taurus</i>	K-WCSKGRCSRSLAELAPVGVVHGHWSWGWPSPCSRSCGGGVITRRRCNNPRPAFGGRT

Mutation p.R398C

<i>Mus musculus</i>	CVGEDLQAKMCNT-ACEKTQLEFMSEQCAQTDQRPLQLSQGTA-SFYHWDAAVQYSQGD
<i>Rattus norvegicus</i>	CVGEDLQAKMCNT-ACEKTQLEFMSEQCAQTDQRPLQLSQGTA-SFYHWDAAVQYSQGD
<i>Papio anubis</i>	CVGADLQAEMCNTQACEKTQLEFMSEQCARTDGGQPLHSSPGGA-SFYHWGAAPVPHSQGD
<i>Homo sapiens</i>	CVGADLQAEMCNT-ACEKTQLEFMSEQCARTDGGQPLRSPGGA-SFYHWGAAPVPHSQGD
<i>Gorilla gorilla</i>	CVGADLQAEMCNT-ACEKTQLEFMSEQCARTDGGQPLRSPGGA-SFYHWGAAPVPHSQGD
<i>Pan troglodytes</i>	CVGADLQAEMCNT-ACEKTQLEFMSEQCARTDGGQPLRSPGGA-SFYHWGAAPVPHSQGD
<i>Ovis aries</i>	CVGSDLQAEMCNT-ACETTQLEFMSEQCAQTDGEPHLHSPGGSTSFYRWGTATLLSPGN
<i>Bos taurus</i>	CVGSDLQAEMCNT-ACEKTQLEFMSEQCAQTDSEPLRLSPGGSTAFYRWGTAEQYSEGN

Mutation p.Q436H

<i>Mus musculus</i>	VWDACQVCGGDNSTCSSRNGSFTAGRAREYVTFLLIVTPNMTNAHIVNRRPLFTHL----
<i>Rattus norvegicus</i>	VWDACQVCGGDNSTCTSQNGSFTAGRAREYVTFLLIVTPNMTSAHVINHRPLFTHL----
<i>Papio anubis</i>	VRDMCQVCGGDNSTCSFRNGSFTAGRAREYVTFLLIVTPNLTSVYIANHRPLFTHLAVRIG
<i>Homo sapiens</i>	VWDRQCQVCGGDNSTCSFRKGSFTAGRAREYVTFLLIVTPNLTSVYIANHRPLFTHLAVRIG
<i>Gorilla gorilla</i>	VWDRQCQVCGGDNSTCSFRKGSFTAGRAREYVTFLLIVTPNLTSVYIANHRPLFTHLAVRIG
<i>Pan troglodytes</i>	VWDRQCQVCGGDNSTCSFRKGSFTAGRAREYVTFLLIVTPNLTSVYIANHRPLFTHLAVRIG
<i>Ovis aries</i>	VRDVCQVCGGDNSTCTCRPQNGSFTAGRAREYVTFLLIVTPNLTISIINRRPLFTHLASRAA
<i>Bos taurus</i>	VRDVCQVCGGDNSTCQPQSGSFTAGRAREYVTFLLIVTPNLTISIYINRRPLFTHLAVRVR

Mutation p.A596V

<i>Mus musculus</i>	GKVYRRYGGEYGLDTHPDIITFTYFQLKQAAWVWTAKRGPCSVSCGAGLRWVITYSCDQA
<i>Rattus norvegicus</i>	GKVYRRYGGEYGLDTHPDIITFTYFQKQAAWVWAAKRGPCSVSCGAGLRWVITYSCDQA
<i>Papio anubis</i>	IQVYRRYGGEYGNLTPDITFTYFQPKPRQAWVWAAVRGPCSVSCGAGLRWVINYSCLDQA
<i>Homo sapiens</i>	IQVYRRYGGEYGNLTPDITFTYFQPKPRQAWVWAAVRGPCSVSCGAGLRWVINYSCLDQA
<i>Gorilla gorilla</i>	IQVYRRYGGEYGNLTPDITFTYFQPKPRQAWVWAAVRGPCSVSCGAGLRWVINYSCLDQA
<i>Pan troglodytes</i>	IQVYRRYGGEYGNLTPDITFTYFQPKPRQAWVWAAVRGPCSVSCGAGLRWVINYSCLDQA
<i>Ovis aries</i>	GRPCRRPGLAEXSPARPDIITFTYFQPEQRRAWAWAALRGPCSVSCGAGLRQVITYSCWDQS
<i>Bos taurus</i>	IQVYRRYSEYGSARPDIITFTYFQPEQRRAWAWAVVQGPCSVSCGAGLRQVITYRCRDQS

Mutation p.A609T

<i>Mus musculus</i>	PCPARWETQVLAPCPVTCGGGRVPLSVRLVQL--DRGHPISVPHSKCSPVPKPQSFEDCS
<i>Rattus norvegicus</i>	PCPARWETRVLAPCPVTCGGGRVPLAHCVQL--DHGRPVSVPHSKCWPAPRPGSFEDCS
<i>Papio anubis</i>	PCPARWQYK-LAACSVCGEVMMRRIILYCARAHGEDDEEILLDTQCQGLPRPEPQEVCS
<i>Homo sapiens</i>	PCPARWQYK-LAACSVCGRGVRRRIILYCARAHGEDDGEILLDTQCQGLPRPEPQEAACS
<i>Gorilla gorilla</i>	PCPARWRYK-LAACSVCGGGVRRRIILYCARAHGEDDGEILLDTQCQGLPRPEPQEAACS
<i>Pan troglodytes</i>	PCPARWRYK-LAACSVCGGGVRRRIILYCARAHGEDDGEILLDTQCQGLPRPEPQEAACS
<i>Ovis aries</i>	PCPARWRYK-LAACSLSCGGVAQRILYCARAHGEDTDEEILLPDTQCQGLPRPEPQEAACS
<i>Bos taurus</i>	PCPARWETRALAPCPVTCGGGQVPLAVRCVVM--DQGRVLSLPHSKCWPMPRPTLEDCS

Mutation p.C977F

<i>Mus musculus</i>	PEPCPAR-----
<i>Rattus norvegicus</i>	PEPCPAR-----
<i>Papio anubis</i>	LEPCPPRWKVTSLGPCSASCLGLTARRSVACVQLDQGDVEVDEAACALVLPQASVPCL
<i>Homo sapiens</i>	LEPCPPRWKVMVSLGPCSASCLGLTARRSVACVQLDQGDVEVDEAACALVLPQASVPCL
<i>Gorilla gorilla</i>	LEPCPPRWKVMVSLGPCSASCLGLTARRSVACVQLDQGDVEVDEAACALVLPQASVPCL
<i>Pan troglodytes</i>	LEPCPPRWKVMVSLGPCSASCLGLTARRSVACVQLDQGDVEVDEAACALVLPQASVPCL
<i>Ovis aries</i>	PGPCPPRWKVTSLGPCSASCLGLGTATRSVACVRLDRGQDTEVDRAACAGLVLPQASIPCI
<i>Bos taurus</i>	LEPCPARWKVTSLGPCSASCLGLTATRSVACVRLDRGQDTEVDGAACAGLVLPQASIPCI

Mutation p.R1060W

3.3.2 FOLD X

The FOLD X scores for mutations and SNPs can be seen in Table 3.2.

Table 3.2 FOLD X $\Delta\Delta G$ scores for mutations and SNPs

Mutation	$\Delta\Delta G$ value prediction (kcal/mol)	Effect on stability of mutation
p.R102H (G305A)	No reliable structural information	
p.T196I (C587T)	No reliable structural information	
p.D217H (G649C)	No reliable structural information	
p.Q436H (G1308C)	0.29	No effect on protein stability
p.R398C (C1192T)	No reliable structural information	
p.R409W (C1225T)	7.95	Severely reduces protein stability
p.Q436H (G1308C)	0.29	No effect on protein stability
p.A596V (C1787T)	1.92	Reduces protein stability
p.A690T (G2068A)	No reliable structural information	
p.C977R (G2930T)	No reliable structural information	
p.R1060W (C3178T)	No reliable structural information	
SNP		
p.R7W (C19T)	No reliable structural information	
p.Q448E (C1342G)	No reliable structural information	
p.P475S (C1423T)	1.70	Reduces protein stability
p.P618A (C1852G)	3.95	Reduces protein stability
p.A732V (C2195T)	No reliable structural information	
p.A900V (C2699T)	No reliable structural information	
p.A1033T (G3097A)	No reliable structural information	

As summarised in Table 3.2, the following mutations and SNPs were found to reduce protein stability (see Figures 3.1-3.4):

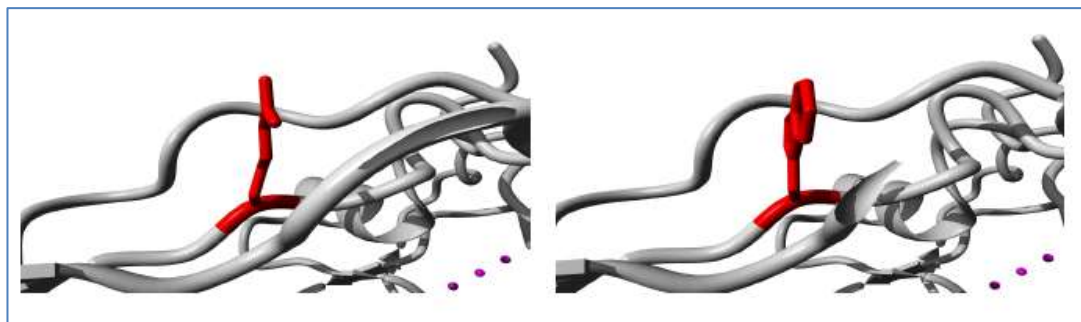


Figure 3.1 Mutation p.R409W from FOLD X analysis: molecular visualisation of the wild type (left) and the variant p.R409W (right) mutation. The residue coloured in red represents the wild type (arginine) and variant residue (tryptophan) respectively.

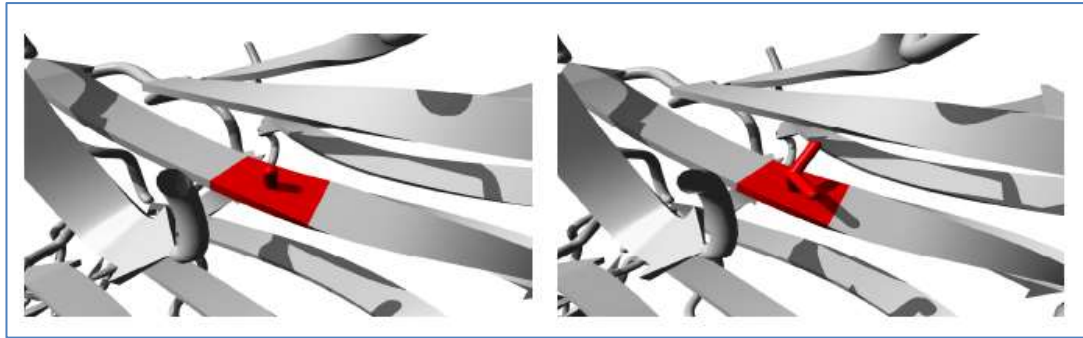


Figure 3.2 Mutation p.A596V from FOLD X analysis: molecular visualisation of the wild type (left) and the variant p.A596V (right) mutation. The residue coloured in red represents the wild type (alanine) and variant residue (valine) respectively.

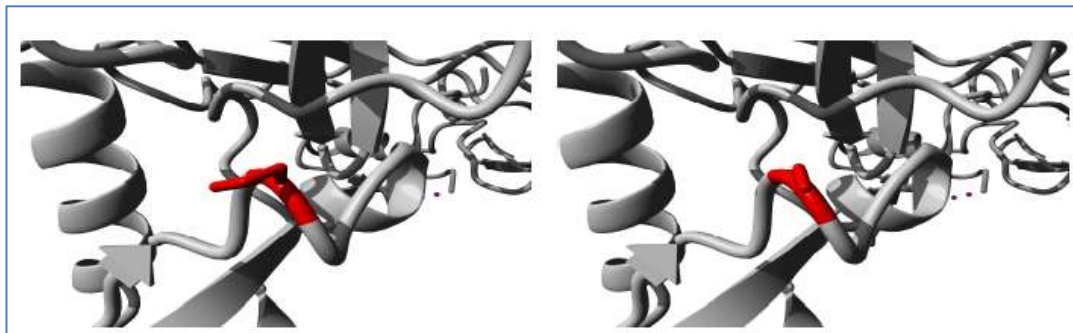


Figure 3.3 SNP p.P475S from FOLD X analysis: molecular visualisation of the WT (left) and the variant p.P475S (right) SNP. The residue coloured in red represents the wild type (proline) and variant residue (serine) respectively.



Figure 3.4 SNP p.P618A from FOLD X analysis molecular visualisation of the wild type (left) and the variant P618A (right) SNP. The residue coloured in red represents the wild type (proline) and variant residue (alanine) respectively.

Table 3.3 Summary of SNP Effect 4.0: FOLD X findings

Mutation	Effect
C1787T p.A596V	Amno acid substitution reduces protein stability
C1308C p.Q436H	Amno acid substitution has no effect on protein stability
C1225T p.R409W	Amno acid substitution i severely reduces protein stability
C1423T p.P475S	Amno acid substitution reduces protein stability
C1852G p.P618A	Amno acid substitution reduces protein stability

All other mutations: no reliable structural informatio

3.3.3 I-Mutant2.0

The results from the I-Mutant 2.0 analysis of mutations and SNPs can be seen in Table 3.4.

Table 3.4 Results from I-Mutant algorithm for mutations and SNPs . $\Delta G = Dg$ (new protein) – ΔG (wild type). The mutation is said to destabilize the protein if $\Delta\Delta G < -0.5$ kcal/mol or largely stabilize if $\Delta\Delta G > +0.5$ kcal/mol. Neutral stability is between $\Delta\Delta G -0.5$ and 0.5 kcal/mol

Mutation	$\Delta\Delta G$ value (kcal/mol)	prediction	Effect on stability of mutation
p.R102H (G305A)	-1.24		Large decrease
p.T196I (C587T)	-0.29		Neutral
p.D217H (G649C)	0.24		Neutral
p.Q436H (G1308C)	-0.49		Neutral
p.R398C (C1192T)	-0.99		Decrease
p.R409W (C1225T)	-0.44		Neutral/decrease
p.A596V (C1787T)	-0.07		Neutral
p.A690T (G2068A)	-0.38		Neutral
p.C977R (G2930T)	-0.04		Neutral
p.R1060W (C3178T)	-0.19		Neutral
SNP			
p.R7W (C19T)	-0.1		Neutral
p.Q448E (C1342G)	0.14		Neutral
p.P475S (C1423T)	-1.5		Large decrease
p.P618A (C1852G)	-1.8		Large decrease
p.A732V (C2195T)	0.02		Neutral
p.A900V (C2699T)	-0.03		Neutral
p.A1033T (G3097A)	-0.59		Decrease

3.3.4 Sorting intolerant from tolerant (SIFT) analysis

The results of the SIFT analysis predicts whether the amino acid substitution will be damaging or not. The scores range from 0 - 1 and is the scaled probability of the substitution being tolerated. Those falling below 0.05 are predicted to alter the protein function (Kumar *et al.*, 2009). The median info content is the conservation value for a position ranging from 0, when all amino acids are observed at a position in the alignment to $\log_2 20$ (=4.32) when only one amino acid is observed at that position. The SIFT scores for mutations and SNPs can be seen in Table 3.5.

Table 3.5 SIFT scores for mutations and SNPs

Mutation	Prediction	SIFT score	Median info content
p.R102H (G305A)	Tolerated	0.28	2.12
p.T196I (C587T)	Damaging	0	2.09
p.D217H (G649C)	Tolerated	0.08	2.09

p.Q436H (G1308C)	Tolerated	0.18	2.09
p.R398C (C1192T)	Damaging	0	2.11
p.R409W (C1225T)	Damaging	0	2.08
p.A596V (C1787T)	Tolerated	0.28	2.09
p.A690T (G2068A)	Tolerated	0.62	2.09
p.C977R (G2930T)	Damaging	0	2.15
p.R1060W (C3178T)	Damaging	0	2.17
SNP			
p.R7W (C19T)	Tolerated	0.09	4.32
p.Q448E (C1342G)	Tolerated	2.09	2.09
p.P475S (C1423T)	Tolerated	0.6	2.10
p.P618A (C1852G)	Tolerated	0.14	2.17
p.A732V (C2195T)	Tolerated	0.26	2.11
p.A900V (C2699T)	Tolerated	0.29	2.17
p.A1033T (G3097A)	Tolerated	2.15	2.15

3.3.5 PolyPhen2.0

The results of the analysis of mutations and SNPs by PolyPhen2.0 can be seen in Table 3.6.

Table 3.6 Results of PolyPhen2.0 analysis for mutations and SNPs (based on HumDiv)

Mutation	Prediction	Score	Sensitivity*	Specificity*
p.R102H (G305A)	Probably damaging	1	0	1
p.T196I (C587T)	Probably damaging	1	0	1
p.D217H (G649C)	Probably damaging	1	0	1
p.Q436H (G1308C)	Probably damaging	1	0	1
p.R398C (C1192T)	Probably damaging	1	0	1
p.R409W (C1225T)	Possibly damaging	0.597	0.87	0.91
p.A596V (C1787T)	Probably damaging	1	0	1
p.A690T (G2068A)	Possibly damaging	0.597	0.87	0.91
p.C977R (G2930T)	Probably damaging	0.997	0.41	0.98
p.R1060W	Probably damaging	0.998	0.27	0.99
SNP				
p.R7W (C19T)	Benign	0	1	0
p.Q448E (C1342G)	Benign	0	1	0
p.P475S (C1423T)	Benign	0.024	0.95	0.81
p.P618A (C1852G)	Probably damaging	1	0	1
p.A732V (C2195T)	Possibly damaging	0.949	0.79	0.95
p.A900V (C2699T)	Benign	0	1	0
p.A1033T	Possibly damaging	0.14	0.14	0.99
p.C977R (G2930T)	Probably damaging	0.997	0.41	0.98
p.R1060W	Probably damaging	0.998	0.27	0.99
p.A1033T	Possibly damaging	0.14	0.14	0.99

Scores between 0.0-0.15 are predicted to be benign; scores between 0.15-1.0 are predicted to be possibly damaging and 0.85-1.0 are more confidently predicted to be damaging

*Sensitivity denotes the true positive rate and specificity is 1 minus the false positive rate.

Highlighted SNPs are predicted to be benign.

3.3.6 Frequency of SNPs in the population

3.3.6.1 The European population

The Exome Aggregation consortium (ExAC) is a coalition of investigators seeking to aggregate and harmonise exome sequencing data from a variety of large-scale sequencing projects. The data set spans 60,706 unrelated individuals sequenced as part of various disease-specific and population genetic studies (Lek *et al.*, 2016). Results of the frequency of SNPs in the European population can be seen in Tables 3.7.

Table 3.7 Frequencies of SNPs in the European population (from: ExAC)

SNP	dbSNP accession number	Allele count	Allele no.	No. homozygous	Allele frequency
p.R7W	rs34024143	11387	121274	691	0.09389
p.Q448E	rs2301612	18000	35440	3655	0.5079
p.P475S	rs11575933	78	29234	1	0.00266
p.P618A	rs28647808	6559	72646	327	0.09287
p.A732V	rs41314453	1095	71486	11	0.1553
p.A900V	rs685523	10062	115078	532	0.08744
p.A1033T	rs28503257	3182	72598	61	0.0438

3.3.6.2 The global population

The frequency of SNPs in the global population can be seen in Table 3.8 (dbSNP <[http:// www.ncbi.nlm.nih.gov/snp](http://www.ncbi.nlm.nih.gov/snp)> [accessed 10/6/2017]).

Table 3.8 Frequency of SNPs in the global population (based on minor allele frequency, MAF)

SNP	dbSNP accession number	Frequency in global population	Annotation (clinical significance)
p.R7W ¹	rs34024143	0.0527	Likely benign
p.Q448E ²	rs2301612	0.2716	Pathogenic
p.P475S ²	rs11575933	0.0561	Likely benign
p.P618A ¹	rs28647808	0.0323	Likely benign
p.A732V ¹	rs41314453	0.0056	Likely benign
p.A900V ³	rs685523	0.0765	Likely benign
p.A1033T ¹	rs28503257	0.0156	Likely benign

Validation by: ¹ 1000G, cluster, frequency; ² 1000G, 2hit 2allele, cluster, frequency, hapmap; ³ 1000G, hapmap, cluster, frequency.

3.3.7 Predict SNP

The results of analysis by Predict SNP with annotations can be seen in Table 3.9.

Table 3.9 Summary of prediction and expected accuracy of prediction for each analytical tool

	PolyPhen 1	PolyPhen 2	MAPP	PhD-SNP	SIFT	SNAP
Expected accuracy	68.1%	69.2%	70.7%	71.5%	70.3%	67.6%

Mutations	PolyPhen 1	PolyPhen 2	MAPP	PhD-SNP	SIFT	SNAP
R102H	Neutral 67%	Neutral 70%	Neutral 79%	Neutral 72%	Deleterious 53%	Deleterious 56%
T196I	Deleterious 74%	Deleterious 68%	Deleterious 57%	Deleterious 82%	Deleterious 79%	Deleterious 72%
D217H	Neutral 61%	Deleterious 56%	Neutral 72%	Neutral 66%	Neutral 68%	Deleterious 72%
R398C	Deleterious 74%	Deleterious 81%	Neutral 64%	Deleterious 86%	Deleterious 79%	Deleterious 85%
R409W	Deleterious 74%	Deleterious 81%	Deleterious 56%	Deleterious 86%	Deleterious 79%	Deleterious 85%
Q436H	Neutral 67%	Deleterious 46%	Neutral 77%	Neutral 58%	Neutral 76%	Deleterious 56%
A596V	Neutral 67%	Deleterious 65%	Deleterious 48%	Deleterious 88%	Deleterious 79%	Deleterious 56%
C977F	Deleterious 74%	Deleterious 81%	Deleterious 66%	Deleterious 86%	Deleterious 79%	Deleterious 85%
R1060W	Deleterious 59%	Deleterious 40%	Deleterious 57%	Deleterious 86%	Deleterious 79%	Deleterious 72%
SNP						
R7W	Neutral 67%	Neutral 87%	Neutral 70%	Neutral 72%	Neutral 60%	Deleterious 68%
Q448E	Neutral 67%	Neutral 72%	Neutral 77%	Neutral 78%	Neutral 90%	Neutral 77%
P475S	Neutral 67%	Neutral 69%	Neutral 85%	Deleterious 82%	Neutral 67%	Neutral 77%
P618A	Neutral 67%	Deleterious 41%	Neutral 70%	Neutral 78%	Deleterious 79%	Neutral 58%
A732V	Neutral 67%	Neutral 68%	Neutral 75%	Neutral 89%	Neutral 61%	Neutral 71%
A1033T	Neutral 67%	Neutral 70%	Neutral 68%	Neutral 66%	Deleterious 53%	Deleterious 62%
A900V	Neutral 67%	Neutral 79%	Neutral 73%	Neutral 83%	Neutral 90%	Neutral 83%

Mutation	PredictSNP	Amino acid change
R102H (G305A)	Neutral 65%	Arginine (polar basic) → histidine (polar basic) No annotation
T196I (C587T)	Deleterious 87%	Threonine (polar neutral) → Isoleucine (hydrophobic non polar) Annotation: natural variant in TT dbSNP rs121908470
D217H (G649C)	Neutral 63%	Aspartic acid (polar acidic) → histidine (polar basic) No annotation
R398C (C1192T)	Deleterious 76%	Arginine (polar basic) → cysteine (polar neutral SH) No annotation
R409W (C1225T)	Deleterious 87%	Arginine (polar basic) → tryptophan (non-polar aromatic) No annotation
Q436H (G1308C)	Neutral 65%	Glutamine (polar neutral) → histidine (polar basic) No annotation
A596V (C1787T)	Deleterious 72%	Alanine (hydrophobic non polar) → valine (hydrophobic non-polar) Annotation: natural variant in TTP dbSNP, rs281875299
C977F (G2930T)	Deleterious 87%	Cysteine (polar neutral S) → phenylalanine (hydrophobic aromatic) No annotation
R1060W (C3778T)	Deleterious 87%	Arginine (polar basic) → tryptophan (hydrophobic aromatic) Annotation: in TTP affects protein secretion, the mutant protein has reduced activity: dbSNP rs142572218
SNP		
R7W	Neutral 75%	Arginine (basic) → tryptophan (non-polar aromatic) Annotation: does not affect protein secretion, dbSNP rs34024143
Q448E (C1342G)	Neutral 83%	Glutamine (neutral polar) → glutamic acid (polar acidic) Annotation: natural variant, does not affect protein secretion, normal proteolytic activity dbSNP rs2301612
P475S (C1423T)	Neutral 75%	Proline (hydrophobic kinky) → Serine (polar neutral) Annotation: natural variant in dbSNP rs11575933
P618A (C1852G)	Neutral 63%	Proline (hydrophobic kinky) → Alanine (hydrophobic) Annotation: natural variant rs28647808
A732V (C2195T)	Neutral 83%	Alanine (hydrophobic) → valine (hydrophobic) Annotation: natural variant in dbSNP rs41314453
A900V (C2699T)	Neutral 83%	Alanine (hydrophobic) → valine (hydrophobic) Annotation: natural variant in dbSNP rs685523
A1033T (G3097A)	Neutral 63%	Alanine (hydrophobic) → threonine (polar neutral) Annotation: natural variant in dbSNP rs 28503257

3.4 Discussion

The prediction of protein structures and the effect a variant will have on the expression and secretion of a protein is very challenging and cannot be considered proof that the predicted structures will form and produce the

predicted effects. However, when backed up by experimental data it can be a useful form of analysis and direct further research. Additionally, a single variant should not be compared to coupled variants within a frequently seen haplotype as there may be some functional synergistic effects (Plaimauer *et al.*, 2006). With respect to variants seen in rare diseases such as congenital TTP, the information regarding the frequency of these variants in different populations is scarce and detailed analysis will not be undertaken until additional data is obtained by sequencing a significant number of patient populations.

This study has analysed the predicted effects of several single mutations and SNPs identified in patients within the UK TTP Registry (Camilleri *et al.*, 2012) where the clinical information is known. Several *in silico* tools have been employed which have looked at changes in $\Delta\Delta G$ estimates of the variants, indicating if the substitution will affect protein stability (I-Mutant and SNP Effect). The degree of the conservation of residues within a protein sequence (MUSCLE alignment of orthologs, SIFT and PolyPhen2.0) has also been analysed, with varying degrees of correlation.

The basic premise that substitutions in highly conserved areas will have a significant effect on protein function has been applied by looking at the MUSCLE alignment between eight species (Table 3.1). Single nucleotide polymorphisms were originally defined as codon substitutions that occur in >1% of the population and are found across the entire human genome coding sequence (Edwards *et al.*, 2012). As such, it may be considered that these polymorphisms contribute to natural variation and are not under significant evolutionary selection pressures. However, SNPs are now classified as genomic variants and it may now no longer be possible to distinguish between SNPs and mutations based on their frequency (Sherry *et al.*, 2001).

3.4.1 Analyses of polymorphisms

The alignment for the SNP p.R7W can be seen in Figure 3.1. This variant (highlighted in yellow) lies within the signal peptide area of the ADAMTS13 protein and, as can be seen, the region shows variance between species and

this area is not highly conserved. In the estimation of $\Delta\Delta G$ using I-Mutant (there is no PDB structure for this region of the protein), the substitution of arginine (a polar, positively charged amino acid) for tryptophan (an aromatic, non-polar amino acid) at this position does not result in a significant Gibbs free energy change and is considered neutral. Using the PredictSNP analysis, the variant is tolerated and considered neutral, which would be expected for a polymorphism occurring at a frequency of 0.0527 of the global population.

The polymorphism p.Q448E, with the substitution of glutamine (a neutral amino acid) for glutamic acid (an acidic, charged amino acid) lies within a more conserved region (see Figure 3.1), which is within the cysteine-rich domain of the protein. As there is no PDB structure for this domain, based on I-Mutant analysis using the amino acid sequence only, it is predicted that there is no change in Gibbs free energy for this substitution. SIFT, PolyPhen2.0 and PredictSNP analyses predict the variant is tolerated, benign and neutral, which is as expected for a SNP with a frequency of 0.217 of the global population.

The polymorphism p.P475S is within a more variable region with respect to the MUSCLE alignment (see Figure 3.1). The variant is within the ADAMTS13 cysteine-rich domain with the substitution of proline (with a hydrophobic kink) for serine (polar and neutral); (see Figure 3.4). As there is structural data on this region, the amino acid substitution has been predicted by SNPEffect and I-Mutant to result in a $\Delta\Delta G$ of +1.7kcal/mol and +1.5kcal/mol respectively, destabilising the protein structure. However, SIFT, PolyPhen2.0 and PredictSNP have predicted the variant to be benign and neutral. The SNP occurs in 0.0561 of the global population, which could indicate a level of selection pressure.

Interestingly, the polymorphism p.P618A, which substitutes proline (a cyclic, non-polar amino acid) for alanine (a hydrophobic amino acid) at amino acid 618 lies within the spacer domain and is also found in a more variable area as seen in Figure 3.5. This SNP has been predicted to induce a $\Delta\Delta G$ of +3.95 and +1.8kcal/mol by SNPEffect and I-Mutant respectively. The variant is predicted to be tolerated by SIFT but probably damaging, with a score of 1, by

PolyPhen2.0. Predict SNP predicts this variant to be likely benign clinically. This data suggests the substitution will reduce protein stability. The SNP occurs at a global frequency of 0.032 but has been reported only in the Japanese population. In expression studies the SNP has been associated with a decrease in secretion levels of ADAMTS13 (Kokame *et al.*, 2002; Plaimauer *et al.*, 2006).

The polymorphism p.A732V, which substitutes alanine (a hydrophobic amino acid) for valine (similarly hydrophobic), is found within the TSP1-2 domain. As can be seen from Figure 3.1, alanine is conserved at this position among species but lies within a more variable area. As there is no structural data for this region of the protein, I-Mutant predicted the substitution to be neutral with no significant $\Delta\Delta G$ based on the amino acid sequence. The variant has been predicted to be tolerated by SIFT. However, it has been predicted to be probably damaging by PolyPhen2.0 with a score of 0.949. This score carries a high false positive rate, with a specificity of 0.95. PredictSNP has annotated this SNP as likely benign clinically. The SNP occurs with a frequency of 0.0056 of the global population which indicates there may be some selection pressure on the SNP.

The polymorphism p.A900V also substitutes alanine for valine and is located in the TSP1-6 domain of the protein. The amino acids in this area are moderately conserved across orthologs (see Figure 3.7) and it has been predicted on the amino acid sequence that there will be no significant $\Delta\Delta G$ increases. SIFT and PolyPhen2.0 analyses predict the polymorphism to be benign and tolerated, which is to be expected in an SNP with a frequency of 7.6% of the global population.

The final polymorphism to be analysed appearing in this group of patients is p.A1033T, which substitutes alanine (a hydrophobic amino acid) for threonine (a hydrophilic amino acid but similar in size to valine) and is located in the TSP1-7 domain of the protein. It is in an amino acid region that is conserved among primates, as seen in MUSCLE alignment (see Table 3.1). There is no structural data for this region of the protein but it has been predicted by I-

Mutant to decrease the structural stability of the protein with a change in $\Delta\Delta G$ of 0.59kcal/mol. On SIFT analysis the substitution is predicted to be tolerated but has been predicted to be possibly damaging by PolyPhen2.0. PredictSNP has annotated this SNP as likely benign However, this is based on a sensitivity score of 0.14 (true positive) which is very low. The SNP occurs in the global population at a frequency of 0.0156.

3.4.2 Analyses of mutations

As missense mutations have been previously been classified as those substitutions causing a change in the amino acid sequence and occur in <1% of the population, it may be assumed that mutations are deleterious and are under considerable evolutionary selection pressures. It may also be assumed that these mutations occur in highly conserved areas of the protein and cause a change in the protein structure, leading to a decrease in activity or secretion of the protein. The mechanism by which this occurs may be due to the decreased structural stability of the protein, leading to enhanced degradation and clearance by the cellular quality control pathways.

The mutation p.R102H was identified as a novel homozygous mutation in a pregnant patient who had three previous live births (Camilleri *et al.*, 2012). As the clinical phenotype can be classified as late-onset, the mutation may not be considered significantly deleterious. The missense mutation is located in the metalloproteinase domain of the protein. This region is highly conserved, as can be seen in Table 3.1. There is no reliable structural data on this domain but from the amino acid sequence it has been predicted to have a large effect on $\Delta\Delta G$ and destabilise the protein (see Table 3.4). However, as can be seen in Table 3.9, it has been predicted to be deleterious only by SIFT and SNAP and overall neutral by PredictSNP.

The mutation p.T196I was found in a three-year-old patient who needed PT prophylaxis treatment as required. Due to the early onset of TTP in this patient, the mutation would be expected to have a significant deleterious effect. The mutation p.T196I is found within the metalloproteinase domain and again there

is no structural information on this region. From Table 3.1 it can be seen that the mutation lies within a highly conserved area across species. On analysis by I-Mutant, the substitution is not predicted to produce a significant change in $\Delta\Delta G$ hence the resultant protein would not be destabilised. However, Predict SNP has annotated the mutation to be deleterious with all prediction tools and this is seen in the clinical phenotype.

The mutation p.D217H was identified in an 18-month-old patient who required FFP prophylaxis treatment infrequently, mainly as a response to severe infection. The mutation is located within the metalloproteinase domain and lies within a highly conserved area (see Table 3.1) within the amino acid sequence. Based on the clinical and alignment data, this mutation would be expected to be deleterious. There is no reliable structural information on this area of the protein but based on I-Mutant analysis the substitution was not predicted to lead to a significant $\Delta\Delta G$ and destabilise the protein. The mutation has been predicted to be deleterious with PolyPhen and SNAP predictive tools but overall to be neutral.

The mutation p.R409W was identified in a patient who showed a more severe clinical phenotype and presented as a neonate, requiring plasma therapy prophylaxis treatment every 1-2 weeks. From the alignment (Table 3.1) the mutation lies within a conserved area in the TSP1-1 domain. Structural data is available for this domain. On analysis by FOLDX, a predicted Gibbs free energy change of 7.75 kcal/mol, predicted the mutation to severely reduce protein stability. The $\Delta\Delta G$ was predicted to be less with I-Mutant (0.44 kcal/mol) but still predicted to affect protein stability. The mutation was also predicted to be deleterious by all tools in Predict SNP. This is aligned to the clinical phenotype.

The mutations p.R398C and p.Q436H were identified as a compound heterozygote in a neonatal patient who presented with a severe clinical phenotype, requiring PT prophylaxis every 1-2 weeks. Both mutations lie within conserved regions (see Table 3.1) which would concur with the clinical phenotype. The p.R398C mutation, lies within the TSP1-1 domain. The

p.Q436H mutation also lies within the TSP1-1 domain. There is no reliable structural information for the p.R398C mutation but based on structural data, p.Q436H is predicted not to result in a $\Delta\Delta G$ thus having no effect on protein stability. Based on the amino acid sequence alone predicted by I-Mutant, p.R398C decreases $\Delta\Delta G$ whereas p.Q436H has no effect. Both mutations are predicted to be deleterious by Predict SNP.

The mutation p.A596V was identified in a pregnant patient, together with another novel mutation p.R1095Q and SNP p.P475S as a compound heterozygote. She had a clinical history of no live births. Another 18-month-old patient also had the p.A596V mutation in homozygous form. The p.A596V mutation is found in a conserved region (see Table 3.1) so would be expected to be deleterious. The p.A596V is found within the spacer domain. Structural data is available and the mutation is predicted to induce a $\Delta\Delta G$ of 1.92kcal/mol with a resultant decrease in protein stability by SNPEffect. However, it is not predicted to have a significant effect by I-Mutant. On analysis by SIFT, the mutation is predicted to be deleterious by Predict SNP. This mutation was identified both in a late-onset TTP patient and an 18-month-old child in homozygous form thus this conflicting analysis may be borne out by the clinical data.

The mutation p.A690T was found as a compound heterozygous genotype (together with the deletion mutation C241_C242del) in a pregnant patient who had a clinical history of one live birth and four losses. The A690T mutation is found in a relatively conserved area of the protein (see Table 3.1). The mutation is found within the TSP1-2 domain of the protein. There is no structural data available for this region but the substitution was predicted to have no significant effect on $\Delta\Delta G$ by I-Mutant. It is predicted to be tolerated by SIFT and possibly damaging by PolyPhen2.0. This was found in a patient with late-onset symptoms as a compound heterozygote, together with a deletion mutation. These results affirm the clinical phenotype.

The final mutation to be analysed, p.C977F, was found in a pregnant patient with a clinical history of one live birth. This indicates that this is not a clinically

severe mutation. The mutation, involving the substitution of the residue cysteine (which is polar and can form disulphide bonds with other cysteine residues and is involved in protein stabilization) with phenylalanine (an aromatic hydrophobic residue which is often located in the interior structure of proteins), is found within the TSP1-5 domain of the protein. The amino acid lies within a moderately conserved area (see Table 3.1). There is no reliable structural information available but I-Mutant has predicted the substitution to be neutral, with no significant change in $\Delta\Delta G$. However, Predict SNP has annotated this mutation as deleterious with all predictive tools.

The mutation p.R1060W is analysed and discussed in Chapter 4.

3.5 Concluding remarks

From the *in silico* analysis of mutations and SNPs using various predictive tools, it can be concluded that the effect of SNPs on the expression of ADAMTS13 will be minimal and have no appreciable clinical effect on the phenotype of TTP patients. However, the effect of the mutations p.T196I, p.R398C, p.R409W, p.596V, C977F and p.R1060W on the phenotype of patients will be clinically significant and have a deleterious effect. The mutations p.R102H, p.D217H and p.Q436H have been predicted to have a neutral effect on clinical phenotype.

In silico tools can be a useful adjunct to experimental data but as they are predictors of structure and function, the results should be interpreted with a degree of caution. It is important to understand the algorithms that are used and the degree of sensitivity and specificity. Further discussion can be found in Chapter 6.

Chapter 4

Pregnancy-associated congenital TTP (Upshaw-Schulman syndrome)

4.1 Introduction

4.1.1 Thrombotic microangiopathies

Thrombotic microangiopathies (TMA) are a group of haemolytic disorders characterised by thrombocytopenia and microangiopathic haemolytic anaemia (MAHA). Pregnancy is known to be a risk factor for the development of TMA, with an incidence of 1 in 25,000 – 100,000 deliveries. This represents 25% of TMA cases in adults (Kentouche *et al.*, 2013). Pregnancy-associated TTP shares similar clinical features but different aetiologies with other TMA disorders such as HELLP syndrome (haemolysis, elevated liver enzymes and low platelet count) and HUS (haemolytic uraemic syndrome), which can make differential diagnosis between these conditions a challenge.

4.1.1.1 Thrombotic thrombocytopenic purpura

The overall prevalence of congenital TTP or Upshaw Schulman syndrome (USS) is 4 -10 cases per million per year and the global mortality rate for both inherited and acquired forms is 20 %, in spite of advances in treatment and diagnosis (Veyradier *et al.*, 2012). The incidence of TTP occurring in pregnancy was found to be much higher than in the general population; in a recent study the occurrence was documented as 1 in 200,000 (Scully *et al.*, 2014). Between 10-30% of cases of TTP were diagnosed during pregnancy or during the post-partum period (Moatti-Cohen *et al.*, 2012; Fujimura *et al.*, 2009).

4.1.1.2 Pregnancy-associated TTP

In the UK over a five-year period, 1% of all maternal deaths were found to be due to TTP (Hunt *et al.*, 2013). A diagnosis of USS is confirmed by low ADAMTS13 activity, the absence of anti-ADAMTS13 antibodies and mutational analysis. The initial presentation is frequently thrombocytopenia, microangiopathic haemolytic anaemia (MAHA) and <13% ADAMTS13 activity

(Scully *et al.*, 2014). If left untreated, mortality remains high for mother and foetus. Pregnancy loss is usually seen in the second trimester caused by inadequate placental function, leading to severe intrauterine growth retardation and foetal loss (Scully *et al.*, 2014). The organs involved in microangiopathic damage are the kidneys, heart, brain and placenta. In TTP patients with foetal loss, all had placental infarction (Kentouche *et al.*, 2013). Plasma therapy (PT) remains the only treatment for USS and the risk of recurrence in subsequent pregnancies is 100% in the absence of PT prophylactic treatment.

Women with the inherited TTP present more frequently in pregnancy compared with those with the acquired form of TTP (Scully *et al.*, 2014). However, pregnancy has been found not to be a risk factor for acquired TTP (Tsai, 2010). Clinically, late-onset TTP appears to follow a quiescent course until a major physiological stress such as pregnancy brings on the first manifestations of the disease. In the majority of cases, no signs and symptoms develop before pregnancy but it has been found that 20% of patients required regular plasma therapy after delivery (Scully *et al.*, 2014). This suggests that genotype alone cannot explain this clinical effect, indicating other environmental factors may be involved.

In a publication of the French TMA Registry, an unexpectedly high frequency of pregnancy-associated TTP was found (24%, or 10 out of 42 cases), with eight out of ten cases being heterozygous carriers of the p.R1060W mutation (Moatti-Cohen *et al.*, 2012). The stillbirth rate in the French cohort was stated as 40% for patients with TTP, with the majority of cases becoming symptomatic in the late-second or early-third trimester. A worse prognosis was associated with the earlier onset of TTP (Fujimura *et al.*, 2009).

In another recent systematic review (Veyradier *et al.*, 2012), 350 cases of TTP or TTP/HUS appeared in the English language literature. However, many cases were not systematically investigated for ADAMTS13 antigen or activity level. Between 1976 and 2011, 32 patients were documented with pregnancy-associated TTP (although eight patients were not assessed for ADAMTS13

levels). In the remaining 24 patients, the level of ADAMTS13 was <10 %, with no anti-ADAMTS13 antibodies present. Fifteen of these cases were genotyped and six cases carried the p.R1060W mutation, either in heterozygous or homozygous form. Interestingly, these cases were seen in the Western world only (Europe or North America). In the nine remaining cases, which were recorded in Japan, miscellaneous mutations were seen. The p.R1060W mutation has not been found in Japanese patients (Fujimura *et al.*, 2009).

4.2 Pathophysiology of pregnancy-associated TTP

4.2.1 Genotype of pregnancy-associated TTP

Patients diagnosed with TTP have been observed on all continents of the world. More than 120 different mutations have been documented, the majority of which are confined to single families. In a study in Norway, patients with homozygous mutations were encountered in areas with a high prevalence of consanguinity (von Krogh *et al.*, 2016). However, two mutations observed in TTP patients of European ancestry were exceptions to this: the frameshift mutation c4143_4144 dupA, which induces a premature termination of the protein at amino acid 1386 and the p.R1060W mutation in exon 24. The p.R1060W lies within the TSP1-7 domain in the ADAMTS13 protein and is a missense mutation with the substitution of arginine with tryptophan (see Figure 4.1).

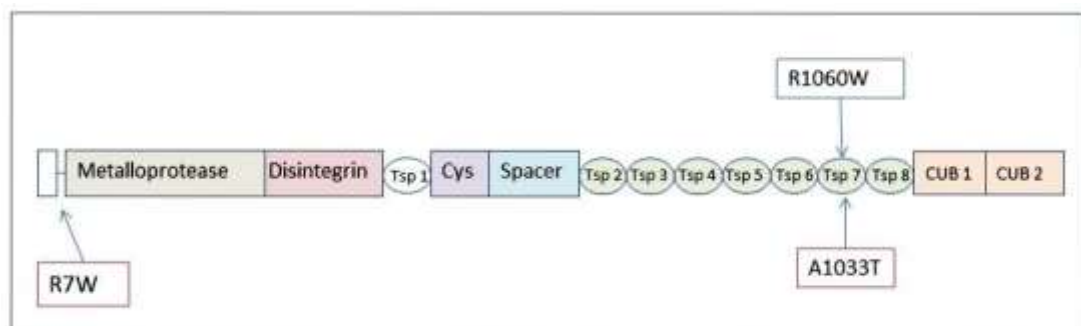


Figure 4.1 Position of the mutation p.R1060W and SNPs p. R7W and p.A1033T within the ADAMTS13 protein

The p.R1060W mutation has been genotyped in patients from Turkey, Central Europe, Scandinavia, Europe and in North Americans of European descent (von Krogh *et al.*, 2016). It causes impaired secretion but has been associated with some residual activity in plasma. The mutation in relation to late-onset TTP was first identified in 2006 (Tao *et al.*, 2006) in a 34-year-old male patient who was compound heterozygous for p.R1060W and a deletion mutation (C365del). The patient had been diagnosed with idiopathic thrombocytopenic purpura as a young adult and was diagnosed with TTP 14 years later. The mutation p.R1060W was subsequently identified by Camilleri *et al.* in a cohort of TTP patients and was identified in six out of 53 cases. Three patients had pregnancy-associated USS and three had chronic/relapsing USS. One patient was homozygous for the p.R1060W mutation and the other five were heterozygous but had ADAMTS13 activity < 5% at presentation (Camilleri *et al.*, 2008).

In a recent prospective study of TTP cases from the UK TTP Registry, 17 out of 23 patients with USS who showed the initial presentation in pregnancy carried the p.R1060W mutation (Scully *et al.* 2014). Out of these patients, six were homozygous for p.R1060W and 11 were compound heterozygotes for p.R1060W and deletion mutations. The SNPs p.R7W and p.A1033T were also co-inherited and were present in 74% and 70% of cases respectively. This was in contrast to the incidence of these SNPs in healthy European controls of 13% and 2% respectively (Scully *et al.* 2014). These SNPs may be inherited as a haplotype with the p.R1060W mutation.

4.2.2 Location of p.R1060W and SNPs in ADAMTS13

The single nucleotide polymorphism (SNP) p.R7W is located in the propeptide domain. In comparison with other ADAMTS or ADAM proteases, the ADAMTS13 propeptide is only 41 residues long and is exceptionally short compared to the approximate 200 residues in other members of this family (Apte, 2009). The propeptides in members of the ADAMTS family act as molecular chaperones, assisting in the correct protein folding and ensuring latency of the protein until it has been trafficked to the correct destination.

However, the propeptide in ADAMTS13 does not have this function and it has been shown not to be required for the secretion and activation of the protein (Majerus *et al.*, 2003).

The mutation p.R1060W and SNP p.A1033T are located in the distal TSP1-7 domain. The number of TSP repeats in members of the ADAMTS proteases varies, however they have been shown to play a role in substrate recognition and cell surface binding (Apte 2009; Turner *et al.* 2009). The TSP1 domains show post-translational modifications but it is unclear whether these have a function *in vivo* (Zheng, 2013). All contain the amino acid sequence WXXW whereby an α -mannosyl group is attached to the first C2 group of tryptophan (W). Seven of the eight TSP1 groups also contain the conserved sequence CSX(S/T)CG whereby the amino acid at position 4 is modified by the disaccharide Glc-Fuc-O-Ser/Thr (Hofsteenge *et al.*, 2001). TSP1 repeats 5-8 appear to bind native VWF through the D4 domain (Zanardelli *et al.* 2009) and the terminal repeats have been shown to interact with the endothelial cell surface receptor CD36 (Asch *et al.*, 1991). This could lead to enhanced proteolytic cleavage under flow conditions (Vomund & Majerus, 2009). Mutations in this area could disrupt these interactions. A further role of the TSP repeats could be to reduce the force of VWF-mediated platelet adhesion and aggregation. The TSP repeats contain free thiols that may react with free thiols on the surface of ULVWF or plasma VWF exposed under shear stress. This interaction may prevent disulphide bond formation between apposed VWF multimers under these conditions (Yeh *et al.*, 2010).

4.3 Previous expression studies of mutation p.R1060W and SNPs

4.3.1 Expression studies of p.R1060W mutation

In previous expression studies, the catalytic activity of p.R1060W was found to be conserved. Carriers of the p.R1060W mutation have been shown to display small residual amounts of secretion. The level of secretion was found to be 11% of wild type (WT) in HeLa cells (Tao *et al.*, 2006) and < 5% in HEK293T cells (Camilleri *et al.*, 2008). This may reflect inherent differences in protein expression between the different cell lines (HeLa cells are derived from

cervical cancer cells whereas HEK are not) thus no direct conclusions can be made. A study of 29 USS patients from four European centres (Milan, the UK, Bergamo and France) found four unrelated USS patients who were homozygous for this mutation displaying residual ADAMTS13 activity of 5-7% normal plasma (Lotta *et al.*, 2012). All were late-onset presentation with pregnancy being the trigger for the first occurrence of TTP.

4.3.2 Expression studies of p.R7W and p.A1033T SNPs with mutation p.R1060W

The SNPs p.R7W and p.A1033T, together with p.R1060W are often inherited as a haplotype. The presence of SNPs have previously been suggested as modifiers of ADAMTS13 expression (Plaimauer *et al.*, 2006; Camilleri *et al.*, 2008). Levy *et al.* first identified the following SNPs in TTP patients: p.R7W, p.Q448E, p.P618A, p.R625H, p.A732V, p.A900V and p.A1033T. These were also identified in 92 unrelated healthy controls (Levy *et al.*, 2001). Tao *et al.* analysed secretion and activity levels of p.A1033T, which is found in the TSP1-7 domain together with p.R1060W and substitutes alanine for threonine. This SNP was found to conserve secretion and activity by 80% (Tao *et al.*, 2006).

Plaimauer *et al.* also carried out expression studies and analysed the effects of four SNPs: p.R7W, p.Q448E, p.P618A and p.A732V in tandem with a rare mutation p.R1336W. It was shown that the effect of a single amino acid substitution in a mutation or SNP can be interactive, altering the phenotype of ADAMTS13 deficiency (Plaimauer *et al.*, 2006). The SNP p.R7W was found to have no effect on ADAMTS13 secretion singly but acted as a positive modifier in the context of p.P618A and p.A732V, which were known to cause secretory defects. In the context of the mutation p.R1336W, the SNP p.R7W enhanced the detrimental effect of the mutation and led to undetectable enzyme activity. It was also observed that the SNPs p.R7W and p.Q448E ameliorated the defects induced by a combination of the SNPs p.P618A and p.A732V.

Edwards *et al.* also carried out expression studies with SNP p.A1033T (Edwards *et al.*, 2012). It was found that p.A1033T increased secretion of

ADAMTS13 by 35% of WT. From this experimental data, it can be concluded that SNPs contribute to modification of ADAMTS13 expression and could explain the course of milder, late onset phenotypes. However, changes in physiology during pregnancy also need to be considered. These include the effect pregnancy has on the ADAMTS13-VWF axis and also the effect of pregnancy hormones on ADAMTS13 itself, which will be discussed in section 4.9.

4.4 Aims of this study

This study investigated the *in vitro* effect of the individual SNPs p.R7W and p.A1033T singly and in combination with the missense mutation p.R1060W on ADAMTS13 expression levels in order to relate genotype to the late-onset phenotype observed in patients with pregnancy-associated TTP.

4.5 Methods

4.5.1 In silico modelling of mutation p.R1060W and SNPs R7W and A1033T
A full description of *in silico* modelling can be seen in Chapter 3. The conservation of amino acids in the ADAMTS13 protein in the region of the mutation p.R1060W and SNPs p.R7W and p.A1033T was investigated by aligning the amino acid sequence of human ADAMTS13 with the amino acid sequence of ADAMTS13 orthologs using the MUSCLE (Multiple Sequence Comparison by Log-Expectation) alignment tool. The results can be seen in Table 3.1.

The likely effect of the amino acid substitutions of mutation p.R1060W and SNPs p.R7W and p.A1033T was predicted using the following computational based tools: I-Mutant, SIFT, PolyPhen2 and PredictSNP (see Chapter 3). A summary of results can be seen in Table 4.1.

Table 4.1 Summary of *in silico* analysis

Predictive software	p.R1060W	p.R7W	p.1033T
MUSCLE alignment	Partially conserved	Not conserved	Conserved
IMutant $\Delta\Delta G$	-0.19 (neutral: no effect on protein stability)	-0.1 (neutral: no effect on protein stability)	-0.59 (Decrease in protein stability)
SIFT	Damaging	Tolerated	Tolerated
PolyPhen2	Probably damaging	Benign	Possibly damaging
PredictSNP	Deleterious	Neutral except SNAP	Neutral except SNAP and SIFT
ExAC population frequency (Europe)	0.12%	9%	4%

4.5.2 *In vitro* expression studies of mutation p.R1060W and SNPs p.R7W and p.A1033T

Site directed mutagenesis (SDM) was used to create a combination of six expression vectors, each containing a mutation, a SNP or mutation and/or SNP in various combinations (see Table 4.2).

Table 4.2 Expression vectors created by site directed mutagenesis

Expression vector	Description
R1060W	Missense mutation
R7W	SNP
A1033T	SNP
R1060W + R7W	Missense mutation + SNP
R1060W + A1033T	Missense mutation + SNP
R1060W + R7W + A1033T	Missense mutation + 2 SNPs

Two complementary mutagenic oligonucleotide primers were designed and purified by HPLC (Eurofins, Germany) to insert nucleotide substitutions into the ADAMTS13 cDNA insert of the pcDNA3.1+ vector (Invitrogen, UK), (see Table 4.3).

Table 4.3 Nucleotide substitutions for site directed mutagenesis primers

Amino acid change	Nucleotide change (cDNA)
1060 R→W	3178 C→T
7 R→W	19 C→T
1033 A→T	3097 G→A

Site directed mutagenesis was performed as previously described in section 2.2. The presence or absence of the nucleotide substitutions were verified by Sanger sequencing (GATC, Germany). Mutant plasmids were amplified and purified with MaxiPrep kits (QIAGEN, UK) prior to transfection into human embryonic kidney cells (HEK293T). To measure transfection efficiency, HEK293T cells were co-transfected with a reporter plasmid expressing *E.coli* β galactosidase in a 1:1 molar ratio. Sub-confluent HEK293T cells were grown in 100mm dishes in DMEM medium until 70-80% confluency. Transient transfections of WT and mutant expression vectors were performed with 33 μ g total DNA and 10mM PEI in Opti-Mem with cells and incubated for 72 hours at 37°C, 5% CO₂ in a humidified incubator.

Transfection efficiency of each construct was examined in three transfections. Transfection efficiency by β -galactosidase activity has been previously described (see section 2.8). Cells were collected, the cells lysed in 20mM Triton X (Sigma-Aldrich, UK) and sonicated prior to protein quantitation by BCA assay (Thermo-Scientific, UK). Conditioned media was harvested and concentrated prior to protein quantitation by BCA assay (Thermo-Scientific, UK). Western blot analyses were performed on cell lysates and conditioned media (see section 2.12). An equal quantity of protein was loaded per well for SDS-PAGE. The housekeeping protein β -actin was used as a loading control (cell lysates only) to normalize protein loading. Recombinant ADAMTS13 was visualized by western blotting using an antibody to the myc insert (Merck Millipore, UK). Alkaline phosphate-conjugated goat anti-mouse IgG was used for the secondary antibody (Abcam, UK). The western blot band intensities were analysed by densitometry using ImageJ software. To correct for sample-to-sample and lane-to-lane variability in SDS-PAGE, the intensity of the ADAMT13 band on the western blot image for each lane was normalized to the internal loading control of the endogenous protein β actin. Blots were assessed for quality of the primary and secondary antibody interactions in relation to band intensities of the housekeeping protein and positive (WT) control and repeated if necessary To monitor the transfection efficiency and to obtain normalized expression values in order to compare the results of transfections with different constructs, the appearance of blue colonies

(indicating the reporter plasmid) was quantified (as described in section 2.8). ADAMTS13 antigen quantitation was performed on the concentrated conditioned media using the commercially available IMUBIND® ADAMTS13 ELISA (Sekisuidiagnostics UK). Values (mean of replicate transfections) are presented as % of WT values ± SEM (WT = 100%).

4.6 Results of transient expression studies of mutation p.R1060W mutation and SNPs

4.6.1 Sanger sequencing of WT ADAMTS13 cDNA insert

Initially the WT expression vector was sequenced by Sanger sequencing to ensure there were no non-synonymous mutations present (i.e. those that would result in an amino acid change). It was found that the ADAMTS13 cDNA contained the following synonymous changes (i.e. those that differ in nucleotide sequence from the reference sequence but would not result in an amino acid change); see Figure 4.2 and Table 4.4.

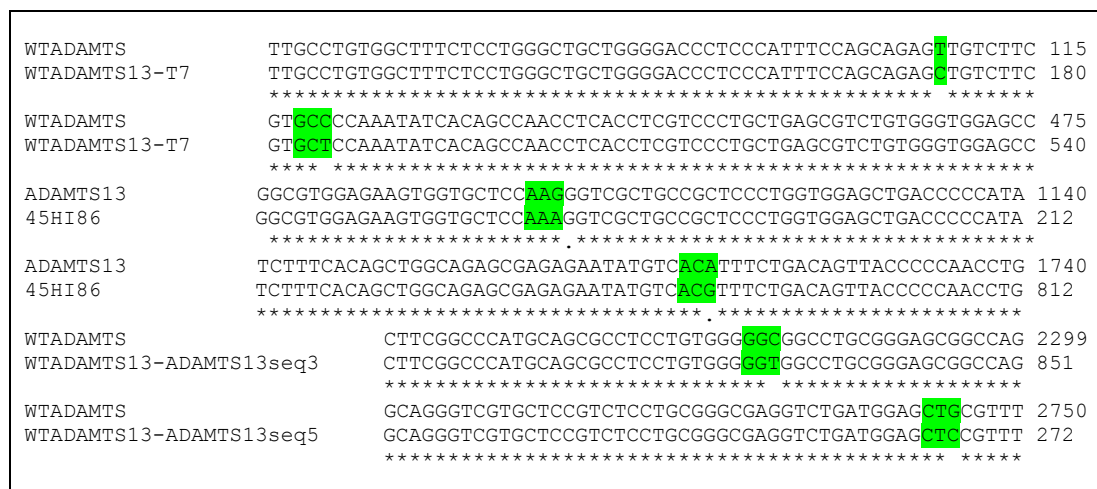


Figure 4.2 Wild type full sequencing *ADAMTS13* results: synonymous changes in WT cDNA insert (shaded). NM_139025.4 was used as the cDNA reference sequence cDNA

Table 4.4 Synonymous changes in WT *ADAMTS13* cDNA insert

Nucleotide change	Codon change		Amino acid
T108C	AGT → AGC		Serine → serine
C420T	GCC → GCT		Alanine → alanine
G1104A	AAG → AAA		Lysine → lysine
A1716G	ACA → ACG		Threonine → threonine
C2280T	GGC → GGT		Glycine → glycine
G2744C	CTG → CTC		Leucine → leucine

Once confirmation by Sanger sequencing had confirmed that the mutation/SNP had successfully been introduced and the full insert was screened for unwanted non-synonymous changes (those that would result in an amino acid substitution), the WT and mutant expression vectors were amplified using the Maxiprep QIAGEN kits according to manufacturer's instructions (QIAGEN). As can be seen from Table 4.5, this often yielded very poor DNA concentrations, even after troubleshooting the method.

Table 4.5 DNA concentration of expression vectors (QIAGEN Maxiprep)

Clone	DNA Concentration (ng/μl)
p.A1033T (3) + C384T (9)	880
p.R1060W (4) + C3484T (2)	91, 93
p.R7W (8) + C3484T (2)	133
p.R7W (8) + p.R1060W (8) + C3484T (2)	34, 36, 567, 694
p.R1060W (4) + p.A1033T (3)+ C3484T(2)	25, 36, 56, 124
p.R7W (8) + p.R1060W (8) + p.A1033T (4) + C3484T (1)	28, 25, 113
X gal reporter plasmid	132
Naked vector	1099
WT	528, 314, 94, 63

4.6.1.1 Non-synonymous mutation introduced by SDM

After SDM and confirmation by Sanger sequencing, a non-synonymous mutation was found in the cDNA ADAMTS13 insert arising at nucleotide position 3484 in several plasmids. This substitution of cytosine for thymine (C>T) resulted in an amino acid change of serine (codon TCC) to proline (codon CCC). This occurred at the same position in several SDM expression vectors and was reverted by a repeat SDM experiment using the primer seen in Figure 4.3.

CCC TGG AGT GGT T CC AGG CCC GG	CCG GGC CTG G A CCA CTC CAG GG
Forward	Reverse

Figure 4.1 Non-synonymous mutation primer design C3484T. The nucleotide substitution is highlighted.

Repeat Sanger sequencing was performed of the cDNA insert to verify the nucleotide sequence had reverted back to the WT sequence and that no other

changes were inserted (see Figures 4.4 – 4.9). It is unclear as to why this nucleotide substitution occurred in all expression vectors.

4.6.1.2 Sanger sequencing of expression vectors

The Sanger sequencing results can be seen in Figures 4.4 - 4.9.

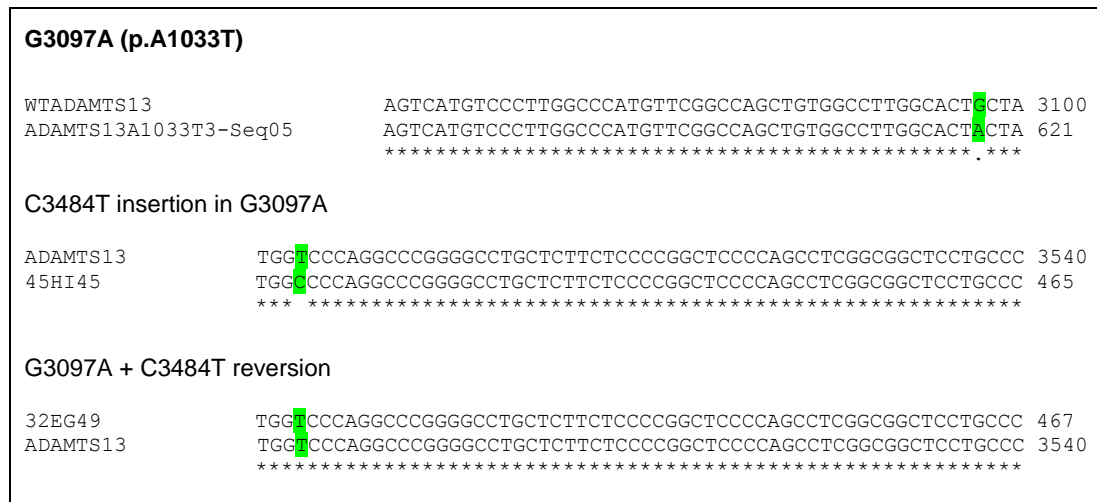


Figure 4.2 Sequencing results of expression vector p.A1033T SNP Sequencing results of expression vector p.A1033T (G3097T) SNP with non-synonymous mutation reverted to WT.

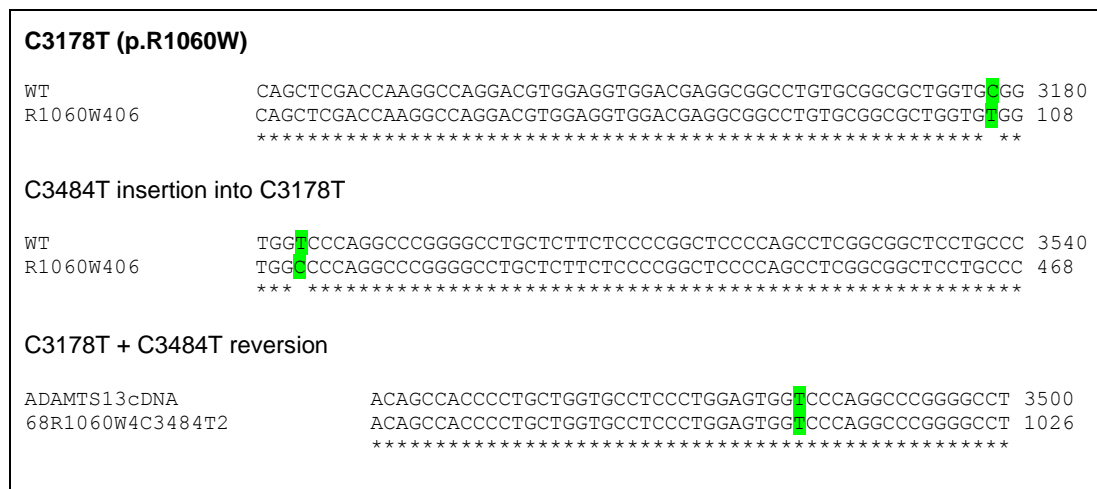


Figure 4.3 Sequencing results of expression vector p.R1060W mutation with non-synonymous mutation reverted to WT.

C19T (p.R7W)

```

ADAMTS13      -----ATGCACCAGCGTCACCCC GGGCAAGATGCCCTCCCCTCTGTGTGGCCGGAATC  54
45HI60        GCCACCATGCACCAGCGTCACCCC GGGCAAGATGCCCTCCCCTCTGTGTGGCCGGAATC  120
                *****

```

C3484T insertion into C19T

```

ADAMTS13      TGGTCCCAGGCCCGGGGCTGCTCTTCTCCCGGCTCCCCAGCCTCGGCGGCTCCTGCCC  3540
45HI79        TGGTCCCAGGCCCGGGGCTGCTCTTCTCCCGGCTCCCCAGCCTCGGCGGCTCCTGCCC  466
                *** *****

```

C19T + C3484T reversion

```

ADAMTS13      TGGTCCCAGGCCCGGGGCTGCTCTTCTCCCGGCTCCCCAGCCTCGGCGGCTCCTGCCC  3540
26R7W8        TGGTCCCAGGCCCGGGGCTGCTCTTCTCCCGGCTCCCCAGCCTCGGCGGCTCCTGCCC  1062
                *****

```

Figure 4.6 Sequencing results of expression vector p.R7W (C19T) SNP with non-synonymous mutation reverted to WT

C19T (p.R7W)

```

C19TcDNA      -----ATGCACCAGCGTCACCCC GGGCAAGATG  29
R7W8R1060W8C3484T2  TGGTGAATTCGCCGCCACCATGCACCAGCGTCACCCC GGGCAAGATG  100
                *****

```

C3187T (p.R1060W)

```

cDNA          GACGAGGCGGCTGTGCGGCGCTGGTG GGGCCGAGGCCAGTGTCCCTG  3200
R7W8R1060W8C3484T2  GACGAGGCGGCTGTGCGGCGCTGGTG GGGCCGAGGCCAGTGTCCCTG  731
                *****

```

C3484T insertion

```

WTADAMTS13    TGGTCCCAGGCCCGGGGCTGCTCTTCTCCCGGCTCCCCAGCCTCGGCGGCTCCTGCCC  3540
67GD97        TGGTCCCAGGCCCGGGGCTGCTCTTCTCCCGGCTCCCCAGCCTCGGCGGCTCCTGCCC  471
                *** *****

```

C3484T reverted

```

ADAMTS13      ACAGCACCCCTGCTGGTGCCTCCCTGGAGTGGTCCCAGGCCCGGGGCT  3500
87DI38R7W+R1060W+C3484T  ACAGCACCCCTGCTGGTGCCTCCCTGGAGTGGTCCCAGGCCCGGGGCT  429
                *****

```

Figure 4.4 Sequencing results of expression vector p.R7W+ p.R1060W SNP + mutation with non-synonymous mutation reverted to WT

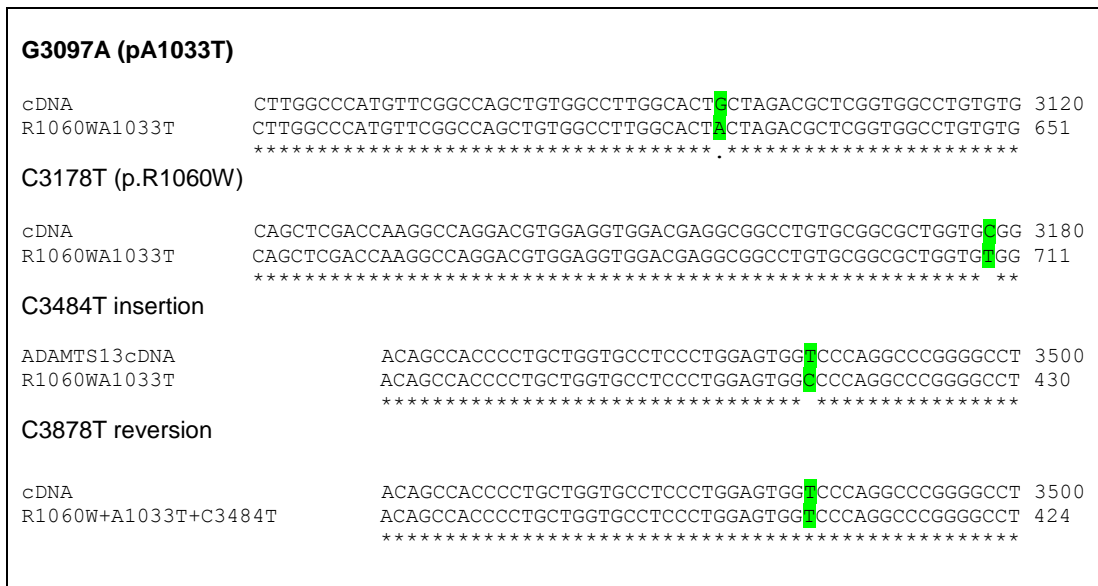


Figure 4.5 Sequencing results of expression vector p.R1060W + p.A1033T with non-synonymous mutation reverted to WT

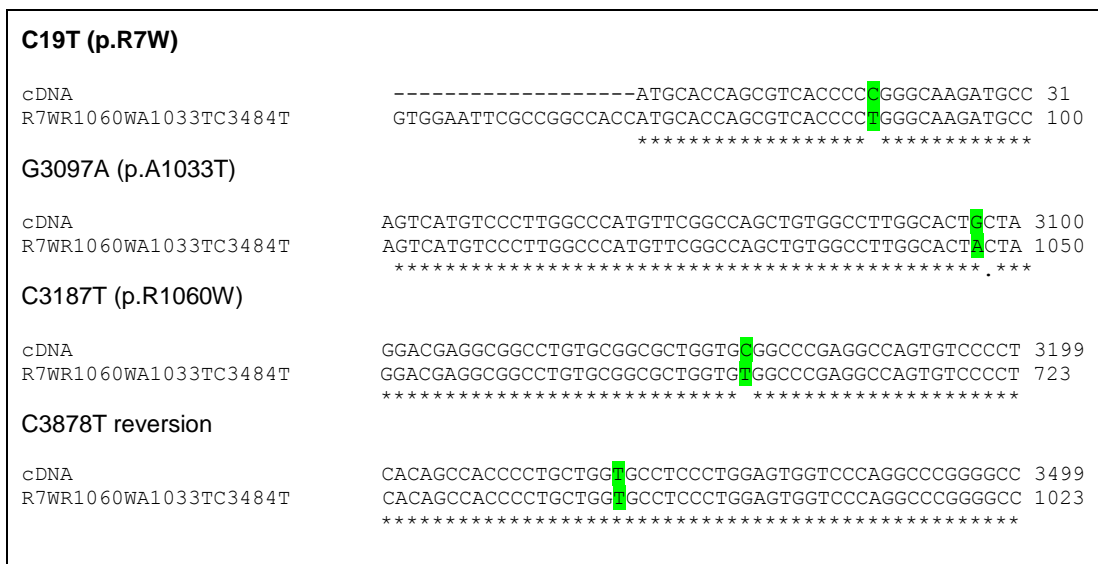


Figure 4.6 Sequencing results of expression vector p.R1060W + p.R7W + p.A1033T with non-synonymous mutation reverted to WT

4.6.2 Transfection efficiencies

A total of five fields were examined microscopically (X100) and a grid overlaid on each image. A differential count of the total number of cells and number of blue cells was performed. Blue coloured cells indicated successful co-transfection with the reporter plasmid containing the *LacZ* gene, producing β -galactosidase. A representative plate from each transfection is shown in Figures 4.10 - 4.17.

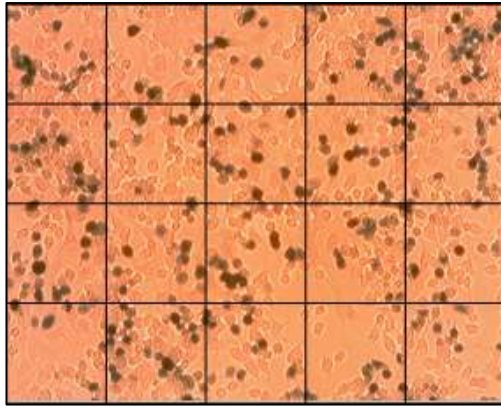


Figure 4.8 Co-transfection negative control

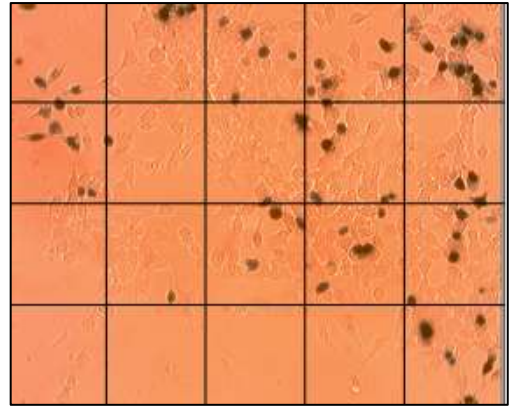


Figure 4.7 Co-transfection positive control

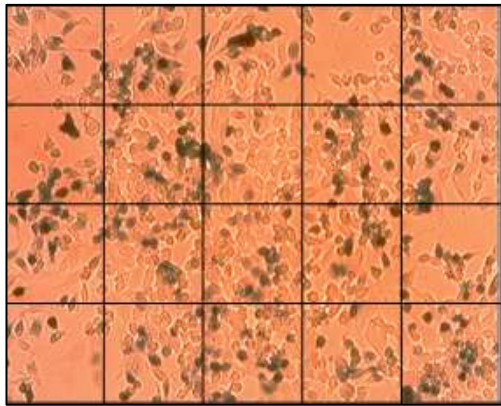


Figure 4.9 Co-transfection p.R1060W

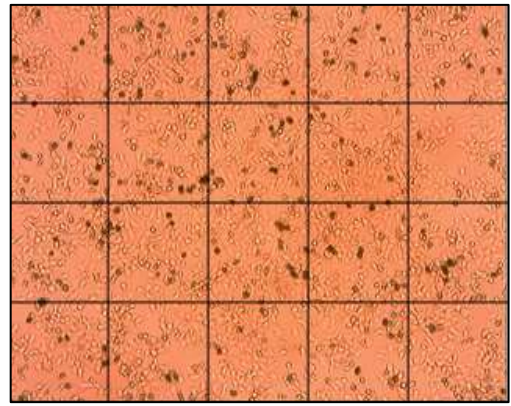


Figure 4.10 Co-transfection p.R7W

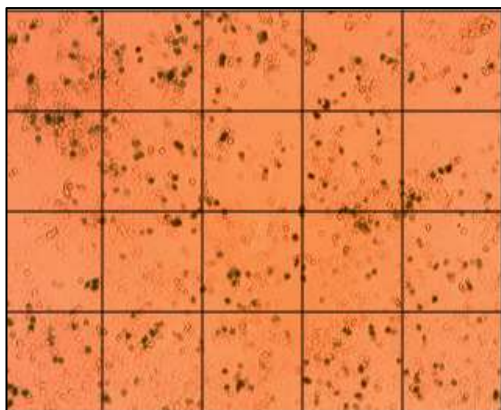


Figure 4.11 Co-transfection p.A1033T

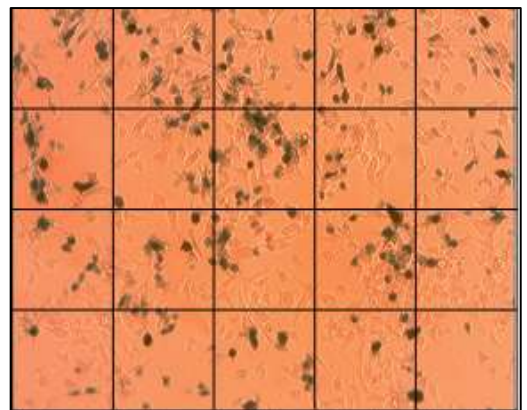


Figure 4.12 Co-transfection p.R1060W + p.R7W



Figure 4.13 Co-transfection p.R1060W + p.A1033T



Figure 4.17 Co-transfection p.R1060W + p.R7W + p.A1033T

From the differential counts, the transfection efficiency for each expression vector can be seen in Table 4.6. The total number of blue stained cells were counted (those successfully transfected with the reporter plasmid) together with the total number of cells to calculate the percentage of cells successfully transfected. It was assumed that the ADAMTS13 expression vector was transfected at the same efficiency as the reporter vector. The protocol was repeated once, as can be seen in Table 4.6.

Table 4.6 Estimated transfection efficiencies of expression vectors

Clone	% transfection efficiencies	% transfection efficiencies (repeat)
WT	18	30
p.A1033T	25	24
p.R1060W	28	26
p.R7W	18	25
p.R7W + p.R1060W	32	20
p.R1060W + p.A1033T	20	22
p.R7W + p.R1060W + p.A1033T	24	35

Quantitation of total protein in cell lysates and conditioned media was performed by BCA assay (Thermo Scientific, UK); for results see Appendix 1.0.

Each expression vector was transiently transfected into HEK293T cells in triplicate. The resultant cell lysate and conditioned media were analysed on western blot. If it was found that the transient transfection was unsuccessful,

only two expression vectors can be seen on western blot. The transient transfection was then repeated.

4.6.3 Western blot analysis of cell lysates

After transient transfection, cells were harvested and initially untreated by cell lysis and sonication (see Figure 4.18). The expected size of ADAMTS13 protein (approx. 180kDa) was seen.

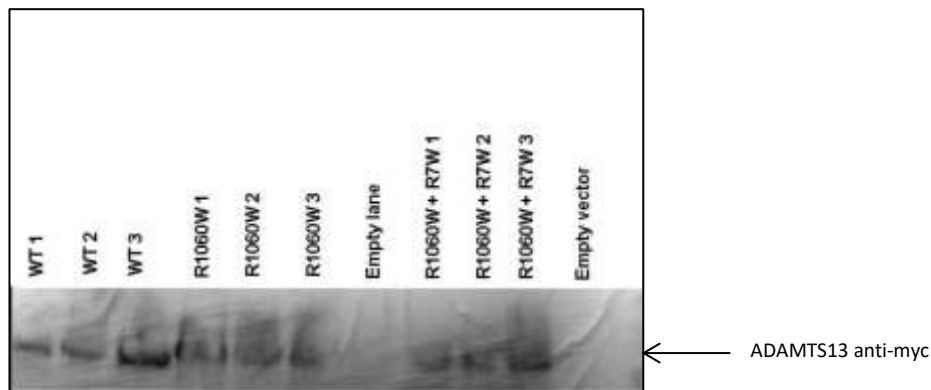


Figure 4.14 Western blot analysis cell lysates (untreated) Western blot of cell lysate (untreated): WT, p.R1060W and p.R1060W + p.R7W (WT 1, 2 and 3 denotes the cell lysates from separate transient transfections)

Due to the difficulty in manipulating and loading the untreated samples, cell lysates were lysed using 20mM Triton X (Sigma-Aldrich UK) and sonicated. An antibody directed against the housekeeping protein β -actin of molecular weight 45kDa was used as a loading control (see Figures 4.19-4.21). An equal amount of total protein was loaded into each well of SDS-PAGE, as determined by BCA assay. The optimal quantity of protein to load to ensure a linear relationship between sample and signal was evaluated and is described in section 2.12.5.

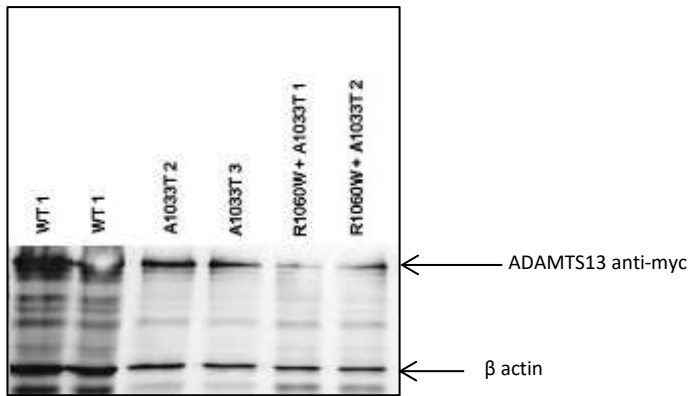


Figure 4.15 Western blot analysis cell lysates p.A1033T, p.A1033T + p.R1060W (β actin was used as a loading control)

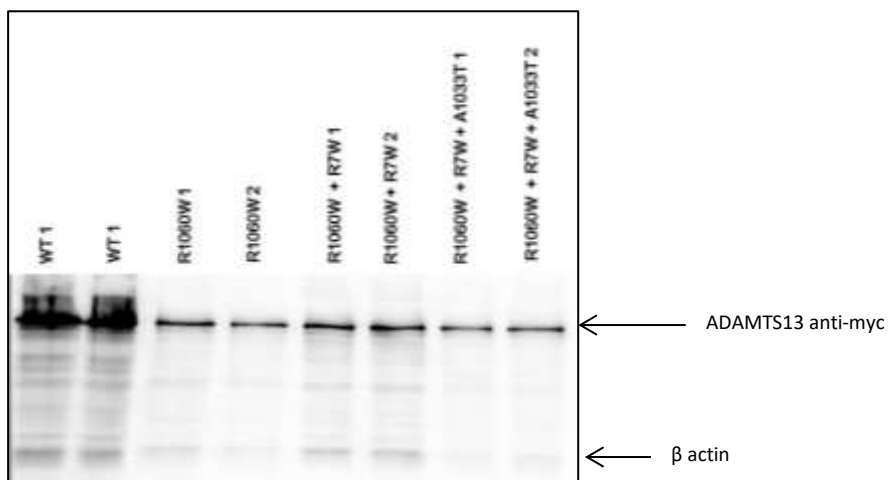


Figure 4.16 Western blot analysis cell lysate p.R1060W, p.R1060W + p.R7W, p.R1060W + p.R7W + p.A1033T

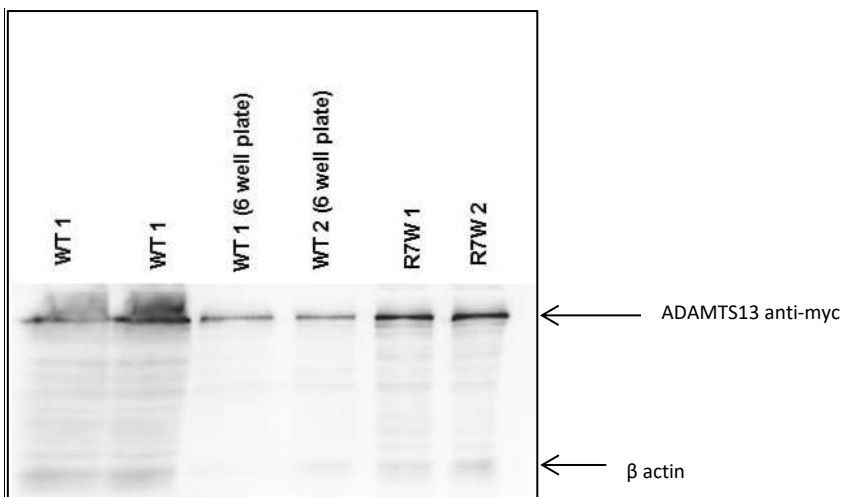


Figure 4.17 Western blot analysis p.R7W

4.6.4 Western blot analysis of conditioned media (concentrated)

The conditioned media of the expression vectors analysed in Figures 4.19 - 4.21 were harvested, concentrated and analysed on western blot as described in section 2.10 – 2.12 (see Figures 4.22 – 4.24).

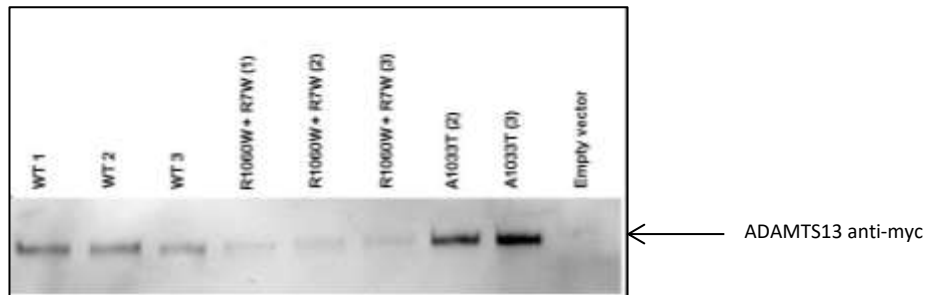


Figure 4.18 Western blot analysis conditioned media (CM) p.R1060W + p.R7W and p.A1033T

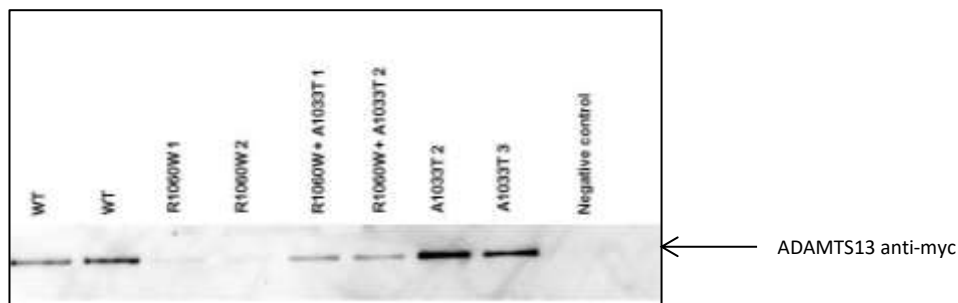


Figure 4.19 Western blot analysis conditioned media p.R1060W, p.R1060W + p.A1033T, p.A1033T

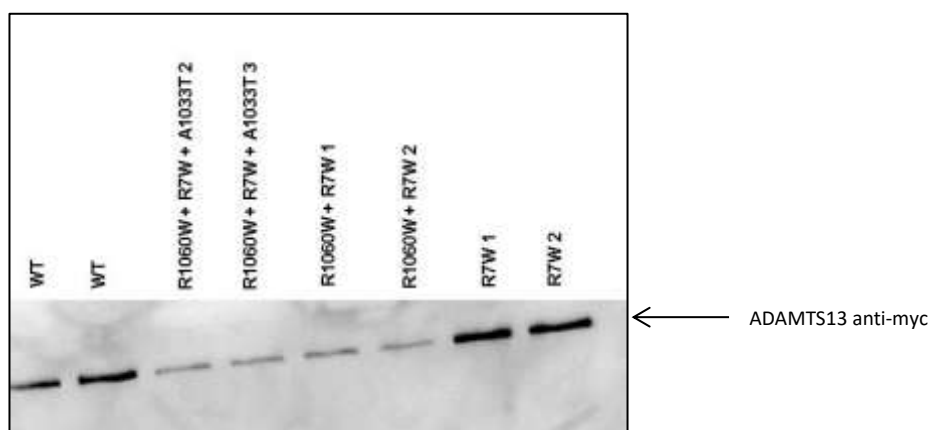


Figure 4.20 Western blot analysis conditioned media p.R1060W + p.R7W + p.A1033T, p.R1060W + p.R7W, p.R7W

4.6.5 Western blot analysis of cell lysates, repeat transient transfections

A repeat transfection was carried out with the same expression vectors using the same protocol and experimental conditions. The cells were lysed and sonicated as previously described and analysed on western blot (see Figures 4.25 - 4.26).

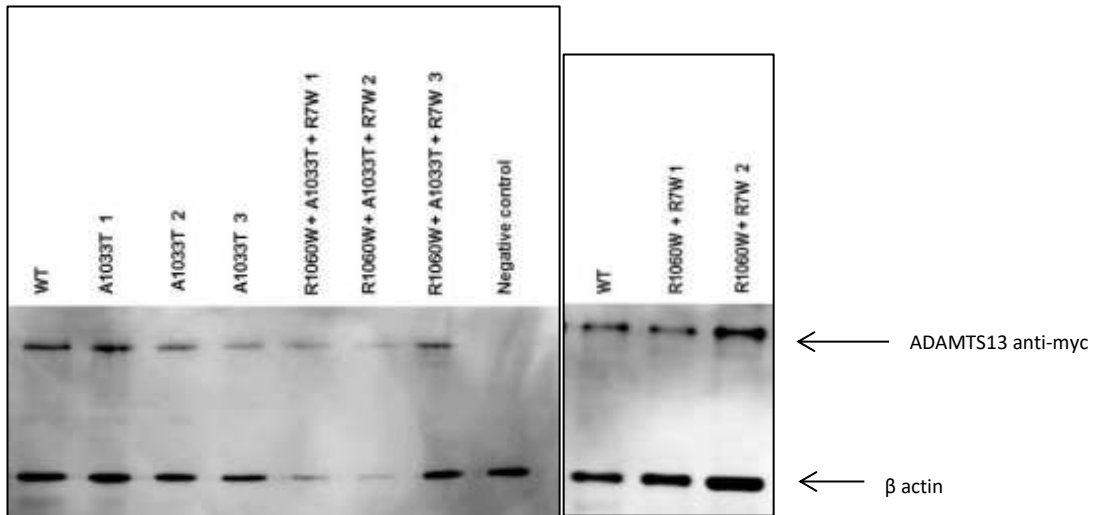


Figure 4.21 Western blot analysis conditioned media p.A1033T, p.R1060W + p.A1033T + p.R7W, R1060W + p.R7W

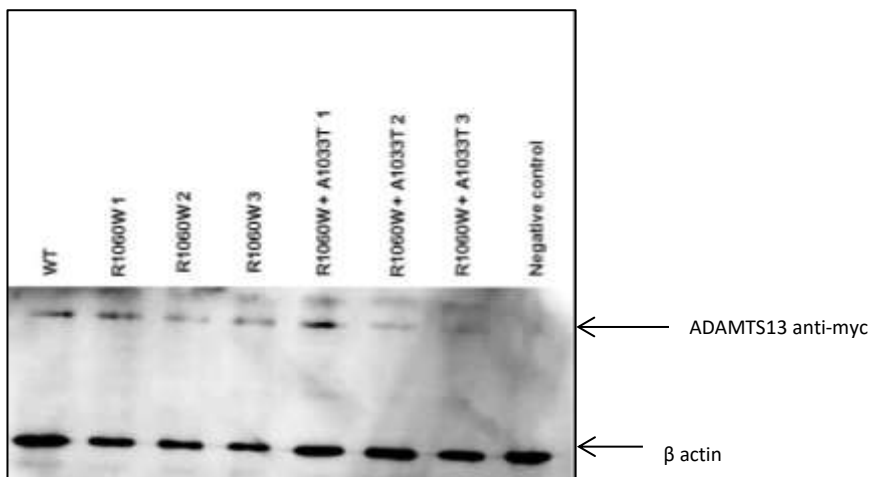


Figure 4.22 Western blot analysis cell lysate (rpt) p.R1060W, p.R1060W + p.A1033T

4.6.6 Western blot analyses of conditioned media, repeat transient transfections

The conditioned media of the expression vectors analysed in Figures 4.25 - 4.26 were harvested and analysed on western blot (see Figures 4.27 – 4.28).

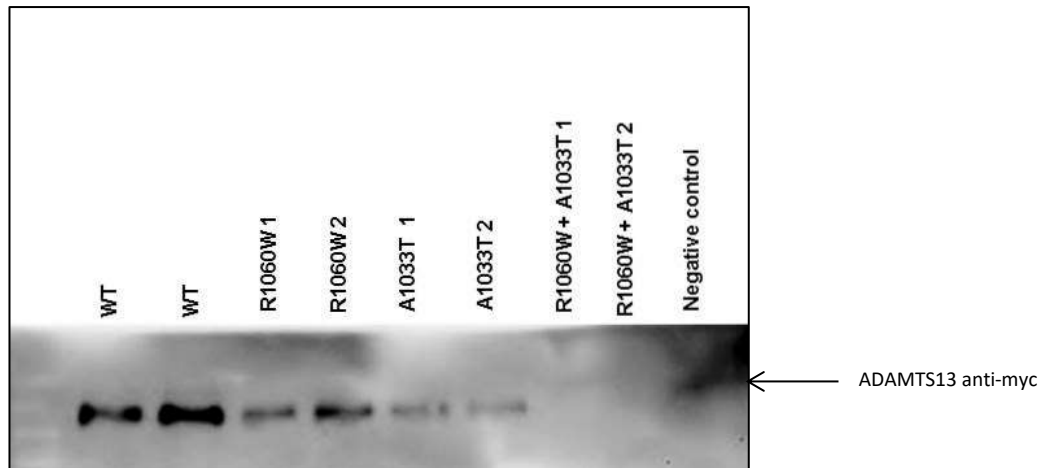


Figure 4.23 Western blot analysis conditioned media (rpt) p.R1060W, p.A1033T, p.R1060W + p.A1033T

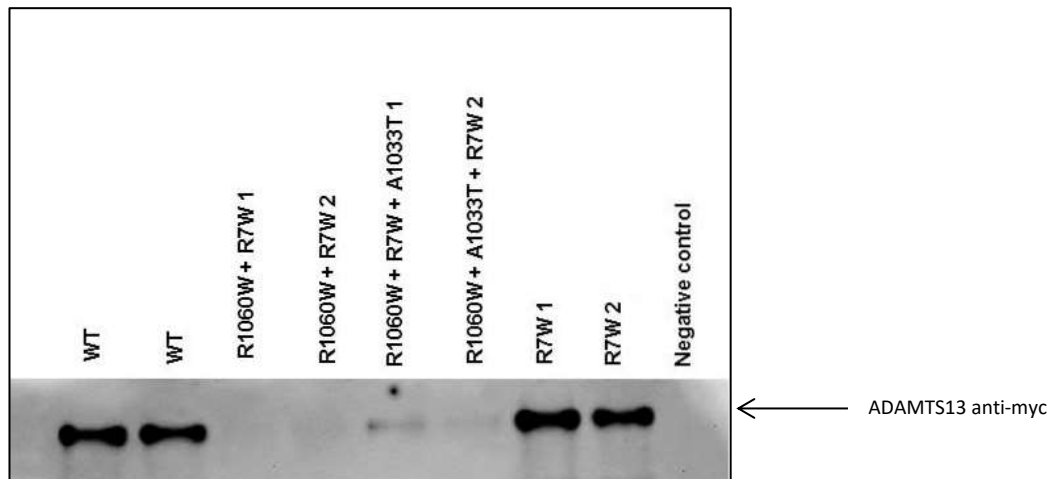


Figure 4.24 Western blot of conditioned media, repeat transient transfection: WT, p.R1060W + p.R7W, p.R1060W + p.R7W + p.A1033T and p.R7W

4.6.7 ImageJ analysis of western blots: cell lysates

The band intensities on western blots were scanned using ImageJ software and the cell lysates normalized to the β -actin housekeeping protein by comparing the signal intensity of the housekeeping protein to the target ADAMTS13 signal. This normalized ADAMTS13 signal was then compared with the positive control (WT) values (%) and the standard error of the mean for each expression vector calculated (see Table 4.7 and Figure 4.29). Each expression vector was transiently transfected in triplicate and analysed on western blot (one lane per transfection). For example, p.R7W1 is transfection 1. Transfection was then repeated in triplicate. As it was found that not all vectors were transfected successfully, only the results from duplicate transfections were analysed (i.e. R7W1 and R7W2).

Table 4.7 Normalized protein ratio of expressed ADAMTS13 in cell lysates samples, %WT ± SEM.

cDNA substitution	Normalized protein ratio	% of WT ± SEM
WT	1.0	100
p.R1060W 1	0.23	23 ± 8.6
p.R1060W 2	0.06	6 ± 8.6
p.R7W 1	1.26	126 ± 6.0
p.R7W 2	1.38	138 ± 6.0
p.A1033T 2	1.07	106 ± 9.0
p.A1033T 3	0.88	88 ± 9.0
p.R1060W + p.R7W 1	0.39	39 ± 5.0
p.R1060W + p.R7W 2	0.49	49 ± 5.0
p.R1060W + p.A1033T 1	0.26	26 ± 13.9
p.R1060W + p.A1033T 2	0.54	54 ± 13.9
p.R1060W + p.R7W + p.A1033T 1	0.08	8 ± - 2.1
p.R1060W + p.R7W + p.A1033T 2	0.12	12 ± - 2.1

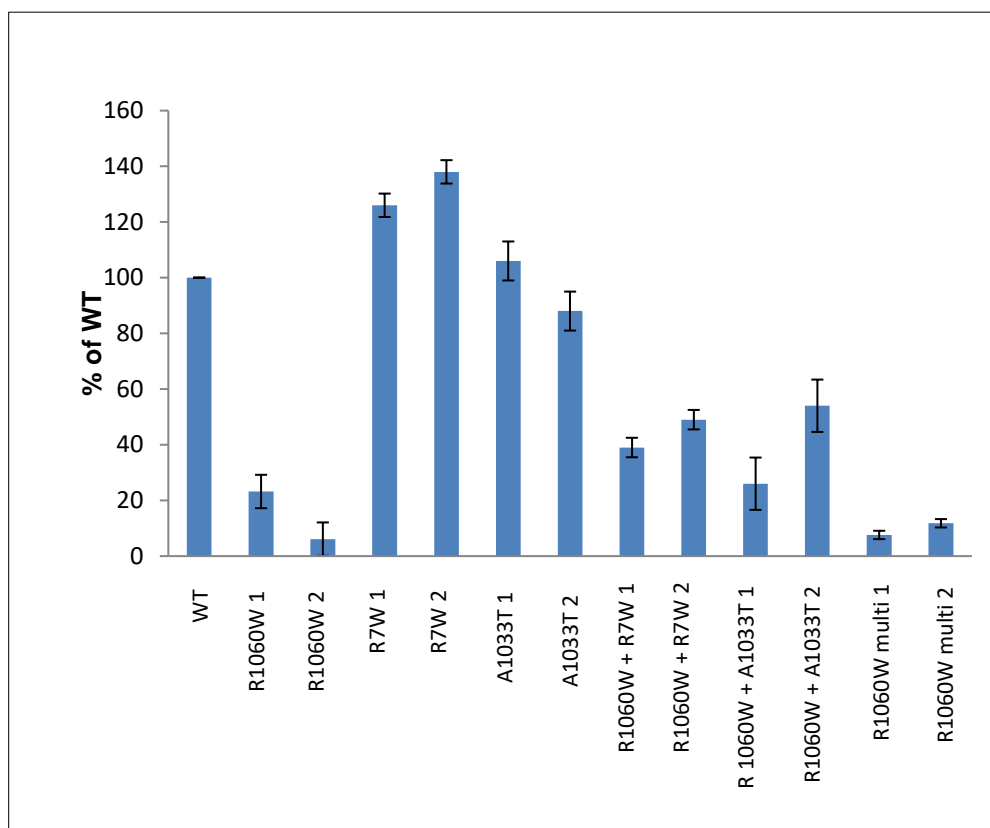


Figure 4.25 Comparison of normalized protein ratio of ADAMTS13 expressed in cell lysate samples, % WT ± SEM. (p.R1060W multi = p.R1060W + p.R7W + p.A1033T)

4.6.8 ImageJ analysis of western blots: conditioned media

The band intensities on western blots were scanned using ImageJ software and the conditioned media samples normalized to the WT positive control on the same blot (values \pm SEM); (see Table 4.8 and Figure 4.30).

Table 4.8 Normalized protein ratio of expressed ADAMTS13 in conditioned media samples, %WT \pm SEM

cDNA substitution	Normalized protein ratio	% of WT \pm SEM
WT	1.00	100
p.R1060W 1	0.06	6 \pm 1.6
p.R1060W 2	0.02	2 \pm 1.6
p.R7W 1	1.28	128 \pm 1.0
p.R7W 2	1.26	126 \pm 1.0
p.A1033T 2	1.52	152 \pm 18.4
p.A1033T 3	1.15	115 \pm 18.4
p.R1060W + R7W 1	0.28	28 \pm 5.6
p.R1060W + R7W 1	0.20	20 \pm 5.6
p.R1060W + A1033T 1	0.32	32 \pm 3.5
p.R1060W + p.A1033T 2	0.25	25 \pm 3.5
p.R1060W + p.R7W + p.A1033T 2	0.26	26 \pm 3.0
p.R1060W + p.R7W + p.A1033T 3	0.20	20 \pm 3.0

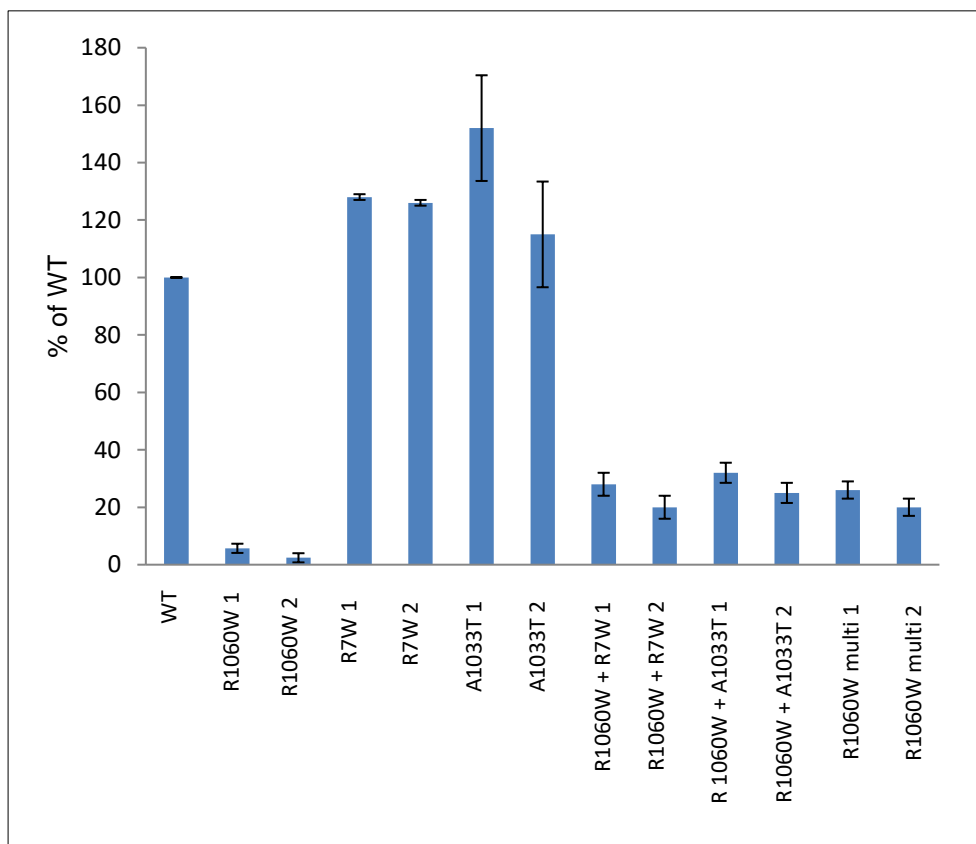


Figure 4.26 Comparison of normalized protein ratio of expressed ADAMTS13 in conditioned media samples, %WT \pm SEM. (p.R1060W multi = p.R1060W + p.R7W + p.A1033T)

4.6.9 ImageJ analysis of cell lysates, repeat transient transfections

The band intensities on western blots for repeat transfections were scanned using ImageJ software and the cell lysates normalized to the β -actin housekeeping protein and compared with positive control (WT) values \pm SEM (see Table 4.9 and Figure 4.31).

Table 4.9 Normalized protein ratio of expressed ADAMTS13 in cell lysate samples, repeat transfections, % WT \pm SEM

cDNA substitution	Normalized protein ratio	% WT \pm SEM
WT	0.41	100
p.A1033T 1	0.73	100 \pm 8.3
p.A1033T 2	0.61	98 \pm 8.3
p.A1033T 3	0.33	81 \pm 8.3
p.R1060W + p.R7W + p.A1033T 1	1.10	144 \pm 16.8
p.R1060W + p.R7W + p.A1033T 2	1.06	141 \pm 16.8
p.R1060W + p.R7W + p.A1033T 3	0.43	57 \pm 16.8
p.R1060W + p.R7W 1	0.28	29 \pm 11.5
p.R1060W + p.R7W 2	0.52	50 \pm 11.5
p.R1060W 1	0.48	119 \pm 5.7
p.R1060W 2	0.27	61 \pm 5.7
p.R1060W 3	0.47	113 \pm 5.7
p.R1060W + p.A1033T 1	0.58	140 \pm 12.1
p.R1060W + p.A1033T 2	0.09	21 \pm 12.1
p.R1060W + p.A1033T 3	0.07	17 \pm 12.1

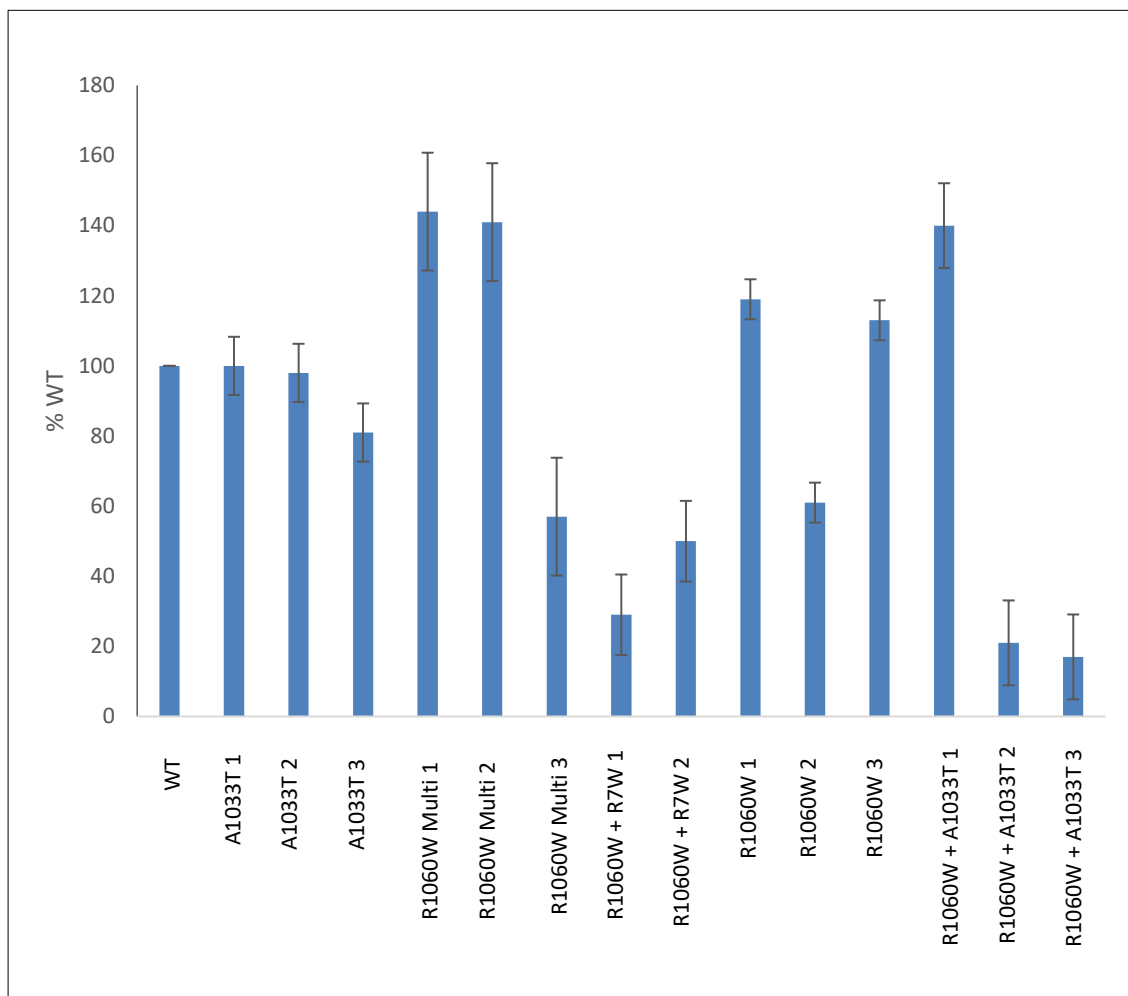


Figure 4.27 Comparison of normalized protein ratio of ADAMTS13 in cell lysate samples, % WT ± SEM, repeat transfections. p.R1060W Multi = p.R1060W + p.R7W + p.A1033T

4.6.10 ImageJ analysis of concentrated conditioned media, repeat transient transfections

The band intensities on western blots were scanned using ImageJ software and the conditioned media samples normalized to the WT positive control (values ± SEM); (see Table 4.10 and Figure 4.32).

Table 4.10 Normalized protein ratio of expressed ADAMTS13 in conditioned media samples, repeat transfections % WT ± SEM

Expression vector	Normalized protein ratio	% WT ± SEM
WT (mean)	1.0	100
p.R1060W 1	0.37	37 ± 11.0
p.R1060W 2	0.59	59 ± 11.0
p.A1033T 1	0.23	23 ± 5.7
p.A1033T 2	0.15	15 ± 5.7
p.R1060W + A1033T 1	0	0
p.R1060W + A1033T 2	0	0
p.R1060W + R7W 1	0.28	28
p.R1060W + R7W 1	0.20	20

p.R1060W + R7W + A1033T 1	0.26	26 ± 3.5
p.R1060W + R7W + A1033T 2	0.20	20 ± 3.5
p.R7W 1	1.48	128 ± 18.5
p.R7W 2	1.11	126 ± 18.5

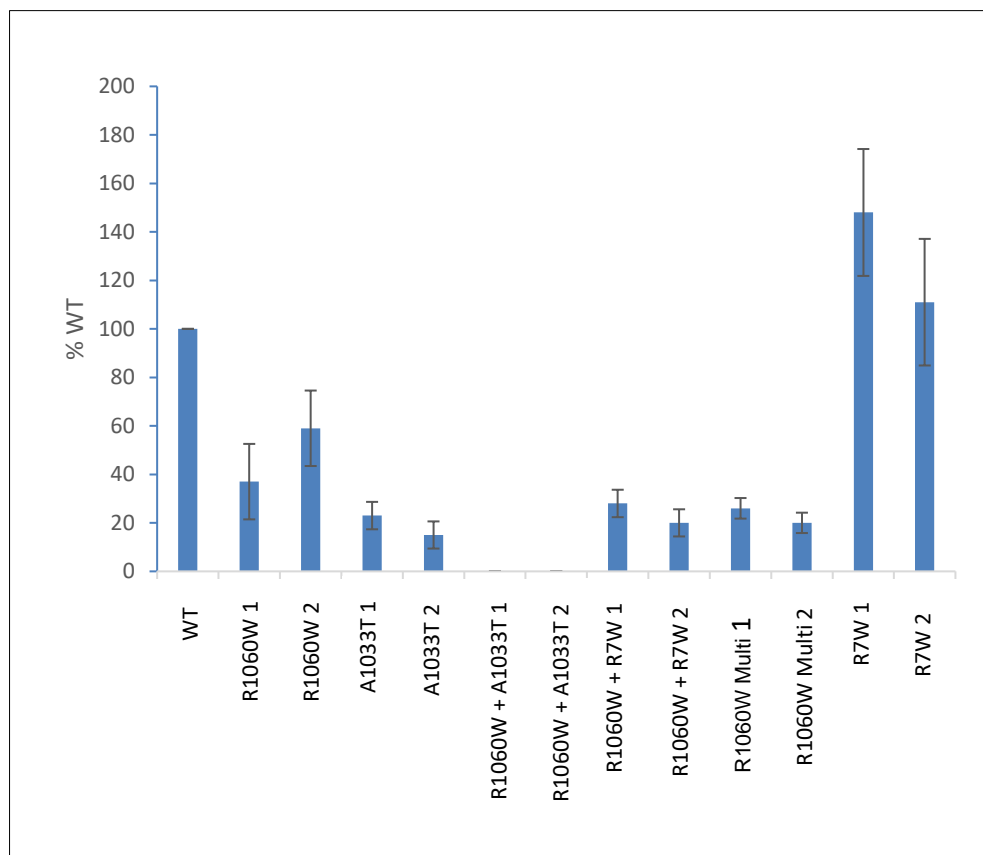


Figure 4.28 Comparison of normalized protein ratio of expressed ADAMTS13 in concentrated conditioned media samples, % WT ± SEM, repeat transfections. (multi = p.R160W + p.R7W + p.A1033T)

4.6.11 ADAMTS13 ELISA analysis of concentrated conditioned media samples

Cell lysate and conditioned media samples were analysed for ADAMTS13 antigen with the commercially available IMUBIND® ADAMTS13 ELISA (Sekisuidiagnostics UK) according to manufacturer's instructions (see Chapter 2). Results can be seen in Table 4.11 and Figure 4.33. The positive control (WT ADAMTS13) was taken as 100% expression and all results were normalized against this value and expressed as % WT. Each sample was repeated in triplicate and standard error of the mean calculated.

Table 4.11 Normalized ADAMTS13 antigen ratio of expressed ADAMTS13 in conditioned media samples, repeat transfections %WT \pm SEM.

Expression vector	ADAMTS13 concentration (ng/ml)	% WT \pm SEM
WT	242.75	100
p.R1060W 1	0	0 \pm 1.6
p.R1060W 2	7.84	3.2 \pm 1.6
p.A1033T 2	27.6	11.4 \pm 4.2
p.A1033T 3	48.23	19.9 \pm 4.2
p.R1060W + p.A1033T 1	20	8.2 \pm 0.6
p.R1060W + p.A1033T 2	16.47	6.8 \pm 0.6
p.R1060W + p.R7W 1	8.24	3.4 \pm 1.0
R1060W + R7W 2	13.33	5.5 \pm 1.0
p.R7W 1	0	0 \pm 0.05
p.R7W 2	2.35	0.1 \pm 0.05
p.R1060W + p.R7W + p.A1033T 1	16.86	6.9 \pm 1.0
p.R1060W + p.R7W + p.A1033T 2	11.76	4.8 \pm 1.0

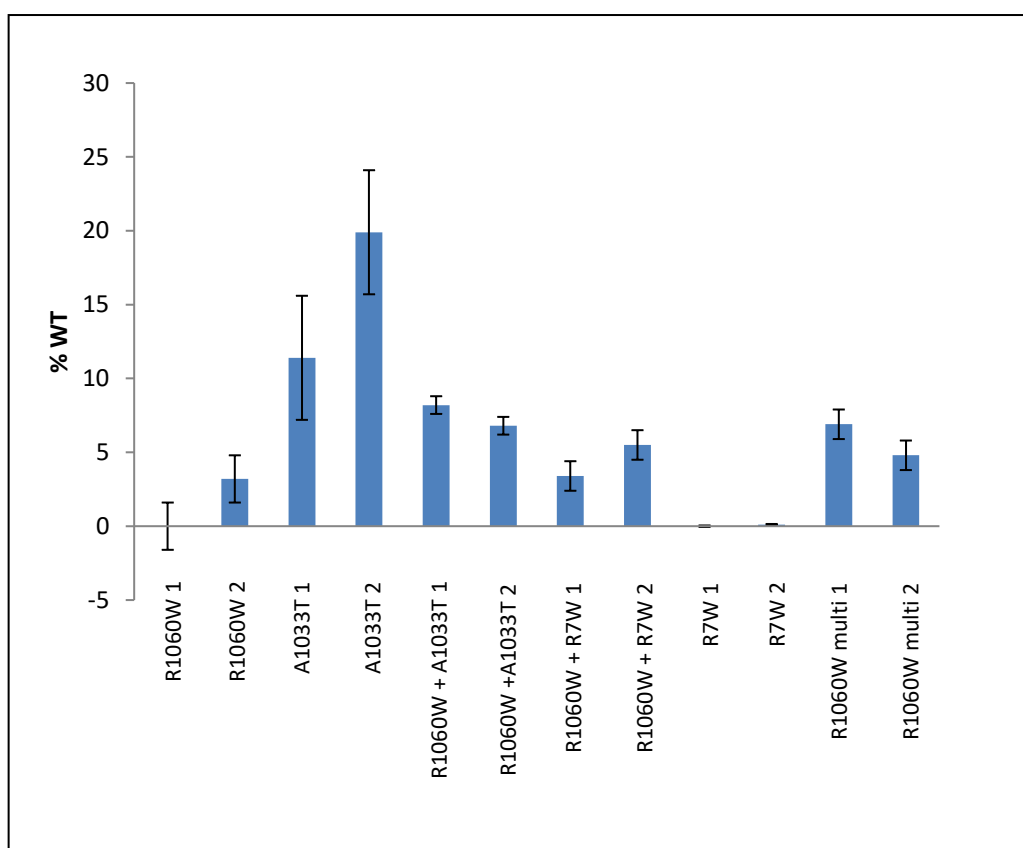


Figure 4.29 ADAMTS13 antigen concentration expressed in conditioned media samples as analysed by ELISA, % WT \pm SEM.

4.7 Statistical analysis

In order to assess the statistical significance of the variation in ADAMTS13 expression between the mutation R1060W and R1060W in combination with SNPs R7W and A1033T singly and in combination with R7W and A1033T, a one way analysis of variance (ANOVA) statistical test was performed. The values for %WT were utilised for each western blot. Results can be seen in Table 4.12

Table 4.12 Results of one way ANOVA analysis for first and repeat transient transfection of R1060W series ($p=0.05$).

Expression vector	Experimental Method	Observed ratio	F	Tabulated ratio ($p=0.05$)	F	Null hypothesis
Cell lysate first transfection	Western blot	0.094		6.59		Accept
CM first transfection	Western blot	0.387		6.59		Accept
Cell lysate repeat transfection	Western blot	2.26		3.59		Accept
CM repeat transfection	Western blot	9.47		18.5		Accept
CM first and repeat transfections	ELISA	0.83		9.23		Accept

In all cases the null hypothesis was accepted in that there is no significant difference between the mean ADAMTS13 expression of vectors p.R1060W, p.R1060W + p.R7W, p.R1060W + p.A1033T and p.R1060W + p.R7W + p.A1033T in cell lysates and conditioned media as analysed by western blot and conditioned media as analysed by ELISA.

4.8 Discussion

The mechanism of the association between ADAMTS13 mutations and disease phenotype is unknown. From previous animal studies (Motto *et al.* 2005; Banno *et al.* 2006), ADAMTS13 deficiency alone and hence genotype, may not be sufficient to cause TTP. There also may be additional triggers required. This can be evidenced clinically in that siblings with the same genotype may present differently with respect to onset and severity of the disease and that some patients with severely reduced ADAMTS13 activity

present later in life, usually after a triggering event such as pregnancy, severe infection or treatment with certain drugs. As explained previously, pregnancy is associated with many physiological changes but whether this event serves to promote ADAMTS13 deficiency or the event serves to trigger a TTP episode is hard to evidence.

This study investigated the *in vitro* effect of the individual SNPs p.R7W and p.A1033T singly and in combination with the missense mutation p.R1060W on ADAMTS13 antigen levels in order to relate genotype to the late-onset phenotype observed in patients with USS.

Usually, to cause severe ADAMTS13 deficiency both alleles of the *ADAMTS13* gene are affected. Heterozygous carriers of a mutation on a single allele are usually asymptomatic and do not present with TTP-like symptoms (Crawley & Scully, 2013). However, several patients diagnosed with late-onset, pregnancy-associated TTP carrying a single p.R1060W mutation, together with several SNPs, have been identified (Camilleri *et al.* 2008). The majority of mutations causing severe ADAMTS13 deficiency cause disruption of ADAMTS13 protein folding during synthesis, leading to severe intracellular retention (Crawley & Scully, 2013). In this study, the homozygous condition was studied due to limitations of the experimental procedure.

From the *in silico* MUSCLE alignment, the p.R7W SNP is located in a variable area with respect to conservation between orthologs. The p.R1060W and p.A1033T are separated by approximately 80 nucleotides and this region is highly conserved in all orthologs except in the mouse and the rat. Conservation of amino acids has been postulated to be the second most predictive factor of the impact of a mutation (Lee *et al.* 2009), with a mutation occurring in a highly conserved area having more impact. The SNPs p.R7W and p.A1033T are predicted to be tolerated by SIFT, which is a sequence homology tool, and p.R7W is predicted to have a benign effect by PolyPhen2.0. The latter tool is based on phylogenetic and structural information. However, p.A1033T is predicted to be possibly damaging by PolyPhen2.0. The p.R1060W mutation is predicted to be damaging by both. Predict SNP has predicted the mutation pR1060W to be deleterious by all predictive software and the p.A1033T SNP

to be deleterious by SIFT and SNAP. However, overall the SNPs have been predicted to be likely benign clinically. The I-Mutant tool, which estimates changes in Gibbs free energy due to the mutation and hence the effect on the stability of the protein, predicted p.R7W and p.R1060W to have no effect but estimated p.A1033T to decrease the stability of the protein. Interestingly, the occurrence of the p.R7W SNP in the global population is 0.0527, the occurrence of p.A1033T 0.0156 and that of p.R1060W, 0.0008 which may reflect the evolutionary pressures on these variants.

From the *in vitro* expression studies, the estimated transfection efficiencies of the WT (positive control) and p.R7W SNP were similar at 18%. The variants p.R1060W + p.A1033T, p.A1033T and p.R1060W + p.R7W + p.A1033T had similar transfection efficiencies of approximately 23%. The variants p.R1060W and p.R1060W + p.R7W had the highest at approximately 30%, despite ensuring an equal number of cells were plated and the transfection performed at 70-80% cell confluency. When interpreting results these differing values should be taken into account.

From the first transfection series, an equal quantity of total protein was loaded in each well during SDS-PAGE. However, a housekeeping antibody was not used and the values have been normalised against the positive control (WT) only. The mean results (expressed as % of WT) for cell lysates are summarised in Table 4.13:

Table 4.13 Summary of mean normalized ADAMTS13 expression in cell lysates expressed as %WT; first transfection

p.R1060W	p.R7W	p.A1033T	p.R1060W + p.R7W	p.R1060W + p.A1033T	p.R1060W + p.R7W + p.A1033T
15 %	132 %	97 %	44 %	40 %	10 %

In consideration of the differing transfection efficiencies, the values could be normalized to reflect %ADAMTS13 in cell lysates as WT and p.R7W transfection efficiencies were 60% of p.R1060W. The transfection efficiencies of p.R1060W + p.R7W were 80% of the other variants. However, the low %

ADAMTS13 expression of p.R1060W (which had the highest transfection efficiency) may indicate that this mutation is causing aberrant folding of the protein and is being targeted and broken down in the cell. However, despite these observations, statistical analysis using one way ANOVA found that there was no statistical significance in the expression of ADAMTS13 in cell lysates between p.R1060W and p.R1060W + SNPs.

The mean quantity of ADAMTS13 secreted into the conditioned media from these variants is summarised in Table 4.14:

Table 4.14 Summary of mean ADAMTS13 secretion in conditioned media, expressed as %WT; first transfection

p.R1060W	p.R7W	p.A1033T	p.R1060W + p.R7W	p.R1060W + p.A1033T	p.R1060W + p.R7W + p.A1033T
4 %	127 %	120 %	24 %	29 %	23 %

From these results, the mean secretion of ADAMTS13 in the media from the p.R7W SNP has not decreased compared to WT as would be expected and is comparable to the cell lysate results. However, expression of ADAMTS13 in the conditioned media by this SNP shows an actual increase of 27% that of WT. Plaimauer *et al.* found that the p.R7W SNP ameliorated the effects of the detrimental SNPs p.P618A and p.A732V (Plaimauer *et al.* 2006). An increase in secretion by the p.R7W may explain this observation. Interestingly it appears that the secretion of ADAMTS13 from the p.A1033T variant is also enhanced. This has also been seen by other researchers (Edwards *et al.* 2012). The decreased secretion of ADAMTS13 from the p.R1060W variant is as expected, particularly when taking into account the lower cell lysate values. However, the combination of the SNPs p.A1033T and p.R7W both singly and in combination with p.R1060W does appear to ameliorate against possible breakdown of ADAMTS13 in the cell and thus leads to an enhanced ADAMTS13 secretion. This could partly explain the late-onset phenotype seen in patients with the p.R1060W mutation and associated SNPs.

The mean ELISA antigen results, expressed as average % WT, are summarised in Table 4.15.

Table 4.15 Summary of mean normalized ADAMTS13 antigen concentrations in conditioned media expressed as %WT; first transfection

p.R1060W	p.R7W	p.A1033T	p.R1060W + p.R7W	p.R1060W + p.A1033T	p.R1060W + R7W + p.A1033T
3.2 %	0.1 %	16 %	4 %	8 %	6%

These results are unexpected and surprisingly low. The IMUBIND® ELISA antigen assay is a commercial assay used in patient diagnostic laboratories and details of the ADAMTS13 epitope targeted by the capture antibody are not available. It could be assumed that this epitope(s) may be altered by the introduction of the mutation or SNP. The quantity of ADAMTS13 secreted from HEK293T cells in a 100mm dish is not comparable to that produced in the body thus the lower limit of detection of the assay may be too great a concentration for this purpose and may give aberrant results. In order to rectify this, the conditioned media could be concentrated further and the assay repeated. As the IMUBIND assay has been developed and validated for diagnostic purposes with plasma or serum used as the matrix, the presence of an unknown inhibitor within the *in vitro* expression experiment cannot be discounted.

These values found on ELISA are below the detection limits for the activity assays (FRETs-VWF) and these were not performed as a result.

The results of the repeat transfections are summarised in Table 4.16:

Table 4.16 Summary of mean normalized ADAMTS13 in cell lysates expressed as %WT; second transfection

p.R1060W	p.R7W	p.A1033T	p.R1060W + p.R7W	p.R1060W + p.A1033T	p.R1060W + p.R7W + p.A1033T
35 %	45 %	51 %	41 %	55 %	70 %

The transfection efficiencies were comparable for the repeat transfections at approximately 25%. However, the p.R1060W + p.R7W + p.A1033T clone was higher at 30%. The quantity of ADAMTS13 secreted in the conditioned media for the repeat transfections are summarised in Table 4.17.

Table 4.17 Summary of mean ADAMTS13 expression in conditioned media %WT; repeat transfection.

p.R1060W	p.R7W	p.A1033T	p.R1060W + p.R7W	p.R1060W + p.A1033T	p.R1060W + p.R7W + p.A1033T
48 %	130 %	19 %	0 %	0 %	13 %

Statistical analysis using one way ANOVA found that there was no statistical significance in the expression of ADAMTS13 in cell lysates or conditioned media between p.R1060W and p.R1060W + SNPs.

There was some variability in the quality of the western blots. In consideration of this, there were some changes with respect to the experimental procedure for the repeat transfections. The imaging system used in the second series of transfections was updated and changed, with a more sensitive camera. This greatly enhanced the background noise on the blots which may have skewed the ImageJ values. All experimental protocols were followed and controls put in place where possible. There was observed variability in the density of signal of the positive control and in the housekeeping protein. Both the antibody to β -actin antibody and the target anti-myc were reused due to lack of resources. However, the secondary antibody was not reused and diluted from frozen stock. There was also no protease inhibitor used which could have caused breakdown of the target ADAMTS13. This could have explained the variability in results.

4.9 Concluding remarks

These results indicate that the SNPs p.R7W and p.A1003T may have a positive modifying effect on the p.R1060W mutation and may, in some part, explain the phenotype of late-onset TTP. However, on statistical analysis, no significant results have been found on the modifying influence of SNPs. The p.R1060W mutation has been shown to decrease ADAMTS13 secretion. However, patients may also have a residual level of activity of ADAMTS13 from the p.R1060W mutation near the endothelial surface where cleavage of the newly synthesized ULVWF occurs. Vascular endothelial cells have been

found to synthesise and secrete ADAMTS13 in small quantities (Turner *et al.*, 2006). A sufficient amount of ADAMTS13 could therefore be produced until a physiologically demanding event such as pregnancy or infection dramatically increases the level of ULVWF produced by activated endothelial cells. ADAMTS13 also has no known natural inhibitor therefore plasma levels remain fairly constant, with a long half- life. The effect of SNPs on RNA processing and stability may also contribute to altered ADAMTS13 expression and is discussed in Chapter 6.

Pregnancy is a hypercoagulable state which may be a physiological adaptation in order to protect against haemorrhage during parturition and the post-partum stage (peri-partum haemorrhage is the leading cause of maternal mortality in the developing world; Drury-Stewart *et al.*, 2014; Khan *et al.*, 2008). Hypercoagulability can be explained by an increase in VWF synthesis with a decrease in the activity of ADAMTS13. The VWF propeptide and activity levels in pregnancy have been measured and have been found to increase by approximately 500% (Kentouche *et al.*, 2013). During the course of pregnancy, VWF levels progressively increase to reach 2.5 - 3 times higher at term (however, peak values follow delivery). ADAMTS13 levels decrease by approximately 30% at term when compared to baseline levels before pregnancy, possibly due to the concomitant increase in VWF levels and consumption of VWF substrate (Kentouche *et al.*, 2013). Elevations in pro-coagulant proteins have also been observed (Brenner, 2004). However, in normal, healthy women, ADAMTS13 levels will stay above 10%. The physiological significance of an increase in VWF during the second trimester may be the trigger for the TTP boom seen in pregnancy-associated TTP as TTP occurring in the first trimester is not seen (Veyradier *et al.*, 2012)

There may also be an effect of pregnancy hormones on ADAMTS13 metabolism. Powazniak *et al.* performed a series of studies evaluating the effect of 17 β -estradiol (E2) on human umbilical vein endothelial cells (HUVEC) on the synthesis and secretion of VWF and ADAMTS13 (Powazniak *et al.*, 2011). Although HUVEC incubated with E2 showed no significant differences in secreted ADAMTS13 levels, intracellular levels increased eight-fold and

ADAMTS13 mRNA increased nine-fold. There was no increase in VWF secretion or intracellular levels. However, VWF mRNA levels increased. ADAMTS13 gene inactivation also upregulated the release and intracellular VWF levels in HUVEC, indicating that E2 may play a role in the regulation of VWF and ADAMTS13 gene expression (Powazniak *et al.* 2011).

Another TTP trigger during pregnancy may be complement activation. Atypical HUS presents with TTP-like symptoms and results in partial inactivation of ADAMTS13. A mutation in factor H has been associated with thrombotic microangiopathy associated with ADAMTS13 deficiency (Chapin *et al.*, 2016). The use of the anti-complement therapy Eculuzimab has also been reported to ameliorate refractory TTP in a patient (Tsai *et al.*, 2013). This indicates that complement may have an effect on the VWF-ADAMTS13 axis.

In summary, the SNPs p.R7W and p.A1033T may positively modify the effect of the p.R1060W mutation to explain the late-onset TTP phenotype although no statistically significant results have been found. However, due to the changes in VWF-ADAMTS13 axis during pregnancy and possible complement activation the genotype is only one in a number of factors to consider. The effect of SNPs on RNA processing and stability may also play a role in varied clinical phenotype.

Chapter 5

The effect of SNPs and mutations on congenital TTP phenotype

5.1 *ADAMTS13* polymorphisms

SNPs have been identified throughout the *ADAMTS13* gene (see Table 5.1) and various studies have reviewed their contribution to disease phenotype (Edwards *et al.*, 2012; Lotta *et al.*, 2010; Plaimauer *et al.*, 2006). Most case studies that report screening of the *ADAMTS13* gene note that, in addition to mutations, patients also carry multiple SNPs. It has been observed that the SNPs p.R7W and p.Q448E exist in greater frequencies in TTP patients than in the general population (Donadelli *et al.*, 2006). The occurrence of SNPs p.R7W and p.A1033T also occur in pregnancy-associated TTP, together with the p.R1060W mutation, at a greater frequency than is seen in the general population (Scully *et al.*, 2014). This may just be an observation that the SNPs have co-evolved with the mutation and it is difficult to make more definitive conclusions without more comprehensive reporting of the full *ADAMTS13* genotype. Interestingly, the SNPs in humans p.R7W, p.Q448E and p.A900V are in the WT in murine species of the C57BL/6J strain, which could indicate these variants have a neutral effect (Bruno *et al.*, 2005).

The effect of a combination of SNPs *in vitro* has been investigated by Plaimauer *et al.* The SNPs p.P618A and p.A732V individually led to a decrease in *ADAMTS13* antigen levels. These SNPs were more detrimental in combination (p.P618A + p.A732V in combination showed 4% WT levels); this would be sufficient to cause TTP if present on both alleles in a *cis*-configuration. The addition of p.R7W or p.Q448E singly increased the *ADAMTS13* activity to 15% and the addition of all four SNPs increased the activity to 40% (Plaimauer *et al.*, 2006). The amino acid substitutions may alter the short or long-range interactions of the protein at the active site, the exosites or sites involved in post-translational modifications, thus affecting function or secretion.

Table 5.1 Missense non-synonymous SNPs identified in the *ADAMTS13* gene (from Lotta *et al.*, 2010)

Nucleotide change	Amino acid change	Domain	dbSNP accession number	Global minor allele frequency*(MAF)
C19T	p.R7W	Signal peptide	rs34024143	0.0527
C1016G	p.T339R	Disintegrin	-	-
C1342G	p.Q448E	Cysteine-rich	rs2301612	0.2716
G1368T	p.Q456H	Cysteine-rich	rs36220239	0.0170
C1370T	p.P457L	Cysteine-rich	rs36220240	0.0063
C1423T	p.P475S	Cysteine-rich	rs11575933	0.0044
G1451A	p.R484K	Cysteine-rich	rs28375042	-
G1810A	p.V604I	Spacer	rs34256013	0.0004
C1852G	p.P618A	Spacer	rs28647808	0.0323
G1874A	p.R625H	Spacer	rs36090624	0.0244
G1900A	p.E634K	Spacer	rs34569244	-
C2195T	p.A732V	TSP1-2	rs41314453	0.0056
G2218A	p.E740K	TSP1-2	rs36221451	0.0120
G2494A	p.V832M	TSP1-4	rs34104386	0.0040
C2699T	p.A900V	TSP1-5	rs685523	0.0765
C2708T	p.S903L	TSP1-5	-	-
G2944A	p.G982R	TSP1-6	rs36222275	0.0014
G3097A	p.A1033T	TSP1-7	rs28503257	0.0156
G3287G	p.R1096H	TSP1-8	rs61751476	0.0146
C3677T	p.T1226I	CUB-1	rs36222894	0.0042

The numbering of nucleotides is relative to the *ADAMTS13* cDNA derived from reference sequence NM_139025.4, genome build 37.1.

For a given SNP, the less conserved the area in which the variant occurs, the greater the variant allele frequency. Thus the rarer SNPs tend to encode more conserved residues as this variation may be unfavourable to the function of the encoded protein (Tseng & Kimchi-Safarty, 2011). This can be evidenced in Chapter 3. It should also be noted that the basal level of *ADAMTS13* is highly variable, even among healthy controls and between patients of different ethnic backgrounds and this should be taken into account when interpreting the possible clinical effect of mutations and SNPs (Peyvandi *et al.*, 2004). However, TTP diagnosis is made on *ADAMTS13* activity levels at <5% normal (for a particular population) in the plasma. The normal range for *ADAMTS13* ranges widely from 740-1420ng/ml within normal, healthy individuals (Reiger *et al.*, 2006) and this is also dependent on the assay method used. There is currently no international standard or recognised quality control material in use.

The aims of this study are to analyse the effect of single nucleotide polymorphisms and mutations, either singly or in combination, on congenital thrombotic thrombocytopenic purpura phenotype based on patient genotype. The mutations and polymorphisms investigated in this study were identified in a cohort of TTP patients referred to the TTP Registry at UCLH, London (Camilleri *et al.*, 2012); see Tables 5.2-5.4 for genotype information. Those mutations for which expression vectors were constructed are marked with * The clinical details of these patients can be seen in Table 5.5.

Table 5.2 Genotype of patients diagnosed with pregnancy-associated TTP (from Camilleri *et al.*, 2012)

Pregnancy-associated TTP	Patient	Nucleotide change	Amino acid change	Domain	SNPs present
	1	C3178T*	p.R1060W	TSP-7	p.R7W + p.A1033T
	2	G794C+ A796T C3178T*	p.C265S+ p.S266C p.R1060W	MP TSP1-7	p.R7W, p.A1033T
	3	C1787T* G3284A	p.A596V p.109Q	Spacer TSP1-8	p.475S
	4	G305A*	p.R102H	MP	p.Q448E + p.618A + p.A900V
	5	G2930T*	p.C977F	TSP1-5	-
	6	719_724del G2068A	p.G241_C242del p.A690T	MP	p.R7W, p.Q448E, p.618A, p.A732V, p.A900V

Table 5.3 Genotype of patients diagnosed with neonatal TTP (from Camilleri *et al.*, 2012)

Neonatal TTP	Patient	Nucleotide change	Amino acid change	Domain	SNPs present
	7	C1225T*	p.R409W	TSP1-1	-
	8	C1192T* G1308C*	p.R398C p.Q436H	TSP1-1 TSP1-1	p.Q448E
	9	719_724del C2728T*	p.G241_C242del p.R910X	MP TSP1-5	p.A900V
10	719_724del C2728T*	p.G241_C242del p.R910X	MP TSP1-5	-	

Table 5.4 Genotype of patients diagnosed with childhood TTP (from Camilleri *et al.*, 2012)

Childhood TTP	Patient	Nucleotide change	Amino acid change	Domain	SNPs present
	11	C1787T*	p.A596V	Spacer	-
	12	C587T*	p.T196I	MP	p.Q448E
	13	T2260C	p.C754R	TSP1-3	p.Q448E
	14	G649C* C3178T*	p.D217H p.R1060W	MP TSP1-7	p.R7W, p.Q448E, p.A1033T
15	G803C G1368T	p.R268P p.Q456H	MP Cysteine-rich	-	

Table 5.5 Clinical details and genotype of TTP patients (from Camilleri *et al.*, 2012)

Mutation	Age at TTP diagnosis	ADAMTS13/antigen level	SNPs
Metalloprotease domain			
p.R102H ¹	18 years*	57ng/ml	p.Q448E ¹ , p.616A ¹ , p.A900V ¹
p.T196I ¹	3 years	Undetectable	p.Q448E ¹
p.D217H + p.R1060W ²	18 months	17ng/ml	p.A1033T ³ , p.R7W ³ , p.Q448E ³
TSP1-1 domain			
p.R398H + p.Q436H ²	Birth	Undetectable	p.Q448E ³
p.R409W	Birth	Undetectable	-
Spacer domain			
p.A596V + p.R1095Q ²	29 years*	<10ng/ml	p.Q448E ³
p.A596V ¹	18 months	11ng/ml	-
TSP1-2, 5 and 7			
p.A690T + 719_724del ²	20 years*	35ng/ml	p.R7W + p.Q448E+ p.418A, p.A732V, p.A900V
p.C977F ¹	24 years*	38 ng/ml	-
p.R1060W2 + p.D217H (as above)	18 months	17ng/ml	p.A1033T3, p.R7W3, p.Q448E3

*Pregnancy associated ¹Homozygous; ²Compound heterozygous; ³Heterozygous, haplotype not specified. Minor allele frequency can be seen in Table 5.1.

The positions of these mutations and polymorphisms as they affect the ADAMTS13 protein can be seen in Figures 5.1 and 5.2. Mutations near the N-terminal would be assumed to be more detrimental as this is the functional part of the protease and more highly conserved. Hing *et al.* determined that a mutation located within this area was an indicator of the severity of clinical phenotype (Hing *et al.*, 2013) although acknowledged that other factors could also affect phenotype.

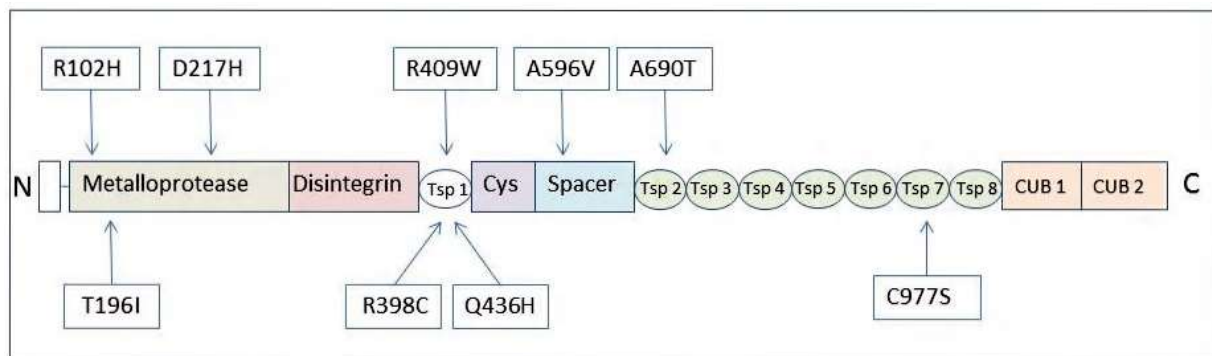


Figure 5.1 Position of mutations within the ADAMTS13 protein

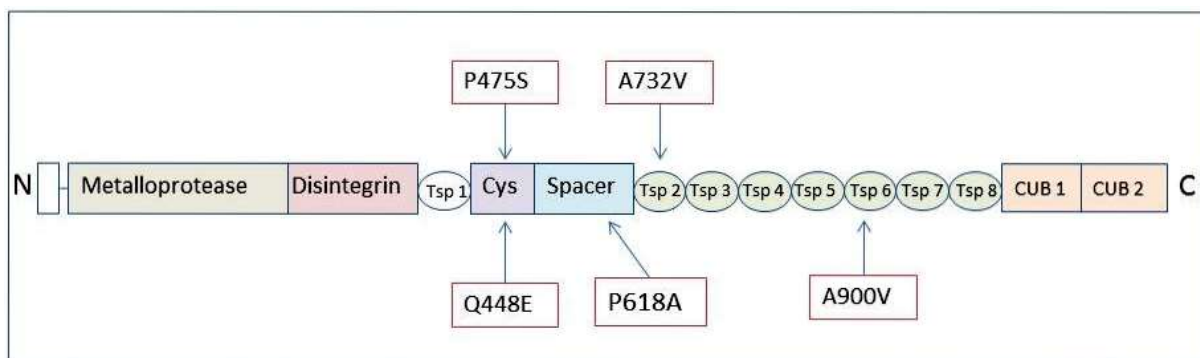


Figure 5.2 Position of SNPs within the ADAMTS13 protein

Previous investigators have utilised *in vitro* expression systems to determine the effect of mutations and SNPs within the *ADAMTS13* gene on ADAMTS secretion and activity. A summary can be seen Table 5.6.

Table 5.6 Previous expression studies of the effect of mutations and SNPs on the secretion and activity of ADAMTS13

Mutation	Cell line	Secretion	Activity	Reference
p.R102H (G305A)	HEK293T	Reduced (28-51%)	12%	Camilleri <i>et al.</i> , 2012
p.T196I*(C587T)	HEK293T	4%	Reduced	Camilleri <i>et al.</i> , 2012
p.D217H (G649C)	HEK293T	29-112%	24%	Camilleri <i>et al.</i> , 2012
p.G241_C242del 719_724del	HEK293T	Abolished (<3%)		Camilleri <i>et al.</i> , 2012
p.C265S+S266C (G794C+A796T)	HEK293T	Reduced (7%)		Camilleri <i>et al.</i> , 2012
p.R268P (G803C)	HeLa HeLa COS-7 HEK293T	Not detectable 38% 25% 5%	No activity No activity No activity 30%	Kokame <i>et al.</i> , 2002 Hommais <i>et al.</i> , 2007 Hommais <i>et al.</i> , 2007 Camilleri <i>et al.</i> , 2012
p.R409W (C1125T)	HEK293T	Abolished (<5%)		Camilleri <i>et al.</i> , 2012
p.R398C (C1192T)	HEK293T	Abolished (<5%)		Camilleri <i>et al.</i> , 2012
p.Q436H (G1308C)	HEK293T	Reduced (64-18%)		Camilleri <i>et al.</i> , 2012
p.Q456H (G1368T)	HEK293T	Increased (117-261%)	Normal*	Camilleri <i>et al.</i> , 2012
p.A596V	HeLa	17%	No activity	Hommais <i>et al.</i> , 2007

(C1787T)	COS-7 HEK293T	20% 7%	25%	Hommais <i>et al.</i> , 2007 Camilleri <i>et al.</i> , 2012
p.A690T (G2068A)	HEK293T	7-38%		Camilleri <i>et al.</i> , 2012
p.C754R (T2260C)	HEK293T	15-4%		Camilleri <i>et al.</i> , 2012
p.R910X*(C2728T)	HEK293T	7%		Camilleri <i>et al.</i> , 2012
p.C977F (G2930T)	HEK293T	<11%		Camilleri <i>et al.</i> , 2012
p.C3178T (R1060W)	HeLa HEK293	11% <5%	100% ¹ ,35% ² 100%	Tao <i>et al.</i> , 2006 Camilleri <i>et al.</i> ,2008
SNPs				
p.R7W	HEK293	99%	86%	Plaimauer <i>et al.</i> , 2006
p.Q448E	HeLa HEK293	Conserved 95%	Conserved 75%	Kokame <i>et al.</i> , 2002 Plaimauer <i>et al.</i> , 2006
p.P475S	HeLa	Conserved	70%	Kokame <i>et al.</i> , 2002
p.P618A	HEK293	27%	14%	Plaimauer <i>et al.</i> , 2006
p.A732V	HEK293	60%	71%	Plaimauer <i>et al.</i> , 2006
p.A1033T	HeLa	Conserved	80%	Tao <i>et al.</i> , 2006

Other researchers have also used *in vitro* studies using transient expression systems to evaluate ADAMTS13 expression both intracellularly (in cell lysates) and extracellularly (secreted levels in conditioned media). The results of studies with several SNP variants can be seen in Table 5.7 (Edwards *et al.*, 2012).

Table 5.7 Results of the effect of SNPs within the *ADAMTS13* gene on extracellular and intracellular expression of ADAMTS13 (Edwards *et al.*, 2012).

SNP	Domain	Extracellular expression as % of WT ADAMTS13	Intracellular expression as % of WT ADAMTS13
p.Q448E	Cysteine rich	100	140
p.P475S	Cysteine rich	105	130
p.P618A	Spacer	31	90
p.A732V	Tsp1-2	80	30
p.A1033T	Tsp1 -7	179	90

Camilleri *et al.* has also investigated the expected effect of *ADAMTS13* mutations on the secretion of ADAMTS13 (see Table 5.8; Camilleri *et al.*, 2012).

Table 5.8 Expected effect of mutations on secretion of ADAMTS13

Mutation	Effect on ADAMTS13 secretion level
Q456H (C1368T)	Increased 117-261%
D217H (G649C)	29-112%WT (also reduced activity)
R102H (G305A)	28-51%WT
C265C+S266C	Reduced
Q436H (G1308C)	Reduced
A690T (G2068A)	Reduced
C754R (T2260C)	Reduced
C977F (G2930T)	Reduced
R109X	Markedly reduced
T196I (C587T)	Markedly reduced
R268P (G803C)	Markedly reduced
R1060W	Severely reduced
G241_C242del	Abolished
R398C (C1192T)	Abolished
R409W (C1225T)	Abolished
A596V (C1787T)	Abolished

5.2 Methods

5.2.1 *In silico* analysis

The following computational tools were used to analyse the putative effects of mutations and SNPs found in cTTP patients on the function of ADAMTS13: SNPEffect4.0, IMutant, SIFT, PolyPhen2.0 and SNP Effect. Full details of methods and results can be seen in Chapter 3.

5.2.2 *In vitro* expression studies

Site directed mutagenesis (SDM) was used to create a series of expression vectors, as seen in Table 5.9. Each vector contained a mutation, an SNP or mutation and/or SNP in various combinations. The multi-SNP vectors p. R102H + p.Q448E + p.P618A + p.A900V and p. D217H + p.R7W + p.Q448E + p.A1033T were constructed by multi-site-directed mutagenesis, as described in Chapter 2. All other vectors were constructed by single-site-SDM. Constructs were validated by Sanger sequencing to ensure that no unwanted nucleotide changes were inserted, leading to non-synonymous variants.

Table 5.9 Expression vectors constructed by site directed mutagenesis

Expression vector	Mutation and/or SNP
p. R102H (G305A)	Mutation
p. R102H + p.Q448E	Mutation + SNP
p. R102H + p.P618A	Mutation + SNP
p. R102H + p.A900V	Mutation + SNP
p. R102H + p.Q448E + p.P618A + p.A900V [‡]	Mutation + 3 SNPs
p. T196I (C587T)	Mutation
p. T196I + p.Q448E	Mutation + SNP
p.D217H (G649C)	Mutation
p. D217H + p.R7W	Mutation + SNP
p. D217H + p.Q448E	Mutation + SNP
p. D217H + p.A1033T	Mutation + SNP
p. D217H + p.R7W + p.Q448E + p.A1033T [‡]	Mutation + 3 SNPs
p. R398C (C1192T)	Mutation
p.R409W (C1225T)	Mutation
p. Q436H (G1308C)	Mutation
p. A596V (C1787T)	Mutation
p. A596V + P475A	Mutation + SNP
p. A690T (G2068A)	Mutation
p. C977F (G2930T)	Mutation
SNPs	
p. R7W (C19T)	SNP
p Q448E (C1342G)	SNP
p. P475S (C1423T)	SNP
p. P618A (C1852G)	SNP
p. A732V (C2195G)	SNP
p. A900V (C2699T)	SNP
p. A1033T (C3097A)	SNP

[‡] denotes vectors constructed by multi- site-directed mutagenesis

The construction of expression vectors in Table 5.10 were attempted but were abandoned due to continual corruption of the nucleotide sequencing around the nucleotide substitution, as confirmed on Sanger sequencing.

Table 5.10 Expression vectors not created

Mutations
p.G241_C242del*
p.C265S+S266C *
p.R268P *
p.Q456H *
p.C754R *

Mutant plasmids were amplified and purified prior to transfection into human embryonic kidney cells (HEK293T). Transfection efficiency was measured by the co-transfection of the reporter vector carrying the *LacZ* gene, as described previously in Chapter 2. Transfection of WT and mutant vectors were performed in 6-well plates as described. After incubation for 72 hours cell lysates were collected, the cells lysed in 20mM Triton X and sonicated prior to protein quantitation by BCA assay. Conditioned media was harvested and concentrated prior to protein quantitation by BCA assay. Western blot analysis was performed on cell lysates and conditioned media. An equal quantity of protein was loaded per well for SDS-PAGE and during blotting the housekeeping antibody anti- β -actin (Abcam, clone 8226) was used as a loading control (cell lysates only). Recombinant ADAMTS13 was visualized by western blotting using an antibody directed towards the anti-myc tag (Merck-Millipore, clone A46). HRP-conjugated goat anti-mouse IgG was used as a secondary antibody (Sigma-Aldrich, A4416). The western blots were band intensities were analysed by densitometry using ImageJ. ADAMTS13 antigen quantitation was performed on the concentrated conditioned media using the commercially available IMUBIND[®] ADAMTS13 ELISA. Values (mean of replicate transfections) are presented as % of 3 replicate WT values \pm SEM (WT = 100%).

5.3 Results

5.3.1 Sequencing data of expression vectors

The sequencing data for each expression vector with mutation \pm SNP inserted can be seen in Figures 5.3- 5.15.

G305A

ADAMTS13 30FD49 GGAGGACACAGAGCCTATGTGCTCACCAACCTCAACATCGGGGCAGAACTGCTTCGGGA 350
GGAGGACACAGAGCACTATGTGCTCACCAACCTCAACATCGGGGCAGAACTGCTTCGGGA 420

C1342G

ADAMTS13 30FD43 ACCCAGCTGGAGTTCATGTGCGAACAGTGCGCCAGGACCGACGGCCAGCCGCTGCGCTCC 1380
ACCCAGCTGGAGTTCATGTGCGAACAGTGCGCCAGGACCGACGGCCAGCCGCTGCGCTCC 456

C1852G

ADAMTS13 07AF24 AGGGCGCTATGTCGTGGCTGGGAAGATGAGCATCTCCCCTAACACCACCTACCCCTCCCT 1859
AGGGCGCTATGTCGTGGCTGGGAAGATGAGCATCTCCCCTAACACCACCTACCCCTCCCT 411

C2699T

ADAMTS13 30FD44 CCCTCCCCATGGGGCAGCATCAGGACGGGGCTCAAGCTGCACACGTGTGGACCCCTGGG 2700
CCCTCCCCATGGGGCAGCATCAGGACGGGGCTCAAGCTGCACACGTGTGGACCCCTGGG 656

Figure 5.3 Sequencing results of expression vector G305A + C1342G + C1852G + C2699T mutation + SNPs

C587T

ADAMTS13 07AE85 ACTAGGTTTGACCTGGAGTTGCCTGATGGTAACCGGCAGGTGCGGGGCGTCAACCAGCTG 594
ACTAGGTTTGACCTGGAGTTGCCTGATGGTAACCGGCAGGTGCGGGGCGTCAACCAGCTG 660

C1342G

ADAMTS13 84CI13 ACCCAGCTGGAGTTCATGTGCGAACAGTGCGCCAGGACCGACGGCCAGCCGCTGCGCTCC 1380
ACCCAGCTGGAGTTCATGTGCGAACAGTGCGCCAGGACCGACGGCCAGCCGCTGCGCTCC 453

Figure 5.4 Sequencing results of expression vector C587T + C1342G mutation + SNP

G649C

ADAMTS13 07AF35 AGCTGGGCGGTGCCTGCTCCCCAACCTGGAGCTGCCTCATTACCGAGGACACTGGCTTCG 649
AGCTGGGCGGTGCCTGCTCCCCAACCTGGAGCTGCCTCATTACCGAGGACACTGGCTTCG 720

C19T

ADAMTS13 07AF35 -----ATGCACCAGCGTCACCCCAGGGCAAGATGCCCTCCCCTCTGTGTGGCCG 49
CGCCGGCCACCATGCACCAGCGTCACCCCAGGGCAAGATGCCCTCCCCTCTGTGTGGCCG 120

C1342G

ADAMTS13 07AF48 ACCCAGCTGGAGTTCATGTGCGAACAGTGCGCCAGGACCGACGGCCAGCCGCTGCGCTC 1379
GACCCAGCTGGAGTTCATGTGCGAACAGTGCGCCAGGACCGACGGCCAGCCGCTGCGCTC 454

G3097A

ADAMTS13 30FD69 CTGGGCCATGTTCCGGCCAGCTGTGGCCTTGGCACTCTAGACGCTCGGTGGCCTGTGTG 3120
CTGGGCCATGTTCCGGCCAGCTGTGGCCTTGGCACTCTAGACGCTCGGTGGCCTGTGTG 651

Figure 5.5 Sequencing results of expression vector G649C + C19T + C1342G + G3097A mutation + SNPs

C1192T

ADAMTS13 GCAGCAGTGCATGGGCGCTGGTCTAGCTGGGGTCCCCGAAGTCCTTGCTCCGCTCCTGC 1200
 45HI66 GCAGCAGTGCATGGGCGCTGGTCTAGCTGGGGTCCCCGAAGTCCTTGCTCCGCTCCTGC 270

C1342G

ADAMTS13 ACCCAGCTGGAGTTCATGTCGAACAGTGCGCCAGGACCGACGGCCAGCCGCTGCGCTCC 1380
 32EG87 ACCCAGCTGGAGTTCATGTCGAACAGTGCGCCAGGACCGACGGCCAGCCGCTGCGCTCC 452

Figure 5.6 Sequencing results of expression vector C1192T + C1342G mutation + SNP

C1225T

ADAMTS13 GGAGGAGGTGTGGTCACCAGGAGGGGCAGTGCACAACCCAGACCTGCCTTTGGGGGG 1260
 36AG24 GGAGGAGGTGTGGTCACCAGGAGGGGCAGTGCACAACCCAGACCTGCCTTTGGGGGG 338

Figure 5.7 Sequencing results of expression vector C1225T mutation

G1308C

ADAMTS13 CGTGCATGTGTTGGTGCTGACCTCCAGGCCGAGATGTGCAACACTCAGCCTGCGAGAAG 1320
 36AG28 CGTGCATGTGTTGGTGCTGACCTCCAGGCCGAGATGTGCAACACTCAGCCTGCGAGAAG 395

Figure 5.8 Sequencing results of expression vector G1308C mutation

C1787T

ADAMTS13 ACCAGTGTCTACATTGCCAACCACAGGCCTCTCTTACACACTTGGGGTGAGGATCGGA 1800
 30FE18 ACCAGTGTCTACATTGCCAACCACAGGCCTCTCTTACACACTTGGGGTGAGGATCGGA 357

C1423T

WTADAMTS13 CTACCACTGGGGTGTGCTGTGTAACACAGCCAAGGGGATGCTCTGTGCA 1450
 C1423T6 CTACCACTGGGGTGTGCTGTGTAACACAGCCAAGGGGATGCTCTGTGCA 521

Figure 5.9 Sequencing results of expression vector C1787T + C1423T mutation + SNP

G2068A

ADAMTS13 AGGCCTGGGTGTGGGCCCTGTGCGTGGGCCCTGCTCGGTGAGCTGTGGG 2100
 G2068A17-Seq03 AGGCCTGGGTGTGGGCCCTGTGCGTGGGCCCTGCTCGGTGAGCTGTGGG 655

Figure 5.10 Sequencing results of expression vector G2068A mutation

```

C2930T
ADAMTS13                GGAGAGGGGTCGTGCGGAGGATCCTGTATTGTGCCCGGGCCCATGGGGAG 2949
87G2930T_3_+C3484T_2_ GGAGAGGGGTCGTGCGGAGGATCCTGTATTGTGCCCGGGCCCATGGGGAG 901
*****

```

Figure 5.11 Sequencing results of expression vector G2930T mutation

```

C1423T
ADAMTS13                TCCCCTGGCGGCGCCTCCTTCTACCACTGGGGTGCTGCTGTATCACACAGCCAAGGGGAT 1440
30FD90                  TCCCCTGGCGGCGCCTCCTTCTACCACTGGGGTGCTGCTGTATCACACAGCCAAGGGGAT 516
*****

```

Figure 5.12 Sequencing results of expression vector C1423T SNP

```

C1852G
ADAMTS13                GGGCGCTATGTCGTGGCTGGGAAGATGAGCATCTCCCTAACACCACCTACCCTCCCTC 1860
45HI82                  GGGCGCTATGTCGTGGCTGGGAAGATGAGCATCTCCCTAACACCACCTACCCTCCCTC 936
*****

```

Figure 5.13 Sequencing results of expression vector C1852G SNP

```

C2195T
WTADAMTS13             ACTGTCCAGTGCCAAGGGAGCCAGCAGCCACCAGGTGGCCAGAGGCCTGCGTGCTCGAA 2220
VN004                  ACTGTCCAGTGCCAAGGGAGCCAGCAGCCACCAGGTGGCCAGAGGCCTGCGTGCTCGAA 168
*****

```

Figure 5.14 Sequencing results of expression vector C2195T SNP

```

C2699T
WTADAMTS13             GCAGGGTCGTGCTCCGTCTCCTGCGGGCGAGGTCTGATGGAGCTCGTTTCCTGTGCATG 2760
BS03-05                GCAGGGTCGTGCTCCGTCTCCTGCGGGCGAGGTCTGATGGAGCTCGTTTCCTGTGCATG 351
*****

```

Figure 5.15 Sequencing results of expression vector C2699T SNP

5.3.1.1 Non synonymous mutation introduced by SDM

It was found that in several vectors, SDM lead to an unwanted amino acid change involving the same nucleotide substitution (resulting in a non-synonymous mutation) at C3484T.

The nucleotide change was reverted back to the WT sequence by with a further SDM experiment, as described in section 4.7.1.1. Interestingly, the unwanted nucleotide change was inserted when the original nucleotide change was implemented in the more distal end of the cDNA insert. Those nucleotide changes implemented at the more proximal end of the insert did not induce this C3484T substitution.

A summary of the vectors which contained the same non synonymous mutation as a result of SDM are summarised in Table 5.11.

Table 5.11 Expression vectors carrying C3484T non-synonymous mutation

C1787T (p.596V)
C1787T + C1423T (p.596V + P475S)
G2068A (p.A690T)
G2930T (p.C977F)
C1423T (p.P475S)
C1852G (p.P618A)
C2195T (p.A732V)
C2699T (p.A990V)

The nucleotide change was reverted back to the WT sequence by with a further SDM experiment, as described in section 4.7.1.1. Interestingly, the unwanted nucleotide change was inserted when the original nucleotide change was implemented in the more distal end of the cDNA insert. Those nucleotide changes implemented at the more proximal end of the insert did not induce this C3484T substitution.

After sequencing and validation as described previously, the expression vectors were cleaned and amplified, yielding the DNA concentrations seen in Table 5.12. In consideration of the poor DNA yield with QIAGEN Maxiprep, the Invitrogen Midiprep was used, yielding a much higher concentration of DNA.

Table 5.12 DNA concentrations of expression vectors following Maxiprep/Midiprep*preparation

Expression vector	Protein concentration ($\mu\text{g}/\mu\text{l}$)
G305A *	180
G305A + C1342G	84
G305A + C1342G * repeat	1631
G305A + C2699T	90
G305A + C1342G + C1852G + C2699T	212
C587T	148
C587T+ C1342G	116
G649C	113
G649C repeat	130
G649C + C19T	54
G649C + C19T repeat	291
G649C + C19T repeat*	1164
G649C + C1342G	113
G649C + C1342G *	1057
G649C + G3097A	76
G649C + C19T + C1342G + G3097A 1	66
C1192T	662
C1192T + C1342G *	469
C1225T	503
C1308C	1212
C1787T	299
C1787T + C1423T	441
G2068A	1435
G2930T	1380
C1342G	87
C1852G	33
C1852G	180
C2195T	677
C2699T	115

As can be seen, DNA yield differs very greatly between expression vectors. It can also be noted that the growth rate and colonial morphology also differed greatly on the LB-Agar plates. This may possibly reflect the differences at the DNA level (possibly reflecting a change in the coiling of the vector) as a result of introducing nucleotide changes.

5.3.2 Transfection efficiencies of expression vectors

The transfection efficiency was measured as previously described in section 2.8; see Table 5.13.

Table 5.13 Transfection efficiencies of expression vectors

Expression vector	Transfection efficiency (%)
p.R102H (G305A)	21
p.R102H + p.A900V(G305A + C2699T)	18
p.R102H + p.Q448E (G305A + C1342G)	20
p.R102H + p.R7W + p. Q448E + p.P618A + p.A1033T (G305A + C19T + C1342G + C1842G + G3097A) multi	15
p.T196I (C587T)	22
p.T196I + p.Q448E (C587T + C1342G)	21
p.D217H (G649C)	20
p.D217H + p.R7W (G649C + R7W)	18
p.D217H + p.A1033T (G649C + G3097A)	18
p. D217H + p.Q448E (G649C + C1342G)	21
p. D217H + p.R7W + p.Q448E + p.A1033T (G649C + C19T + C1342G + D3097A) (multi)	18
p.R398C (C1192T)	18
p.R398C + p.Q448E (C1192T + C1342G)	20
p.R409W (C1225T)	14
p. Q436H (G1308C)	19
p.A596V (C1787T)	22
p.A596V + p.Q448E (C1787T + C1342G)	20
p.A690T (G2068A)	19
p.C977F (G2930T)	19
p.P475S (C1423T)	15
p.Q448E (C1342G)	13
p.P618A (C1852G)	12
p.A732V (C2195T)	16
p.A900V (C2699T)	14

Following harvesting, lysing (cell lysates) and concentrating (conditioned media) the samples were assayed for total protein concentration by BCA assay; for results see Appendix 1.

5.3.3 Western blot analyses

5.3.3.1 Western blots p.R102H series

The cells were harvested, lysed and sonicated as previously described before analysing by western blot (see Figures 5.16 –5.17.).The expected size of ADAMTS13 protein (approx. 180kDa) was seen. The housekeeping protein β -actin of molecular weight 45kDa was used as a loading control. An equal

amount of total protein was loaded into each well of the SDS-PAGE gel, as determined by BCA assay.

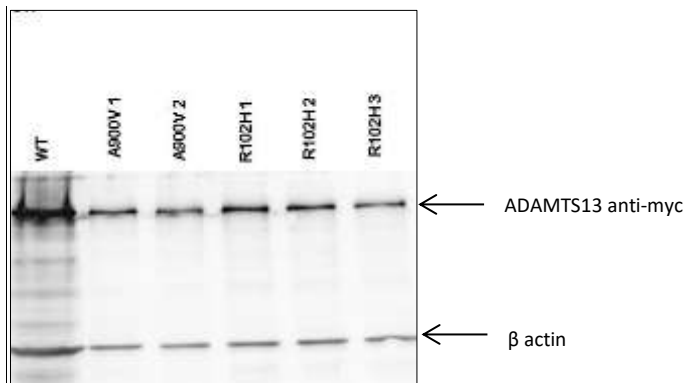


Figure 5.16 Western blot analysis cell lysate p.A900V and p.R102H

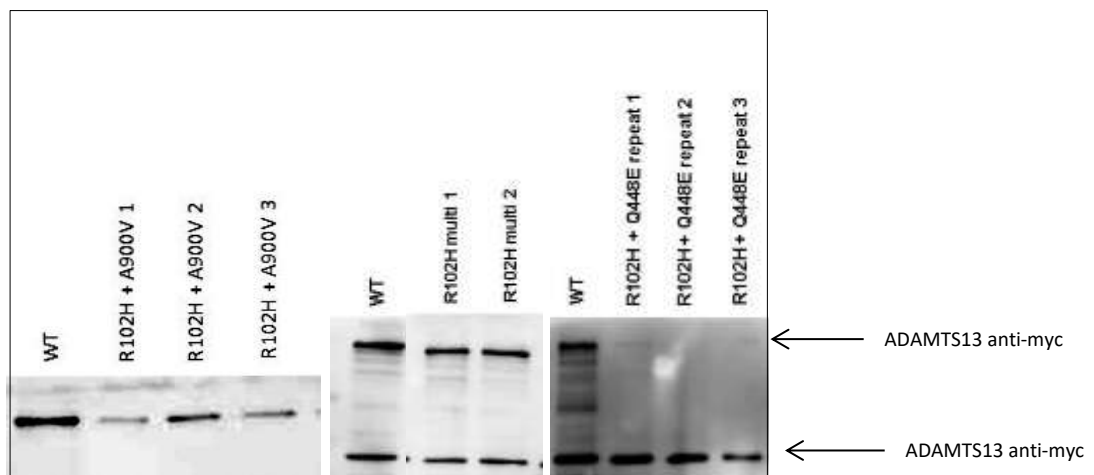


Figure 5.17 Western blot analysis cell lysates p.R102H + p.A900V; p.R102H + p.Q448E repeat transfection; and p.R102H multi SNPs (p.R102H + p.Q448E + p.P618A + p.A900V).

The conditioned media of the expression vectors analysed in Figures 5.16 - 5.17 were harvested, concentrated and analysed on western blot (see Figure 5.18).

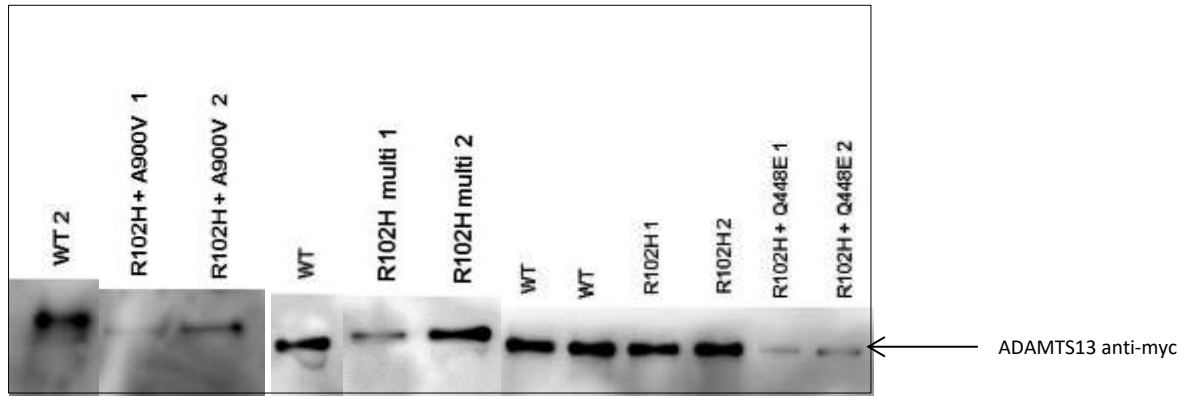


Figure 5.18 Western blot conditioned media: WT, p.R102H + p.A900V, p.R102H + multi SNPs (p.R102H + p.Q448E + p.P618A + p.A900V), p.R102H and p.R102H + Q448E

The band intensities on western blots were scanned using ImageJ software and the cell lysate values normalized to the β -actin housekeeping protein and compared with positive control (WT) values % WT \pm SEM (see Table 5.14 and Figure 5.19).

Table 5.14 ImageJ analysis of p.R102H series, cell lysates

Expression vector	Normalized protein ratio (sample/actin)	% normalised WT \pm SEM
WT	1.0	100
p.R102H 1	0.64	64 \pm 5
p.R102H 2	0.58	58 \pm 5
p.R102H 3	0.49	49 \pm 5
p.R102H + A900V 1	n/a	45 \pm 12
p.R102H + A900V 2	n/a	68 \pm 12
p.R102H + A900V 3	n/a	63 \pm 12
p. R102H + p.Q448E 1 Rpt	0.19	19 \pm 5
p.R102H + p.Q448E 2 Rpt	0.10	9 \pm 5
p.R102H + p.Q448E 3 Rpt	0.29	15 \pm 5
p.R102H + p.Q448E + p.P618A + A900V (multi) 1	1.5	145 \pm 33
p.R102H + p.Q448E + p.P618A + A900V multi 2	1.0	97 \pm 33

*Repeat transfection. The expression vectors p.R102H + p.618A were not transfected.

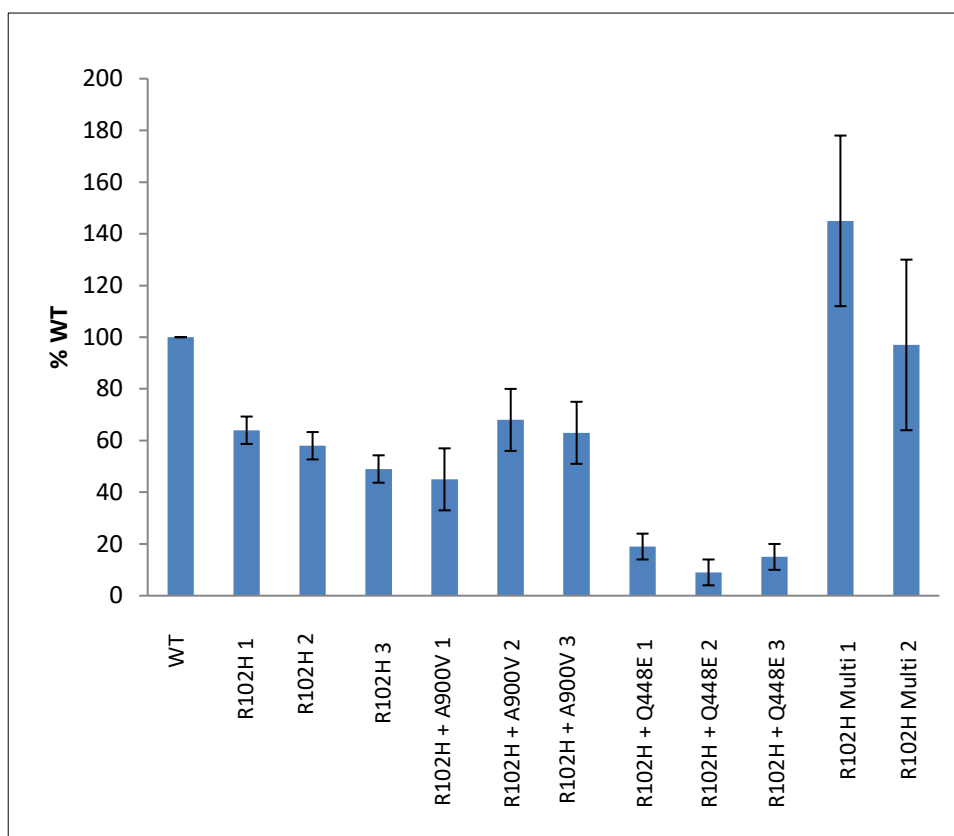


Figure 5.19 Comparison of %WT \pm SEM ADAMTS13 expression in cell lysates, p.R102H series (multi = p.R102H + p.Q448E + p.P618A + A900V).

The band intensities on western blots were scanned using ImageJ software and the conditioned media samples normalized to the WT positive control on the same blot (values % WT \pm SEM); (see Table 5.15 and Figure 5.20).

Table 5.15 ImageJ analysis of p.R102H series, conditioned media

Expression vector	Normalized protein ratio	% WT \pm SEM
WT	1.0	100
p.R102H 1	1.07	107 \pm 29
p.R102H 2	1.5	149 \pm 29
p.R102H + p.A900V 1	0.22	22 \pm 1.4
p.R102H + p.A900V 2	0.24	24 \pm 1.4
p.R102H + p.Q448E 1	0.37	37 \pm 1.4
p.R102H + p.Q448E 2	0.39	39 \pm 1.4
p.R102H + p.Q448E + p.P618A + A900V (multi) 1	0.67	67 \pm 13
p.R102H + p.Q448E + p.P618A + A900V (multi) 2	0.86	86 \pm 13

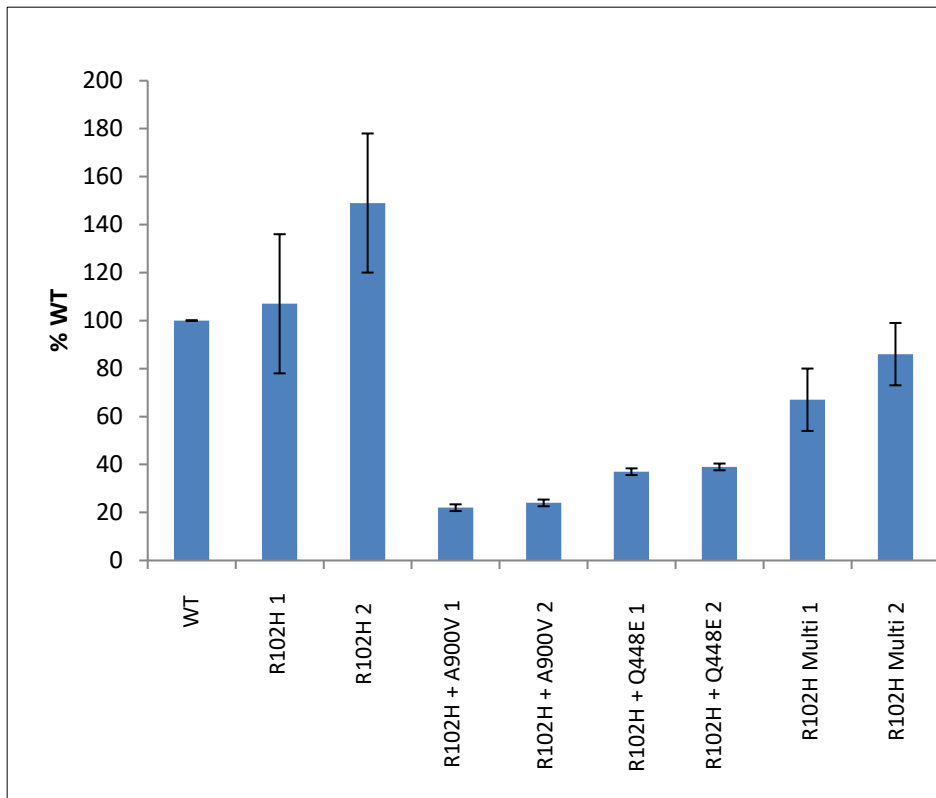


Figure 5.20 Comparison of %WT \pm SEM ADAMTS13 expression in conditioned media, p.R102H series

Conditioned media samples were analysed for ADAMTS13 antigen with the commercially available IMUBIND® ADAMTS13 ELISA kit according to manufacturer's instructions. Results can be seen in Table 5.16 and Figure 5.21.

Table 5.16 ELISA ADAMTS13 antigen concentration p.R102H series, expressed as %WT conditioned media

Expression vector	ADAMTS13 concentration (ng/ml)	% WT \pm SEM
p.R102H 1	218	90 \pm 9.0
p.R102H 2	174	72 \pm 9.0
p.R102H + A900 1	9	4 \pm 1.6
p.R102H + A900V2	1	1 \pm 1.6
p.R102H + p.Q448E + p.P618A + A900V (multi) 1	73	30 \pm 1.0
p.R102H + p.Q448E + p.P618A + A900V (multi) 2	78	32 \pm 1.0
p.D102H + p.Q448E 1	15	7 \pm 1.3
p.D102H + p.Q448E 2	9	4 \pm 1.3

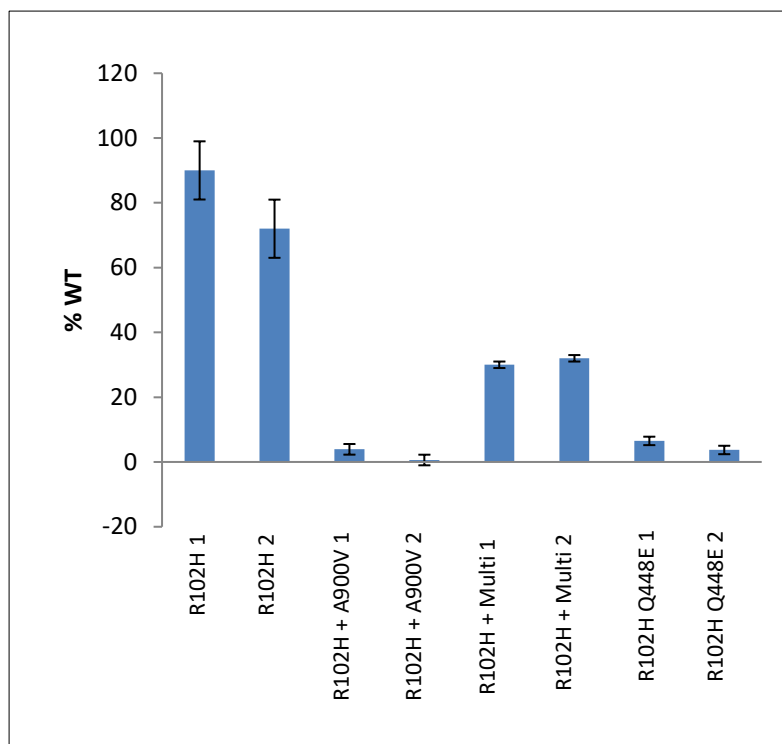


Figure 5.21 ELISA analysis of ADAMTS antigen concentration, %WT ± SEM of conditioned media, p.R102H series

In order to assess the statistical significance of the variation in ADAMTS13 expression between the mutation p.R102H in combination with SNPs p.Q448E and A900V singly and in combination with, a one way analysis of variance (ANOVA) statistical test was performed. The values for %WT were utilised for each western blot (not all shown) with outlying % WT values excluded. Results can be seen in Table 5.17. In the analysis of cell lysates and conditioned media by western blot, there was no statistical significance found in ADAMTS13 expression between the mutation and mutation + SNPs. However, a statistical significant difference was found on analysis of ADAMTS13 expression in conditioned media as analysed by ELISA.

Table 5.17 One way ANOVA analysis of p.R102H + SNPs

Expression vector	Experimental Method	Observed ratio	F	Tabulated ratio (p=0.05)	F	Null hypothesis
Cell lysate	Western blot	0.01		4.35		Accept
CM	Western blot	0.98		4.35		Accept
CM	ELISA	39.2		9.28		Reject

5.3.3.2 Western blot analyses p.D217H series

The cells were harvested, lysed and sonicated as previously described before analysing by western blot (see Figure 5.21- 5.23). The expected size of ADAMTS13 protein (approx. 180kDa) was seen. An antibody directed against the housekeeping protein β -actin of molecular weight 45kDa was used as a loading control. An equal amount of total protein was loaded into each well of SDS-PAGE, as determined by BCA assay.

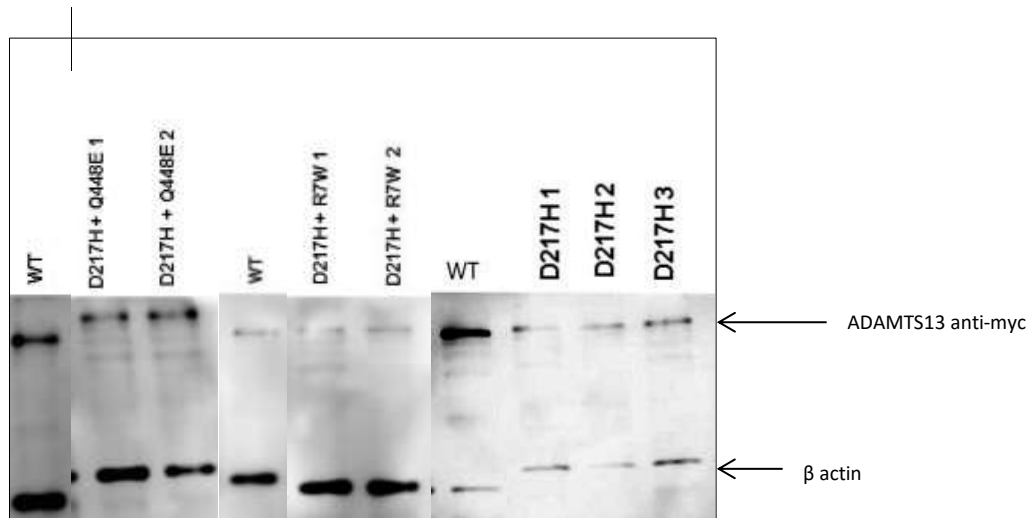


Figure 5.22 Western blot analyses of cell lysate: WT, p.D217H + p.Q448E p.D217H + p.R7W; p.D217H.

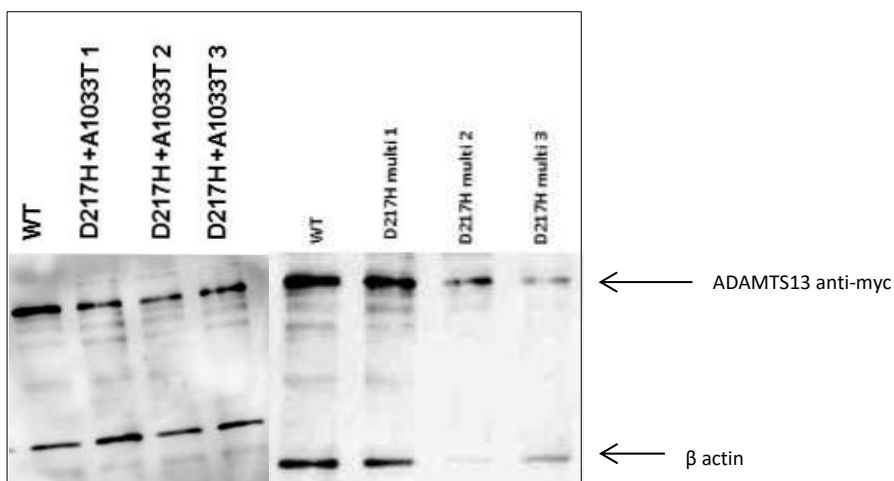


Figure 5.23 Western blot analyses of cell lysate: p.D217H + p.A1033T; E: p.D217H + multi SNPs (p.R7W + p.Q448E + p.A1033T).

The conditioned media of the expression vectors analysed in Figure 5.22-5.23 were harvested, concentrated and analysed on western blot (see Figure 5.24).

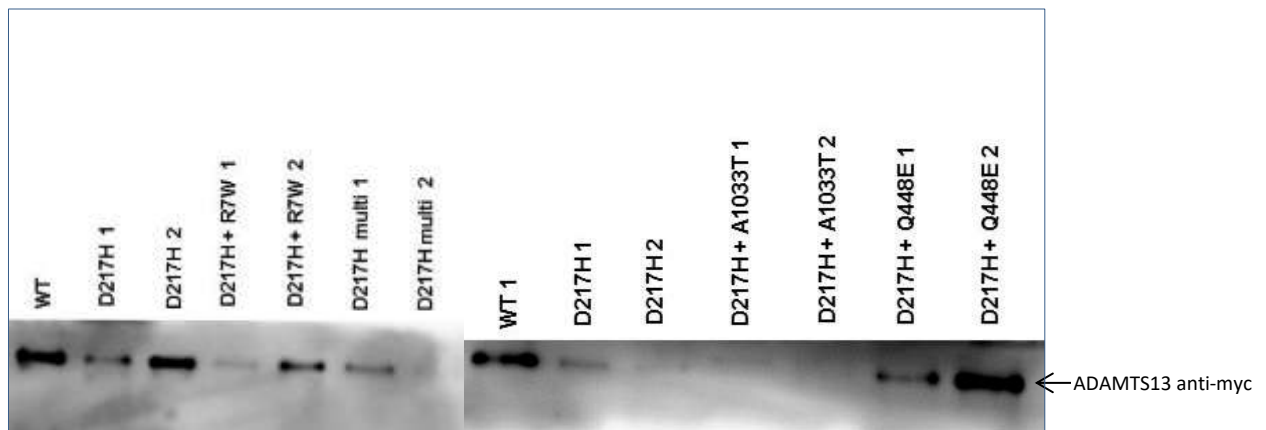


Figure 5.24 Western blot analyses conditioned media: p.D217H, p.D217H + R7W, p.D217H + multi SNPs. (p.R7W + p.Q448E + p.A1033T), p.D217H + p.A1033T and p.D217H + p.Q448E.

The band intensities on western blots were scanned using ImageJ software and the cell lysates normalized to the β -actin housekeeping protein and compared with positive control (WT) values % WT \pm SEM (see Table 5.18 and Figure 5.25).

Table 5.18 ImageJ analysis of p.D217H series, cell lysates

Expression vector	Normalized protein ratio	% WT \pm SEM
WT	1.0	100
p. D217H 1	1.5	149 \pm 24
p. D217H 2	1.1	160 \pm 24
p. D217H 3	1.6	114 \pm 24
p. D217H + p.R7W 2 rpt	1.1	112 \pm 34
p. D217H + p.R7W 3 rpt	0.6	64 \pm 34
p. D217H + p.Q448E 1 rpt	0.7	65 \pm 18
p. D217H + p.Q448E 2 rpt	0.9	90 \pm 18
p. D217H + p.A1033T 1	1.1	110 \pm 5
p. D217H + p.A1033T 2	1.2	120 \pm 5
p. D217H + p.A1033T 3	2.6	111 \pm 5
p. D217H + p.R7W + Q448E + A1033T (multi) 1	2.59	40 \pm 100
p. D217H + p.R7W + Q448E + A1033T (multi) 2	0.9	0 \pm 100
p. D217H + p.R7W + Q448E + A1033T (multi) 3	0.8	80 \pm 100

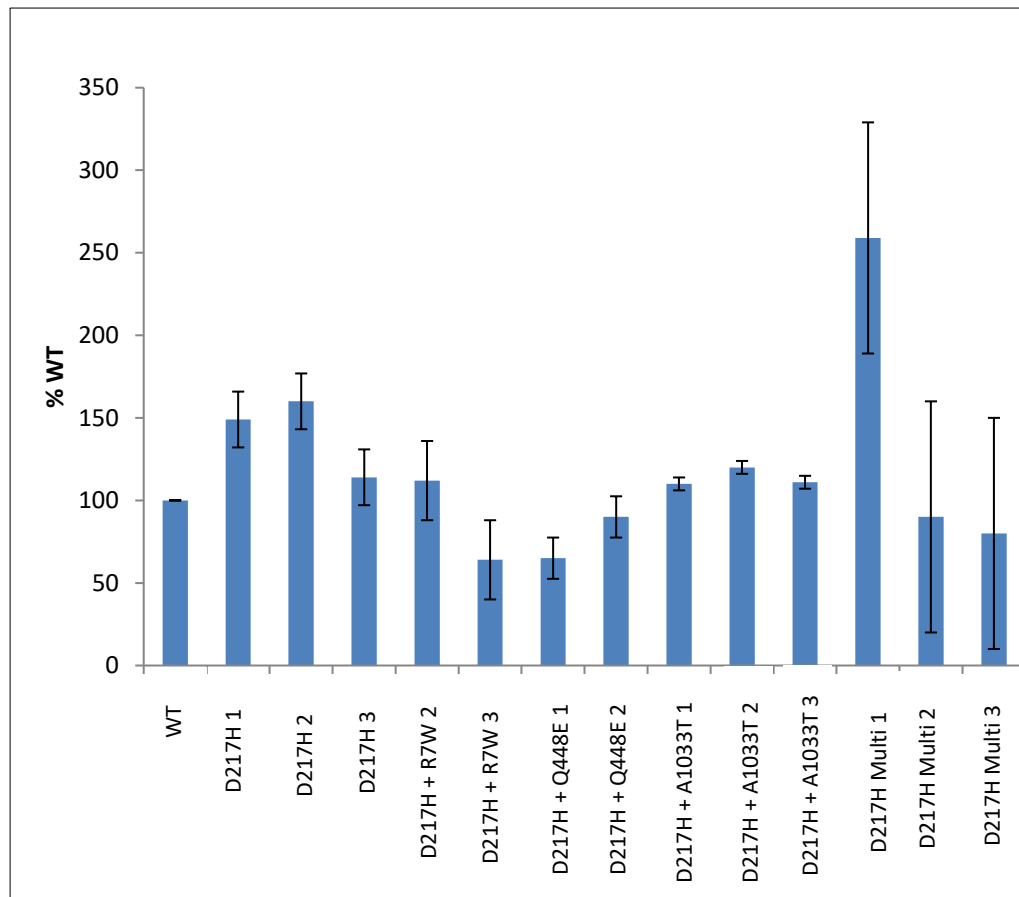


Figure 5.25 Comparison of %WT ADAMTS13 expression in cell lysates ADAMTS13 expression, p.D217H series.

The band intensities on western blots were scanned using ImageJ software and the conditioned media samples normalized to the WT positive control on the same blot (values % WT \pm SEM); (see Table 5.19 and Figure 5.26).

Table 5.19 ImageJ analysis of p.D217H series, conditioned media

Expression vector	Normalized protein ratio	% WT \pm SEM
WT	1	100
p. D217H 1	0.5	50 \pm 41
p. D217H 2	0.3	30 \pm 41
p. D217H 3	1.0	100 \pm 41
p. D217H + p.R7W 1 rpt	0.3	30 \pm 28
p. D217H + p.R7W 2 rpt	0.7	70 \pm 28
p. D217H + p.Q448E 1	0.7	70 \pm 56
p. D217H + p.Q448E 2	1.5	150 \pm 56
p. D217H + p.A1033T 1	0.2	23 \pm 2
p. D217H + p.A1033T 2	0.2	20 \pm 2
p. D217H + p.R7W + Q448E + A1033T 1	0.4	40 \pm 14
p. D217H + p.R7W + Q448E + A1033T 2	0.2	20 \pm 14

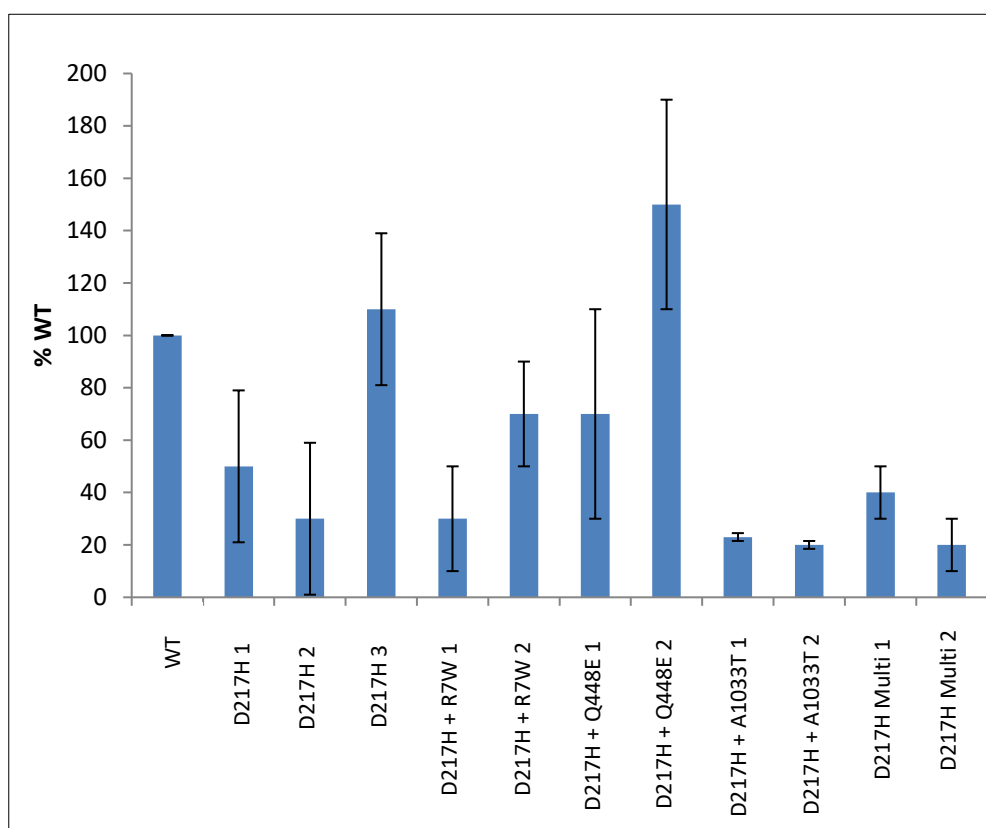


Figure 5.26 Comparison of %WT ADAMTS13 expression in conditioned media, p.D217H series.

Conditioned media samples were analysed for ADAMTS13 antigen with the commercially available IMUBIND® ADAMTS13 ELISA kit according to manufacturer's instructions. Results can be seen in Table 5.20 and Figure 5.27.

Table 5.20 ELISA ADAMTS13 antigen concentration p.D217H series, expressed as %WT conditioned media

Expression vector	ADAMTS13 concentration (ng/ml)	% WT
WT	273	100
p. D217H 1	17.3	7.1
p. D217H 2	108.0	44.4
p. D217H + p.R7W Rpt 1	76.0	31.2
p. D217H + p.R7W Rpt 2	40.0	17
p. D217H + p.Q448E Rpt 1	0	0
p. D217H + p.Q448E Rpt 2	0	0
p. D217H + p.A1033T 1	56.0	23
p. D217H + p.A1033T 2	55.0	23
p.D217H + p.R7W + p.Q448E + p.A1033T (multi) 1	161.0	66.4
p.D217H + p.R7W + p.Q448E + p.A1033T (multi) 2	222.0	91.6

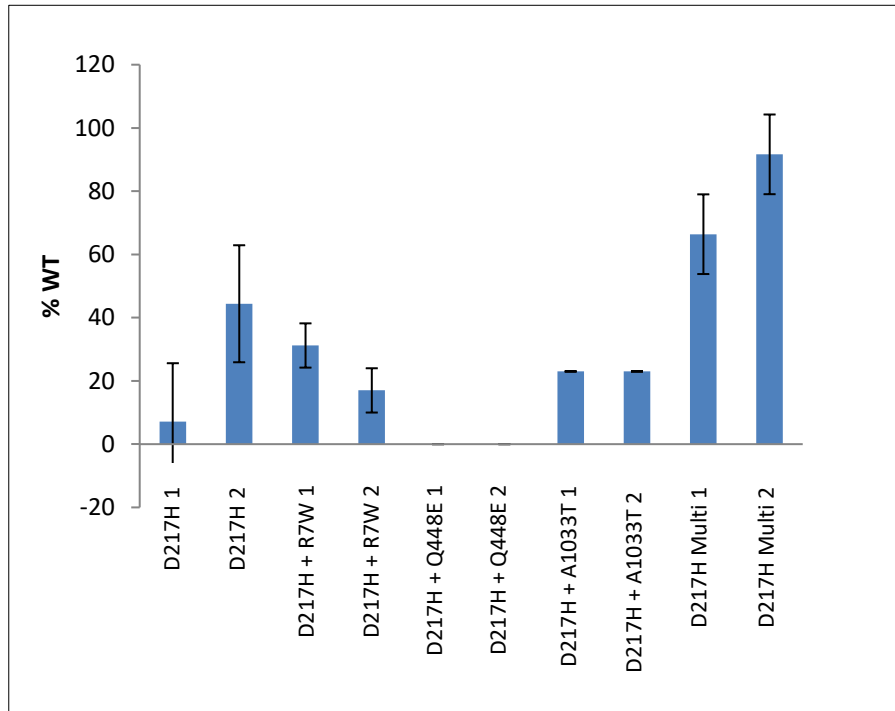


Figure 5.27 ELISA analysis of ADAMTS antigen concentration, %WT ± SEM of conditioned media, p.D217H series.

In order to assess the statistical significance of the variation in ADAMTS13 expression between the mutation p.D217H in combination with SNPs p.R7W, p.Q448E and A1033T singly and in combination, a one way analysis of variance (ANOVA) statistical test was performed. The values for %WT were utilised for each western blot (not all are shown) Results can be seen in Table 5.21.

Table 5.21 One way ANOVA results, p.D217H + SNPs ($p=0.05$)

Expression vector	Experimental Method	Observed F ratio	Tabulated F ratio ($p=0.05$)	Null hypothesis
Cell lysate	Western blot	1.169	3.84	Accept
Conditioned media	Western blot	2.04	3.84	Accept
Conditioned media	ELISA	67.2	4.12	Reject

In the analysis of cell lysates and conditioned media by western blot, there was no statistical significance found in ADAMTS13 expression between the mutation and mutation + SNPs. However, a statistical significant difference was found on analysis of ADAMTS13 expression in conditioned media as analysed by ELISA.

5.3.3.3 Western blots analyses SNP series

The cells were harvested, lysed and sonicated as previously described before analysing by western blot (see Figures 5.28 – 5.29). The expected size of ADAMTS13 protein (approx. 180kDa) was seen. An antibody directed against the housekeeping protein β -actin of molecular weight 45kDa was used as a loading control. An equal amount of total protein was loaded into each well of SDS-PAGE, as determined by BCA assay.

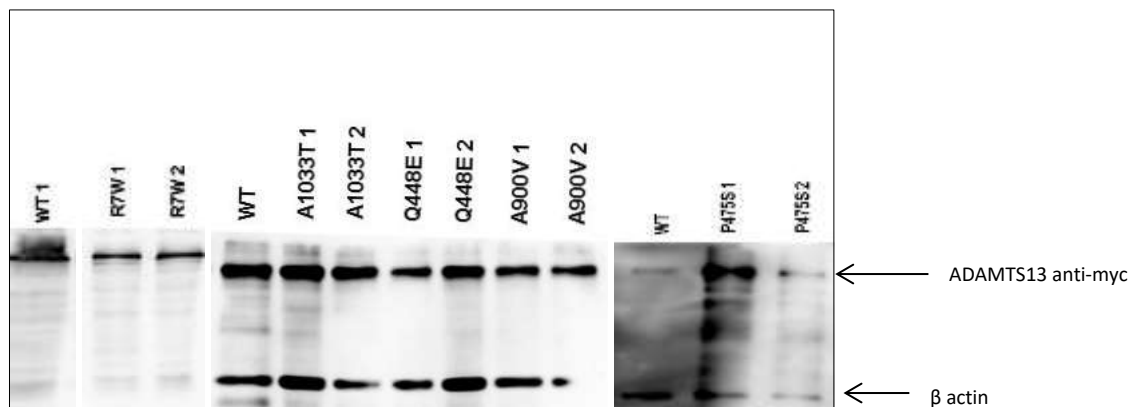


Figure 5.28 Western blot analyses SNPs, cell lysates p. R7W, p.A1033T, p.Q448E, p.A900V and p.P475S

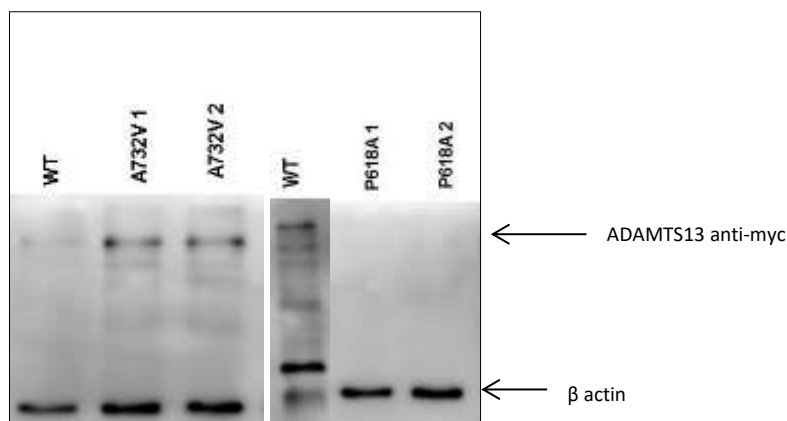


Figure 5.29 Western blot analyses SNPs cell lysates p. A732V and p.P618A

The conditioned media of the expression vectors analysed in Figure 5.29 -5.29 were harvested, concentrated and analysed on western blot (see Figure 5.30). The SNP p.A1033T has previously been analysed in sections 4.6.7 and 4.6.8 in Chapter 4.

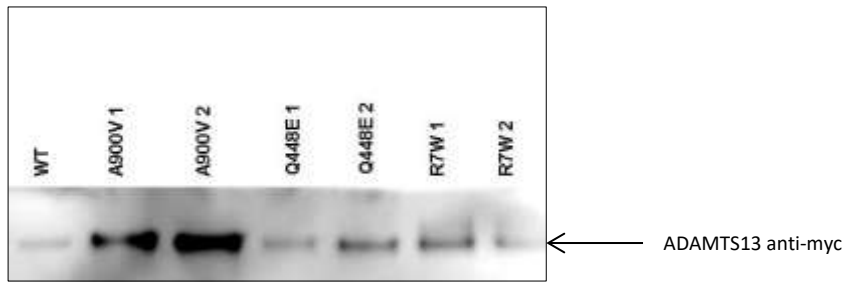


Figure 5.30 Western blot analyses SNPs, conditioned media p.A900V, p.Q448E and p.R7W

No bands were visualised for p.457S, p. A732V and p.P618A after repeat transfections.

The band intensities on western blots were scanned using ImageJ software and the cell lysates normalized to the β -actin housekeeping protein and compared with positive control (WT) values % WT \pm SEM (see Table 5.22 and Figure 5.31).

Table 5.22 ImageJ analysis of SNP series, cell lysates

Expression vector	Normalized protein ratio	% WT
WT	1.0	100
p.R9W 1	0.75	75
p.R7W 2	0.80	80
p.Q448E 1	0.9053	90 \pm 6.5
p.Q448E 2	0.7769	77 \pm 6.5
p.P475S 1	0.6	60 \pm 20.4
p.P475S 3	0.55	55 \pm 20.4
p.P618A 1	0	0
p.P618A 2	0	0
p.A732V 1	0.5774	57 \pm 6.0
p.A732V 3	0.6972	69 \pm 6.0
p.A900V 1 blot 1	0.9396	93 \pm 142
p.A900V 2 blot 1	1.6	166 \pm 142
p.1033T 1	0.73	73
p.1033T 2	0.75	75

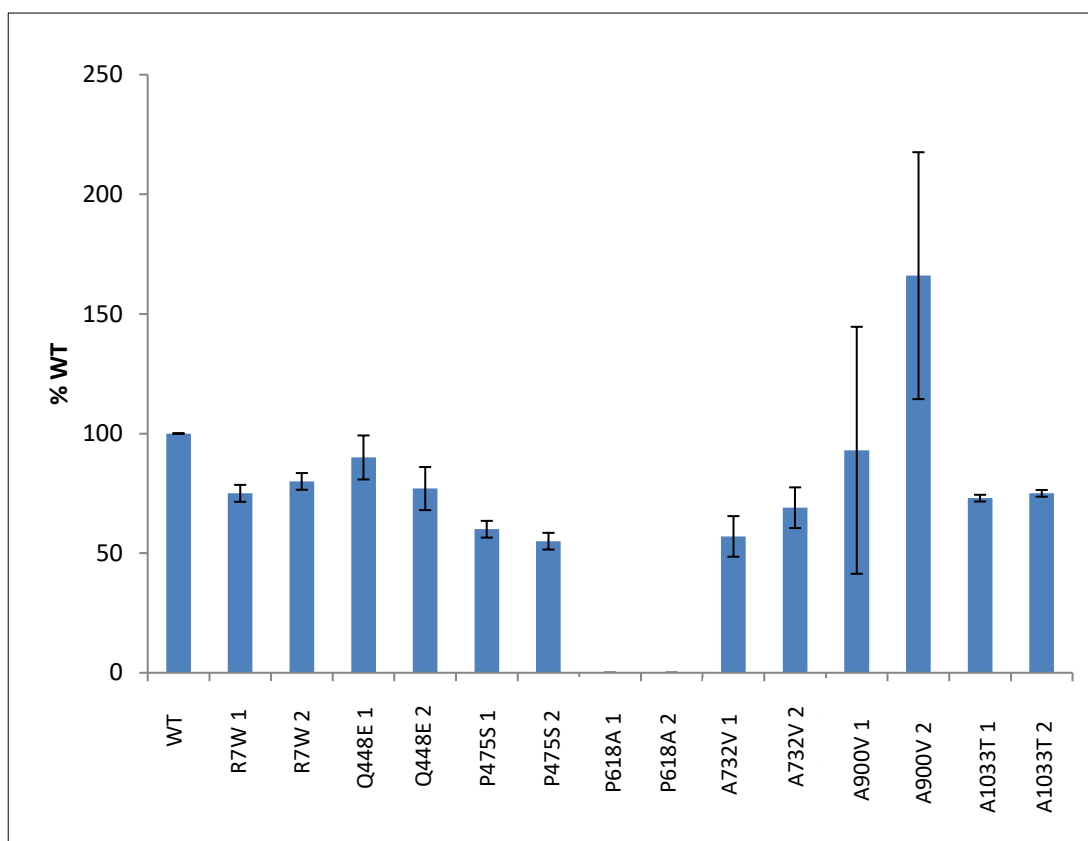


Figure 5.31 Comparison of ADAMTS13 expression cell lysates %WT ± SEM, SNP series

The band intensities on western blots were scanned using ImageJ software and the conditioned media samples normalized to the WT positive control on the same blot (values % WT ± SEM); (see Table 5.23 and Figure 5.32).

Table 5.23 ImageJ analysis of SNP series, conditioned media

Expression vector	Normalized protein ratio	% WT ± SEM
WT		
p.Q448E 1 blot 1	1.0	103 ± 4.24
p.Q448E 2 blot 1	1.1	109 ± 4.24
p.P475S 1	0	0
p.P475S 3	0	0
p.P618A 1 blot 2	0	0
p.P618A 2 blot 2	0	0
p.A732V 1	0	0
p.A732V 3	0	0
p.A900V 1	2.3	233 ± 65
p.A900V 2	1.0	103 ± 65

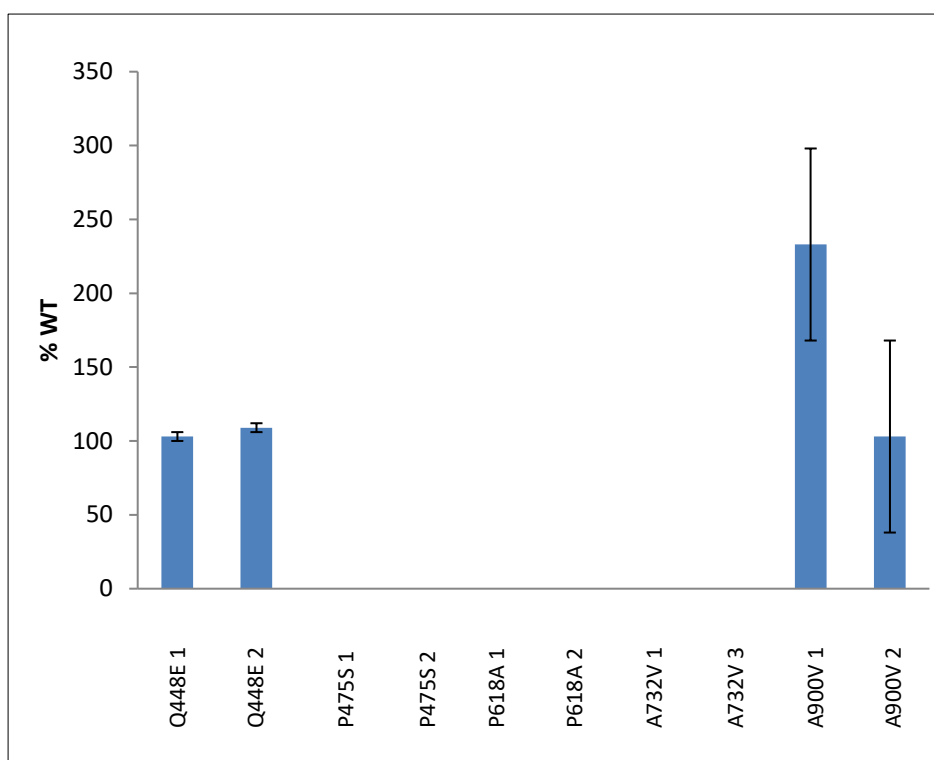


Figure 5.32 Comparison of ADAMTS13 expression conditioned media %WT ± SEM, SNP series

Conditioned media samples were analysed for ADAMTS13 antigen with the commercially available IMUBIND® ADAMTS13 ELISA kit according to manufacturer's instructions. Results can be seen in Table 5.24 and Figure 5.33.

Table 5.24 ELISA ADAMTS13 antigen concentration SNP series, expressed as %WT conditioned media

Expression vector	ADAMTS13 concentration (ng/ml)	% WT
WT	242	100
p.Q448E 1	100	41 ± 21
p.Q448E 2	202	83 ± 21
p.P475S 1	0	0
p.P475S 2	0	0
p.P618A 1	137	56.4 ± 28
p.P618A 2	0	0 ± 28
p.A732V 1	70	29 ± 3.5
p.A732V 3	89	36 ± 3.5
p.A900V 1	10	4.1 ± 6.4
p.A900V 2	42	17 ± 6.4

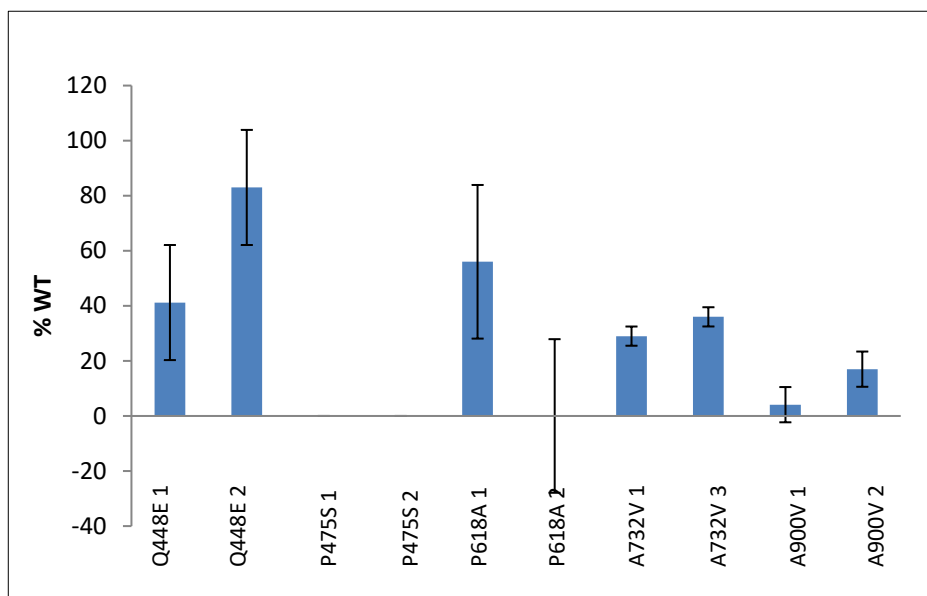


Figure 5.33 ELISA analysis of ADAMTS antigen concentration, %WT \pm SEM of conditioned media, SNP series

In order to assess the statistical significance of the variation in ADAMTS13 expression between the SNPs p.R7W, p.Q448E, p.P475S, p.A732V, p.A900V and p.A1033T, a one way analysis of variance (ANOVA) statistical test was performed. The values for %WT were utilised for each western blot (not all are shown). Results can be seen in Table 5.25.

Table 5.25 One way ANOVA results, SNP series ($p=0.05$)

Expression vector	Experimental Method	Observed F ratio	Tabulated F ratio ($p=0.05$)	Null hypothesis
Cell lysate	Western blot	0.55	4.39	Accept
CM	Western blot	0.58	6.59	Accept
CM	ELISA	0.87	3.84	Accept

In the analysis of cell lysates and conditioned media by western blot, there was no statistical significance found in ADAMTS13 expression between the SNPs on western blot or ELISA.

5.3.3.4 Western blot analysis p.R409W and p.R398C series

The cells were harvested, lysed and sonicated as previously described before analysing by western blot (see Figure 5.34). The expected size of ADAMTS13 protein (approx. 180kDa) was seen. An antibody directed against the housekeeping protein β -actin of molecular weight 45kDa was used as a

loading control. An equal amount of total protein was loaded into each well of SDS-PAGE, as determined by BCA assay.

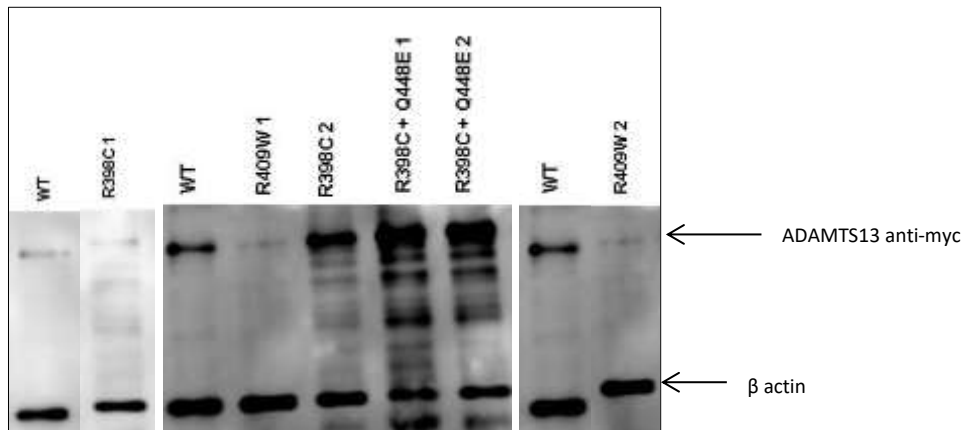


Figure 5.34 Western blot analysis of cell lysate: p.R398C, p.R409W, and p.R398C + p.Q448E.

The conditioned media of the expression vectors analysed in Figures 5.34 was harvested, concentrated and analysed on western blot (see Figure 5.35).

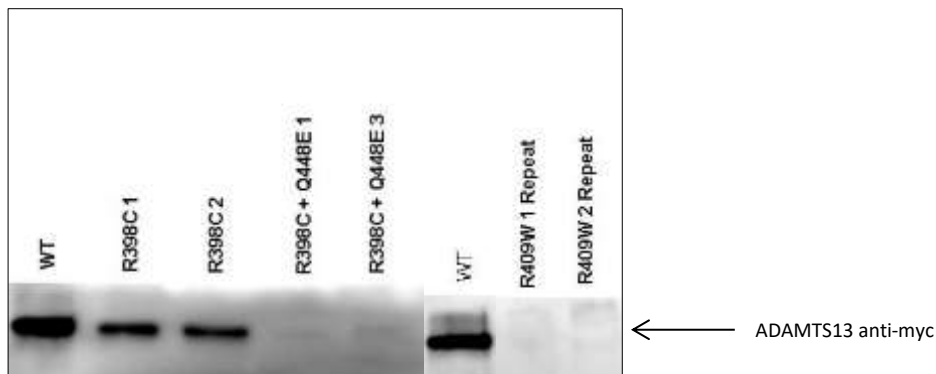


Figure 5.35 Western blot analysis of conditioned media: p.R398C, p.R398C + p.Q448E and p.R409W.

The band intensities on western blots were scanned using ImageJ software and the cell lysates normalized to the β -actin housekeeping protein and compared with positive control (WT) values $\% \text{ WT} \pm \text{SEM}$ (see Table 5.26 and Figure 5.36).

Table 5.26 ImageJ analysis of p.R409W and p.R398C series, cell lysates

Clone	Normalized protein ratio	% WT \pm SEM
p.R409W 1	0.5	57 \pm 2.5
p.R409W 2	0.5	52 \pm 2.5
p.R398C 1	0.2	24 \pm 38.7
p.R398C 2	1.0	101 \pm 38.7
p.R398C + p.Q448E 1	0.85	85 \pm 14.5
p.R398C + p.Q448E 2	1.14	114 \pm 14.5

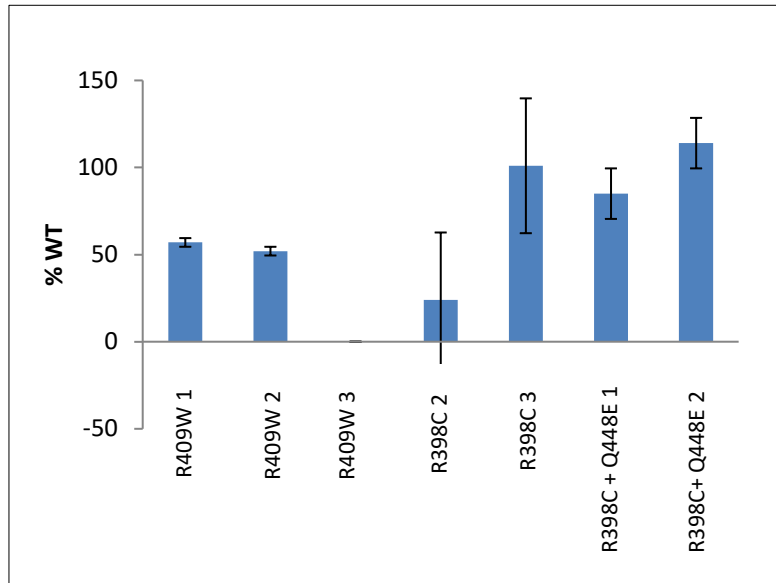


Figure 5.36 Comparison of %WT \pm SEM ADAMTS13 expression cell lysates, p.R409W and p.R398C series

The band intensities on western blots were scanned using ImageJ software and the conditioned media samples normalized to the WT positive control on the same blot (values % WT \pm SEM); (see Table 5.27 and Figure 5.37).

Table 5.27 ImageJ analysis p.R409W and p.R398C series, conditioned media

Clone	Normalized protein ratio	% WT \pm SEM
p.R409W 1	0	0
p.R409W 2	0	0
p.R398C 1	0.8	87 \pm 0.5
p.R398C 2	0.8	86 \pm 0.5
p.R398C + p.Q448E1	0.1	12 \pm 7.0
p.R398C + p.Q448E 2	0.2	26 \pm 7.0

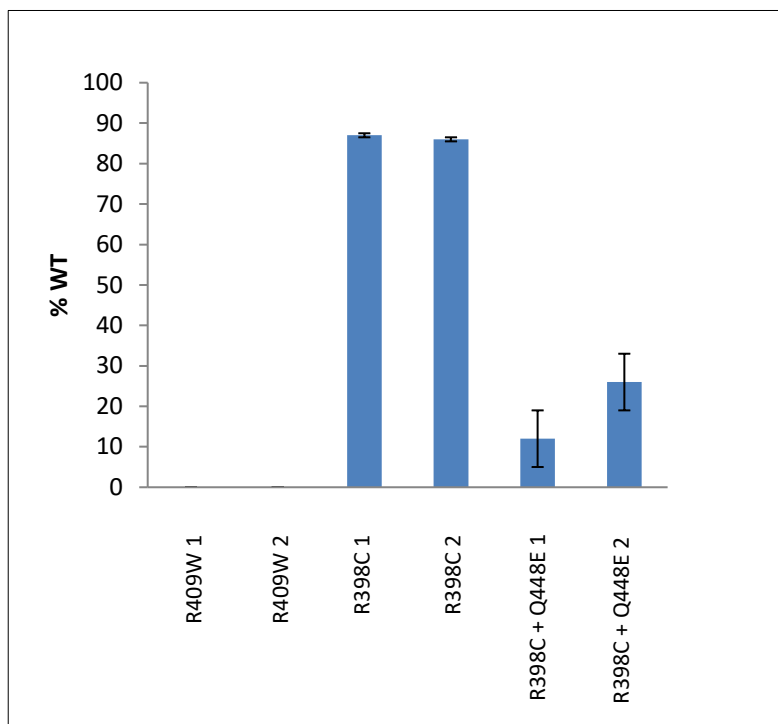


Figure 5.37 Comparison of %WT \pm SEM ADAMTS13 expression conditioned media, p.R409W and p.R398C series

Conditioned media samples were analysed for ADAMTS13 antigen with the commercially available IMUBIND® ADAMTS13 ELISA kit according to manufacturer's instructions. Results can be seen in Table 5.28 and Figure 5.38.

Table 5.28 ELISA ADAMTS13 antigen concentration p.R409W and p.R398C series, expressed as %WT conditioned media

Clone	ADAMTS13 concentration (ng/ml)	% WT \pm SEM
WT	243	100
p.R409W 1	0	0
p.R409W 2	0	0
p.R398C 1	0	0
p.R398C 2	50	21 \pm 10.4
p.R398C + p.Q448E 1	22.1	9 \pm 12.4
p.R398C + p.Q448E 2	83.0	34 \pm 12.4

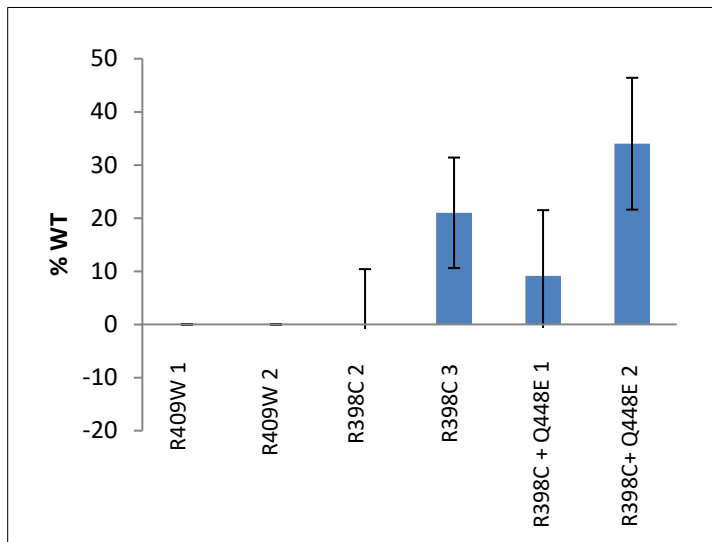


Figure 5.38 ELISA analysis of ADAMTS antigen concentration, %WT \pm SEM of conditioned media, p.R409W and p.R398C series

A paired sample student's t test was performed to analyse if there was any significant difference between % ADAMTS13 expression in cell lysates and conditioned media between p.R398C and p.R398C + p.Q448E, ($p=0.05$). The calculated result = 0.00123 lysates and 0.0019 in conditioned media. The tabulated value with one degree of freedom = 12.71.

The null hypothesis can be accepted that there is no significant difference between ADAMTS13 expression with mutation p.R398C and the mutation with p.Q448E SNP in cell lysates or conditioned media. However, due to the small sample size, any conclusions drawn from this data must be interpreted with caution.

5.3.3.5 Western blot analysis p.A596V and p.A690T

The cells were harvested, lysed and sonicated as previously described before analysing by western blot (see Figures 5.39). An antibody directed against the housekeeping protein β -actin of molecular weight 45kDa was used as a loading control. An equal amount of total protein was loaded into each well of SDS-PAGE, as determined by BCA assay.

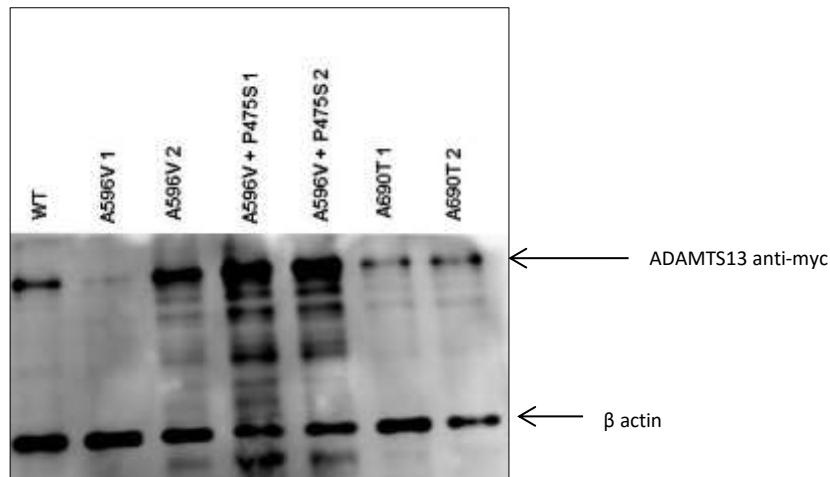


Figure 5.39 Western blot analyses cell lysates p.A596V, p. A596V + p.P475S and p.A690T A690T

The conditioned media of the expression vectors analysed in Figure 5.39 was harvested, concentrated and analysed on western blot (see Figure 5.40).

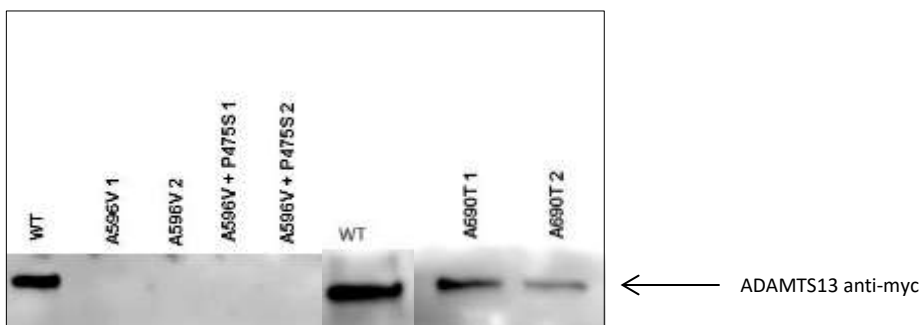


Figure 5.40 Western blot analysis of conditioned media: p.A596V, p.A596V + p.P475S and p. A690T.

The band intensities on western blots were scanned using ImageJ software and the cell lysates normalized to the β -actin housekeeping protein and compared with positive control (WT) values % WT \pm SEM (see Table 5.29 and Figure 5.41).

Table 5.29 ImageJ analysis of cell lysates p.A596V series and p.A690T

Clone	Normalized protein ratio	% WT \pm SEM
p.A596V 1	0.85	85 \pm 43
p.A596V 2	1.7	171 \pm 43
p.A596V + p.P475S 1	1.6	155 \pm 31
p.A596V + p.P475S 2	2.2	217 \pm 31
p.A690T 1	0.95	95 \pm 39
p.A690T 2	1.73	173 \pm 39

The band intensities on western blots were scanned using ImageJ software and the conditioned media samples normalized to the WT positive control on the same blot (values \pm %WT SEM); (see Table 5.30 and Figure 5.43).

Table 5.30 ImageJ analysis conditioned media p.596V series and p.A690T

Clone	Normalized protein ratio	% WT \pm SEM
p.A596V 1	0	0
p.A596V 2	0	0
p.A596V + p.P475S 1	0	0
p.A596V + p.P475S 2	0	0
p.A690T 1	1.06	106 \pm 26
p.A690T 2	0.54	54 \pm 26

ELISA antigen concentration of conditioned media of all expression vectors: 0ng/ml

A paired sample student's t test was performed to analyse if there was any significant difference between % ADAMTS13 expression in cell lysates and between p.A596V and p.A596V + p.P475S, ($p=0.05$). The calculated result = 0.0013. The tabulated value with one degree of freedom = 12.71.

The null hypothesis can be accepted that there is no significant difference between ADAMTS13 expression with mutation p.A596V and the mutation with p.P475V SNP in cell lysates.

5.3.3.6 Western blot analysis cell analysis p.T196I series cell lysate

The cells were harvested, lysed and sonicated as previously described before analysing by western blot (see Figures 5.41). An antibody directed against the housekeeping protein β -actin of molecular weight 45kDa was used as a loading control. An equal amount of total protein was loaded into each well of SDS-PAGE, as determined by BCA assay.

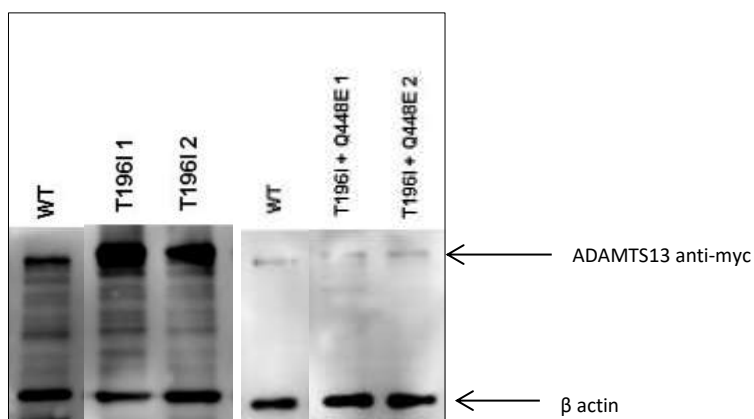


Figure 5.41 Western blot analyses cell lysates p.T196I, p.T196I + p.Q448E

The conditioned media of the expression vectors analysed in Figure 5.41 was harvested, concentrated and analysed on western blot (see Figure 5.42).

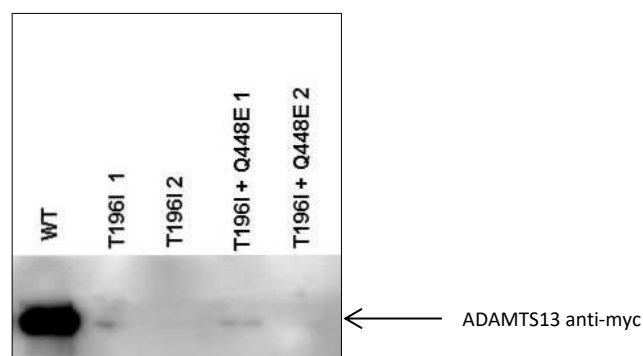


Figure 5.42 Western blot analyses conditioned media p.T196I, p.T196I + p.Q448E

The band intensities on western blots were scanned using ImageJ software and the cell lysates normalized to the β -actin housekeeping protein and compared with positive control (WT) values % WT \pm SEM (see Table 5.31 and Figure 5.43).

Table 5.31 ImageJ analysis of p.T196I series, cell lysates

Clone	Normalized protein ratio	% WT \pm SEM
p.T196I 2	1.27	127 \pm 17
p.T196I 3	0.85	85 \pm 17
p.T196I	0.76	76 \pm 17
p.T196I + p.Q448E	0.72	72 \pm 25
p.T196I + p.Q448E	1.2	123 \pm 25

The band intensities on western blots were scanned using ImageJ software and the conditioned media samples normalized to the WT positive control on the same blot (values % WT \pm SEM); (see Table 5.32 and Figure 5.44).

Table 5.32 ImageJ analysis of p.T196I series, conditioned media

Clone	Normalized protein ratio	% WT
p.T196I 2	0	0
p.T196I 3	0	0
p.T196I + p.Q448E 2	0	0
p.T196I + p.Q448E 3	0	0

ELISA antigen concentration of conditioned media: 0ng./ml

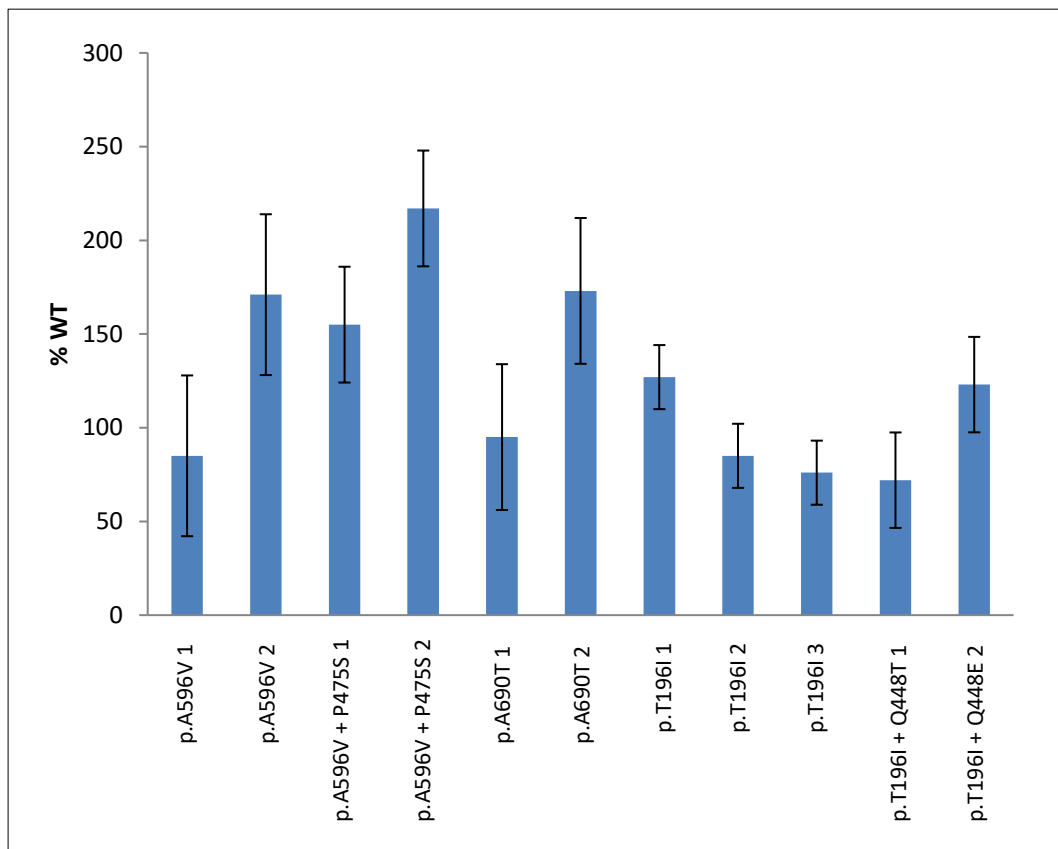


Figure 5.43 Comparison ADAMTS13 expression cell lysates p.A596V series, p.A690T, p.T196I series

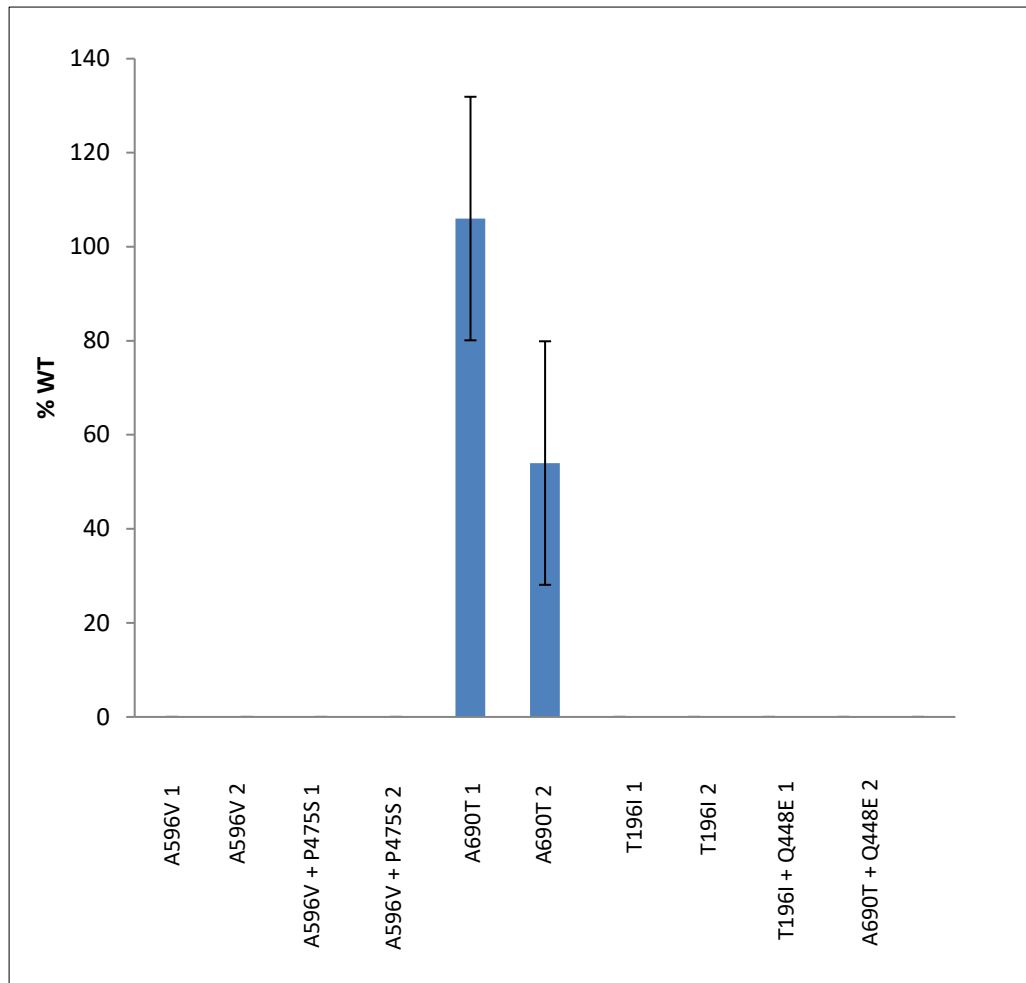


Figure 5.44 Comparison of %WT \pm SEM ADAMTS13 expression conditioned media p.A596V series, p.A690T and p.T196I series

ELISA antigen concentration of conditioned media: 0ng./ml

A paired sample student's t test was performed to analyse if there was any significant difference between % ADAMTS13 expression in cell lysates and between p.T196I and p.T196I + p.Q448E, ($p=0.05$). The calculated result = 0.0008. The tabulated value with one degree of freedom = 12.71.

The null hypothesis can be accepted that there is no significant difference between ADAMTS13 expression with mutation p.T196I and the mutation with p.Q448E SNP in cell lysates.

5.3.3.7 Western blot cell analysis p.Q436H

The cells were harvested, lysed and sonicated as previously described before analysing by western blot (see Figure 5.45). An antibody directed against the

housekeeping protein β -actin of molecular weight 45kDa was used as a loading control. An equal amount of total protein was loaded into each well of SDS-PAGE, as determined by BCA assay.

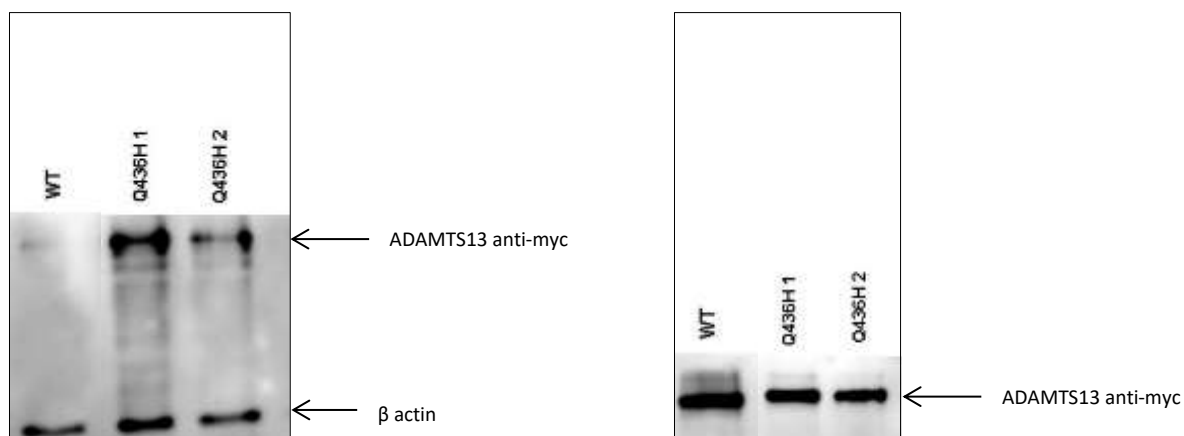


Figure 5.45 Western blot analyses: Left: cell lysate p.Q436H; right: conditioned media p.Q436H

The conditioned media of the expression vector was harvested, concentrated and analysed on western blot (see Figures 5.45).

The band intensities on western blots were scanned using ImageJ software and the cell lysates normalized to the β -actin housekeeping protein and compared with positive control (WT) values % WT \pm SEM (see Table 5.33 and Figure 5.46).

Table 5.33 ImageJ analysis of p.Q436H, cell lysates

Clone	Normalized protein ratio	% WT \pm SEM
p.Q436H 1	0.7751	77 \pm 1.5
p.Q436H 2	0.7443	74 \pm 1.5

The band intensities on western blots were scanned using ImageJ software and the conditioned media samples normalized to the WT positive control on the same blot (values % WT \pm SEM); (see Table 5.34 and Figure 5.46).

Table 5.34 ImageJ analysis of p.Q436H, conditioned media

Clone	Normalized protein ratio	% WT \pm SEM
p.Q436H 1	0.699	70 \pm 1.0
p.Q436H 2	0.6801	68 \pm 1.0

Conditioned media samples were analysed for ADAMTS13 antigen with the commercially available IMUBIND® ADAMTS13 ELISA kit according to manufacturer's instructions. Results can be seen in Table 5.35 and Figure 5.46.

Table 5.35 ELISA ADAMTS13 antigen concentration p.Q436H expressed as %WT conditioned media

Clone	ADAMTS13 concentration (ng/ml)	% WT ± SEM
WT	242.75	100
p.Q436H 1	0.36	36 ± 9.5
p.Q436H 2	0.55	55 ± 9.5

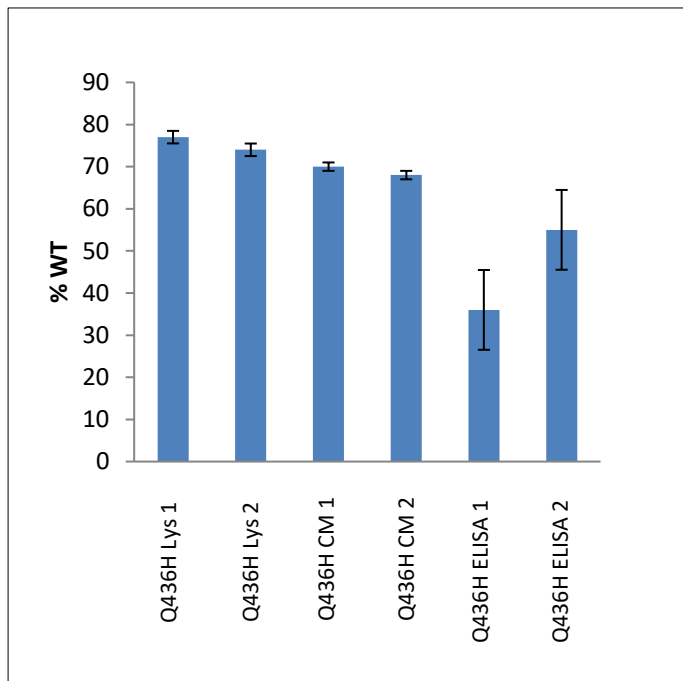


Figure 5.46 Comparison of %WT ± SEM ADAMTS13 p.Q436H cell lysates (Lys), conditioned media (CM) and ELISA antigen

5.3.3.8 Western blot analysis p.C977F

The cells were harvested, lysed and sonicated as previously described before analysing by western blot (see Figure 5.47). The expected size of ADAMTS13 protein (approx. 180kDa) was seen. An antibody directed against the housekeeping protein β -actin of molecular weight 45kDa was used as a loading control. An equal amount of total protein was loaded into each well of SDS-PAGE, as determined by BCA assay.

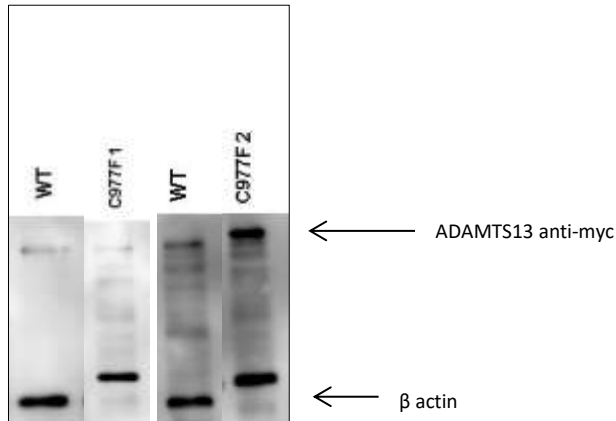


Figure 5.47 Western blot analyses cell lysates p.C977F

The conditioned media of the expression vector analysed in Figures 5.47 was harvested, concentrated and analysed on western blot (see Figure 5.48).

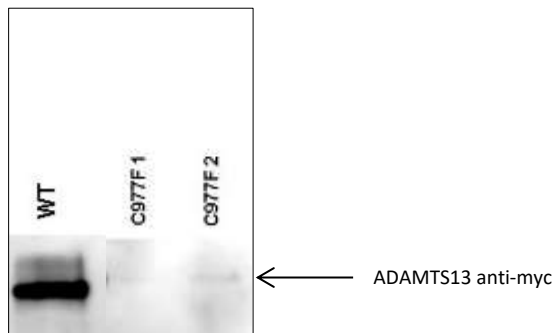


Figure 5.48 Western blot analyses conditioned media p.C977F

The band intensities on western blots were scanned using ImageJ software and the cell lysates normalized to the β -actin housekeeping protein and compared with positive control (WT) values % WT \pm SEM (see Table 5.36 and Figure 5.49).

Table 5.36 ImageJ analysis p.C977F cell lysate

Clone	Normalized protein ratio	% WT \pm SEM
p.C977F 1	0.9	93 \pm 7.5
p.C977F 2	0.78	78 \pm 7.5

The band intensities on western blots were scanned using ImageJ software and the conditioned media samples normalized to the WT positive control on the same blot (values % WT \pm SEM); (see Table 5.37 and Figure 5.49).

Table 5.37 ImageJ analysis p.C977F conditioned media

Clone	Normalized protein ratio	% WT
p.C977F 2	0	0
p.C977F 3	0	0

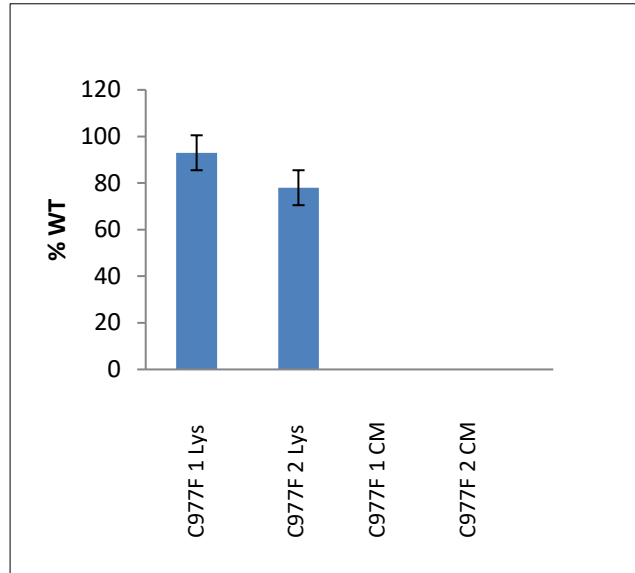


Figure 5.49 Comparison of %WT \pm SEM ADAMTS13 expression p.C977F cell lysates (Lys) and conditioned media (CM)

ELISA antigen concentration of conditioned media: 0ng./ml

5.4 Discussion

When comparing *in vitro* expression levels of constructs and clinical data, the mean levels of ADAMTS13 in citrated plasma from normal donors (n=49) was determined as 740 ± 110 ng/mL (Peyvandi *et al.*, 2004).

5.4.1 Challenges in the methodology

Several setbacks were encountered in this study. The construction of a number of expression vectors was abandoned due to the difficulty in obtaining clean nucleotide sequences (i.e. as the wild type sequence) after the mutation had been inserted. The method was altered by adding 5% DMSO to the PCR mixture, decreasing the T_m to 58°C and increasing the melting temperature to 98°C in the PCR cycling conditions. These expression vectors were the double mutation G794C + A796T, G803C and C1368T. The nucleotide changes were located in particularly rich in G-C areas, which may explain why these vectors

were difficult to construct. The deletion mutation 719_724del (a deletion of six nucleotides) was not successfully inserted, possibly due to the high fidelity and proofreading ability of the *pfu* Ultra polymerase used in the SDM mutagenesis kit.

The insertion of the unwanted nucleotide change C3484T, which would lead to a non-synonymous variant, was inserted in all constructs after attempting nucleotide substitutions after and including nucleotide 1787. In those vectors with nucleotide changes before 1787, this was not observed. This was puzzling to the manufacturer of the SDM kit (Agilent Technologies, UK) and was corrected only by performing another SDM procedure to revert the nucleotide change back to the WT sequence. Possibly the attachment of the *pfu* polymerase to the dsDNA created a torsion within the DNA at one particular point in the strand, resulting in the nucleotide change. Thymine and cytosine are pyrimidine bases with one carbon-ring therefore the substitution would be more energetically favourable compared to the substitution of pyrimidine bases. The reversion to WT by SDM was invariably successful.

5.4.2 Mutation p.R102H series

The transfection efficiencies for expression vectors p.R102H, p.R102H + p.Q448E, p.D102H and p.D102H + p.A900V were similar. However, the transfection efficiency for p.D102H multi was lower at 15%. Based on the densitometry analysis of band intensities on western blots, the average synthesis of ADAMTS13 in cell lysates, which have been normalized to the housekeeping protein β -actin and expressed as % of WT, were 41% for p.R102H, 19% for p.R102H + p.Q448E, 39% for p.D102H + p.A900V and 121% for p.R102H multi (p.R102H+ p.R7W + p.Q448E + p.A900V). This is interesting in consideration of the apparent lower transfection efficiency for p.R102H multi. The densitometry analysis of the conditioned media of the same vectors were 61% of WT for p.R102H, 69% for p.R102H + p.Q448E, 64% for p.D102H + p.A900V and 68% for p.R102H multi. In the analysis of cell lysates and conditioned media by western blot, there was no statistical significance found in ADAMTS13 expression between the mutation and mutation + SNPs. However, a statistically significant difference was found on

analysis of ADAMTS13 expression in conditioned media as analysed by ELISA. The values for ADAMTS13 antigen concentration by IMUBIND ELISA was not in agreement with the western blot analysis and thus appeared spurious. The ELISA should be repeated in order to make a valid conclusion. Based on these low concentrations, the ADAMTS13 activity was not assessed. In conclusion, the mutation p.R102H caused a decreased secretion of ADAMTS13 (average 61% of WT) by analysis on western blot and the presence of SNPs either singly or in combination did not affect ADAMTS13 secretion.

The disparity between the cell lysate values and the secretion has also been documented by other researchers (Edwards *et al.*, 2012). The level of ADAMTS13 secretion is in agreement with another expression study, which was 51% (Camilleri *et al.*, 2012). This is also in agreement with the clinical picture of the patient who developed TTP during her first pregnancy. At approximately 60% normal ADAMTS13 secretion, it could be argued that this level of ADAMTS13 would be adequate until the changes in the ADAMTS-VWF axis during pregnancy induced a TTP episode.

5.4.3 Mutation p.D217H series

The p.D217H mutation was identified in an 18-month-old patient with prophylactic PT needed only in severe infections. Based on the densitometry analysis of western blots, the average synthesis of ADAMTS13 in cell lysates, which have been normalized to the housekeeping protein β -actin and expressed as % of WT, were 146% for p.D217H, 88% for p.D217H + p.R7W, 76% for p.D217H + p.Q448E, 349% for p.D217H + p.A1033T and 231% for p.D217H multi (p.D217H + p.R7W + p.Q448E + p.A1033T). The transfection efficiencies were similar, at between 18-20%. There is an apparent increase in synthesis of the recombinant ADAMTS13 protein on the addition of the SNPs p.A1033T and all four SNPs (which also contains p.A1033T). The densitometry analyses of the conditioned media of the same vectors were: 63% of WT for p.D217H, 70% for p.D217H + p.R7W 179% for p.D217H + p.Q448E, 40% for p.D217H + p.A1033T and 90% for p.D217H multi.

Comparing the intracellular synthesis to the extracellular synthesis, there is a decrease in secretion in the mutation p.D217H, a comparable value for p.D217H + p.R7W, an increase in secretion in p.D217H + p.Q448E, a decrease in secretion in p.D217H + p.A1033T and a decrease in p.D217H multi. This is in agreement with the research performed by Edwards *et al.* who reported on the SNPs p.Q448E and p.A1033T (Edwards *et al.*, 2012). However, in the analysis of cell lysates and conditioned media by western blot in this study, there was no statistical significance found in ADAMTS13 expression between the mutation and mutation + SNPs. However, a statistical significant difference was found on analysis of ADAMTS13 expression in conditioned media as analysed by ELISA.

Previous expression studies performed by Camilleri *et al.* found the mutation p.D217H caused an increased secretion at 112% WT and this study found a secretory decrease of 63%, which is not in agreement (Camilleri *et al.*, 2012). The mutation in the patient was found as a compound heterozygote with p.R1060W, which is associated with late-onset TTP. These mutations acting in tandem could precipitate TTP at a younger age when challenged with a physiological stress such as severe infection. In conclusion, SNPs in addition to the mutation p.D217H does appear to alter the secretion of rADAMTS13. However, as haplotype data has not been specified it is difficult to directly relate this to the clinical picture.

5.4.4 Mutation p.T196I series

The p.T196I mutation was identified in a 21-year-old patient who was first diagnosed with TTP at aged three. The transfection efficiencies of the mutation p.T196I and p.T196I + p.Q448E were similar at 21% and 22% respectively. Based on the densitometry analysis of western blots, the average synthesis of ADAMTS13 in cell lysates was 96% for p.T196I and 98% for p.T196I + p.Q448E. Densitometry analysis of western blots of the conditioned media from the same expression vectors was 0% for p.T196I and p.T196I + p.Q448E. In a previous expression study the secretion level was not assessed by western blot but was 4% WT on antigen assay (Camilleri *et al.*, 2012). This is

in agreement with the clinical picture. In conclusion, the SNP p.Q448E has no influence on the effect of the mutation p.T196I, which is found in the metalloprotease domain.

5.4.5 Mutation p.R409W

The mutation p.R409W was found in a patient in homozygous form with no SNPs and was diagnosed as a neonate with a requirement for frequent prophylactic PT. The transfection efficiency of the expression vector was low at 15%. Based on the densitometric analysis of western blots, the average synthesis of ADAMTS13 in cell lysates, which has been normalized to the housekeeping protein β -actin and expressed as % of WT, was 55%. The densitometry analysis of the conditioned media was 0% WT and this was also seen on ELISA. As this mutation was seen in a neonate with a requirement for frequent PT this expression study is in agreement with the clinical picture.

5.4.6 Mutation p.R398H

The p.R398H mutation was identified in a patient diagnosed with TTP as a neonate, requiring frequent PT. It was in compound heterozygous form with the mutation p.Q436H and SNP p.Q448E. The transfection efficiencies for expression vectors p.R398H and R398H + p.Q448E were 18% and 20% respectively. Based on normalized densitometry analysis of band intensities on western blot, the average synthesis of ADAMTS13 in cell lysates were 82% p.R398H and 100% R398H + p.Q448E. Densitometry analysis of the conditioned media, expressed as %WT, was 86% for the mutation p.R398H and 21% for the mutation + SNP p.R398H + p.Q448E. Interestingly the ELISA results were 21% for the p.R398H mutation and 21% for the mutation + SNP p.R398H + p.Q448E. If this mutation was in homozygous form this genotype may present as a different phenotype. However, the mutation was identified as a part of a compound heterozygote thus relationship of genotype and phenotype is difficult to correlate in this case. These results also do not concur with previous expressions studies (Camilleri *et al.*, 2012) where secretion was greatly reduced.

5.4.7 Mutation p.Q436H

This mutation was identified as a heterozygote with the mutation p.R398C as described above. It was identified in a neonate who required frequent PT prophylactic treatment. Densitometry analysis on the band intensities on western blot showed the normalized secretion of ADAMTS13 in cell lysates to be 76% of WT and the secretion of 69% WT in conditioned media. Previous *in vitro* expression studies showed the secretion to be 18% WT on western blot and 64% on ELISA (Camilleri *et al.*, 2012). The latter figure is more in agreement with the findings of western blot analysis in this study. As the patient was a compound heterozygote and no other patients have presented in homozygous form, the relationship of genotype to clinical phenotype is difficult to establish with this mutation.

5.4.8 Mutation p.A596V

The mutation p.A596V was found in homozygous form in a patient who was diagnosed with TTP at aged 18 months. The transfection efficiency for the expression vector was 22 % of WT. The densitometry analysis of band intensities on western blots revealed the average synthesis of rADAMTS13 in cell lysates to be 128% WT and that of the conditioned media and ELISA 0% WT. The low levels of secretion would explain childhood onset TTP, although the patient would have been more expected to present as a neonate. This mutation was also found in another patient as a compound heterozygote with p.R1095Q and SNP p.Q448E. The patient was diagnosed with TTP during pregnancy. The densitometry analysis of normalized cell lysates on western blots was 166% p.A596V + p.Q448E. The western blot analysis of the conditioned media was 0% p.A596V + p.Q448E. The ELISA result was 0ng/mL for both the mutation and mutation + SNP. Previous expression studies found the mutation p.A596V abolished secretion (Camilleri *et al.*, 2012). This is in agreement. As p.A596V was a compound heterozygote with p.R1095Q, it could be argued the latter mutation 'rescues' ADAMTS13 levels and TTP does not present until the physiological stress of pregnancy. As p.A596V is a severe mutation the SNP was not able to modulate its effects.

5.4.9 Mutation p.A690T

The mutation p.A690T was identified in a pregnant patient who had a clinical history of one live pregnancy and four losses and an ADAMTS13 antigen level of 35ng/mL. Genotype analysis revealed the p.A690T mutation together with the deletion mutation G241_C242del and no SNPs. The p.A690T mutation is located in TSP1-8 domain. The densitometry analysis of band intensities on western blots revealed the average synthesis of rADAMTS13 in cell lysates to be 134% WT and that of the conditioned media to be 80% WT expression. The deletion mutation G241_C242del has been previously been identified in three 18-month-old children. The p.A690T mutation as a compound heterozygote could be argued to 'rescue' the ADAMTS13 levels producing the later onset phenotype with the TTP boot being precipitated by pregnancy.

5.4.10 Mutation p.C977F

The mutation p.C977F was found in homozygous form in a patient who was diagnosed with TTP in pregnancy. The densitometry analysis of band intensity on western blots revealed the average synthesis of ADAMTS13 in cell lysates to be 85% of WT and in conditioned media and ELISA 0%. i.e., the mutation in homozygous form would abolish secretion. A previous expression study reported secretion was much reduced at <11% ADAMTS13 (Camilleri *et al.*, 2012). Despite the low ADAMTS13 secretory levels this patient presented a late-onset phenotype which highlights the varied clinical nature of TTP and suggests there are other factors involved in the pathophysiology that have not yet been identified.

5.4.11 Single nucleotide polymorphisms

On analysis of the secretion of the singular SNPs, the transfection efficiencies were low at between 12-16% that of wild type but they were comparable with each other. Based on the densitometry analysis of band intensities on western blots, the average synthesis of rADAMTS13 in cell lysates, which have been normalized to the housekeeping protein β -actin and expressed as % of WT, were 84% p.Q448E, 120% p.P475S, 0% p.P618A, 63% p.A732V and 235% p.A900V. The expression vector p.P618A was transfected twice but showed

no bands on western blot. The densitometry analysis of western blots of the conditioned media of the same vectors were 106% p.Q448E, 0% p.P475S, 0% p.P618A, 32% p.A732V and 168% p.A900V. Interestingly the ELISA results were 62% p.Q448E, 56% p.P618A (in only one vector, which showed no visible banding on western blot), 32% p.A732V and 17% p.A900V. The SNP p.P618A has been shown to have decreased secretory levels (Kokame *et al.*, 2002). These results also concur with the different pattern in synthesis and secretion for p.Q448E (an increase in cellular synthesis compared with secretion) and p.A732V (a decrease in secretion compared to intracellular synthesis); (Edwards *et al.*, 2012). This provides further evidence that SNPs can have an impact on secretion of rADAMTS and possibly affect phenotype in TTP.

5.5 Concluding remarks

In conclusion, this study has found that, on analysis of western blot SNPs do not have a statistically significant modifying effect on the effect of mutations within the *ADAMTS13* gene. Clinically there may be other environmental factors involved that have not been defined; these may be in non-exonic regions, such as the promoter region or other parts of the genome, the effects of SNPs which alter RNA processing and stability, or epigenetic factors.

Chapter 6

Discussion and conclusions

6.1 Aim of this study

The aim of this study was to correlate the effects of mutations and SNPs, either singly or in combination, identified in a UK cohort of TTP patients on the secretion of rADAMTS13 and to relate genotype to phenotype in congenital TTP.

The results of the computational tools used to predict the effect of mutations and SNPs in this study can be summarised in Table 6.1

Table 6.1 Summary of predicted effect of SNPs and mutations on ADAMTS13 expression

Variant	Prediction by computational tools (Predict SNP)	Effect on stability of mutation $\Delta\Delta G$
R102H	Deleterious by SIFT and SNAP	Large decrease
T196I	Deleterious*	Neutral
D217H	Deleterious by PolyPhen and SNAP	Neutral
R398C	Deleterious by all tools except MAPP	Decrease
R409W	Deleterious*	Neutral/decrease
Q436H	Deleterious by PolyPhen and SNAP	Neutral
A596V	Deleterious by all tools except PolyPhen	Neutral
C977F	Deleterious*	Neutral
R1060W	Deleterious *	Neutral

Variant	Prediction by computational software	MAF	Effect on stability of mutation $\Delta\Delta G$
R7W	Neutral	0.09389	Neutral
Q448E	Neutral	0.5079	Neutral
P475S	Neutral	0.00266	Large decrease
P618A	Neutral	0.09287	Large decrease
A732V	Neutral	0.1553	Neutral
A900V	Neutral	0.0438	Neutral
A1033T	Neutral	0.08744	Decrease

*Deleterious = by all computational tools

Summary of accuracy and computational tools referred to in table above.

	PolyPhen 1	PolyPhen 2	MAPP	PhD-SNP	SIFT	SNAP
Expected accuracy	68.1%	69.2%	70.7%	71.5%	70.3%	67.6%

In the analysis of cell lysates and conditioned media by western blot of mutations p.R102H, p.D217H, p.R398C, p.A596V and p.R1060W there was no statistical significance found in ADAMTS13 expression between the mutation and mutation + SNPs either singly or in combination. A statistical significant difference was found on analysis of ADAMTS13 expression in conditioned media as analysed by ELISA in p.R102H and p.D217H. However, the antigen levels as analysed by ELISA were not in agreement with the analysis of ADAMTS13 expression levels in conditioned media by western blot analysis. These results should thus be interpreted with caution. As discussed previously, the ELISA used from a commercial source has been validated for use in the clinical diagnostic setting with plasma/serum used as a matrix rather than reagents used in an *in vitro* expression system. The nature of epitope(s) of the ADAMTS 13 capture antibody used is also not in the public domain thus any conclusions regarding the specificity or the avidity of the antibody which may cause low antigen results cannot be made.

6.2 Discussion of methods used

A series of expression vectors was created containing nucleotide substitutions that were identified in patient genotype and rADAMTS13 was transiently expressed in HEK293T cells containing the missense mutation or SNP. Several expression vectors with nucleotide changes in a G-C rich area of the ADAMTS13 cDNA insert proved difficult to construct, possibly due to the enhanced H-bonding in the nucleotide sequence in that region of the DNA strand. The nucleotide changes in these vectors were specifically the double missense mutation G794C+A796T and the single mutations G803C and G1368T. Vectors containing the individual mutations G794C and A796T could be constructed singly but, possibly due to the high fidelity proofreading ability

of the proprietary *pfu* polymerase enzyme, the double nucleotide change proved problematic.

Modelling of the cDNA nucleotides 700 – 1400 using the MFold server (<http://www.unafold.rna.albany.edu>) revealed H-bonding between many nucleotides within this area. As a result the dsDNA strand may resist denaturation needed for the DNA polymerase to bind. In the light of this, the PCR conditions were changed to increase the temperature of the denaturation step to 98°C and 5% DMSO was added to the PCR mixture to facilitate breakage of the H-bonds. The T_m was also decreased to 58°C. It was found that the desired nucleotide change was inserted but the nucleotide sequence approximately 20 base pairs following the substitution became corrupted. This indicated that the primer design was suitable but the polymerase appeared to detach from the cDNA strand, possibly due to torsional strains in the strand as a result of DNA coiling.

The construction of an expression vector carrying the deletion mutation 719_724del was also attempted but proved problematic. The design of the primer used in the SDM method included the six nucleotide deletion located in the central region of the primer. As the *pfu* polymerase (Agilent Technologies) has high-fidelity proofreading ability, this appears to have led to the non-amplification of the DNA insert. However, by changing the protocol in future work, an expression vector containing the desired mutation could be created.

An alternative method published by Pérez-Pinera *et al.* excludes the amplification of the fragment to be deleted through the design of primers to include a restriction enzyme target at the 5' sequence. Briefly, following PCR amplification the plasmid is digested with *DpnI* to digest the template DNA strand together with the chosen restriction enzyme and ligated. The method has been reported to obtain 100% of transformants containing the desired mutation (Pérez-Pinera *et al.*, 2006). The limitation of the method is the selection of the restriction enzyme target sequence that must not be present in the original plasmid. Restriction enzymes have been identified that do not appear in the ADAMTS13 cDNA (see Table 6.2):

Table 6.2: Restriction enzymes that can be used in a vector construct that would not target *ADAMTS13* cDNA

Table 6.2 Restriction enzymes which would not target *ADAMTS13* cDNA

<i>TfiI</i>	<i>ApaI</i>	<i>PfI</i>	<i>DrdI</i>	<i>FspI</i>	<i>XmnI</i>
<i>Tth111I</i>	<i>ARSi</i>	<i>AscI</i>	<i>BcgI</i>	<i>BspHI</i>	<i>AccI</i>
<i>PshAI</i>	<i>BsaI</i>	<i>BsmBI</i>	<i>MreI</i>	<i>SgrAI</i>	<i>BmgBI</i>
<i>ArrI</i>	<i>AseI</i>	<i>BssSI</i>	<i>AndI</i>	<i>kpnI</i>	<i>BsaWI</i>
<i>Acc65I</i>	<i>Scal</i>				

It was observed that the DNA yields found in the amplification of the validated constructs were very low compared to expected DNA concentrations (see Tables 4.9; 5.11). The quality of DNA was checked with each measurement of DNA concentration (the absorption ratio at 260nm:280nm ~1.8-2.0) to ensure the DNA was of the appropriate quality. The vector used (pcDNA3.1) is classified as a high copy plasmid but due to the large *ADAMTS13* insert cDNA this could impede copy number. Troubleshooting was performed as per the protocol and the problem was identified to be the lysis stage. It was ensured that the starter culture containing selective media was diluted 1/500-1/1000 times and incubated in a vessel four-fold greater than the volume of inoculant. This was incubated for 12-16 hours and shaken at approx. 230 RPM. The optical density at 600nm was measured to ensure growth was in the logarithmic phase (OD_{600} 0.8-1.2) and, after centrifugation, the wet pellet weight (biomass) was in the region of 3g/L. This reflected a cell density of 3×10^4 , as per the protocol. The protocol was performed as per high copy number plasmid and per low plasmid copy number. A new kit was also purchased. However, the DNA yield still remained low and the QIAGEN Maxiprep kit was changed for the Invitrogen MidiPrep kit and the problem regarding DNA concentration was resolved.

The use of a reporter vector to assess the transfection efficiency does not measure the true transfection efficiency of the vector containing the variant. It does, however, indicate that the transfection has worked, i.e. can be used as a positive control and does provide an indication of transfection efficiency. To measure the true transfection efficiency a reporter would ideally be tagged

onto the variant vector. However, depending on the size of the reporter itself, it could be argued that this may affect the translation of the variant protein. The transfection efficiencies found in this study, which used the β -galactosidase reporter, were lower than expected. Alternative reporter vectors could be used. These include the luciferase reporter vector (Vesuna, 2005) which contains the gene from the sea pansy *Renilla reniformis*, chloramphenicol acetyl transferase (CAT) and green fluorescent protein (GFP). The luciferase reporter is reported to be used widely (Vesuna, 2005) due to its detection sensitivity and ease of quantification when compared to other systems (de Wet *et al.*, 1987). However, there have been reports of aberrant activation or repression of the control reporter genes by the constructs and the reporter promoters used such as simian virus (SV40), cytomegalovirus (CMV) or thymidine kinase (TK) (Farr & Roman, 1992; Mulholland *et al.*, 2004). This can alter the levels of the control reporter expression which could lead to the spurious expression of the control reporter, leading to a bias in the normalization of the data. An alternative reporter is enhanced green fluorescent protein (eGFP) and this has been reported as robust, with the production of consistent results and can also be measured *in vivo*. The β -galactosidase reporter used in this study can only be used on fixed cells.

To allow valid comparison for each expression study, a number of control measures were put in place during the ADAMTS13 expression studies (intracellular and extracellular). Transfections were performed in triplicate together with the transfection of WT to allow comparison among variants transfected concurrently. The number of viable HEK293T cells, with viability assessed with the use of trypan blue, was counted by haemocytometer and an equal number of cells plated for each culture dish. An empty vector was used (with no cDNA insert) for the negative control. Transfection efficiencies were assessed by the use of co-transfection with a reporter vector containing the *LacZ* gene and on positive transfection the number of blue cells, as a percentage of the total number of cells, was quantified (see above). For the SDS-PAGE step the appropriate quantity of protein to load was assessed initially, as loading too much protein would lead to signal saturation and too little would produce too little signal. A WT positive control was used and

differing protein concentrations were loaded. Both target protein antibody (anti-myc) and housekeeping protein (β -actin) were used and, after densitometry analysis of the western blots, the protein load that gave the quantitative reading in the linear dynamic range was chosen. This quantity of total protein was used for all blots, as assessed by BCA assay. After blotting, the uniform transfer of protein onto the nitrocellulose membrane was assessed with the use of Ponceau S staining and those blots with inadequate or non-uniform transfer were discarded. On completion of western each blot, the positive control lanes (WT ADAMTS13) were assessed compared to the housekeeping protein and the protein of interest. An assessment was made of the quality of the primary antibody interaction with ADAMTS13: a low signal with both WT and target protein indicated the exhaustion of the ADAMTS13 anti-myc antibody and the blot was discarded. The data was not included in the data set. If all lanes showed a low signal on densitometric analysis, poor interaction with secondary antibody was indicated and the blot was discarded and the data excluded. The protocols used for each expression study did not vary. Ideally, the western blots would be repeated three times for densitometry analysis and the average taken. However, this was not possible due to time and resource constraints. All values of cell lysates were normalized against the housekeeping protein β -actin.

6.3 The relationship between patient genotype and clinical phenotype

It has been argued by Edwards *et al.* that the effect of a single SNP should not be compared to that of SNPs in combination that often appear together as a haplotype as the combination may have an alternative significant effect (Edwards *et al.*, 2010). Until more data is produced on this rare disorder this is difficult to evidence.

Lotta *et al.* 2010 found that patients with the same *ADAMTS13* genotype were found to have a similar age of onset (Lotta *et al.*, 2010). A lower residual *ADAMTS13* was also associated with the age at first TTP episode requiring PT. The results from their study also related the amount of residual *ADAMTS13* activity and the clinical features of the disease. A total of 51% of

the mutations described to date in TTP patients are missense and 71% of these missense mutations whose data was analysed are localized in the N' terminal end of the protein. The N-terminal domain mutations were associated with lower activity and more severe disease in an allele-dosage-dependent way. This area contains the catalytic domains and is the area where the highest degree of conservation occurs (Lotta *et al.*, 2010). It was also found that missense SNPs do not show evidence of skewed distribution. Residual plasmatic activity, as measured by SELDITOF mass spectrometry, was inversely correlated with the clinical severity of the phenotype.

Some features of this research can also be seen in the results of this expression study. Those mutations located nearer to the N-terminal end of ADAMTS13 showed less secretory levels which would result in a more severe clinical phenotype. The mutations nearer the C-terminal end of the protein tended to present a less severe clinical phenotype such as p.R1060W and the effect of SNPs could modify the effect of these secretions on ADAMTS13 expression.

6.4 The effect of mRNA processing on ADAMTS13 expression

In higher eukaryotes only a small fraction of changes at the proteome level is directly reflected by changes at the transcriptome level. There is thus an important role played by the translation and post-translational controls of gene expression.

Changes in messenger RNA (mRNA) structure/folding may represent one of the reasons for altered protein production. In eukaryotes, mRNA is bound to messenger ribonucleoprotein complexes (mRNPs). Variants may produce changes in the mRNA sequence/structure affecting its association with specific proteins and thus alter the fate of the encoded protein. However, most effects may be due to altered mRNA conformation and stability rather than efficiency of protein translation. The abundance of mRNA may also affect extracellular protein expression levels. Significantly lower mRNA expression levels compared to WT may account for lower intracellular protein levels and

SNPs may affect the levels of mRNA levels. This has been found in the multidrug resistant polypeptide MRD1 which is an efflux transporter of drugs. An SNP has been associated with decreased mRNA and protein levels via an unknown mechanism (Wang et al., 2005). Calculations of mRNA folding using software programmes has suggested the decreased level is due to an effect on the secondary structure of mRNA.

Changes in protein expression levels could also be explained by alternative RNA splicing. This would not affect mRNA levels but could affect the efficiency of translation.

6.5 Improvement of the method of protein detection

The results from analysis of band intensities seen on western blot for cell lysate and conditioned media showed a variation in results despite various controls put in place in the experimental design (as discussed previously). As western blotting involves a sequence of steps, variability can be introduced at each stage which may bias the results. However, new techniques for the measurements of low concentrations of proteins have now been developed and validated and are in use in diagnostic laboratories. Lotta *et al.*, recognised that the sensitivity and reproducibility of the commonly used ADAMTS13 assays were questionable at low concentrations of the protein and used the more sensitive surface-enhanced laser desorption/ionization time-of-flight mass spectrometry (SELDITOF) (Lotta *et al.*, 2012). A method published in 2006 measured ADAMTS13 plasmatic activity with high analytical sensitivity (limits of detection 0.5%) which was 5-10 fold higher than most commercially available assays (Jin *et al.*, 2006; Jin *et al.*, 2008). Not only is this method more sensitive but would be more reproducible compared to western blotting. The latter method has a relatively high limit of detection and scarce reproducibility at low ADAMTS13 concentrations (Tripodi *et al.*, 2004, 2008).

6.6 Synonymous SNPs

Synonymous variants, whereby the primary structure of the protein (the amino acid sequence) does not change, occurs as a consequence of the wobble of transfer RNA (tRNA) base pairing during translation and the redundancy in the genetic code. However, single base pair changes require different tRNAs to decode them even though the tRNA is charged with the same amino acid. It has been previously assumed that synonymous variants or sSNPs are inconsequential as the primary structure of the protein is retained. However, a number of studies have questioned this, mainly through showing these sSNPs are under evolutionary pressure and may have a functional consequence such as the alteration in structure, function and expression levels of the protein. These synonymous variants exist throughout the entire genome, both within exons and in non-coding regions which include promoters and transcription factor binding-sites. The mechanism by which these variants can affect the structure, function or expression levels of a protein is through messenger RNA (mRNA) stability, mRNA structure or alteration of the rate of protein folding, as mentioned previously.

The genotype of patients with TTP is now well-documented but has largely been focused on the coding regions of the *ADAMTS13* gene. As TTP is a complex, variable disorder that does not have a direct genotype-phenotype correlation, sequencing the whole *ADAMTS13* gene and assessing sSNPs may provide more data to understand this heterozygous disease.

6.7 Concluding remarks

Phenotypic severity in TTP appears to be a result of multiple environmental and genetic factors. Although hundreds of genetic variants certain mutations near the N-terminal, functional end of *ADAMTS13* seem to have a greater impact on phenotype and not be as influenced by physiological factors. Those mutations near the C-terminal end of the *ADAMTS13* protein appear to have a lesser impact on phenotype. SNPs and environmental factors such as

hormone levels and the immune system may have greater influence on the TTP phenotype in these cases.

Congenital TTP is considered an orphan disease as it is very rare in the population. Obtaining more genotype data for the whole *ADAMTS13* gene and the reporting of synonymous mutations would contribute more data and encourage further research in this area. Research into the role of *ADAMTS13* in more widespread conditions such as MI and stroke may give more insight into this heterogeneous disease.

References

- Adzhubei, I., Jordan, D. M. and Sunyaev, S. R. (2013) Predicting functional effect of human missense mutations using PolyPhen-2. *Current Protocols in Human Genetics*, Oxford: John Wiley & Sons, Unit 7.20-71.
- Ai, J., Smith, P., Wang, S., Zhang, P. and Zheng, X. L. (2005) The proximal carboxyl-terminal domains of ADAMTS13 determine substrate specificity and are all required for cleavage of von Willebrand factor. *Journal of Biological Chemistry*. **280**(33), 29428–29434.
- Akiyama, M., Takeda, S., Kokame, K., Takagi, J. and Miyata, T. (2009a) Crystal structures of the noncatalytic domains of ADAMTS13 reveal multiple discontinuous exosites for von Willebrand factor. *Proceedings of the National Academy of Sciences of the United States of America*. **106**(46), 19274–9.
- Akiyama, M., Takeda, S., Kokame, K., Takagi, J. and Miyata, T. (2009b) Production, crystallization and preliminary crystallographic analysis of an exosite-containing fragment of human von Willebrand factor-cleaving proteinase ADAMTS13. *Acta crystallographica. Section F, Structural biology and crystallization communications*. **65**(Pt 7), 739–42.
- Amorosi, E. and Ultmann, J. (1966). Thrombotic thrombocytopenic purpura: report of 16 cases and review of the literature. *Medicine*. **45**, 139-160.
- Anderson, P. J., Kokame, K. and Sadler, J. E. (2006) Zinc and calcium ions cooperatively modulate ADAMTS13 activity. *Journal of Biological Chemistry*. **281**(2), 850–857..
- Apte, S. S. (2004) A disintegrin-like and metalloprotease (reprolysin type) with thrombospondin type 1 motifs: The ADAMTS family. *International Journal of Biochemistry and Cell Biology*. **36**(6), 981–985.
- Apte, S. S. (2009) A disintegrin-like and metalloprotease (reprolysin-type) with thrombospondin type 1 motif (ADAMTS) superfamily: Functions and mechanisms. *Journal of Biological Chemistry*. **284**(46), 31493–31497.
- Arya, M., Anvari, B., Romo, G. M., Cruz, M. A., Dong, J. F., McIntire, L. V., Moake, J. L. and López, J. A. (2002) Ultralarge multimers of von Willebrand factor form spontaneous high-strength bonds with the platelet glycoprotein Ib-IX complex: Studies using optical tweezers. *Blood*. **99**(11), 3971–3977.
- Asch, A. S., Tepler, J., Silbiger, S. and Nachman, R. L. (1991). Cellular attachment to thrombospondin: Cooperative interactions between receptor systems. *Journal of Biological Chemistry*. **266**(3), 1740–1745.
- Banno, F., Kokame, K., Okuda, T., Honda, S., Miyata, S., Kato, H. and Tomiyama, Y. (2006). Complete deficiency in ADAMTS13 is prothrombotic, but it alone is not sufficient to cause thrombotic thrombocytopenic purpura. **107**(8), 3161–3166.
- Baehr, G., Klemperer, P., Schifrin, A. (1936). An acute febrile anemia and thrombocytopenic purpura with diffuse platelet thrombosis of capillaries and arterioles. *Trvts Assoc Am Physicians*. **51**, 43-58.
- Bendl, J., Stourac, J., Salanda, O., Pavelka, A., Wieben, E.D., Zendulka, J., Brezovsky, J., Damborsky, J. (2014) PredictSNP: Robust and Accurate Consensus Classifier for Prediction of Disease-Related Mutations. *PLoS Computational Biology*. **10**, e1003440.
- Bernardo, A., Ball, C., Nolasco, L., Moake, J. F. and Dong, J. F. (2004) Effects of inflammatory cytokines on the release and cleavage of the endothelial cell-derived ultralarge von Willebrand-factor multimers under flow. *Blood*, **104**(1), pp. 100–106.

Brenner, B. (2004). Haemostatic changes in pregnancy. *Thrombosis Research*. **114**, 409–414.

Bruno, K., Völkel, D., Plaimauer, B., Antoine, G., Pable, S., Motto, D. G., Lemmerhirt, H. L., Dorner, F., Zimmermann, K. and Scheiflinger, F. (2005) Cloning, expression and functional characterization of the full-length murine ADAMTS-13. *Journal of Thrombosis and Haemostasis*, **3**(5), pp. 1064–1073.

Callewaert, F., Roodt, J., Ulrichs, H., Stohr, T., Van Rensburg, W. J., Lamprecht, S., Rossenu, S., Priem, S., Willems, W. and Holz, J. B. (2012). Evaluation of efficacy and safety of the anti-VWF Nanobody ALX-0681 in a preclinical baboon model of acquired thrombotic thrombocytopenic purpura. *Blood*, **120**(17), 3603–3610.

Camilleri, R. S., Cohen, H., Mackie, I. J., Scully, M., Starke, R. D., Crawley, J. T. B., Lane, D. and Machin, S. J. (2008). Prevalence of the ADAMTS-13 missense mutation R1060W in late onset adult thrombotic thrombocytopenic purpura. *Journal of Thrombosis and Haemostasis*. **6**(2), 331–8.

Camilleri, R. S., Scully, M., Thomas, M., Mackie, I. J., Liesner, R., Chen, W. J., Manns, K. and Machin, S. J. (2012). A phenotype-genotype correlation of ADAMTS13 mutations in congenital thrombotic thrombocytopenic purpura patients treated in the United Kingdom. *Journal of Thrombosis and Haemostasis*. **10**(9), 1792–801.

Capriotti, E., Calabrese, R. and Casadio, R. (2006). Predicting the insurgence of human genetic diseases associated to single point protein mutations with support vector machines and evolutionary information. *Bioinformatics*. **22**(22), 2729–2734.

Cataland, S., Peyvandi, F., Mannucci, P., Lammle, B., Hovinga, J., Machin, S., Scully, M., Rock, G., Gilbert, J., Yang, S., Wu, H., Jilma, B. and Knoebi, P. (2012). Initial experience from a double-blind, placebo-controlled, clinical outcome study of ARC1779 in patients with thrombotic thrombocytopenic purpura. *American Journal of Hematology*. **87**(4), 430–432.

Chapin, J., Eyler, S., Smith, R., Tsai, HS, Laurence, J. (2016). Complement factor H mutations are present in ADAMTS13-deficient, ticlopidine-associated thrombotic microangiopathies. *Blood*. **121**(19), 4012–4014.

Chapman, K., Seldon, M., Richards, R. (2012) Thrombotic Microangiopathies , Thrombotic Thrombocytopenic purpura and ADAMTS-13. *Seminars in Thrombosis and Hemostasis*. **38**, 47–54.

Chromas Lite (<<http://www.technelysium.com.au/wp/chromas>>).

Clustal Omega (<<http://www.ebi.ac.uk/Tools/msa/clustalo/>>)

Crawley, J. T. B., de Groot, R., Xiang, Y., Luken, B. M. and Lane, D. (2011). Unraveling the scissile bond: how ADAMTS13 recognizes and cleaves von Willebrand factor. *Blood*. **118**(12), 3212–21.

Crawley, J. T. B., Lam, J. K., Rance, J. B., Mollica, L. R., O'Donnell, J. S. and Lane, D. A. (2008). Proteolytic inactivation of ADAMTS13 by thrombin and plasmin. *Blood*. **105**(3), 1085–1093.

Crawley, J.T, Lane, D.A., Woodward, M., Rumley, A. and Lowe, G.D. (2008). Evidence that high von Willebrand factor and low ADAMTS13 levels independently increase the risk of non-fatal heart attack. *Journal Thrombosis and Haemostasis*. **6**, 583-588.

Crawley, J. T. B. and Scully, M. (2013) Thrombotic thrombocytopenic purpura: basic pathophysiology and therapeutic strategies. *Hematology: The Education Program of the American Society of Hematology. American Society of Hematology. Education Program*, 292–9.

Davis, A. K., Makar, R. S., Stowell, C. P., Kuter, D. J. and Dzik, W. H. (2009). ADAMTS13 binds to CD36: A potential mechanism for platelet and endothelial localization of ADAMTS13. *Transfusion*. **49**(2), 206–213.

dbSNP database: < www.ncbi.nlm.nih.gov/snp > [Accessed 15/6/15].

Donadelli, R., Banterla, M., Capoferri, C., Bucchioni, S., Gastoldi, S., Nosari, S., Monteferrante, G., Ruggeri, Z., Bresin, E., Scheifflinger, F., Rossi, E., Martinez, C., Coppo, R., Remuzzi and G. Noris, M. (2006). In vitro and in vivo consequences of mutations in the von Willebrand factor cleaving protease ADAMTS13 in thrombotic thrombocytopenic purpura. *Thrombosis and Haemostasis*. **96**(4), 454–464.

Drury-Stewart, D. N., Lannert, K. W., Chung, D. W., Teramura, G. T., Zimring, J. C., Konkle, B. A., Gammill, H. S. and Johnsen, J. M. (2014). Complex changes in Von Willebrand Factor-associated parameters are acquired during uncomplicated pregnancy. *PLoS ONE*. **9**(11), 1–11.

Edwards, N. C., Hing, Z., Perry, A., Blaisdell, A., Kopelman, D. B., Fathke, R., Plum, W., Newell, J., Allen, C., Shapiro, A., Okunji, C., Kostic, I., Shomron, N., Grigoryan, V., Przytycka, T. M., Sauna, Z. E., Salari, R., Mandel-Gutfreund, Y., Komar, A. and Kimchi-Sarfaty, C. (2012). Characterization of coding synonymous and non-synonymous variants in ADAMTS13 using ex vivo and in silico approaches. *PLoS One*, **7**(6), p. e38864.

ExAC <<http://www.exac.broadinstitute.org>> [Accessed 10/6/2017]

Farr, A. and Roman, A. (1992) A pitfall of using a second plasmid to determine transfection efficiency. *Nucleic Acids Research*. **20**(4), 920.

Feys, H. B., Anderson, P. J., Vanhoorelbeke, K., Majerus, E. M. and Sadler, J. E. (2009) Multi-step binding of ADAMTS-13 to von Willebrand factor. *Journal of Thrombosis and Haemostasis*. **7**(12), 2088–2095.

Feys, H. B., Pareyn, I., Vancaenenbroeck, R., De Maeyer, M., Deckmyn, H., Van Geet, C. and Vanhoorelbeke, K. (2009) Mutation of the H-bond acceptor S119 in the ADAMTS13 metalloprotease domain reduces secretion and substrate turnover in a patient with congenital thrombotic thrombocytopenic purpura. *Blood*. **114**(21), 4749–52.

Feys, H. B., Roodt, J., Vandeputte, N., Pareyn, I., Lamprecht, S., van Rensburg, W. J., Anderson, P. J., Budde, U., Louw, V. J., Badenhorst, P. N., Deckmyn, H. and Vanhoorelbeke, K. (2010). Thrombotic thrombocytopenic purpura directly linked with ADAMTS13 inhibition in the baboon (*Papio ursinus*). *Blood*. **116**(12), 2005–10.

Feys, H. B., Roodt, J., Vandeputte, N., Pareyn, I., Mottl, H., Hou, S., Lamprecht, S., Rensburg, W. J. Van, Deckmyn, H., Vanhoorelbeke, K., Feys, H. B., Roodt, J., Vandeputte, N., Pareyn, I., Mottl, H., Hou, S., Lamprecht, S., Rensburg, W. J. Van, Deckmyn, H. and Vanhoorelbeke, K. (2014). Inhibition of von Willebrand factor–platelet glycoprotein Ib interaction prevents and reverses symptoms of acute acquired thrombotic thrombocytopenic purpura in baboons. *Thrombosis and Hemostasis*. **120**(17), 3611–3614.

FOLD X (<<http://www.foldx.embl.de/>>).

Fuchs, T. A., Hovinga, J. A. K., Schatzberg, D., Wagner, D. and La, B. (2013). Circulating DNA and myeloperoxidase indicate disease activity in patients with thrombotic microangiopathies. *Blood*. **120**(6), 1157–1164.

Fujikawa, K. (2001) Purification of human von Willebrand factor-cleaving protease and its identification as a new member of the metalloproteinase family. *Blood*, **98**(6), 1662–1666.

- Fujimura, Y., Matsumoto, M., Kokame, K., Isonishi, A., Soejima, K., Akiyama, N., Tomiyama, J., Natori, K., Kuranishi, Y., Imamura, Y., Inoue, N., Higasa, S., Seike, M., Kozuka, T., Hara, M., Wada, H., Murata, M., Ikeda, Y., Miyata, T. and George, J. N. (2009). Pregnancy-induced thrombocytopenia and TTP, and the risk of fetal death, in Upshaw-Schulman syndrome: a series of 15 pregnancies in 9 genotyped patients. *British Journal of Haematology*. **144**(5), 742–54.
- Fujimura, Y., Titani, K., Holland, L. Z., Russell, S. R., Roberts, J. R., Elder, J. H., Ruggeri, Z. M. and Zimmerman, T. S. (1986) Von Willebrand factor: A reduced and alkylated 52/48-kDa fragment beginning at amino acid residue 449 contains the domain interacting with platelet glycoprotein Ib. *Journal of Biological Chemistry*. **261**(1), 381–385.
- Furlan, M., Robles, R., Galibusera, M., Remuzzi, G., Kyrle, P., Brenner, B., Krause, M., Scharrer, I., Aumann, V., Mittler, U., Solenthaler, M., Lämmle, B. (1998) Von willebrand factor–cleaving protease in thrombotic thrombocytopenic purpura and the hemolytic–uremic syndrome. *New England Journal of Medicine*. **339**, 1578–1584.
- Furlan, M., Robles, R. and Lämmle, B. (1996) Partial purification and characterization of a protease from human plasma cleaving von Willebrand factor to fragments produced by in vivo proteolysis. *Blood*, **87**(10), 4223–34.
- Furlan, M., Robles, R., Solenthaler, M., Wassmer, M., Sandoz, P. and La, B. (1997) Deficient Activity of von Willebrand Factor – Cleaving Protease in Chronic Relapsing Thrombotic Thrombocytopenic Purpura. *Blood*, **89**(9), 3097–3103.
- Gao, W., Anderson, P. J. and Sadler, J. E. (2008). Extensive contacts between ADAMTS13 exosites and von Willebrand factor domain A2 contribute to substrate specificity. *Blood*. **112**(5), 1713–1719.
- Gardner, M. D., Chion, C. K. N. K., Groot, R. De, Shah, A., Crawley, J. T. B., Lane, D. (2014). A functional calcium-binding site in the metalloprotease domain of ADAMTS13. *Thrombosis and Hemostasis*. **113**(5), 1149–1157.
- George, J. N., Hovinga, J. A. K., Terrell, D. R. and Vesely, S. K. (2008). The Oklahoma Thrombotic Thrombocytopenic Purpura – Hemolytic Uremic Syndrome Registry : the Swiss connection. *European Journal of Hematology*. **80**, 277–286.
- Giblin, J.P., Hewlett, L.J and Hannah, M.J. (2008). Basal secretion of von Willebrand factor from human endothelial cells. *Blood*. **11**, 957-964.
- Gill, J., Endres-Brooks, J., Bauer, P., Marks, W. and Montgomery, R. (1987) The effect of ABO blood group on the diagnosis of von Willebrand disease. *Blood*. **69**, 1691–1695.
- Ginsburg, D., Handin, R., Bonthron, D., Donlon, T., Bruns, G., Latt, S. and Orkin, S. (1985) Human von Willebrand Factor (vWF): Isolation of complementary (cDNA) clones and chromosomal localization. *Science*. **228**, 1401–1406.
- de Groot, R., Bardhan, A., Ramroop, N., Lane, D. and Crawley, J. T. B. (2009) Essential role of the disintegrin-like domain in ADAMTS13 function. *Blood*. **113**(22), 5609–16.
- de Groot, R., Lane, D. and Crawley, J. T. B. (2010) The ADAMTS13 metalloprotease domain: roles of subsites in enzyme activity and specificity. *Blood*. **116**(16), 3064–72.
- de Groot, R. De, Lane, D. and Crawley, J. T. B. (2015) The role of the ADAMTS13 cysteine-rich domain in VWF binding and proteolysis. *Thrombosis and Haemostasis*. **125**(12), 1968–1976.

Hing, Z., Schiller, T., Wu, A., Hamasaki-Katagiri, N., Struble, E. B., Russek-Cohen, E. and Kimchi-Sarfaty, C. (2013). Multiple in silico tools predict phenotypic manifestations in congenital thrombotic thrombocytopenic purpura. *British Journal of Haematology*. **160**(6), 825–837.

Hofsteenge, J., Huwiler, K. G., Macek, B., Hess, D., Lawler, J., Mosher, D. F. and Peter-Katalinic, J. (2001). C-Mannosylation and O-Fucosylation of the Thrombospondin Type 1 Module. *Journal of Biological Chemistry*. **276**(9), 6485–6498.

Hunt, B.J., Thomas-Dewing, R.R., Bramham, K. and Lucas, S.B. (2013). Preventin maternal deaths due to acquired thrombotic thrombocytopenic purpura. *Journal Obstetrics and Gynaecology Research*. **39**(1), 347-350.

I-Mutant2.0 <<http://www.folding.biofold.org/i-mutant/i-mutant2.0.html>> [Accessed 15/5/15].

ImageJ (<http://www.imageJ.net>)

Jia, W., Lu, Z., Fu, Y., Wang, H.-P., Wang, L.-H., Chi, H., Yuan, Z.-F., Zheng, Z.-B., Song, L.-N., Han, H.-H., Liang, Y.-M., Wang, J.-L., Cai, Y., Zhang, Y.-K., Deng, Y.-L., Ying, W.-T., He, S.-M. and Qian, X.-H. (2009). A strategy for precise and large scale identification of core fucosylated glycoproteins. *Molecular & Cellular Proteomics*. **8**(5), 913–923.

Jin, M., Casper, T. C., Cataland, S. R., Kennedy, M. S., Lin, S., Li, Y. J. and Wu, H. M. (2008) Relationship between ADAMTS13 activity in clinical remission and the risk of TTP relapse. *British Journal of Haematology*. **141**(5), 651–658.

Jin, M., Cataland, S., Bissell, M. and Wu, H. M. (2006) A Rapid Test for the Diagnosis of Thrombotic Thrombocytopenic Purpura Using Surface Enhanced Laser Desorption/Ionization Time-of-flight (SELDI-TOF)-Mass Spectrometry. *Journal of Thrombosis and Haemostasis*. **4**(2), 333–338.

Jin, S., Skipwith, C. G. and Zheng, X. L. (2012) Amino acid residues Arg 659 , Arg 660 , and Tyr 661 in the spacer domain of ADAMTS13 are critical for cleavage of von Willebrand factor. **115**(11), 2300–2310.

Jin, S. Y., Skipwith, C. G., Shang, D. and Zheng, X. L. (2009) Von Willebrand factor cleaved from endothelial cells by ADAMTS13 remains ultralarge in size. *Journal of Thrombosis and Haemostasis*. **7**(10), 1749–1752.

Kelwick, R., Desanlis, I., Wheeler, G. N. and Edwards, D. R. (2015) The ADAMTS (A Disintegrin and Metalloproteinase with Thrombospondin motifs) family. *Genome Biology*. **16**, 113.

Kentouche, K., Voigt, a, Schleussner, E., Schneppenheim, R., Budde, U., Beck, J. F., Stefańska-Windyga, E. and Windyga, J. (2013). Pregnancy in Upshaw-Schulman syndrome. *Hämostaseologie*. **33**(2), 144–8.

Khan, K. S., Wojdyla, D., Say, L., Imezoglu, A. M. and Van Look, P. F. (2006). WHO analysis of causes of maternal death: a systematic review. *Lancet*. **367**(9516), 1066–1074.

Kim, J., Zhang, C.-Z., Zhang, X. and Springer, T. A. (2010) A mechanically stabilized receptor-ligand flex-bond important in the vasculature. *Nature*. **466**(7309), 992–5.

Klaus, C., Plaimauer, B., Studt, J. D., Dorner, F., Lämmle, B., Mannucci, P. M. and Scheiflinger, F. (2004). Epitope mapping of ADAMTS13 autoantibodies in acquired thrombotic thrombocytopenic purpura. *Blood*. **103**(12), 4514–4519.

- Kokame, K., Aoyama, Y., Matsumoto, M., Fujimura, Y. and Miyata, T. (2008) Inherited and de novo mutations of ADAMTS13 in a patient with Upshaw-Schulman syndrome. *Journal of Thrombosis and Haemostasis*. **6**(1), 213–215.
- Kokame, K., Matsumoto, M., Soejima, K., Yagi, H., Ishizashi, H., Funato, M., Tamai, H., Konno, M., Kamide, K., Kawano, Y., Miyata, T. and Fujimura, Y. (2002). Mutations and common polymorphisms in ADAMTS13 gene responsible for von Willebrand factor-cleaving protease activity. *Proceedings of the National Academy of Sciences of the United States of America*. **99**(18), 11902–7.
- von Krogh, A. S., Quist-Paulsen, P., Waage, A., Langseth, O., Thorstensen, K., Brudevold, R., Tjønnfjord, G. E., Largiadèr, C. R., Lämmle, B. and Kremer Hovinga, J. A. (2016). High prevalence of hereditary thrombotic thrombocytopenic purpura in central Norway: From clinical observation to evidence. *Journal of Thrombosis and Haemostasis*. **14**(1), 73–82.
- Kumar, P., Henikoff, S. and Ng, P. C. (2009). Predicting the effects of coding non-synonymous variants on protein function using the SIFT algorithm. *Nature Protocols*. **4**(7), 1073–81.
- Lee, S. I., Dudley, A. M., Drubin, D., Silver, P. A., Krogan, N. J., Pe'er, D. and Koller, D. (2009) Learning a prior on regulatory potential from eQTL data. *PLoS Genetics*. **5**(1).
- Levy, G. G., Nichols, W. C., Lian, E. C., Foroud, T., McClintick, J. N., McGee, B. M., Yang, a Y., Siemieniak, D. R., Stark, K. R., Gruppo, R., Sarode, R., Shurin, S. B., Chandrasekaran, V., Stabler, S. P., Sabio, H., Bouhassira, E. E., Upshaw, J. D., Ginsburg, D. and Tsai, H. M. (2001) Mutations in a member of the ADAMTS gene family cause thrombotic thrombocytopenic purpura. *Nature*, **413**(6855), 488–94.
- Liu, T., Qian, W. J., Gritsenko, M., Camp, D. G., Monroe, M. E., Moore, R. J. and Smith, R. D. (2005). Human plasma N-glycoproteome analysis by immunoaffinity subtraction, hydrazide chemistry, and mass spectrometry. *Journal of Proteome Research*. **4**(6), 2070–2080.
- Lotta, L. a, Garagiola, I., Palla, R., Cairo, A. and Peyvandi, F. (2010) ADAMTS13 mutations and polymorphisms in congenital thrombotic thrombocytopenic purpura. *Human Mutation*, **31**(1), 11–9.
- Lotta, L., Wu, H. M., Mackie, I. J., Noris, M., Veyradier, A., Scully, M., Remuzzi, G., Coppo, P., Liesner, R., Donadelli, R., Loirat, C., Gibbs, R., Horne, A., Yang, S., Garagiola, I., Musallam, K. M. and Peyvandi, F. (2012). Residual plasmatic activity of ADAMTS13 is correlated with phenotype severity in congenital thrombotic thrombocytopenic purpura. *Blood*. **120**(2), 440–8.
- De Maeyer, B., De Meyer, S. F., Feys, H. B., Pareyn, I., Vandeputte, N., Deckmyn, H. and Vanhoorelbeke, K. (2010) The distal carboxyterminal domains of murine ADAMTS13 influence proteolysis of platelet-decorated VWF strings in vivo. *Journal of Thrombosis and Haemostasis*. **8**(10), 2305–2312.
- Majerus, E. M., Zheng, X., Tuley, E. A. and Sadler, J. E. (2003). Cleavage of the ADAMTS13 Propeptide Is Not Required for Protease Activity. *Journal of Biological Chemistry*. **278**(47), 46643–46648.
- Majerus, E. M., Zheng, X., Tuley, E. a. and Sadler, J. E. (2003) Cleavage of the ADAMTS13 Propeptide Is Not Required for Protease Activity. *Journal of Biological Chemistry*. **278**(47), 46643–46648.
- Malina, M., Roumenina, L. T., Seeman, T., Le Quintrec, M., Dragon-Durey, M.-A., Schaefer, F. and Fremeaux-Bacchi, V. (2012). Genetics of hemolytic uremic syndromes. *Presse Médicale* **41**(3), e105-14.

Mancuso, D. J., Tuley, E. A., Westfield, L. a, Worrall, N. K., Shelton-Inloes, B. B., Sorace, J. M., Alevy, Y. G. and Sadler, J. E. (1989) Structure of the gene for human von Willebrand factor, *The Journal of Biological Chemistry*, **264**, 19514–19527.

Matsui, T., Titani, K. and Mizuochi, T. (1992) Structures of the Asparagine-linked Oligosaccharide Chains of Human von Willebrand Factor. *Journal of Biological Chemistry*. **267**(13), 8723–8731.

Miyata, T. (2015). GWA study for ADAMTS13 activity. *Blood*. **125**(25), 3833–3834.

Moatti-Cohen, M., Garrec, C., Wolf, M., Boisseau, P., Galicier, L., Azoulay, E., Stepanian, A., Delmas, Y., Rondeau, E., Bezieau, S., Coppo, P. and Veyradier, A. (2012). Unexpected frequency of Upshaw-Schulman syndrome in pregnancy-onset thrombotic thrombocytopenic purpura. *Blood*. **119**(24), 5888–97.

Morgand, M., Buffet, M., Busson, M., Loiseau, P., Malot, S., Amokrane, K., Fortier, C., London, J., Bonmarchand, G., Wynckel, A., Provôt, F., Poullin, P., Vanhille, P., Presne, C., Bordessoule, D., Girault, S., Delmas, Y., Hamidou, M., Mousson, C., Vigneau, C., Lautrette, A., Pourrat, J., Galicier, L., Azoulay, E., Pène, F., Mira, J. P., Rondeau, E., Ojeda-Urbe, M., Charron, D., Maury, E., Guidet, B., Veyradier, A., Tamouza, R. and Coppo, P. (2014). High prevalence of infectious events in thrombotic thrombocytopenic purpura and genetic relationship with toll-like receptor 9 polymorphisms: Experience of the French Thrombotic Microangiopathies Reference Center. *Transfusion*. **54**(2), 389–397.

Moschcowitz, E. (1924) Hyaline thrombosis of the terminal arterioles and capillaries: a hitherto undescribed disease. *Proc NY Pathol Soc*. **24**, 21–24.

Motto, D. G., Chauhan, A. K., Zhu, G., Homeister, J., Lamb, C. B., Desch, K. C., Zhang, W., Tsai, H., Wagner, D. D. and Ginsburg, D. (2005). Shigatoxin triggers thrombotic thrombocytopenic purpura in genetically susceptible ADAMTS13-deficient mice. *Journal of Clinical Investigation*. **115**(10), 2752–2761.

Mulholland, D. J., Cox, M., Read, J., Rennie, P. and Nelson, C. (2004) *Androgen* responsiveness of Renilla luciferase reporter vectors is promoter, transgene, and cell line dependent. *Prostate*. **59**(2), 115–119.

MUSCLE alignment: <<http://www.ebi.ac.uk/Tools/msa/muscle/>> [Accessed 30/9/15]

Nachman, R., Levine, R. and Jaffe, E.A. (1977). Synthesis of Factor VIII antigen by cultured guinea pig megakaryocytes. *Journal of Clinical Investigation*. **60**(4), 914-921.

NCBI dbSNP Human Build 146. Available from: <http://www.ncbi.nlm.nih.gov/projects/SNP/snp_ref.cgi?rs¼10065172> [Accessed 10/6/2017].

Ng, P. C. and Henikoff, S. (2006). Predicting the effects of amino acid substitutions on protein function. *Annual Review of Genomics and Human Genetics*. **7**, 61–80.

Niiya, M., Uemura, M., Zheng, X. W., Pollak, E. S., Dockal, M., Scheifflinger, F., Wells, R. G. and Zheng, X. L. (2006). Increased ADAMTS-13 proteolytic activity in rat hepatic stellate cells upon activation in vitro and in vivo. *Journal of thrombosis and haemostasis*. **4**(5), 1063–70.

Noris, M., Mescia, F. and Remuzzi, G. (2012) STEC-HUS, atypical HUS and TTP are all diseases of complement activation. *Nature Reviews. Nephrology*. **8**(11), 622–33.

Noris, M., Ruggenenti, P., Perna, A., Orisio, S., Caprioli, J., Skerka, C., Vasile, B., Zipfel, P. F. and Remuzzi, G. (1999). Hypocomplementemia discloses genetic predisposition to hemolytic uremic syndrome and thrombotic thrombocytopenic purpura: role of factor H abnormalities. *Journal of the American Society of Nephrology*. **10**(2), 281–293.

Palla, R., Lavoretano, S., Lombardi, R., Garagiola, I., Karimi, M., Afrasiabi, A., Ramzi, M., De Cristofaro, R. and Peyvandi, F. (2009). The first deletion mutation in the TSP1-6 repeat domain of ADAMTS13 in a family with inherited thrombotic thrombocytopenic purpura. *Haematologica*. **94**(2), 289–93.

Perez-Pinera, P., Menendez-Gonzalez, M. and Vega, J. (2006). Deletion of DNA sequences using a polymerase chain reaction approach. *Electronic Journal of Biotechnology*. **9**(5), 604–609.

Peyvandi, F., Ferrari, S., Lavoretano, S., Canciani, M. T. and Mannucci, P. M. (2004) Von Willebrand factor cleaving (ADAMTS-13) and ADAMTS-13 neutralizing autoantibodies in 100 patients with thrombotic thrombocytopenic purpura. *British Journal of Haematology*. **127**(4), 433–439.

Plaimauer, B., Fuhrmann, J., Mohr, G., Wernhart, W., Bruno, K., Ferrari, S., Konetschny, C., Antoine, G., Rieger, M. and Scheifflinger, F. (2006). Modulation of ADAMTS13 secretion and specific activity by a combination of common amino acid polymorphisms and a missense mutation. *Blood*. **107**(1), 118–25.

Polley, M.J. and Nachman, R. (1978). The human complement system in thrombin-mediated platelet function. *Journal Experimental Medicine*. **147**(6), 1713–1726.

PolyPhen2.0 <<http://www.genetics.bwh.harvard.edu/pph2/>> [Accessed 23/5/15].

Porter, S., Clark, I.M., Kevorkian, L. and Edwards, D.R. (2005). The ADAMTS metalloproteinases. *Biochem J*. **386**(1), 15–27.

Pos, W., Crawley, J. T. B., Fijnheer, R., Voorberg, J., Lane, D. A. and Luken, B. M. (2010) An autoantibody epitope comprising residues R660, Y661, and Y665 in the ADAMTS13 spacer domain identifies a binding site for the A2 domain of VWF. *Blood*, **115**(8), 1640–1649.

Powazniak, Y., Kempfer, A. C., Pereyra, J. C. C., Palomino, J. P. and Lazzari, M. A. (2011). VWF and ADAMTS13 behavior in estradiol-treated HUVEC. *European Journal of Haematology*. **86**(2), 140–7.

Predict SNP <https://loschmidt.chemi.muni.cz/predictsnp>

Reiger, M., Ferrari, S., Kremer Hovinga, J.A., Konetschny, C., Herzog, A., Koller, L., Weber, A., Renuzzi, G., Dockal, M., Plaimauer, B. and Scheifflinger, F. (2006) Relation between ADAMTS13 activity and ADAMTS13 antigen levels in healthy donors and patients with TMA. *Thrombosis and Haemostasis*. **95**(2), 212–30.

Reti, M., Farkas, P., Csuka, D., Razso, K., Schlamadinger, A., Udvardy, M.L., Madach, K., Domjan, G., Reusz, G.S., Szabo, A.J. and Prohaszka, Z. (2012). Complement activation in thrombotic thrombocytopenic purpura. *Journal Thrombosis and Haemostasis*. **10**, 791–8.

Ricketts, L. M., Dlugosz, M., Luther, K. B., Haltiwanger, R. S. and Majerus, E. M. (2007). O-fucosylation is required for ADAMTS13 secretion. *The Journal of Biological Chemistry*. **282**(23), 17014–23.

Rossi, E., Mannucci, P. M., Canciani, M. T., Forza, I., Lussana, F., Lattuada, A. and Factor, W. (2001). Changes in health and disease of the metalloprotease that cleaves von Willebrand factor. **98**(9), 2730–2736.

Ruiz-Torres, M.P., Casiraghi, F., Galbusera, M., Macconi, D., Todeschini, M., Porrati, F., Belotti, D., Pogliani, E.M., Noris, M. and Remuzzi, G. (2005). Complement activation: the missing link between ADAMTS-13 deficiency and microvascular thrombosis of thrombotic microangiopathies. *Thrombosis and Haemostasis*. **93**(3), 443–452.

Sadler, J. E. (1998) Biochemistry and Genetics of von Willebrand factor. *Biochemistry*. **67**, 395–424.

Sadler, J. E. (2002) A new name in thrombosis, ADAMTS13. *Proceedings of the National Academy of Sciences of the United States of America*. **99**(18), 11552–4.

Salamanca, S., Li, L., Vendrell, J., Aviles, F. X. and Chang, J. Y. (2003). Major kinetic traps for the oxidative folding of leech carboxypeptidase inhibitor. *Biochemistry*. **42**(22), 6754–6761.

Scheiflinger, F., Kno, P., Trattner, B., Plaimauer, B., Mohr, G. and Dockal, M. (2003) Nonneutralizing IgM and IgG antibodies to von Willebrand factor – cleaving protease (ADAMTS-13) in a patient with thrombotic thrombocytopenic purpura. *Blood*. **102**(9), 3241–3243.

Schneider, S.W., Nuschelle, S., Wixforth, A. et al. (2007). Shear-induced unfolding triggers adhesion of von Willebrand factor fibers. *Proceedings of the National Academy of Sciences, USA*. **104** (19), 7899-7903.

Schneppenheim, R., Budde, U., Oyen, F., Angerhaus, D., Aumann, V., Drewke, E., Hassenpflug, W., Ha, J., Kentouche, K., Kohne, E., Kurnik, K., Mueller-wiefel, D. and Obser, T. (2003) von Willebrand factor cleaving protease and ADAMTS13 mutations in childhood TTP. *Haemostasis, Thrombosis and Vascular Biology*. **101**(5), 1845–1850.

Schulman, Z., Pierce, I., Lukens, M., Currimbhoy, A. (1960). Studies on thrombopoiesis. A factor in normal human plasma required for platelet production: chronic thrombocytopenia due to its deficiency. *Blood*. **16** (1), 943-957.

Schwameis, M., Schörghofer, C., Assinger, A., Steiner, M. M. and Jilma, B. (2015) VWF excess and ADAMTS13 deficiency: a unifying pathomechanism linking inflammation to thrombosis in DIC, malaria, and TTP. *Thrombosis and Haemostasis*. **113**(4), 708–18.

Schymkowitz, J., Borg, J., Stricher, F., Nys, R., Rousseau, F. and Serrano, L. (2005) The FoldX web server: An online force field. *Nucleic Acids Research*. **33**(Suppl.2), 382–388.

Scully, M., Gattens, M., Khair, K. and Liesner, R. (2006) 'The use of intermediate purity factor VIII concentrate BPL 8Y as prophylaxis and treatment in congenital thrombotic thrombocytopenic purpura. *British Journal of Haematology*. **135**(1), 101–104.

Scully, M., Hunt, B. J., Benjamin, S., Liesner, R., Rose, P., Peyvandi, F., Cheung, B. and Machin, S. J. (2012). Guidelines on the diagnosis and management of thrombotic thrombocytopenic purpura and other thrombotic microangiopathies. *British Journal of Haematology*. **158**(3), 323–35.

Scully, M., McDonald, V., Cavenagh, J., Hunt, B. J., Longair, I., Cohen, H. and Machin, S. J. (2011) A phase 2 study of the safety and efficacy of rituximab with plasma exchange in acute acquired thrombotic thrombocytopenic purpura. *Blood*. **118**(7), 1746–53.

Scully, M., Thomas, M., Underwood, M., Watson, H., Langley, K., Camilleri, R. S., Clark, A., Creagh, D., Rayment, R., McDonald, V., Roy, A., Evans, G., McGuckin, S., Ni Ainle, F., Maclean, R., Lester, W., Nash, M., Scott, R. and O'Brien, P. (2014) Congenital and acquired thrombotic thrombocytopenic purpura and pregnancy: presentation, management and outcome of subsequent pregnancies. *Blood*. **124**(2), 211–219.

Scully, M., Yarranton, H., Liesner, R., Cavenagh, J., Hunt, B., Benjamin, S., Bevan, D., Mackie, I. and Machin, S. (2008) Regional UK TTP registry: correlation with laboratory ADAMTS 13 analysis and clinical features. *British Journal of Haematology*, **142**(5) 819–26.

Shang, D., Zheng, X. W., Niiya, M. and Zheng, X. L. (2006). Apical sorting of ADAMTS13 in vascular endothelial cells and Madin-Darby canine kidney cells depends on the CUB domains and their association with lipid rafts. *Blood*. **108**(7), 2207–2215.

Sherry, S.T. et al., (2001) dbSNP: the NCBI database of genetic variantation. *Nucleic Acids Research*. **29**, 308-311.

Shida, Y., Nishio, K., Sugimoto, M., Mizuno, T., Hamada, M., Kato, S., Matsumoto, M., Okuchi, K., Fujimura, Y. and Yoshioka, A. (2008) Functional imaging of shear-dependent activity of ADAMTS13 in regulating mural thrombus growth under whole blood flow conditions. *Blood*. **111**(3), 1295–1298.

Siedlecki, C. a, Lestini, B. J., Kottke-Marchant, K. K., Eppell, S. J., Wilson, D. L. and Marchant, R. E. (1996) Shear-dependent changes in the three-dimensional structure of human von Willebrand factor. *Blood*. **88**(8), 2939–50.

SIFT <<http://www.sift.jcvi.org>> [Accessed 23/5/15].

Sim, N.-L., Kumar, P., Hu, J., Henikoff, S., Schneider, G. and Ng, P. C. (2012). SIFT web server: predicting effects of amino acid substitutions on proteins. *Nucleic Acids Research*, **40**(Web Server issue), W452-7.

Singer, K., Bornstein, F.P., Wile, S.A. (1947). Thrombotic thrombocytopenic purpura. Hemorrhagic diathesis with generalized platelet thromboses. *Blood*. **2** (6), 542-554.

SNPEdia <<http://www.snpedia.com/index.php/ADAMTS13>>[accessed 13/9/2017]

SNP Effect 4.0: <<http://www.snpeffect.switchlab.org/>>[Accessed 20/7/15].

Soejima, K., Matsumoto, M., Kokame, K., Yagi, H., Ishizashi, H., Maeda, H., Doc, W. and Nozaki, C. (2010). von Willebrand factor cleavage ADAMTS-13 cysteine-rich / spacer domains are functionally essential for von Willebrand factor cleavage. *Blood*. **102**(9), 3232–3237.

Sorvillo, N., Kaijen, P. H., Matsumoto, M., Fujimura, Y., van der Zwaan, C., Verbij, F. C., Pos, W., Fijnheer, R., Voorberg, J. and Meijer, A. B. (2014). Identification of N-linked glycosylation and putative O-fucosylation, C-mannosylation sites in plasma derived ADAMTS13. *Journal of Thrombosis and Haemostasis*. **12**, 670-679.

Tao, Z., Anthony, K., Peng, Y., Choi, H., Nolasco, L., Rice, L., Moake, J. L. and Dong, J.-F. (2006). Novel ADAMTS-13 mutations in an adult with delayed onset thrombotic thrombocytopenic purpura. *Journal of Thrombosis and Haemostasis*. **4**(9), 1931–5.

Tripodi, A., Chantarangkul, V., Böhm, M., Budde, U., Dong, J.-F., Friedman, K. D., Galbusera, M., Girma, J.-P., Moake, J., Rick, M. E., Studt, J.-D., Turecek, P. L. and Mannucci, P. M. (2004) Measurement of von Willebrand factor cleaving protease (ADAMTS-13): results of an international collaborative study involving 11 methods testing the same set of coded plasmas. *Journal of Thrombosis and Haemostasis*. **2**, 1601–1609.

Tripodi, A., Peyvandi, F., Chantarangkul, V., Palla, R., Afrasiabi, A., Canciani, M. T., Chung, D. W., Ferrari, S., Fujimura, Y., Karimi, M., Kokame, K., Kremer Hovinga, J. A., Lämmle, B., de Meyer, S. F., Plaimauer, B., Vanhoorelbeke, K., Varadi, K. and Mannucci, P. M. (2008) Second international collaborative study evaluating performance characteristics of methods measuring the von Willebrand factor cleaving protease (ADAMTS-13). *Journal of Thrombosis and Haemostasis*. **6**(9), 1534–41.

Tsai, E., Chapin, J., Laurence, J. C. and Tsai, H. M. (2013) Use of eculizumab in the treatment of a case of refractory, ADAMTS13-deficient thrombotic thrombocytopenic purpura: Additional data and clinical follow-up. *British Journal of Haematology*. **162**(4), 558–559.

- Tsai, H. M. (1996) Physiologic cleavage of von Willebrand factor by a plasma protease is dependent on its conformation and requires calcium ion. *Blood*. **87**(10), 4235–44.
- Tsai, H. M. (2010). Pathophysiology of thrombotic thrombocytopenic purpura. *International Journal Hematology*. **91**, 1-19.
- Tsai, H.-M. and Lian, E. C. (1998) Antibodies to von Willebrand factor-cleaving protease in acute thrombotic thrombocytopenic purpura. *New England Journal Medicine*. **339**, 1585–1594.
- Tseng, S. and Kimchi-Safarty, C. (2011). SNPs in ADAMTS13. *Pharmacogenomics*, **12**(8), 1147–1160.
- Turner, N, Nolasco, L., Tao, Z., Dong J.F., Moake, J. (2006) Human endothelial cells synthesize and release ADAMTS13. *Journal of Thrombosis and Haemostasis*, **4**, 1396.
- Turner, S. L., Blair-Zajdel, M. E. and Bunning, R. A. D. (2009). ADAMs and ADAMTSs in cancer. *British Journal of Biomedical Science*. **66**(2), 117–128.
- Uemura, M., Tatsumi, K., Matsumoto, M., Fujimoto, M., Matsuyama, T., Ishikawa, M. and Iwamoto, T. (2005). Localization of ADAMTS13 to the stellate cells of human liver. *Alcohol*. **106**(3), 922–924.
- Veyradier, A., Stepanian, A. and Coppo, P. (2012). ADAMTS13 , Thrombotic Thrombocytopenic Purpura and Pregnancy. *Hereditary Genetics*. **S1:002**, 1–6.
- Veyradier, A., Lavergne, J. M., Ribba, A. S., Obert, B., Loirat, C., Meyer, D. and Girma, J. P. (2004). Ten candidate ADAMTS13 mutations in six French families with congenital thrombotic thrombocytopenic purpura (Upshaw-Schulman syndrome). *Journal of Thrombosis and Haemostasis*. **2**(3), 424–429.
- Vomund, A. N. and Majerus, E. M. (2009) ADAMTS13 bound to endothelial cells exhibits enhanced cleavage of von Willebrand factor. *Journal of Biological Chemistry*. **284**(45), 30925–30932.
- De Vries, P. S., Boender, J., Sonneveld, M. A. H., Rivadeneira, F., Ikram, M. A., Rottensteiner, H., Hofman, A., Uitterlinden, A. G., Leebeek, F. W. G., Franco, O. H., Dehghan, A. and De Maat, M. P. M. (2015). Genetic variants in the ADAMTS13 and SUPT3H genes are associated with ADAMTS13 activity. *Blood*. **125**(25), 3949–3955.
- Wagner, D. D., Olmsted, J. B. and Marder, V. J. (1982) Immunolocalization of von Willebrand protein in Weibel-Palade bodies of human endothelial cells. *Journal of Cell Biology*. **95**(1), 355–360.
- Wang, D., Johnson, A.D., Papp, A.C., Kroetz, D.L., Sadee, W. (2005) Multidrug resistance polypeptide 1 (MRD1, ABCB1) variant 3435 C>T affects mRNA stability. *Pharmacogenetics Genomics*. **15**(10) 693-704.
- Weiss, H. J., Sussman, I. I. and Hoyer, L. W. (1977) Stabilization of factor VIII in plasma by the von Willebrand factor. Studies on posttransfusion and dissociated factor VIII and in patients with von Willebrand's disease. *Journal of Clinical Investigation*. **60**(2), 390–404.
- de Wet, J. R., Wood, K. V, De Luca, L. M., Helinski, D. R. and Subramani, S. (1987) Firefly luciferase gene: structure and expression in mammalian cells. *Molecular and Cellular Biology*. **7**(2), 725–737.
- Xiang, Y., Groot, R. De, Crawley, J. T. B. and Lane, D. A. (2011) Mechanism of von Willebrand factor scissile bond cleavage by a disintegrin and metalloproteinase with a thrombospondin type 1 motif , member 13 (ADAMTS13). *Proceedings of the Natural Academy of Sciences USA*. **13**, 1–6.

- Xiao, J., Jin, S. Y., Xue, J., Sorvillo, N., Voorberg, J. and Zheng, X. L. (2011) Essential domains of a disintegrin and metalloprotease with thrombospondin type 1 repeats-13 metalloprotease required for modulation of arterial thrombosis. *Arteriosclerosis, Thrombosis, and Vascular Biology*. **31**(10), 2261–2269.
- Xu, A. J. and Springer, T. A. (2013). Mechanisms by which von Willebrand disease mutations destabilize the A2 domain. *Journal of Biological Chemistry*. **288**(9), 6317–6324.
- Yeh, H. C., Zhou, Z., Choi, H., Tekeoglu, S., May, W., Wang, C., Turner, N., Scheiflinger, F., Moake, J. L. and Dong, J. F. (2010). Disulfide bond reduction of von Willebrand factor by ADAMTS-13. *Journal of Thrombosis and Haemostasis*. **8**(12), 2778–2788.
- Zanardelli, S., Chion, A. C. K., Groot, E., Lenting, P. J., Mckinnon, T., Laffan, M., Tseng, M. and Lane, D. (2009) A novel binding site for ADAMTS13 constitutively exposed on the surface of globular VWF. *Thrombosis and Haemostasis*. **114**(13), 2819–2828.
- Zhang, Q., Zhou, Y.-F., Zhang, C.-Z., Zhang, X., Lu, C. and Springer, T. (2009) Structural specializations of A2, a force-sensing domain in the ultralarge vascular protein von Willebrand factor. *Proceedings of the National Academy of Sciences of the United States of America*. **106**(23), 9226–9231.
- Zheng, X., Chung, D., Takayama, T. K., Majerus, E. M., Sadler, J. E. and Fujikawa, K. (2001). Structure of von Willebrand Factor-cleaving Protease (ADAMTS13), a Metalloprotease Involved in Thrombotic Thrombocytopenic Purpura. *Journal of Biological Chemistry*. **276**(44), 41059–41063.
- Zheng, X.L. (2010). ADAMTS13 testing: Why bother? *Blood*. **115**, 1475-1476.
- Zheng, X. L. (2012). ADAMTS13 , TTP and Beyond. *Hereditary Genetics*. **1**(4), 13–14.
- Zheng, X. L. (2013). Structure-function and regulation of ADAMTS-13 protease. *Journal of thrombosis and haemostasis*. **11** (Suppl 1), 11–23.
- Zheng, X.L. (2015). ADAMTS13 and von Willebrand factor in thrombotic thrombocytopenic purpura. *Annual Reviews of Medicine*. **66**, 211-225.
- Zheng, X., Nishio, K., Majerus, E. M. and Sadler, J. E. (2003) Cleavage of von Willebrand factor requires the spacer domain of the metalloprotease ADAMTS13. *Journal of Biological Chemistry*. **278**(32), 30136–30141.
- Zhou, Z., Behymer, M. and Guchhait, P. (2010). Role of extracellular haemoglobin in thrombosis and vascular occlusion in patients with sickle cell anemia. *Anemia*. **2011**, 918916.

Appendices

Appendix 1

Reagents and media

Triton X cell lysis buffer

20 mM Tris-HCl (Sigma) (0.6304 g)
150 mM NaCl (Fisher) (1.75 g)
0.1 % v/v Triton X-100 (Sigma) (0.2 ml)
Made up to 200 ml with distilled water

X-gal buffer

Deoxycholic acid (Sigma Aldrich)	10 mM (0.05 g)
Potassium ferrocyanate (Sigma Aldrich)	5 mM (1.056 g)
Potassium ferricyanide III (Sigma Aldrich)	5 mM (0.823 g)
Magnesium chloride (Sigma Aldrich)	4.3 mM (0.203 g)
Igepal CA-630 (Sigma Aldrich)	0.02 % v/v (0.1 ml)
Phosphate buffered saline (Sigma Aldrich)	500ml

X-gal (Fisher Scientific) was diluted in DMSO (AppliChem) to give a final concentration of 40mg/ml and stored at -20°C.

For each 10cm dish, 25µl X-gal was added to 2ml buffer.

Site directed mutagenesis

LB media/l, pH 7.0	NZY ⁺ broth/l, pH 7.5
25 g LB Broth, Miller (Fisher)	10 g N-Z-Amine [®] (Sigma-Aldrich)
Distilled water to 1 l	5 g NaCl (Fisher)
	5 g yeast extract (Sigma-Aldrich)
	Distilled water to 1 l
	After autoclaving, prior to use add:
	12.5 ml 1 M magnesium chloride* (Sigma-Aldrich)
	12.5 ml 1 M magnesium sulfate* (Sigma-Aldrich)
	20 ml 20 % (w/v) glucose (Sigma-Aldrich)

*filter sterilized through 0.2 µl size filter

LB-ampicillin agar/l	10 mM IPTG/10 ml
20 g agar (Sigma-Aldrich)	24 mg IPTG (Fisher)
1 l LB media (Fisher)	10 ml sterile distilled water
1 ml 1 mg/ml filter sterilized ampicillin sodium salt (Calbiochem), added on cooling of LB agar to 55 °C	Spread 100 µl per LB-agar plate

2 % X-gal/ 10 ml
0.2 g X-gal (Fisher)
10 ml DMSO (Applichem)
Spread 100 µl per LB-agar plate

SDS gel electrophoresis

Laemmli buffer (x4)

Reagent	Quantity
1 M Tris (adjusted to pH 6.8 with HCl) (Fisher)	1.25 ml
Glycerol (VWR)	0.5 ml
SDS (Sigma-Aldrich)	0.4 g
Bromophenol blue (Fisher)	0.004 g
β mercaptoethanol (Sigma-Aldrich)	1 ml
Deionised water	7.25 ml

Resolving gel buffer 1.5 M Tris HCl (adjusted to pH to 8.8 with HCl)

Tris base (Fisher)	3.63 g
--------------------	--------

Stacking gel buffer 0.5 M Tris HCl (adjusted to pH 6.8 with HCl)

Tris base (Fisher)	1.21 g
--------------------	--------

10 % acrylamide resolving gel (x2)

Reagent	Volume
40 % bis-acrylamide solution (Fisher)	2.5 ml
Deionized water	3.3 ml
1.5 M Tris buffer (Fisher)	3.8 ml
10 % sodium dodecyl sulfate (Sigma-Aldrich)	100 μ l
15 % ammonium persulphate (APS) (Sigma-Aldrich)	50 μ l
TEMED (Sigma-Aldrich)	5 μ l

4% acrylamide stacking gel (x2)

Reagent	Volume
40 % bis-acrylamide solution (Fisher)	0.25 ml
Deionized water	1.5 ml
0.5 M Tris buffer (Fisher)	0.63 ml
10 % sodium dodecyl sulfate (Sigma-Aldrich)	25 μ l
15 % ammonium persulphate (APS) (Sigma-Aldrich)	12.5 μ l
TEMED (Sigma-Aldrich)	2.5 μ l

Running buffer (1 L)

Reagent	Quantity
Tris base (Fisher)	14.4 g
Glycine (Fisher)	3.03 g
SDS (1 % w/v) (Sigma-Aldrich)	1 ml

Western blot

Transfer buffer (x 5), pH 8.3	Transfer buffer (x 1)
15.5 g Tris base (Fisher)	5 x transfer buffer
72 g glycine (Fisher)	600 ml deionized water
1 l deionized water	200 ml methanol (Fisher Chemical)

Tris buffered saline (TBS) x 10, adjusted to pH 7.5 with 5 N NaOH

TBS	Quantity
NaCl (Fisher) 150 mM	8.76 g

Tris (Fisher) 50 mM	6.05 g
Deionized water	1 l

Ponceau S stain

0.1 % w/v Ponceau S (Sigma-Aldrich)
5 % (v/v) Acetic acid glacial (Fisher Scientific)

Blocking buffer (3%)

3 g Marvel original Dried skimmed milk powder (Premier Foods Group)
100 ml 1 x TBS

TBST (0.05%)

50 μ l Tween [®] -20
100 ml TBS

Antibodies (per blot)

5 μ l Anti-myc tag, clone 4A6 (mouse monoclonal) IgG ₁ , 1 mg/ml (Merck Millipore)
10ml 3 % blocking buffer in TBS

10 μ l β actin, clone 8226 (mouse monoclonal) IgG ₁ (Abcam, clone 8226)
10ml 3% blocking buffer in TBS

2 μ l secondary goat anti-mouse IgG monoclonal antibody with HRP (Sigma Aldrich)
10ml 3% blocking buffer in TBS

Appendix 2

Results of BCA assay, cell lysates

Clone	Protein concentration ($\mu\text{g}/\mu\text{l}$)
G305A 1*	378
G305A 2*	338
G305A 3*	350
G305A+C1342G 1	209
G305A+C1342G 2	232
G305A+C1342G 3	179
G305A + Q448E 1 Rpt	243
G305A + Q448E 2 Rpt	305
G305A + Q448E 3 Rpt	284
G305A multi 1	209
G305A multi 2	255
G305A multi 3	289
C587T 1*	577
C587T 2*	571
C587T 3*	529
C587T+ Q448E 1	255
C587T+ Q448E 2	308
C587T+ Q448E 3	317
G649C 1	214
G649C 2	241
G649C 3	242
G649C + R7W 1	171
G649C + R7W 2	181
G649C + R7W 3	182
G649C+Q448E 1	199
G649C+Q448E 2	187
G649C+Q448E 3	200
G649C + 1033T 1	263
G649C + 1033T 2	248
G649C + 1033T 3	271
G649C multi 1	238
G649C multi 2	233
G649C multi 3	266
G649C + R7W 1 Rpt	250
G649C + R7W 2 Rpt	275
G649C + R7W 3 Rpt	286
G649C + Q448E 1 Rpt	295
G649C + Q448E 2 Rpt	302
G649C + Q448E 3 Rpt	292
C1192T 1	243
C1192T 2	199
C1192T 3	247
C1192T + Q448E 1	197
C1192T + Q448E 2	193
C1192T + Q448E 3	221

C1225T 1	288
C1225T 2	307
C1225T 3	340
C1225T 1 Rpt	466
C1225T 2 Rpt	508
C1225T 3 Rpt	479
C1787T 1	240
C1787T 2	262
C1787T 3	215
C1787T + C1423T 1	279
C1787T + C1423T 2	268
C1787T + C1423T 3	247
C1787T + C1423T 1 Rpt	400
C1787T + C1423T 2 Rpt	530
C1787T + C1423T 3 Rpt	517
G2068A 1	702
G2068A 2	732
G2068A 3	553
G2068A 1 Rpt	516
G2068A 2 Rpt	476
G2068A 3 Rpt	518
R910X 1 C2728T	765
R910X 2	775
R910X 3	816
R910X 1 Rpt	475
R910X 2 Rpt	397
G2930T 1	283
G2930T 2	283
G2930T 3	253
Q448E 1*	414
Q448E 2*	498
A900V 1*	381
A900V 2*	380
C2195T 1	286
C2195T 2	252
C2195T 3	265

*denotes 10cm cell culture plates. All other cell lysates derived from 6 well plates

Results of BCA assay, cell lysates

Clone	Protein concentration ($\mu\text{g}/\mu\text{l}$)
WT 1	308
WT 2	314
R7W 1	346
R7W 2	441
R7W 3	419
A1033T 2	304
A1033T 3	251
R1060W + A1033T 1	361

R1060W + A1033T 2	374
R1060W 1	346
R1060W 2	436
R1060W 3	352
R1060W + R7W 1	362
R1060W + R7W 2	445
R1060W + R7W 3	342
R1060W + R7W + A1033T 1	796
R1060W + R7W + A1033T 2	802
R1060W + R7W + A1033T 3	711
Negative	372

Results of BCA assay, conditioned media

Clone	Concentration ($\mu\text{g}/\mu\text{l}$)
WT 2 (31/7/15) 10 ml	340
R1060W 1	282
R1060W 2	298
R1060W + A1033T 1	301
R1060W + A1033T 2	288
A1033T 2	287
A1033T 3	278
R7W 1	325
R7W 2	360
R1060W+A1033T+R7W 1	294
R1060W+A1033T+R7W 3	288
R1060W + R7W 1	340
R1060W + R7W 2	349
Neg	250

Results of BCA assay cell lysates from repeat transfections

Clone	Concentration ($\mu\text{g}/\mu\text{l}$)
R1060W 1 rpt 10ml	384
R1060W 2 rpt 10ml	671
R1060W 3 rpt 10ml	530
A1033T 1 rpt	425
A1033T 2 rpt	424
A1033T 3 rpt	411
R1060W+A1033T Rpt 1	362
R1060W+A1033T Rpt 2	445
R1060W+A1033T Rpt 3	342
R1060W+A1033T+R7W 1 Rpt	796
R1060W+A1033T+R7W 2 Rpt	802
R1060W+A1033T+R7W 3 Rpt	711

Results of BCA assay results repeat transfections: conditioned media

Clone	Concentration ($\mu\text{g}/\mu\text{l}$)
R1060W 1 rpt 10ml	1,148
R1060W 2 rpt 10ml	1,041
R1060W 3 rpt 10ml	1,067
A1033T 1 rpt	1,137
A1033T 2 rpt	1,033
A1033T 3 rpt	1,124
R1060W+A1033T Rpt 1	1,231
R1060W+A1033T Rpt 2	1,117
R1060W+A1033T Rpt 3	1,172
R1060W+A1033T+R7W 1 Rpt	760
R1060W+A1033T+R7W 2 Rpt	830
R1060W+A1033T+R7W 3 Rpt	751

Results of BCA assay conditioned media

Clone conditioned media	Protein concentration ($\mu\text{g}/\mu\text{l}$)
G305A 1*	159
G305A 2*	169
G305A 3*	127
G305A+C1342G 1	257
G305A+C1342G 2	287
G305A+C1342G 3	226
G305A + Q448E 1 Rpt	869
G305A + Q448E 2 Rpt	800
G305A + Q448E 3 Rpt	1020
G305A + A900V 1	301
G305A + A900V 2	263
G305A + A900V 3	239
G305A multi 1	243
G305A multi 2	304
G305A multi 3	229
C587T 1*	645
C587T 2*	682
C587T 3*	842
C587T+ Q448E 1	1605
C587T+ Q448E 2	1594
C587T+ Q448E 3	1541
G649C 1	253
G649C 2	303
G649C 3	389
G649C + R7W 1	237
G649C + R7W 2	289
G649C + R7W 3	275
G649C+Q448E 1	
G649C+Q448E 2	
G649C+Q448E 3	
G649C + 1033T 1	353

G649C + 1033T 2	327
G649C + 1033T 3	475
G649C multi 1	300
G649C multi 2	332
G649C multi 3	393
G649C + R7W 1 Rpt	845
G649C + R7W 2 Rpt	849
G649C + R7W 3 Rpt	650
G649C + Q448E 1 Rpt	923
G649C + Q448E 2 Rpt	936
G649C + Q448E 3 Rpt	876
C1192T 1	1657
C1192T 2	1640
C1192T 3	2519
C1192T + Q448E 1	1393
C1192T + Q448E 2	1834
C1192T + Q448E 3	1421
C1225T 1	977
C1225T 2	784
C1225T 3	919
C1225T 1 Rpt	569
C1225T 2 Rpt	524
C1225T 3 Rpt	623
C1787T 1	2105
C1787T 2	1561
C1787T 3	2108
C1787T + C1423T 1	778
C1787T + C1423T 2	951
C1787T + C1423T 3	811
C1787T + C1423T 1 Rpt	584
C1787T + C1423T 2 Rpt	589
C1787T + C1423T 3 Rpt	805
G2068A 1	2409
G2068A 2	2189
G2068A 3	1481
G2068A 1 Rpt	615
G2068A 2 Rpt	542
G2068A 3 Rpt	675
R910X 1 C2728T	3375
R910X 2	2442
R910X 3	1791
R910X 1 Rpt	545
R910X 2 Rpt	461
G2930T 1	2224
G2930T 2	3523
G2930T 3	2236
Q448E 1*	196
Q448E 2*	180
A900V 1*	180
A900V 2*	190

C2195T 1	2280
C2195T 2	2685
C2195T 3	2501